

**Aus dem Institut für Physiologie und Pathophysiologie
Geschäftsführender Direktor: Prof. Dr. Dr. Jürgen Daut**

des Fachbereichs Medizin der Philipps-Universität Marburg



**Molecular Properties and Pathophysiological Relevance of the
Predominant K⁺ Conductance in Cochlear Outer Hair Cells**

Inaugural-Dissertation zur Erlangung des Doktorgrades der Naturwissenschaften

dem Fachbereich Medizin der Philipps-Universität Marburg

vorgelegt von

Michael Georg Leitner
(geb. in St. Johann in Tirol, Österreich)

Marburg, 2012

Angenommen vom Fachbereich Medizin der Philipps-Universität Marburg
am: 9. August 2012 (Tag der Disputation)

Gedruckt mit Genehmigung des Fachbereichs

Dekan: Prof. Dr. Matthias Rothmund

Referent: Prof. Dr. Dominik Oliver

Korreferent: Prof. Dr. Joachim Hoyer

Diese Doktorarbeit macht von der Möglichkeit Gebrauch, gesammelte Publikationen als Dissertationsleistung anzuerkennen (kumulative Dissertation) wie in der „Promotionsordnung der Mathematisch-Naturwissenschaftlichen Fachbereiche und des Medizinischen Fachbereiches für seine mathematisch-naturwissenschaftlichen Fächer der Philipps-Universität Marburg vom 15.7.2009 (§9)“ erläutert. Demnach besteht diese Arbeit aus einer gemeinsamen Einleitung, einer Zusammenfassung der folgenden, im Anhang angeführten Publikationen und einer Diskussion.

Michael G. Leitner, Christian R. Halaszovich and Dominik Oliver. Aminoglycosides inhibit KCNQ4 channels in cochlear outer hair cells via depletion of phosphatidylinositol(4,5)bisphosphate. *Molecular Pharmacology*. 2011 Jan:79(1):51-60

Michael G. Leitner, Anja Feuer, Olga Ebers, Daniela N. Schreiber, Christian R. Halaszovich and Dominik Oliver. Restoration of ion channel function in deafness-causing KCNQ4 mutations by chemical openers. *British Journal of Pharmacology* (2012) 165 2244-2259

Moritz Lindner, **Michael G. Leitner**, Christian R. Halaszovich, Gerald R.V. Hammond and Dominik Oliver. Probing the regulation of TASK potassium channels by PI(4,5)P₂ with switchable phosphoinositide phosphatases. *Journal of Physiology*. 2011 Jul 1:589 (Pt 13):3149-62

Jérôme Lacroix, Christian R. Halaszovich, Daniela N. Schreiber, **Michael G. Leitner**, Francisco Bezanilla, Dominic Oliver and Carlos A. Villalba-Galea. Controlling the activity of PTEN by membrane potential. *Journal of Biological Chemistry*. 2011 May 20:286(20):17945-53

Äußere Haarsinneszellen (ÄHZ) des Corti'schen Organs im Innenohr werden biophysikalisch charakterisiert durch den K^+ Strom $I_{K,n}$, dessen molekulare Grundlage der spannungsabhängige K^+ Kanal KCNQ4 (Kv7.4) ist. $I_{K,n}/KCNQ4$ dominiert die elektrischen Eigenschaften der ÄHZ Zellmembran und ist darüber hinaus essentiell für das Überleben der Zellen. Im *knock-out* Tiermodell führte der Verlust der KCNQ4 Kanalaktivität zum Untergang der ÄHZ und zu Taubheit. Dies ist klinisch bedeutend, da im Menschen KCNQ4 Mutationen die Ursache für die erbliche Taubheit DFNA2 sind. Der Mechanismus, der zum Haarzelluntergang führt, ist noch unklar, doch korreliert das Überleben von ÄHZ direkt mit der Funktion von KCNQ4. Obwohl der durch Giftstoffe oder Lärm bewirkte Haarzelluntergang (erworbener Hörverlust) dem KCNQ4-bedingten ÄHZ Verlust ähnelt, wurde eine Verbindung zwischen $I_{K,n}/KCNQ4$ und erworbenem Hörverlust bisher noch nicht experimentell erfasst. In der vorliegenden Arbeit habe ich mich mit der pathophysiologischen Rolle von $I_{K,n}/KCNQ4$ in klinisch relevantem Haarzelluntergang beschäftigt, der durch Aminoglykosid (AG) Antibiotika hervorgerufen wird. Des Weiteren wurde untersucht, ob chemische KCNQ Kanalöffner die Funktion von $I_{K,n}$ trotz pathophysiologisch relevanter Inhibition wiederherstellen können, um eventuell Protektion der ÄHZ zu ermöglichen.

Ich konnte erstmalig zeigen, dass AG Antibiotika schnell in Haarzellen eindringen und $I_{K,n}$ inhibieren. Die Inhibition war darauf zurückzuführen, dass AG über elektrostatische Wechselwirkungen negativ geladene Phospholipide funktionell depletieren, die für die Funktion von $I_{K,n}$ essentiell sind. Verschiedene AG zeigen unterschiedliches ototoxisches Potential: Neomycin führt zum Untergang von ÄHZ, während Gentamycin vestibuläre Haarzellen schädigt. Das Ausmaß der $I_{K,n}$ Kanal inhibition korrelierte (Neomycin > Gentamycin) mit dem Grad der Phospholipid Bindung und mit dem ototoxischen Potential der AG. Dies legt nahe, dass die hohe Anfälligkeit der ÄHZ gegenüber Neomycin auf die Inhibition von $I_{K,n}$ zurückzuführen ist. Des Weiteren konnte gezeigt werden, dass die Aktivität von $I_{K,n}$ durch chemische KCNQ Kanalöffner verstärkt wird. Die AG-induzierte Hemmung von $I_{K,n}$ konnte aufgehoben und die Kanalaktivität vollkommen wiederhergestellt werden.

In heterozygoten DFNA2 Patienten werden $I_{K,n}$ Ströme durch einen dominant-negativen Effekt mutierter KCNQ4 Kanaluntereinheiten verringert, was den ÄHZ Untergang bewirkt. Es ist mir im heterologen System gelungen, mittels chemischer KCNQ Kanalöffner KCNQ4 von dieser dominant-negativen Inhibition zu befreien. Die Ströme in Gegenwart der Kanalöffner waren vergleichbar mit Strömen unter Kontrollbedingungen, was gleichbedeutend mit der vollständigen Wiederherstellung der Kanalfunktion war.

Zusammenfassend kann gesagt werden, dass ich in dieser Arbeit erstmals eine Rolle der Kaliumleitfähigkeit $I_{K,n}$ in erworbenem Hörverlust demonstrieren konnte. Dies kann die verstärkte Anfälligkeit von ÄHZ gegenüber ototoxischen Einflüssen erklären. Darüber hinaus stabilisieren chemische Kanalöffner $I_{K,n}$ in Anwesenheit von AG und stellen die Funktion von rekombinanten KCNQ4 Kanälen trotz dominant-negativer Inhibition wieder her. Dies könnte Haarzellen vor KCNQ4-bedingtem Untergang schützen. Es bleibt allerdings offen, ob die Substanzen den Verlust der ÄHZ verzögern und Taubheit abwenden können.

Cochlear outer hair cells (OHCs) are characterised by the voltage-dependent K^+ conductance $I_{K,n}$ that previously was shown to be mediated by KCNQ4 (Kv7) channel subunits. $I_{K,n}$ /KCNQ4 dominates the electrical properties of the OHC cell membrane and furthermore is essential for OHC survival. Genetic deletion of KCNQ4 causes progressive degeneration of OHCs and deafness. Similarly, KCNQ4 loss-of-function mutations cause the progressive form of hereditary deafness DFNA2. The molecular mechanism leading to OHC degeneration remains elusive, but the survival of OHCs has been linked directly to KCNQ4 channel function. Strikingly, the loss of OHCs is phenotypically similar to OHC degeneration caused by ototoxic substances and noise damage (acquired hearing loss), but a role of $I_{K,n}$ /KCNQ4 in acquired hearing loss has never been investigated so far. In the present study I investigated the pathophysiological relevance of $I_{K,n}$ for OHC degeneration caused by aminoglycoside (AG) antibiotics. Since KCNQ4 channel function is essential for OHC survival, chemical current augmentation may provide a protective strategy against KCNQ4-related hearing loss. Thus, I analysed whether chemical KCNQ channel openers rescued $I_{K,n}$ currents from pathological inhibition.

In brief, I found that AGs rapidly entered OHCs and that entry was necessary for $I_{K,n}$ current inhibition. The inhibition was caused by functional depletion of phospholipids by the AGs that are essential for the function of $I_{K,n}$ /KCNQ4. Various AGs exhibit different ototoxic potential, i.e. neomycin causes OHC degeneration whereas gentamicin damages vestibular hair cells. Strikingly, the degree of $I_{K,n}$ inhibition (neomycin > gentamicin) correlated with the phospholipid binding efficiency and with the ototoxic potential of the respective AG. Given the dependence of OHCs on $I_{K,n}$, the ototoxic potential of AGs thus may be determined by their chemical nature and by their inhibitory impact on $I_{K,n}$. Furthermore, I showed that $I_{K,n}$ was sensitive to current augmentation by chemical KCNQ channel openers. A combination of openers rescued $I_{K,n}$ from AG-induced inhibition to wild-type levels indicating full restoration of $I_{K,n}$ activity.

Most DFNA2 patients are heterozygous carriers of KCNQ4 mutations that reduce $I_{K,n}$ through a dominant-negative effect. This reduction of $I_{K,n}$ activity causes OHC degeneration. Residual currents in the dominant-negative situation were essentially rescued to wild-type levels by the application of KCNQ channel openers, at least in a heterologous expression system. The current rescue indicated that KCNQ channel openers might be used to stabilise $I_{K,n}$ in heterozygous DFNA2 patients.

In summary, the present work demonstrated for the first time a role of the essential OHC K^+ conductance $I_{K,n}$ in acquired hearing loss. The dependence of OHCs on $I_{K,n}$ may explain the high vulnerability of OHCs towards ototoxic influences. $I_{K,n}$ current augmentation by chemical KCNQ openers may be used to stabilise $I_{K,n}$ in OHCs and protect the sensory cells from KCNQ4-related degeneration. KCNQ openers rescued $I_{K,n}$ from AG-induced inhibition in OHCs and recombinant KCNQ4 from dominant-negative inhibition by mutant subunits. However, it remains elusive whether chemical KCNQ agonists alleviate OHC degeneration and protect from hearing loss.

TABLE OF CONTENTS

1	INTRODUCTION	- 1 -
1.1	Auditory Hair Cells Mediate the Transduction of Sound	- 1 -
1.2	Outer Hair Cells and the Cochlear Amplifier	- 3 -
1.2.1	The Electrophysiology of Outer Hair Cells	- 4 -
1.2.2	$I_{K,n}$ is the Predominant K^+ Current of Outer Hair Cells	- 5 -
1.2.3	KCNQ4 Mediates $I_{K,n}$, But Both Channels Show Biophysical Differences	- 6 -
1.2.4	$I_{K,n}$ /KCNQ4 is Essential for the Survival of Outer Hair Cells	- 7 -
1.2.5	Other Outer Hair Cell Pathologies May Be Related to KCNQ4 Dysfunction	- 9 -
2	AIMS AND CONTRIBUTIONS	- 11 -
2.1	Objectives	- 11 -
2.2	My Contributions to the Articles Presented	- 12 -
3	RESULTS	- 14 -
3.1	The Outer Hair Cell K^+ Current $I_{K,n}$ Requires PI(4,5)P ₂ for Activation	- 14 -
3.2	Inhibition of $I_{K,n}$ by Aminoglycosides is Pathophysiologically Relevant	- 15 -
3.3	$I_{K,n}$ is Sensitive to Chemical KCNQ Openers	- 16 -
3.4	KCNQ Channel Openers Rescue $I_{K,n}$ from AG-induced Inhibition and Reconstitute Channel Function of Deafness-Causing KCNQ4 Mutants	- 16 -
3.5	The Biophysical Properties and the Molecular Nature of $I_{K,n}$	- 17 -
3.6	Development of Novel Tools to Experimentally Alter PI Levels in Living Cells	- 19 -
4	DISCUSSION	- 20 -
4.1	Biophysical and Pharmacological Differences of $I_{K,n}$ and Recombinant KCNQ4: Implications for the Molecular Identity of $I_{K,n}$	- 20 -
4.2	The Role of $I_{K,n}$ Inhibition in AG-induced Hair Cell Loss	- 21 -
4.3	Potential Use of KCNQ Openers to Protect from KCNQ4-related Hearing Loss	- 22 -
4.4	Outlook	- 23 -
5	REFERENCES	- 25 -
6	SUBMITTED PUBLICATIONS	- 31 -
7	APPENDIX	vii

ABBREVIATIONS

AG	Aminoglycoside
Akt	Protein kinase B
BM	Basilar membrane
CFP	Cyan fluorescent protein
CHO	Chinese hamster ovary
Ci-VSP	<i>Ciona intestinalis</i> voltage-sensing phosphatase
DAG	Diacylglycerol
DFNA2	Deafness-associated autosomal dominant locus 2
GFP	Green fluorescent protein
IHC	Inner hair cell
IP ₃	Inositol-(3,4,5)-trisphosphate
KCNQ	Voltage-gated potassium channel family 7 (Kv7)
M1R	Muscarinic acetylcholine receptor type 1
MET	Mechano-electrical transduction
OHC	Outer hair cell
PBM	Phosphatidylinositol binding motif
PD	Phosphatase domain
PH	Pleckstrin homology
PI	Phosphoinositide
PI(4)P	Phosphatidylinositol-(4)-phosphate
PI(4,5)P ₂	Phosphatidylinositol-(4,5)-bisphosphate
PI(3,4)P ₂	Phosphatidylinositol-(3,4)-bisphosphate
PI(3,4,5)P ₃	Phosphatidylinositol-(3,4,5)-trisphosphate
PI3K	Phosphatidylinositol-3 kinase
PLC	Phospholipase C
PTEN	Phosphatase and tensin homolog deleted from chromosome 10
TASK	TWIK-related acid sensing potassium channel
TIRF	Total internal reflection fluorescence
TEA	Tetraethylammonium
VSD	Voltage sensor domain
VSP	Voltage-sensing phosphatase
Wt	Wild-type
ZnP/Ret	Zinc pyrithione plus retigabine

1 Introduction

Hearing is a complex process that involves the transduction of mechanical sound stimuli into electrical neuronal signals and the processing of the information in higher auditory brain areas (for review see Fettiplace and Hackney, 2006; Schwander et al., 2010). Malfunction at any of these hierarchic steps causes hearing impairment and deafness in humans (Smith et al., 2008). Hearing impairment can only be mitigated by the use of hearing aids or cochlear implants, but hereditary hearing loss cannot be averted successfully (Smith et al., 2008). The voltage-gated potassium channel KCNQ4 (Kv7.4) constitutes the predominant K^+ conductance, $I_{K,n}$, of outer hair cells (OHCs) in the organ of Corti and was shown to be mutated in hereditary progressive hearing loss, DFNA2 (deafness-associated autosomal dominant locus 2) (Housley and Ashmore, 1992; Kubisch et al., 1999; Kharkovets et al., 2006). Loss of KCNQ4 channel function causes progressive loss of OHCs and profound deafness in affected individuals (Kharkovets et al., 2006; Nie, 2008). OHC degeneration was linked to the dysfunction of $I_{K,n}$ /KCNQ4, but the mechanism leading to the loss of the sensory cells remain unclear (Kharkovets et al., 2006). Given the necessity of KCNQ4 channel function for OHC survival, the potential benefits of KCNQ4 current rescue by chemical channel openers are obvious. Interestingly, KCNQ channel agonists are already used successfully against KCNQ-linked epilepsies (Wulff et al., 2009), but have never been tested in the treatment of KCNQ4-related deafness.

In this thesis fundamental biophysical and pharmacological properties of $I_{K,n}$ were analysed to evaluate the potencies of chemical KCNQ agonists in the treatment of KCNQ4-related hearing impairment. In the following section the role of OHCs in the transduction of sound and the importance of $I_{K,n}$ for OHCs will be discussed.

1.1 Auditory Hair Cells Mediate the Transduction of Sound

The human inner ear detects mechanical displacements below one nanometre (Sellick et al., 1982), displays an amazing frequency range of perception from 20 Hz to 20 kHz, and discriminates frequency differences of only 0.2% (Dallos, 1992; Fettiplace and Hackney, 2006). This performance is achieved by anatomical and physiological specialisations: First, mechanical vibrations are represented on the basilar membrane (BM) as travelling waves with local frequency-specific maxima along the cochlear axis. These maxima are facilitated by the mechanical properties of the BM that is stiffer with smaller diameter at the base than at the apex (Von Békésy, 1960). This produces a frequency map along the cochlea where high frequencies are represented at the base and low frequencies at the apex (see Figure 1A). Complex sounds are dispersed into distinct frequency components and lead to multiple amplitude maxima on the BM (Von Békésy, 1960). Second, the relative movement of the BM towards the tectorial membrane and local fluid acceleration displace apical stereocilia of inner (IHCs) and outer hair cells (OHCs) which opens or closes mechano-sensitive ion channels (mechano-electrical transduction channels, MET) (Schwander et al., 2010). Accordingly, hair

cells at different positions along the cochlea are excited by different frequencies, i.e. the characteristic frequency of the hair cell (Figure 1A and B). Third, locally activated OHCs increase the frequency tuning of the cochlea by active amplification of BM motion (Figure 1B and C) (Sellick et al., 1982; Dallos, 1992; Ashmore et al., 2010).

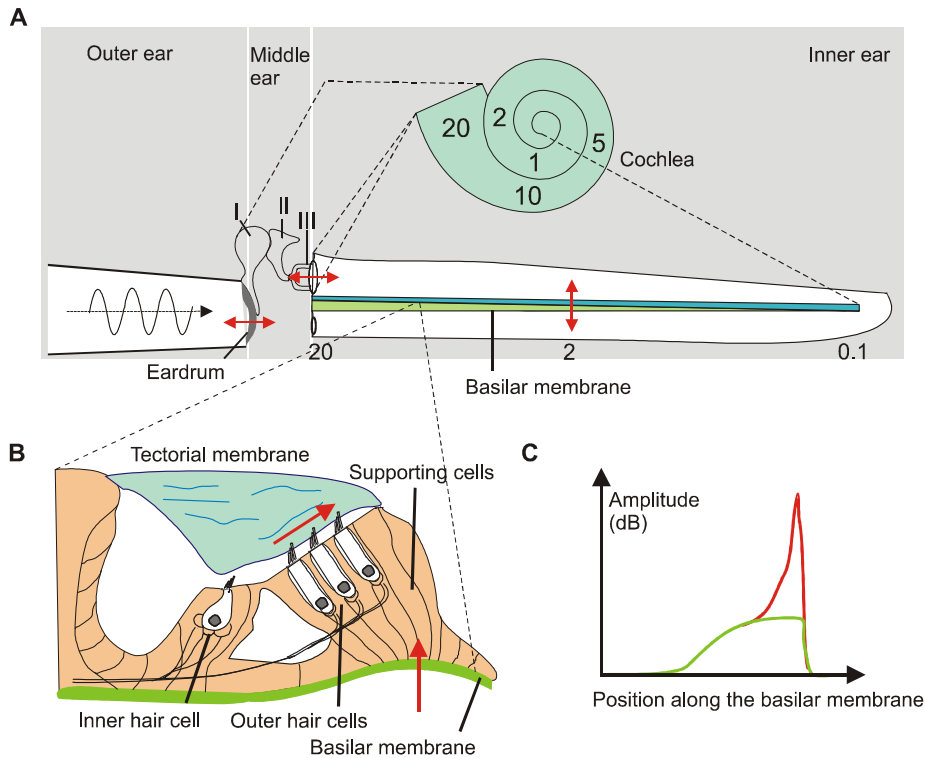


Figure 1: The organ of Corti in the inner ear mediates the transduction of sound.

A, Schematic representation of the coiled cochlea (*top*) and for clarity presented as straight (*bottom*). Sound-induced eardrum vibrations produce frequency-specific movements of the BM. High frequencies are represented in the cochlear base and low frequencies in the apex. The numbers indicate frequency range of the human cochlea (in kHz). (Middle ear bones: (I) malleus, (II) incus, (III) stapes; red arrows indicate direction of mechanical movement)

B, Mechanical movements (*red arrows*) of the BM displace apical stereocilia of hair cells in the organ of Corti, which opens or closes mechano-sensitive ion channels.

C, Cochlear amplification increases frequency discrimination. The *green* trace shows passive BM motion in the dead cochlea. In the living cochlea this movement is increased actively and refined by OHCs (*red*) (see text) (A and B were adopted and modified from Fettiplace and Hackney, 2006).

In the human cochlea sensory hair cells are organised in one row of IHCs and three rows of OHCs (Pickles, 1988; Dallos et al., 1996; Schwander et al., 2010). Hair cells are polarised epithelial cells with a cylindrical cell body presenting the apical part towards the tectorial membrane and the basal (subnuclear) pole towards supporting cells and the tunnel of Corti (Dallos et al., 1996). Accordingly, the apical part of hair cells is bathed in endolymph (with high K^+ and low Na^+ concentration) whereas the basal pole is surrounded by perilymph (with low K^+ and high Na^+) (Dallos et al., 1996). The unique feature of the sensory cells is the apical mechano-sensitive apparatus with three rows of actin-based stereocilia of increasing length

(Lim, 1980). The stereocilia of IHCs and OHCs are made-up by the same molecular components and resemble each other in size, geometry and mechanics (Russell et al., 1986b; Russell et al., 1986a; Russell et al., 1992), but only the OHC hair bundle is embedded into the tectorial membrane (Lim, 1980) (see Figure 1B). Thus, the bundle of OHCs is believed to be displaced by movements of the tectorial membrane relative to the BM, whereas the bundle of IHCs is displaced by motions of the surrounding fluid induced by BM acceleration (Dallos, 1986; Fettiplace and Hackney, 2006). Displacement of the stereocilia towards the longest row opens (gates) MET channels, whereas deflection into the opposing direction closes the channels (Corey and Hudspeth, 1983; Russell and Richardson, 1987). It is believed that MET channel gating is mediated via elastic "gating springs", but neither the molecular nature of the gating spring nor the molecular components of MET channels have been identified so far (Gillespie and Muller, 2009; Schwander et al., 2010). K^+ -carried currents through the MET channels (transduction currents) depolarise IHCs and OHCs. In IHCs depolarisation stimulates Ca^{2+} -dependent glutamate release from the basal pole that increases the action potential frequency of postsynaptic neurons (Moser et al., 2006; Meyer and Moser, 2010). In contrast, voltage changes drive active length changes of the OHC's cell body, which is the mechanism underlying cochlear amplification.

1.2 Outer Hair Cells and the Cochlear Amplifier

In the dead cochlea the low sensitivity, low frequency selectivity and linear dependence of BM movements from stimulus intensity are determined by the mechanical properties of the BM and can be explained by passive movement of the involved structures (Figure 1C, green trace). (Von Békésy, 1960; Pickles, 1988; Dallos, 1992). The structure of the BM, however, does not explain transduction at low stimulus levels, when viscous dampening of the BM and additional passive filtering by involved structures should cause total loss of the energy (Von Békésy, 1960). In contrast, in the living cochlea even low stimulus levels produce robust BM movements that are maximal and sharpest at the characteristic frequency of the respective BM portion (Figure 1C, red trace) (Sellick et al., 1982). Such frequency tuning indicates active amplification of BM movements. Indeed, OHCs were shown to generate additional mechanical output in response to BM displacement which increases BM movement and sharpens cochlear frequency selectivity (Ryan and Dallos, 1975; Dallos and Harris, 1978; Dallos, 1992; Fettiplace and Hackney, 2006). This active enhancement of BM movements by OHCs is referred to as cochlear amplification for which two mechanisms have been proposed: active hair bundle movement and somatic electromotility. Hair bundle movements originate from Ca^{2+} -dependent MET channel desensitisation that actively moves the hair bundle back to its resting position (Fettiplace and Hackney, 2006; Ashmore et al., 2010). Such movement was identified in lower vertebrates (e.g. turtle and frog) and may also exist in mammals, but it remains controversial whether the generated force is sufficient to contribute to the amplification of BM movements (Benser et al., 1996; Martin and Hudspeth, 1999; Ricci et al., 2000; Chan and Hudspeth, 2005;

Kennedy et al., 2005). The more accepted mechanism of cochlear amplification is length changes of the OHC's cell body driven by the membrane potential, also referred to as somatic electromotility. Depolarisation (by gating of MET channels) results in contraction and hyperpolarisation in elongation of the cells. The length changes are mediated by voltage-dependent conformational changes of prestin, a protein in the lateral membrane of OHCs (Brownell et al., 1985; Ashmore, 1987; Zheng et al., 2000; Fettiplace and Hackney, 2006). Since acoustic stimulation changes the membrane potential of OHCs (see 1.2.1), length changes follow audio frequencies and produce a "cycle-by-cycle" force on the BM and the tectorial membrane driven by depolarisation followed by hyperpolarisation (Dallos et al., 1996; Johnson et al., 2011). This mechanical output increases the amplitude of BM movements in response to acoustic stimulation and is the cellular mechanism underlying cochlear amplification (Liberman et al., 2002; Dallos et al., 2008).

In summary, OHCs mediate cochlear amplification through two specialisations: First, mechanical movement of the BM produces a receptor potential that, second, generates mechanical force and enhances BM movement. This requires membrane potential changes as well as conformational responses of prestin and consequently somatic length changes of OHCs. The electrical properties of OHCs enabling cochlear amplification will be discussed in the following section.

1.2.1 The Electrophysiology of Outer Hair Cells

The membrane potential of OHCs is determined by depolarising K^+ currents through the MET channels and by hyperpolarising currents through K^+ channels in the hair cell's basolateral membrane (in the nuclear region of the cell). At rest (without displacement of the hair bundle) approximately 50% of the MET channels are active, setting the membrane potential to around -40 mV (Johnson et al., 2011). Additional gating of MET channels causes K^+ -dependent depolarisation, whereas closing of the MET channels hyperpolarises the membrane potential (Corey and Hudspeth, 1983; Johnson et al., 2011). Accordingly, mechanical displacement of the hair bundle by acoustic stimulation causes sinusoidal variations around the resting potential, i.e. an alternating current (AC) receptor potential (Dallos et al., 1996; Hille, 2001). The AC receptor potential will be attenuated above a certain stimulus frequency due to low-pass filtering of biological membranes. In other words, above this cut-off frequency the receptor potential cannot follow the stimulus anymore and its amplitude is attenuated (Hille, 2001). This is relevant for prestin-driven somatic electromotility. Active amplification of BM movements via positive feedback requires "cycle-by-cycle" length changes in response to alternating depolarisation and hyperpolarisation (Johnson et al., 2011). Thus, OHCs amplify BM movement only if they respond to acoustic stimulation with somatic length changes. If the stimulus frequency exceeds the cut-off frequency of the OHC, attenuation of the receptor potential attenuates prestin-mediated electromotility. This truncates positive feedback and

theoretically limits cochlear amplification to the low frequencies where the receptor potential is not attenuated, since the stimulus frequency is lower than the cut-off frequency.

The cut-off frequency of the circuit is determined by the time constant (τ) that describes the time needed to recharge a capacitor through a resistor ($\tau = R \times C$ where R and C are the input resistance and membrane capacitance, respectively). Accordingly, the cut-off frequency increases with faster time constants of the membrane (Hille, 2001). The input resistance (R) of biological membranes depends on the amount of functional ion channels, i.e. the resistance decreases with increasing number of activated ion channels. In OHCs voltage-dependent K^+ channels are located in the basolateral membrane that dominate the OHC-membrane time constant and shape the receptor potential (Hille, 2001; Johnson et al., 2011). The K^+ channels are activated completely at rest (around -40 mV), which lowers the membrane resistance and speeds the membrane time constant substantially (Johnson et al., 2011). In fact, in OHCs K^+ and MET current amplitudes are bigger in the cochlear base than in the apex, resulting in a high cut-off frequency in high frequency OHCs (Dallos et al., 1982; Dallos, 1985; Housley and Ashmore, 1992; Johnson et al., 2011). Accordingly, complete activation of K^+ channels at the basolateral OHC membrane enables fast prestin-driven electromotility and cochlear amplification even at the highest frequencies in the cochlea. The following chapter describes the K^+ channels of OHCs.

1.2.2 $I_{K,n}$ is the Predominant K^+ Current of Outer Hair Cells

The predominant voltage-dependent K^+ conductance in OHCs is $I_{K,n}$ that shows an unusually negative voltage range of activation. $I_{K,n}$ currents activate at -110 mV and current amplitudes saturate around -40 mV. Thus, $I_{K,n}$ is fully activated at the OHC resting membrane potential, i.e. $I_{K,n}$ is a physiologically constitutively open current ("background current") (Housley and Ashmore, 1992; Mammano and Ashmore, 1996; Nenov et al., 1997; Marcotti and Kros, 1999; Johnson et al., 2011). Thus, as $I_{K,n}$ provides the main K^+ conductance at all potentials it dominates the membrane time constant of OHCs, presumably enabling cochlear amplification at high frequencies (see 1.2.1) (Housley and Ashmore, 1992; Johnson et al., 2011). In murine OHCs the developmental appearance of $I_{K,n}$ concurs with the onset of somatic electromotility around postnatal days eight to ten, implicating the involvement of the conductance in the biophysical and structural maturation of OHCs around the onset of hearing (days 10 to 12) (Marcotti and Kros, 1999; Oliver and Fakler, 1999).

Additional basolateral K^+ currents in OHCs are I_K and I_{SK} . I_K was identified as large conductance voltage- and calcium-activated K^+ current (BKCa; Maxi-K) (Housley and Ashmore, 1992; Mammano et al., 1995; Mammano and Ashmore, 1996; Ruttiger et al., 2004). It resembles a conductance in IHCs and contributes to the fine-tuning of the receptor potential (Ruttiger et al., 2004; Thurm et al., 2005; Oliver et al., 2006). OHCs also express small conductance calcium-activated K^+ channels (I_{SK}) at the basal cell pole that mediate fast efferent inhibition (Dallos et al., 1996). Acetylcholine increases Ca^{2+} levels in OHCs via

postsynaptic nicotinic acetylcholine receptors. Elevated Ca^{2+} levels in turn activate SK channels that through K^+ currents hyperpolarise the hair cell (Elgoyhen et al., 1994; Oliver et al., 2000).

Taken together, the physiology of OHCs largely depends on K^+ channels at the basolateral membrane. The electrical properties of the OHC membrane are dominated by $I_{\text{K,n}}$ that exhibits unusual biophysical properties. The following section discusses these characteristics also considering the voltage-dependent K^+ channel KCNQ4 (Kv7.4) that was shown to constitute $I_{\text{K,n}}$ in OHCs (Kharkovets et al., 2006).

1.2.3 KCNQ4 Mediates $I_{\text{K,n}}$, but Both Channels Show Biophysical Differences

KCNQ4 (Kv7.4) is a member of the KCNQ family (KCNQ1 - KCNQ5, Kv7) of voltage-dependent potassium channels and was shown to mediate $I_{\text{K,n}}$ (Kharkovets et al., 2006; Holt et al., 2007). Whereas other KCNQ isoforms (e.g. KCNQ2/KCNQ3) are expressed throughout the nervous system (reviewed in Jentsch, 2000), the expression profile of KCNQ4 seems to be restricted to hair cells of the inner ear, neurons of the auditory brainstem, mechano-receptors in the skin and vascular smooth muscle cells (Heidenreich et al.; Kharkovets et al., 2000; Chambard and Ashmore, 2005; Yeung et al., 2007). KCNQ4 was identified as the molecular correlate of $I_{\text{K,n}}$ based on various findings: First and most convincing, genetic disruption of KCNQ4 eliminates $I_{\text{K,n}}$ in OHCs (Kharkovets et al., 2006). Second, co-expression of KCNQ4 subunits carrying loss-of-function mutations reduces $I_{\text{K,n}}$ by a dominant-negative effect, i.e. the function of the native channel complex is disrupted by mutant KCNQ4 subunits (Holt et al., 2007). Third, $I_{\text{K,n}}$ is sensitive to specific KCNQ channel inhibitors, XE991 and linopirdine, identifying the conductance as carried by KCNQ subunits (Marcotti and Kros, 1999). Fourth, KCNQ4 was shown to be expressed in the basolateral membrane of OHCs. In addition, the developmental expression of KCNQ4 around days eight to ten matches well with the appearance of $I_{\text{K,n}}$ (Kubisch et al., 1999; Kharkovets et al., 2000). Taken together, compelling evidence points to KCNQ4 as the molecular correlate of $I_{\text{K,n}}$. However, native $I_{\text{K,n}}$ shows biophysical characteristics that are not reproduced by recombinant KCNQ4 (Housley and Ashmore, 1992; Kubisch et al., 1999). Most obviously, $I_{\text{K,n}}$ activates at hyperpolarised potentials (half-maximal voltages of activation, V_h , -80 mV) compared to recombinant KCNQ4 (V_h between around -20 mV) (Mammano and Ashmore, 1996; Kubisch et al., 1999; Marcotti and Kros, 1999). The gating kinetics of $I_{\text{K,n}}$ are substantially faster than of recombinant KCNQ4 (Housley and Ashmore, 1992; Mammano and Ashmore, 1996). In addition, the pharmacological properties of $I_{\text{K,n}}$ differ from heterologously expressed KCNQ4. $I_{\text{K,n}}$ displays higher sensitivity to inhibition by KCNQ antagonists linopirdine and XE991 (Sogaard et al., 2001; for IHCs see Oliver et al., 2003; Xu et al., 2007). Moreover, $I_{\text{K,n}}$ is largely insensitive to the K^+ channel inhibitor tetraethylammonium (TEA) which potently blocks recombinant KCNQ4 (Housley and Ashmore, 1992; Marcotti and Kros, 1999; Hadley et al., 2000).

The extraordinary biophysical properties of $I_{K,n}$ cannot be explained by KCNQ4 channel subunits alone. Since heterologous expression systems normally reproduce biophysical properties of ion channels quite well, these findings imply an OHC-specific mechanism responsible for the negative voltages of activation of $I_{K,n}$. Attractive hypothesis arise from the presence of hitherto unidentified accessory channel subunits, posttranslational modification or a yet unknown mechanism. In any case, an OHC-specific mechanism seems to be the most likely explanation, but its molecular mechanism still needs to be elucidated. One possibility may be the presence of additional KCNQ subunits (e.g. KCNQ3) in the native channel complex. Co-expression of KCNQ4 together with KCNQ3 produced currents with amplitude and gating kinetics similar to $I_{K,n}$, but failed to reproduce the negative voltage range of activation (Kubisch et al., 1999; Bal et al., 2008). Also the low TEA sensitivity of $I_{K,n}$ might be explained by the co-expression of KCNQ4 with KCNQ subunits with low TEA sensitivity (e.g. KCNQ3; Hadley et al., 2000). However, it remains controversial whether KCNQ3 is expressed functionally in OHCs (Kubisch et al., 1999; Kharkovets et al., 2000). Another possibility emerges from the presence of accessory KCNE β -subunits that have been shown to alter the biophysical and pharmacological properties of the KCNQ α -subunit (McCrossan and Abbott, 2004). All KCNE isoforms were identified in the cochlea and all isoforms seem to co-assemble with recombinant KCNQ4 (Strutz-Seeböhm et al., 2006). However, none of the KCNE isoforms produced biophysical characteristics of KCNQ4 explaining the properties of $I_{K,n}$ (Strutz-Seeböhm et al., 2006).

Taken together, an OHC-specific mechanism produces the biophysical properties of $I_{K,n}$, but the molecular nature of this mechanism remains elusive. Since the biophysical and pharmacological properties of KCNQ channels depend on the subunit composition of the channel tetramer, the pharmacological characterisation of $I_{K,n}$ may help to identify channel subunits apart from KCNQ4 in the native channel complex. Thus, one aspect of this thesis was the analysis of fundamental biophysical and pharmacological "KCNQ-like" characteristics of $I_{K,n}$ and the comparison of these properties to recombinant KCNQ channels.

1.2.4 $I_{K,n}$ /KCNQ4 is Essential for the Survival of Outer Hair Cells

It is well established that $I_{K,n}$ /KCNQ4 is essential for the survival of OHCs (Kharkovets et al., 2000; Winter et al., 2006). Pharmacological inhibition, genetic ablation and loss of KCNQ4 channel function in human hereditary deafness DFNA2 lead to progressive OHC degeneration that starts at the cochlear base and proceeds to the apex (reviewed in Jentsch, 2000; Nouvian et al., 2003; Kharkovets et al., 2006; Nie, 2008). Basal OHCs with highest KCNQ4 expression and biggest $I_{K,n}$ current amplitudes are most susceptible to degeneration whereas apical OHCs with smallest $I_{K,n}$ currents remain unaffected (Housley and Ashmore, 1992; Kubisch et al., 1999; Beisel et al., 2000; Nouvian et al., 2003; Kharkovets et al., 2006). The base-to-apex loss of OHCs causes progressive hearing impairment that starts at high and proceeds to low frequencies (Kharkovets et al., 2006; Smith and Hildebrand, 2008). In affected humans,

hearing loss starts in the second or third decade of life and culminates in profound deafness at later ages (Nie, 2008; Smith and Hildebrand, 2008). The disease phenotype was recapitulated by the KCNQ4 knock-out mouse demonstrating that profound hearing impairment was caused by loss of OHCs and absent cochlear amplification (Kharkovets et al., 2006; Smith and Hildebrand, 2008). Although KCNQ4 was reported to be expressed also in IHCs (Marcotti et al., 2003; Oliver et al., 2003), vestibular type I hair cells (Rusch and Eatock, 1996; Holt et al., 2007) and neurons of the auditory brainstem (Kubisch et al., 1999; Kharkovets et al., 2000) the degree of hearing impairment does not implicate the involvement of IHCs or neuronal deficits (Kharkovets et al., 2006). However, profound deafness in elderly DFNA2 patients does not totally rule out additional loss of IHCs at later disease stages (Oliver et al., 2003). Vestibular defects have not been reported consistently from affected humans or from the KCNQ4 knock-out mouse (Kharkovets et al., 2006; Smith and Hildebrand, 2008). Hearing loss was attributed to the loss of KCNQ4 channel function, but the molecular mechanism causing hair cell degeneration remains elusive. Since KCNQ4 is expressed in the basolateral membrane of OHCs, the channel was proposed to serve as the basolateral exit path of K^+ ions to the tunnel of Corti (see Figure 1B) (Housley and Ashmore, 1992; Jentsch, 2000; Jentsch et al., 2000). Thus, $I_{K,n}/KCNQ4$ may regulate K^+ levels in OHCs serving as a key element for the recycling of K^+ ions back to the endolymph via a system of gap junctions and the *stria vascularis* (Mistrik and Ashmore, 2009). From this follows that loss of KCNQ4 channel function disturbs the K^+ homeostasis of OHCs together with persistent K^+ influx through the MET channels. Most probably, sustained K^+ overload causes prolonged Ca^{+2} influx through voltage-dependent Ca^{2+} channels and Ca^{2+} -dependent OHC degeneration (Zenner et al., 1994; Jentsch, 2000; Jentsch et al., 2000).

KCNQ4 loss-of-function causes hair cell degeneration and deafness in DFNA2 patients (Kubisch et al., 1999; Kharkovets et al., 2006). Several DFNA2-causing KCNQ4 mutations have been identified that disturb channel function through disruption of ion permeation or by a reduction of channels expressed at the cell surface (summarised in Smith and Hildebrand, 2008). Accordingly, KCNQ4 mutations reduce $I_{K,n}$, which initiates OHC degeneration (Kharkovets et al., 2006; Holt et al., 2007). A variety of chemical KCNQ channel openers are available, and some of these substances are already in clinical use for the treatment of neurological disorders (Wulff et al., 2009). Importantly, some KCNQ channel agonists (e.g. retigabine, zinc pyrithione) were shown to rescue channel function of epileptogenic KCNQ2 mutants (Biervert et al., 1998; Schroeder et al., 1998; Xiong et al., 2007; Xiong et al., 2008). In analogy, chemical KCNQ openers may rescue $I_{K,n}/KCNQ4$ -mediated currents in DFNA2 patients offering a protective strategy against OHC degeneration. Despite the obvious benefits of such current augmentation, it has never been tested so far whether the substances rescue channel function of DFNA2 relevant KCNQ4 mutants or whether $I_{K,n}$ is sensitive to chemical current potentiation. Thus, this thesis aims to evaluate the potency of KCNQ channel openers in the treatment of KCNQ4-related hearing loss, DFNA2.

1.2.5 Other Outer Hair Cell Pathologies May Be Related to KCNQ4 Dysfunction

Ototoxic agents, noise exposure or aging cause the irreversible loss of OHCs and acquired hearing impairment. Basal OHCs are far more vulnerable to degeneration than apical whereas IHCs are not affected (Smith et al., 2008). The different hair cell susceptibility cannot be explained so far. However, the loss of OHCs correlates directly with the dependence of OHCs on $I_{K,n}$ /KCNQ4 (Nouvian et al., 2003; Kharkovets et al., 2006). Although a potential role of KCNQ4 in age-related deafness has been proposed previously, the involvement of $I_{K,n}$ /KCNQ4 in acquired hearing loss has never been investigated (Van Eyken et al., 2006).

A clinically relevant form of acquired hearing loss is caused by aminoglycosides (AGs): AG-antibiotics (e.g. neomycin) exhibit high efficiency in the treatment of bacterial infections, but their use is limited, since most treated patients develop profound hearing impairment (Forge and Schacht, 2000; Rybak and Ramkumar, 2007). Hearing loss is induced by irreversible degeneration of OHCs that starts in the cochlear base and proceeds to the apex. Yet, this base-to-apex loss of OHCs cannot be explained (Forge and Schacht, 2000). Noteworthy, it resembles KCNQ4-related OHC degeneration (Kharkovets et al., 2006). AGs induce hair cell death following entry into the cell from the endolymph via a not fully resolved entry pathway, possibly via the MET channels (Alharazneh et al., 2011). The mechanisms leading to OHC degeneration may involve the disruption of mitochondrial function (Dehne et al., 2002), the production of reactive oxygen species (Rybak and Ramkumar, 2007), and the disturbance of phosphoinositide (PI) metabolism (Jiang et al., 2006a; Goodyear et al., 2008). AGs have been shown to chelate membrane-resident PIs via electrostatic interactions (Gabev et al., 1989). This links AG-induced OHC loss to $I_{K,n}$ /KCNQ4, since KCNQ channels essentially require membrane-resident phosphatidylinositol-(4,5)-bisphosphate ($PI(4,5)P_2$) for channel activation (Li et al., 2005; Suh et al., 2006). Accordingly, reduction of $PI(4,5)P_2$ inhibits the channel (Suh and Hille, 2002).

The dependence of OHC survival on $I_{K,n}$, the $PI(4,5)P_2$ dependence of KCNQ channels and the chelation of PIs by AGs strongly indicate a contribution of AG-induced $I_{K,n}$ /KCNQ4 inhibition to AG-mediated OHC loss. The role of $I_{K,n}$ in ototoxic hair cell insult has never been investigated so far, but $I_{K,n}$ inhibition by AGs may explain the high vulnerability of OHCs. Positive evaluation of this hypothesis makes KCNQ4 a promising target in the treatment of acquired hearing loss. Accordingly, this thesis evaluates the relevance of $I_{K,n}$ /KCNQ4 inhibition for AG ototoxicity and the use of KCNQ channel openers to rescue $I_{K,n}$ function from AG-induced inhibition.

AGs bind to PIs, which reduces their availability to ion channels. However, the degree of current inhibition depends on the PI affinity and dependence of the respective channel. Although the dependence on membrane-resident $PI(4,5)P_2$ is the characteristic feature of the KCNQ channel family, the phospholipid requirement for channel activation of $I_{K,n}$ has never been investigated so far. The PI dependence of cellular processes has been investigated previously using voltage-sensing phosphatases (VSPs) that, in contrast to unspecific PI

chelation by AGs, specifically deplete certain PI species (Murata et al., 2005). VSPs are modular enzymes that consist of a voltage-sensing domain (VSD) with high homology to voltage-dependent ion channels coupled to a phosphatase domain (PD) (Murata et al., 2005). Typically VSPs respond to membrane depolarisations with 5-phosphatase activity towards PI(4,5)P₂ and PI(3,4,5)P₃ (Halaszovich et al., 2009). Strikingly, the homology of the PD to the 3-phosphatase PTEN (phosphatase and tensin homolog deleted from chromosome 10) may enable the design of engineered VSPs with altered substrate specificity (Iwasaki et al., 2008; Halaszovich et al., 2009). Once transfected into cells these enzymes can be used to analyse the PI dependence and affinity of ion channels in straightforward electrophysiological experiments. Even though VSPs are available, the difficult handling of OHCs in culture and insufficient transfection efficiencies prevented these experiments so far. Thus, technically refined tools and experimental settings are needed to analyse the PI dependence of I_{K,n}. Detailed knowledge of the PI dependence and specificity of I_{K,n} allows for a more precise evaluation of the impact of AGs on the native channel complex in OHCs. Thus, one aspect of this thesis is the design and the characterisation of a novel VSP that contains the VSD of prototypic Ci-VSP together with the 3-phosphatase PTEN. Native and designed VSP will be used in combination to study the PI dependence of I_{K,n} in future studies.

2 Aims and Contributions

2.1 Objectives

$I_{K,n}$ dominates the electrical properties of cochlear OHCs, enables prestin-mediated cochlear amplification and is essential for the survival of OHCs. Nothing is known about the OHC-specific molecular mechanism that determines the characteristic properties of $I_{K,n}$. The involvement of $I_{K,n}$ /KCNQ4 in acquired hearing loss is likely, but has not been investigated so far. The work presented in this thesis aims to analyse the molecular properties of the conductance, to evaluate the pathophysiological relevance and mechanisms of $I_{K,n}$ in AG ototoxicity and to estimate potential benefits of chemical channel openers in the treatment of KCNQ4-related hearing impairment.

I. The role of $I_{K,n}$ /KCNQ4 in AG-induced hair cell loss

The PI-dependence of ion channels has been investigated repeatedly by intracellular application of AGs that functionally deplete PIs (Gabev et al., 1989; e.g. Schulze et al., 2003). In the present work, AGs were used to estimate the PI affinity of $I_{K,n}$ allowing for the comparisons with heterologously expressed KCNQ isoforms. Given the clinical relevance of AG-mediated hair cell loss (see 1.2.5), in these experiments the physiological role of AG-induced $I_{K,n}$ inhibition was evaluated.

II. The sensitivity of $I_{K,n}$ to chemical KCNQ channel openers and their potential for the treatment of KCNQ4-related hearing impairment

Loss of KCNQ4 channel function causes progressive OHC degeneration and hearing loss (Nouvian et al., 2003; Kharkovets et al., 2006; Holt et al., 2007). Dysfunction of other KCNQ isoforms (e.g. KCNQ2) causes epileptic seizures that are treated successfully with chemical KCNQ channel openers (Biervert et al., 1998; Schroeder et al., 1998; Wulff et al., 2009). In analogy, $I_{K,n}$ /KCNQ4 current potentiation by the openers may be used as protective strategy for DFNA2 patients and against AG-induced hair cell loss (see (I)). The benefits of chemical augmentation depend on the sensitivity of $I_{K,n}$ to channel openers. First, $I_{K,n}$ was characterised pharmacologically and the sensitivity of $I_{K,n}$ towards chemical KCNQ openers was determined. Second, the reconstitution of $I_{K,n}$ from AG-induced inhibition was assessed. Third, rescue of DFNA2-causing KCNQ4 mutations by chemical KCNQ openers was investigated (Nie, 2008; Smith and Hildebrand, 2008).

III. Analysis of the KCNQ subunit composition of the native channel complex in OHCs

The contribution of KCNQ channel subunits apart from KCNQ4 to native $I_{K,n}$ is still controversial. The pharmacological properties and biophysical characteristics of KCNQ channels depend on the subunit composition of the channel tetramer (Hadley et al., 2000; Hernandez et al., 2008; Xiong et al., 2008; Hernandez et al., 2009; Zhang et al., 2011). The sensitivity towards chemical current augmentation and the PI-dependence of activation of $I_{K,n}$ were analysed and compared to heterologously expressed KCNQ channel subunits to draw

conclusions about the subunit composition of the native channel complex. Furthermore, recombinant KCNQ4 was established as a sensor for physiologically relevant of PI(4,5)P₂ level changes.

IV. Technically-refined tools to investigate PI-dependent processes

AGs chelate PIs without any preference for a certain PI species. However, the impact of AGs on channel function depends on the PI specificity and affinity of the channel. Accordingly, knowledge of the PI affinity allows more detailed estimation of AG-induced channel inhibition. The PI affinity of ion channels can be determined using stepwise activation of a VSP by stepwise depolarisation. Since prototypic VSPs are PI(4,5)P₂- and PI(3,4,5)P₃-specific 5-phosphatases, the enzymes can be used to determine the affinity of an ion channel towards these PI species. Voltage-controlled PI(3,4,5)P₃ 3-phosphatases are not yet available, but the cytoplasmic 3-phosphatase PTEN shares high sequence homology to the PD of prototypic VSPs (Okamura and Dixon, 2011). This homology presumably enables the design of a voltage-dependent 3-phosphatase consisting of the VSD of Ci-VSP coupled to PTEN. In the work presented, the enzymatic activity and substrate specificity of this chimera were analysed and the potential of designed VSPs in the analysis of the PI-dependence of ion channels was evaluated. Further studies will make use of this work for detailed analysis of the PI dependence of I_{K,n} in OHCs.

2.2 My Contributions to the Articles Presented

In this section, I state my contributions to the publications presented in this thesis.

- (1) **Michael G. Leitner**, Christian R. Halaszovich and Dominik Oliver. Aminoglycosides inhibit KCNQ4 channels in cochlear outer hair cells via depletion of phosphatidylinositol(4,5)bisphosphate. *Molecular Pharmacology*. 2011 Jan;79(1):51-60 **(Leitner et al., 2011)**

I designed the research together with Prof. Dr. Dominik Oliver, performed all electrophysiological and imaging experiments including the data analysis and wrote the paper together with Prof. Dr. Dominik Oliver.

- (2) **Michael G. Leitner**, Anja Feuer, Olga Ebers, Daniela N. Schreiber, Christian R. Halaszovich and Dominik Oliver. Restoration of ion channel function in deafness causing KCNQ4 mutations by chemical openers. *British Journal of Pharmacology* (2012) **165 2244-2259 (Leitner et al., 2012)**

I conceived the project, performed the electrophysiological experiments with data analysis and wrote the paper together with Prof. Dr. Dominik Oliver.

- (3) Moritz Lindner, **Michael G. Leitner**, Christian R. Halaszovich, Gerald R. V. Hammond and Dominik Oliver. Probing the regulation of TASK potassium channels by PI(4,5)P₂. *Journal of Physiology*. 2011 Jul 1; 589 (Pt 13):3149-62 (**Lindner et al., 2011**)

This study is part of the doctoral thesis of Moritz Lindner in the group of Prof. Dr. Dominik Oliver. I planned, performed and analysed experiments presented in Figure 1 (Receptor-mediated inhibition of TASK channels and concomitant depletion of PI(4,5)P₂) and Figure 2B (TASK-currents are insensitive to depletion of PI(4,5)P₂ by Ci-VSP).

- (4) Jérôme Lacroix, Christian R. Halaszovich, Daniela N. Schreiber, **Michael G. Leitner**, Francisco Bezanilla, Dominik Oliver and Carlos A. Villalba-Galea. Controlling the activity of PTEN by membrane potential. *Journal of Biological Chemistry*. 2011 May 20; 286(20): 17945-53 (**Lacroix et al., 2011**)

This project was realised in collaboration with Prof. Dr. Francisco Bezanilla (Chicago, Illinois, USA) and Carlos A. Villalba-Galea (Richmond, Virginia, USA). In summary, my contributions to this study are experiments and data analysis shown in Figure 2 (Ci-VSPTEN displays voltage-activated lipid phosphatase activity; all panels), Figure 5 (Binding of the PBM is essential for phosphatase activation by the VSD) and Figure 6A (Experimental control of Ci-VSPTEN activity in intact cells without use of electrophysiological instrumentation).

Hiermit bestätige ich die Richtigkeit der unter 2.2 gemachten Angaben bezüglich des Eigenanteiles von Michael Leitner an den aufgeführten Publikationen.

Marburg, März 2012



Michael Leitner
(Autor)

Prof. Dr. Dominik Oliver
(Betreuer)

3 Results

3.1 The Outer Hair Cell K^+ Current $I_{K,n}$ Requires $PI(4,5)P_2$ for Activation

The PI dependence of ion channels has been investigated repeatedly by intracellular application of AGs. The positively charged substances bind to the polyanionic PIs, thereby functionally depleting PIs and reducing their availability to the ion channel (Gabev et al., 1989; Oliver et al., 2004). In these experiments AGs were applied via a whole cell patch pipette and $I_{K,n}$ or recombinant KCNQ4 were recorded (**Leitner et al., 2011**). Introduction of AGs into OHCs inhibited $I_{K,n}$. The time course of inhibition was rapid suggesting direct action of the chelators on the channels rather than inhibition via intracellular messenger systems (**Leitner et al., 2011; Figure 1**). The degree of current inhibition correlated with the amount of positive charges in the descending order of neomycin > gentamicin > kanamycin. Intracellular neomycin dose-dependently inhibited $I_{K,n}$, whereas ampicillin, a structurally not related antibiotic, was ineffective. These findings indicated that $I_{K,n}$ inhibition depended on the positive charges of the substances. Analogous experiments with KCNQ4 heterologously expressed in Chinese hamster ovary (CHO) cells revealed that the same substances also robustly inhibited recombinant KCNQ4 (**Leitner et al., 2011; Figure 2**). The rank order of KCNQ4 current inhibition was similar to native $I_{K,n}$, albeit current inhibition by the chelators was more pronounced compared to $I_{K,n}$. These findings indicated higher sensitivity to AG-mediated inhibition of heterologously expressed KCNQ4. Given the well known binding of AGs to phospholipids and the dependence of KCNQ channel activation on $PI(4,5)P_2$, these findings strongly suggested inhibition of $I_{K,n}$ /KCNQ4 via the depletion of PIs (Gabev et al., 1989; Suh and Hille, 2002). I monitored the availability of free PIs upon intracellular dialysis of neomycin and kanamycin using the $PI(4,5)P_2$ sensor tubby-Cterm-GFP and total internal reflection fluorescence (TIRF) microscopy (Halaszovich et al., 2009; **Leitner et al., 2011; Figure 3**). In brief, the membrane-association of tubby-Cterm is a direct measure for membrane-resident $PI(4,5)P_2$. Since in TIRF microscopy only membrane-bound fluorophores are excited, the fluorescence intensity of GFP-labelled tubby-Cterm directly reports on the amount of $PI(4,5)P_2$ at the membrane (Santagata et al., 2001; Halaszovich et al., 2009). Introduction of neomycin or kanamycin via the patch pipette into CHO cells expressing tubby-Cterm-GFP caused rapid decline of membrane-associated fluorescence indicating the functional depletion of $PI(4,5)P_2$ (**Leitner et al., 2011; Figure 3**). The degree of $PI(4,5)P_2$ chelation was stronger for neomycin than for kanamycin, i.e. neomycin with more positive charges bound $PI(4,5)P_2$ more efficiently than kanamycin. Of special note, these findings are in agreement with stronger current inhibition of $I_{K,n}$ and recombinant KCNQ4 by neomycin than by kanamycin. In addition, the time course of $PI(4,5)P_2$ depletion matched the electrophysiological experiments (**compare to Leitner et al., 2011 Figure 1 and 2**). To see whether KCNQ4 current reduction by AGs depended on the availability of free $PI(4,5)P_2$ I increased basal $PI(4,5)P_2$ levels in CHO cells by over-expression of

a PI(4)-5-kinase (e.g. Li et al., 2005). In these cells KCNQ4 current inhibition was significantly reduced compared to control cells (**Leitner et al., 2011, Figure 3**).

Taken together, these findings strongly suggested inhibition of $I_{K,n}$ and recombinant KCNQ4 by functional sequestration of PI(4,5)P₂ through AGs. Additionally, I demonstrated the PI-dependence of $I_{K,n}$, which indicated a role of $I_{K,n}$ current inhibition in AG ototoxicity. Furthermore, I was able to show that KCNQ4 currents can be used along with fluorescent PI sensors to monitor PI(4,5)P₂ changes in living cells (**Lindner et al., 2011**).

3.2 Inhibition of $I_{K,n}$ by Aminoglycosides is Pathophysiologically Relevant

Given the inhibition of $I_{K,n}$ by AGs and the degeneration of OHCs caused by KCNQ4 dysfunction, I investigated the relevance of $I_{K,n}$ in AG ototoxicity (Kharkovets et al., 2006; Rybak and Ramkumar, 2007). In the experiments presented in 3.1 AGs were introduced into the cell. However, ototoxic degeneration of OHCs occurs subsequent to entry of AGs into hair cells from the endolymph (Forge and Schacht, 2000; Marcotti et al., 2005; Dai et al., 2006; Wang and Steyger, 2009). Thus, I examined whether AG entry into OHCs was sufficient to cause relevant $I_{K,n}$ current inhibition (**Leitner et al., 2011; Figure 4**). I applied AGs from the extracellular side and recorded $I_{K,n}$ currents in OHCs. When applied from the extracellular side, AGs inhibited $I_{K,n}$ with the same rank order of current inhibition as upon intracellular application (neomycin > kanamycin) (**compare to Leitner et al., 2011; Figure 1**). Noteworthy, the potency of the substances matched the clinical ototoxic potential with neomycin having the most detrimental impact on OHCs (Forge and Schacht, 2000). Extracellularly applied AGs robustly depolarised OHCs highlighting the physiological relevance of AG-induced $I_{K,n}$ inhibition (**Leitner et al., 2011; Figure 6**). Analogous experiments in CHO cells showed that AGs did not inhibit recombinant KCNQ4 when applied from the extracellular side (**Leitner et al., 2011; Figure 6**). These findings strongly suggested OHC specific inhibition of $I_{K,n}$. Since AGs were shown to enter hair cells specifically, we hypothesised that AGs rapidly entered OHCs and inhibited $I_{K,n}$ via intracellular depletion of PI(4,5)P₂. To see whether the AG entry was reasonably fast to explain $I_{K,n}$ inhibition, I investigated the entry of AGs into hair cells with fluorescently labelled neomycin and confocal microscopy. Indeed, confocal imaging with neomycin conjugated to Texas Red revealed fast accumulation of AGs in hair cells as detected by rapid increase of cellular fluorescence (**Leitner et al., 2011; Figure 5**). AGs specifically entered hair cells and the time course was rapid enough to explain $I_{K,n}$ inhibition (**Leitner et al., 2011; Figure 5**). In contrast, CHO cells did not take up AGs in agreement with absent current inhibition of recombinant KCNQ4 by AGs applied from the extracellular side (**Leitner et al., 2011; Supplemental Figure 2**).

Taken together, I demonstrated rapid entry of AGs into OHCs from the extracellular (endolymphatic) side and AG-induced inhibition of $I_{K,n}$ via functional depletion of PI(4,5)P₂. These findings strongly suggest a role of $I_{K,n}$ inhibition in AG ototoxicity.

3.3 $I_{K,n}$ is Sensitive to Chemical KCNQ Openers

Loss of KCNQ4 channel function causes OHC degeneration and deafness (Kharkovets et al., 2006). Since OHC survival was directly attributed to $I_{K,n}$ /KCNQ4 function, it can be hypothesised that augmentation of $I_{K,n}$ by previously described channel openers may alleviate or even avert this pathology. However, the benefit depends on the sensitivity of native $I_{K,n}$ to the channel openers. Thus, I characterised the sensitivity of recombinant KCNQ4 and $I_{K,n}$ towards KCNQ agonists (Leitner et al., 2011; Leitner et al., 2012). The substances robustly potentiated recombinant KCNQ4 currents and shifted the voltage-dependence of activation to hyperpolarised voltages (Leitner et al., 2012; Figure 1). The rank order of current potentiation was flupirtine < retigabine < BMS-204352 < zinc pyrithione << zinc pyrithione/retigabine (ZnP/Ret) in line with reports from other KCNQ isoforms (Tatulian et al., 2001; Xiong et al., 2007; Xiong et al., 2008). The combination of ZnP/Ret was most effective and shifted the voltage dependence of activation of heterologously expressed KCNQ4 by -40 mV (Leitner et al., 2012; Supplemental Figure 1). Similarly, KCNQ openers robustly augmented $I_{K,n}$ in OHCs and shifted the voltage-dependence of activation to hyperpolarised voltages (Leitner et al., 2012; Figure 7). The rank order of current enhancement was similar, but current potentiation was less pronounced for $I_{K,n}$ than for recombinant KCNQ4 (Leitner et al., 2012, Figures 1 and 7). Of special interest, retigabine that is clinically used as antiepileptic drug also increased $I_{K,n}$ (Leitner et al., 2012, Figure 7).

In conclusion, $I_{K,n}$ was sensitive to current potentiation by chemical KCNQ openers, albeit the degree of current potentiation was lower than for recombinant KCNQ4. The sensitivity of $I_{K,n}$ to KCNQ channel openers, especially to retigabine, may be used to rescue $I_{K,n}$ in case of KCNQ4 dysfunction.

3.4 KCNQ Channel Openers Rescue $I_{K,n}$ from AG-induced Inhibition and Reconstitute Channel Function of Deafness-Causing KCNQ4 Mutants

Next I tested whether KCNQ channel agonists rescued $I_{K,n}$ from pathophysiologically relevant loss of function. I started with AG-induced inhibition of $I_{K,n}$ (Leitner et al., 2011). In brief, neomycin inhibited $I_{K,n}$ and substantially depolarised OHCs (Leitner et al., 2011; Figures 6 and 7). ZnP/Ret rescued $I_{K,n}$ and fully reversed AG-induced depolarisation to control levels before AG application (Leitner et al., 2011; Figure 7). $I_{K,n}$ current amplitudes and the membrane potential of the cells treated with ZnP/Ret in presence of AGs were indistinguishable from normal control cells. These findings showed that KCNQ agonists could be used to stabilise the KCNQ conductance in OHCs despite the presence of AGs. KCNQ channel openers thus might offer a protective strategy against AG-mediated OHC degeneration through augmentation of $I_{K,n}$ (Leitner et al., 2011; Figure 7).

Several KCNQ4 loss-of-function mutations have been shown to cause hereditary hearing loss in humans (Nie, 2008; Smith and Hildebrand, 2008; Kim et al., 2011). I tested whether KCNQ openers rescued channel function of DNFA2 relevant KCNQ4 mutations (Leitner et al., 2012). I over-expressed mutant KCNQ4 subunits in CHO cells and performed whole cell patch clamp

experiments. Recombinant KCNQ4 channels carrying a mutation in the pore region could not be rescued by KCNQ agonists, which suggested total loss of function in these mutants (**Leitner et al., 2012; Figure 3**). A mutation localised close to the C-terminus of KCNQ4 produced small currents under control conditions. Application of ZnP/Ret uncovered voltage-dependent KCNQ4 currents mediated by the mutant subunits. The ZnP/Ret-induced currents through the mutant channels were slightly smaller than KCNQ wild-type (wt) control currents, i.e. the mutant was rescued partially to wt levels (**Leitner et al., 2012; Figure 4**). Most affected individuals are heterozygous carriers of KCNQ4 mutations, which reduces $I_{K,n}$ by a dominant-negative effect, i.e. a single mutant subunit disrupts the function of the tetrameric channel (Kubisch et al., 1999; Holt et al., 2007; Kim et al., 2011). Accordingly, heterozygous patients produce the same amount of wt and mutant KCNQ4 subunits, which leaves behind only 6.25% functional homomeric wt channels at the cell surface. This reduction of functional channels causes the decrease of overall currents. Co-expression of recombinant wt KCNQ4 with mutants in CHO cells reproduced the dominant-negative situation (**Leitner et al., 2012; Figure 5**). Whole cell currents were strongly reduced as predicted from co-assembly of wt and mutant subunits and disruption of channel function by the mutants. Strikingly, application of ZnP/Ret rescued the minute residual currents to wt levels, i.e. currents were indistinguishable from KCNQ4 control currents (**Leitner et al., 2012; Figure 5**). This demonstrates full rescue of KCNQ4 currents from dominant-negative inhibition by KCNQ channel openers. In the dominant-negative situation, the channel population at the cell membrane comprises homomeric wt channels, homomeric mutant channels and heteromeric channels of both, wt and mutant subunits. At this point, it was not clear whether also otherwise dysfunctional heteromeric channels and with homomeric mutant channels contributed to ZnP/Ret-mediated current rescue. We constructed concatamers of wt and mutant channel subunits to obtain homogenous channel populations in the cell membrane and tested whether KCNQ openers rescued the function of the resulting channels. Using the protein concatamers, I showed that channel function of tetramers containing mutant subunits was not restored by the channel openers. Current rescue resulted solely from potentiation of currents through remaining homomeric wt channels. However, this current potentiation was sufficient to account for the complete rescue of KCNQ4 from dominant-negative inhibition (**Leitner et al., 2012; Figure 6**). Taken together, these findings showed that KCNQ channel openers rescued KCNQ4 from dominant-negative inhibition. Since native $I_{K,n}$ (see 3.3) was robustly augmented by KCNQ channel agonists as well, these substances may be used to stabilise the conductance in OHCs. This may postpone profound hearing loss or even protect OHCs from degeneration in DFNA2 patients.

3.5 The Biophysical Properties and the Molecular Nature of $I_{K,n}$

The subunit composition determines the biophysical and pharmacological properties of tetrameric KCNQ channels (Hadley et al., 2000; Hernandez et al., 2009). Accordingly, it may be possible to draw conclusions on the subunit composition from the biophysical properties. In brief, I found that

$I_{K,n}$ was inhibited by depletion of PIs via introduction of AGs. This is expected, since PI(4,5)P₂-dependent KCNQ4 subunits contribute to the native channel complex (**Leitner et al., 2011**). However, the IC₅₀ for neomycin of $I_{K,n}$ was significantly higher than for recombinant KCNQ4 ($I_{K,n}$ 0.59 mM; KCNQ4 0.13 mM), indicating lower sensitivity to neomycin-induced current inhibition for $I_{K,n}$ than of recombinant KCNQ4. Since current inhibition was caused by PI depletion (see 3.1), the degree of current decrease allowed to estimate the PI affinity of the respective channel. Accordingly, these results indicated higher PI affinity of $I_{K,n}$ than of recombinant KCNQ4 (**Leitner et al., 2011; Figures 1 and 2**). Equal neomycin concentrations (500 μM) inside the patch pipette inhibited recombinant KCNQ4 more pronounced (approximately 80% inhibition) than $I_{K,n}$, (30% inhibition) albeit the time course of current inhibition was similar. Noteworthy, currents through recombinant KCNQ3 with high PI(4,5)P₂ affinity were reduced by only 10% upon dialysis of the cells with 500 μM neomycin (Hernandez et al., 2009; **Leitner et al., 2011; Figures 1, 2 and 3**). These differences strongly suggested intermediate PI affinity of $I_{K,n}$ between recombinant KCNQ4 and KCNQ3. Similarly, co-expression of KCNQ2 with low PI(4,5)P₂ affinity and KCNQ3 resulted in heteromeric channels with intermediate PI(4,5)P₂ affinity in previous reports (Hernandez et al., 2009). In analogy, my findings suggested the contribution of additional subunits with high PI affinity to $I_{K,n}$ in OHCs. Additionally, these experiments established recombinant KCNQ4 as a perfect read-out for physiologically relevant PI(4,5)P₂ changes. This makes KCNQ4 a *bona fide* PI(4,5)P₂ sensor that can be used to study the PI dependence of cellular processes (**Lindner et al., 2011**).

Also the pharmacological profile of $I_{K,n}$ suggested the presence of additional subunits in OHCs. Current potentiation by KCNQ openers was less pronounced for $I_{K,n}$ than for recombinant KCNQ4 (**Leitner et al., 2012; Figure 1 and 7**). Similarly, also the agonist-mediated shift of the voltages of activation to hyperpolarised potentials was smaller for the native channel complex. Since KCNQ3 shows lowest sensitivities towards chemical current potentiation of all KCNQ isoforms, co-expression of KCNQ3 may be responsible for the special pharmacological profile of $I_{K,n}$. Thus, I co-expressed KCNQ4 together with KCNQ3 and analysed the sensitivity towards chemical current potentiation of heteromeric channels (**Leitner et al., 2012; Supplemental Figure 5**). As previously reported, current amplitudes through heteromeric channels were increased and activation kinetics were accelerated compared to homomeric KCNQ4 wt channels (Kubisch et al., 1999). However, the voltage-dependence of the heteromers was not altered (**Leitner et al., 2012; Supplemental Figure 5**). Also the sensitivities towards chemical KCNQ channel openers was not different from KCNQ4 wt channels, indicating that co-assembly of KCNQ4 together with KCNQ3 does not explain the unusual pharmacological properties of $I_{K,n}$ (**Leitner et al., 2012**).

Taken together, although the PI sensitivity of $I_{K,n}$ suggested the co-expression of KCNQ3 subunits, the pharmacological properties of $I_{K,n}$ argued against the presence of KCNQ3 subunits in OHCs. Thus, the molecular nature of $I_{K,n}$ remains unknown.

3.6 Development of Novel Tools to Experimentally Alter PI Levels in Living Cells

Ciona intestinalis VSP (Ci-VSP) is a voltage-sensing phosphatase that exhibits PI(3,4,5)P₃ and PI(4,5)P₂ 5-phosphatase activity upon membrane depolarisation (Murata et al., 2005; Iwasaki et al., 2008; Halaszovich et al., 2009). The PD of Ci-VSP shows high homology to the tumour suppressor PTEN, a 3-phosphatase (Maehama and Dixon, 1998; Okamura and Dixon, 2011). We constructed a chimera of PTEN coupled to the voltage sensor of Ci-VSP, termed Ci-VSPTEN. The substrate specificity of the chimera was characterised in whole cell voltage clamp experiments together with TIRF microscopy utilising fluorescent PI sensors (**Lacroix et al., 2011**). I found PI(3,4,5)P₃ and PI(3,4)P₂ 3-phosphatase activity of Ci-VSPTEN fully reproducing the substrate specificity of wt PTEN (**Lacroix et al., 2011; Figure 1**). Voltage-dependent enzymatic activity was conferred by a phosphoinositide binding motif in the linker between the VSD and PD, as shown by mutations inside the motif that functionally uncoupled the VSD from phosphatase activity (**Lacroix et al., 2011; Figure 5**).

Taken together, we engineered a novel voltage-dependent 3-phosphatase by conferring voltage-sensitivity to an otherwise cytoplasmic enzyme. These findings promise future design of voltage-dependent phosphatases with desired substrate specificity. VSPs can be used to elucidate the PI dependence of ion channels in their native environment. Thus, future studies will utilise designed and native VSPs to analyse the PI-dependence of I_{K,n}/KCNQ4 channel gating in OHCs.

4 Discussion

4.1 Biophysical and Pharmacological Differences of $I_{K,n}$ and Recombinant KCNQ4: Implications for the Molecular Identity of $I_{K,n}$

Strong evidence indicates that KCNQ4 channel subunits mediate $I_{K,n}$ in OHCs (Kharkovets et al., 2006). However, native and recombinant currents show different biophysical characteristics. Most obviously $I_{K,n}$ activates at more negative potentials than recombinant KCNQ4, the activation kinetics of $I_{K,n}$ are faster and $I_{K,n}$ displays less sensitivity to chemical current inhibition (Mammano and Ashmore, 1996; Kubisch et al., 1999; Marcotti and Kros, 1999). The molecular explanation for these unique properties remains elusive. Here, I extend the knowledge to the PI dependence and to the sensitivity towards current augmentation by chemical KCNQ openers (Leitner et al., 2011; Leitner et al., 2012).

Intracellular application of AGs inhibited $I_{K,n}$ and heterologous KCNQ4 currents by depletion of PI(4,5)P₂ (Leitner et al., 2011). The sensitivity of $I_{K,n}$ to AG-induced current inhibition was intermediate between recombinant KCNQ4 and KCNQ3. These findings suggested intermediate PI(4,5)P₂ dependence of $I_{K,n}$ between KCNQ4 with low affinity and KCNQ3 with high affinity (Li et al., 2005). Since co-assembly of KCNQ channel subunits with low and high PI(4,5)P₂ affinity (e.g. KCNQ2/3) produced tetrameric channels with intermediate affinity (Hernandez et al., 2008; Hernandez et al., 2009), the PI affinity of $I_{K,n}$ suggests the co-assembly of KCNQ4 with KCNQ3 or another yet unknown K⁺ channel subunit with high PI(4,5)P₂ affinity. Indeed, KCNQ3 has been identified on transcript level in OHCs and has been reported to co-assemble with KCNQ4, but evidence for functional KCNQ3 protein is still missing (Kubisch et al., 1999; Beisel et al., 2000; Kharkovets et al., 2000; Kharkovets et al., 2006). Although KCNQ3/KCNQ4 may explain the PI(4,5)P₂ dependence of $I_{K,n}$, such heteromers failed to reproduce the voltages of activation of $I_{K,n}$ (Kubisch et al., 1999; Leitner et al., 2012). Further work may include the specific knock-down of KCNQ3 channel subunits in OHCs to elucidate the presence of functional KCNQ3 in the native hair cell channel complex.

My findings also showed that the pharmacological profile of $I_{K,n}$ differs from recombinant KCNQ4 (Leitner et al., 2012). Thus, current potentiation and the activation shift to hyperpolarised voltages by ZnP/Ret were less pronounced for $I_{K,n}$ than for heterologously expressed KCNQ4 (Leitner et al., 2012). Most strikingly, BMS-204352 failed to augment $I_{K,n}$ despite robust increase of currents through recombinant KCNQ4. The reason for the lower sensitivity of $I_{K,n}$ may be one of the following: First, OHC-specific mechanisms produce an $I_{K,n}$ channel complex by posttranslational modification or special subunit composition that is less sensitive to current augmentation by KCNQ openers than homomeric KCNQ4. The OHC-specific mechanism and KCNQ channel openers may change the biophysical properties of KCNQ4 via a similar molecular mechanism, which occludes further current potentiation by the openers. It has been reported that the zinc pyrithione sensitivity of KCNQ1 in complex with the accessory β -subunit KCNE1 was strongly reduced, since the molecular determinant of current potentiation was already occupied by the β -

subunit (Gao et al., 2008). Similarly, in OHCs the sensitivity of $I_{K,n}$ may be reduced by additional yet not identified interaction partners (Kubisch et al., 1999; Kharkovets et al., 2006). Since KCNQ3 shows lowest sensitivity towards chemical current potentiation, co-assembly of KCNQ3 with KCNQ4 may also explain the low sensitivity of $I_{K,n}$. However, KCNQ3/4 heterotetramers failed to reproduce the sensitivity of $I_{K,n}$ again indicating that KCNQ3 may rather not be present in OHCs (Leitner et al., 2012). Second, one explanation for the different sensitivities may be derived from the molecular mechanism of current augmentation by the openers. KCNQ agonists have been shown to increase KCNQ-mediated currents via an increase of the channel open probability (Xiong et al., 2007). The low open probability of recombinant KCNQ4 under control conditions thus allows for the dramatic current potentiation by the openers (Tatulian et al., 2001; Xiong et al., 2008). Indeed, KCNQ4 in presence of ZnP/Ret closely resembles native $I_{K,n}$ (Leitner et al., 2012). This strongly suggests high resting open probability of $I_{K,n}$ that limits maximal possible current potentiation by the openers. However, the open probability of $I_{K,n}$ at saturating voltages is not known, but once elucidated it will allow the evaluation of the maximal current augmentation that can be achieved by KCNQ openers.

Taken together, my findings add to the biophysical differences of $I_{K,n}$ and KCNQ4. These findings showed that "KCNQ-like" features such as the PI dependence and chemical current augmentation of $I_{K,n}$ are markedly different from recombinant KCNQ4, but the OHC-specific mechanism remains elusive and requires further work. An interesting aspect is whether this mechanism is specific for KCNQ4, i.e. OHC-specific interaction partners specifically alter the voltage range of activation of KCNQ4 in OHCs. Further work will thus focus on the presence of specific interaction KCNQ4 partners in OHCs (see 4.4: Outlook).

Since $I_{K,n}$ exhibits larger current amplitudes and markedly different voltage sensitivity, it is likely that the pore structure of $I_{K,n}$ is altered compared to KCNQ4. Tetraethylammonium (TEA) potently inhibits K^+ channels via subunit specific binding to the pore domain of the tetrameric channel. Accordingly, TEA and chemically related substances were used to test the pore structure of K^+ channels repeatedly (e.g. Piechotta et al., 2011). Strikingly, decreased TEA sensitivity of $I_{K,n}$ was reported compared to recombinant KCNQ4 (Marcotti and Kros, 1999), strongly suggesting altered architecture of the channel's pore in OHCs. Since in the tetrameric channel all subunits contribute to the structure of the pore, lower TEA sensitivity of $I_{K,n}$ thus suggests the presence of additional K^+ channel subunits in the native channel complex. Accordingly, future studies will investigate the TEA sensitivity of $I_{K,n}$.

4.2 The Role of $I_{K,n}$ Inhibition in AG-induced Hair Cell Loss

I showed for the first time that AG antibiotics rapidly entered into hair cells from the extracellular, endolymphatic side and inhibited the predominant K^+ conductance in OHCs (Leitner et al., 2011). Given robust depolarisation caused by this inhibition and the established importance of $I_{K,n}$ for the survival of OHCs, it seems likely that AG-induced inhibition of $I_{K,n}$ contributes to AG-induced OHC degeneration (Nouvian et al., 2003; Kharkovets et al., 2006). This idea is well supported by the

fact that hair cells exhibit the same vulnerability towards AGs as to KCNQ4 dysfunction, highlighted by the phenotypical similarities of AG-induced OHC degeneration with KCNQ4-related hair cell loss (Kharkovets et al., 2006; Rybak and Ramkumar, 2007). Among different hair cell types in the inner ear $I_{K,n}$ /KCNQ4 provides the predominant K^+ conductance only in OHCs and this cell type is most susceptible to AG-induced degeneration (Housley and Ashmore, 1992; Forge and Schacht, 2000; Kharkovets et al., 2006). Loss of KCNQ4 channel function causes specific OHC degeneration, whereas IHCs and vestibular hair cells remain widely unaffected (Kharkovets et al., 2006). Moreover, the varying vulnerability of OHCs along the cochlear axis also matches well with the appearance of KCNQ4 with higher current densities and expression levels in basal, highly susceptible OHCs than in apical OHCs (Beisel et al., 2000; Beisel et al., 2005; Kharkovets et al., 2006). Since the involvement of reactive oxygen species or mitochondrial dysfunction in AG-induced hair cell loss is well established (Jiang et al., 2006b; Rybak and Ramkumar, 2007), we do not believe that the mechanism presented here is the major cause for hair cell loss. However, it is plausible that AG-induced $I_{K,n}$ inhibition contributes to hair cell degeneration. We hypothesise that the dependence of OHC survival from KCNQ4 and the inhibition of the conductance by AGs may explain the high susceptibility of OHCs towards ototoxic insult (Leitner et al., 2011). Additionally, our findings may explain differences in the ototoxic potential of various AGs. Neomycin is more ototoxic for hair cells in the organ of Corti than kanamycin, whereas gentamicin mainly affects vestibular hair cells (Forge and Schacht, 2000). Indeed, the detrimental potential correlated well with the PI chelating efficiency of each AG and the potency of $I_{K,n}$ current inhibition (Leitner et al., 2011). Thus, the chemical nature of the substance and the resulting degree of $I_{K,n}$ current inhibition may determine the ototoxic potential of AGs. However, the mechanisms leading to hair cell degeneration may be different for OHCs and vestibular hair cells, without the involvement of the KCNQ conductance in the vestibular system.

4.3 Potential Use of KCNQ Openers to Protect from KCNQ4-related Hearing Loss

Since KCNQ4 channel dysfunction causes OHC degeneration, rescue of $I_{K,n}$ by chemical openers may protect from OHC loss and thus from deafness (Kharkovets et al., 2006). We showed that $I_{K,n}$ was sensitive to chemical augmentation by KCNQ agonists (Leitner et al., 2012). Finally, the most important question remains: Can KCNQ channel openers protect OHCs from KCNQ4-related degeneration?

KCNQ4 knock-out mice suffer from progressive degeneration of OHCs and thus progressive hearing loss, suggesting a similar phenotype in DFNA2 patients with KCNQ4 loss-of-function mutations (Kharkovets et al., 2006). Interestingly, small residual $I_{K,n}$ currents in a dominant-negative mouse model with a heterozygous KCNQ4 mutation were sufficient to delay hair cell degeneration and hearing loss significantly (Kharkovets et al., 2006). Thus, it is likely that even moderate current potentiation by chemical channel openers alleviates KCNQ4-related OHC

degeneration. However, the benefits of $I_{K,n}$ potentiation may be different for patients treated with AGs or humans carrying a DFNA2 mutation.

Due to slow turn-over AGs accumulate in hair cells which initiates OHC degeneration even months after the treatment with the drugs (Forge and Schacht, 2000; Rybak and Ramkumar, 2007). Thus, the critical period for OHCs comprises the time during the treatment with the drugs and some months afterwards. Accordingly, stabilisation of $I_{K,n}$ may be needed during this time only. Since retigabine is already in clinical use and no side-effects have been reported, such treatment does not bear any risk for the patient. Thus, we propose concomitant treatment of retigabine with AGs over the critical period until hair cells are cleared from the AGs. This may serve as a protective strategy to alleviate OHC degeneration AGs by activation of $I_{K,n}$. Similarly, the up-regulation of neuronal K^+ channels is believed to alleviate neuronal damage under pathological conditions (Czuczwar et al., 2011). Of course, such treatment needs to be tested in adequate cell culture and animal models first, but we think that it may provide a yet unknown protective strategy against KCNQ-related OHC degeneration (see 4.4).

In DFNA2-affected humans the situation is somewhat different. To our knowledge, most DFNA2 patients are heterozygous carriers of KCNQ4 mutations (Smith and Hildebrand, 2008). In these patients $I_{K,n}$ currents are reduced by a dominant-negative effect, which drastically decreases the amount of functional channels at the membrane (Kubisch et al., 1999; Holt et al., 2007). For recombinant KCNQ4 we essentially rescued the remaining currents back to control levels, and we expect current potentiation of remaining channels also in OHCs (Leitner et al., 2012). We believe that even slight $I_{K,n}$ current increase by chemical openers may significantly postpone hearing loss in DFNA2 patients. However, such treatment may require life-long treatment with KCNQ openers (e.g. retigabine) and it is not yet known to what extent the substances prevent KCNQ4-related OHC degeneration.

4.4 Outlook

The work presented here offers new insight into the physiology and pathophysiology of the predominant K^+ conductance of OHCs, $I_{K,n}$. My findings raise a couple of interesting questions: The first concerns the actual $PI(4,5)P_2$ dependence of the native conductance. So far, we only estimated the PI dependence of $I_{K,n}$ by intracellular dialysis of AGs that globally deplete cellular PIs. Graded PI depletion using voltage-dependent phosphatases with specific PI phosphatase activity should allow for a substantially improved determination of the PI affinity of the channel (Halaszovich et al., 2009). Such experiments require the over-expression of voltage-dependent phosphatases (e.g. Ci-VSP, Ci-VSPTEN) in OHCs. Low transfection efficiency can be overcome with viral transduction that already has been used successfully on OHCs (Holt et al., 2007; Schaechinger et al., 2011). Accordingly, future work may include the design of viral constructs and the production of virus particles for the transduction of OHCs with genetically-encoded PI-manipulating enzymes and subsequent electrophysiological recordings from infected OHCs.

Second, as shown for other members of the KCNQ channel family, $I_{K,n}$ may be modulated by synaptic input (e.g. from the olivo-cochlear cholinergic system) (Brown and Adams, 1980; Wang et al., 1998; Shapiro et al., 2000; Suh and Hille, 2002). This may include $I_{K,n}$ current inhibition through G-protein coupled receptors and phospholipase C-mediated $PI(4,5)P_2$ depletion. Muscarinic receptors have been shown to be expressed in OHCs (Khan et al., 2002), but the efferent modulation of $I_{K,n}$ has never been investigated. This work will substantially improve the understanding of the physiological regulation of $I_{K,n}$ in OHCs

Third, it remains elusive whether KCNQ agonists rescue OHCs from KCNQ4-related degeneration also *in vivo*. We showed that KCNQ agonists rescued KCNQ4 from dominant-negative inhibition by mutant subunits at least in an expression system (Leitner et al., 2012). Although these results seemed promising, evidence for *in vivo* protection of OHCs is still missing. Future work will investigate whether chemical KCNQ openers alleviate hearing loss in a dominant-negative KCNQ4 mouse model and whether the substances rescue OHCs isolated from these and from KCNQ4 knock-out mice (Kharkovets et al., 2006). Additionally, it will be interesting to see whether KCNQ agonists reduce OHC degeneration in cultured organs of Corti treated with AG antibiotics.

Fourth, the molecular nature of $I_{K,n}$ still needs to be determined. Because other KCNQ isoforms differ from KCNQ4 in terms of sequence homology and possible interaction partners, it is likely that the OHC-specific environment does not affect these subunits. Thus, a promising strategy to identify OHC-specific interaction partners might be the transfection of KCNQ subunits into OHCs of KCNQ4 knock-out mice. This will produce currents either resembling $I_{K,n}$ or heterologously expressed KCNQ channels. Transfection of chimeric proteins of KCNQ4 with different parts of a KCNQ subunit that is not affected by the OHC environment may identify amino acid sequences necessary for the restoration of $I_{K,n}$. These protein stretches will be used to identify interaction partners of KCNQ4 in OHCs. In any case, further work is needed to unravel the OHC-specific mechanism that determines the biophysical properties of $I_{K,n}$.

5 References

- Alharazneh A, Luk L, Huth M, Monfared A, Steyger PS, Cheng AG, Ricci AJ (2011) Functional hair cell mechanotransducer channels are required for aminoglycoside ototoxicity. *PLoS one* 6:e22347.
- Ashmore J, Avan P, Brownell WE, Dallos P, Dierkes K, Fettiplace R, Grosh K, Hackney CM, Hudspeth AJ, Julicher F, Lindner B, Martin P, Meaud J, Petit C, Sacchi JR, Canlon B (2010) The remarkable cochlear amplifier. *Hear Res* 266:1-17.
- Ashmore JF (1987) A fast motile response in guinea-pig outer hair cells: the cellular basis of the cochlear amplifier. *The Journal of physiology* 388:323-347.
- Bal M, Zhang J, Zaika O, Hernandez CC, Shapiro MS (2008) Homomeric and Heteromeric Assembly of KCNQ (Kv7) K⁺ Channels Assayed by Total Internal Reflection Fluorescence/Fluorescence Resonance Energy Transfer and Patch Clamp Analysis. *The Journal of biological chemistry* 283:30668-30676.
- Beisel KW, Nelson NC, Delimont DC, Fritzschn B (2000) Longitudinal gradients of KCNQ4 expression in spiral ganglion and cochlear hair cells correlate with progressive hearing loss in DFNA2. *Brain Res Mol Brain Res* 82:137-149.
- Beisel KW, Rocha-Sanchez SM, Morris KA, Nie L, Feng F, Kachar B, Yamoah EN, Fritzschn B (2005) Differential expression of KCNQ4 in inner hair cells and sensory neurons is the basis of progressive high-frequency hearing loss. *J Neurosci* 25:9285-9293.
- Benser ME, Marquis RE, Hudspeth AJ (1996) Rapid, active hair bundle movements in hair cells from the bullfrog's sacculus. *J Neurosci* 16:5629-5643.
- Biervert C, Schroeder BC, Kubisch C, Berkovic SF, Propping P, Jentsch TJ, Steinlein OK (1998) A potassium channel mutation in neonatal human epilepsy. *Science* 279:403-406.
- Brown DA, Adams PR (1980) Muscarinic suppression of a novel voltage-sensitive K⁺ current in a vertebrate neurone. *Nature* 283:673-676.
- Brownell WE, Bader CR, Bertrand D, de Ribaupierre Y (1985) Evoked mechanical responses of isolated cochlear outer hair cells. *Science* 227:194-196.
- Chambard JM, Ashmore JF (2005) Regulation of the voltage-gated potassium channel KCNQ4 in the auditory pathway. *Pflugers Arch* 450:34-44.
- Chan DK, Hudspeth AJ (2005) Ca²⁺ current-driven nonlinear amplification by the mammalian cochlea in vitro. *Nat Neurosci* 8:149-155.
- Corey DP, Hudspeth AJ (1983) Kinetics of the receptor current in bullfrog saccular hair cells. *J Neurosci* 3:962-976.
- Czuczwar P, Wojtak A, Cioczek-Czuczwar A, Parada-Turska J, Maciejewski R, Czuczwar SJ (2011) Retigabine: the newer potential antiepileptic drug. *Pharmacol Rep* 62:211-219.
- Dai CF, Mangiardi D, Cotanche DA, Steyger PS (2006) Uptake of fluorescent gentamicin by vertebrate sensory cells in vivo. *Hear Res* 213:64-78.
- Dallos P (1985) Membrane potential and response changes in mammalian cochlear hair cells during intracellular recording. *J Neurosci* 5:1609-1615.
- Dallos P (1986) Neurobiology of cochlear inner and outer hair cells: intracellular recordings. *Hear Res* 22:185-198.
- Dallos P (1992) The active cochlea. *J Neurosci* 12:4575-4585.
- Dallos P, Harris D (1978) Properties of auditory nerve responses in absence of outer hair cells. *J Neurophysiol* 41:365-383.

R E F E R E N C E S

- Dallos P, Santos-Sacchi J, Flock A (1982) Intracellular recordings from cochlear outer hair cells. *Science* 218:582-584.
- Dallos P, Popper AN, Fay RR (1996) *The Cochlea*. New York: Springer.
- Dallos P, Wu X, Cheatham MA, Gao J, Zheng J, Anderson CT, Jia S, Wang X, Cheng WH, Sengupta S, He DZ, Zuo J (2008) Prestin-based outer hair cell motility is necessary for mammalian cochlear amplification. *Neuron* 58:333-339.
- Dehne N, Rauen U, de Groot H, Lautermann J (2002) Involvement of the mitochondrial permeability transition in gentamicin ototoxicity. *Hear Res* 169:47-55.
- Fettiplace R, Hackney CM (2006) The sensory and motor roles of auditory hair cells. *Nat Rev Neurosci* 7:19-29.
- Forge A, Schacht J (2000) Aminoglycoside antibiotics. *Audiol Neurootol* 5:3-22.
- Gabev E, Kasianowicz J, Abbott T, McLaughlin S (1989) Binding of neomycin to phosphatidylinositol 4,5-bisphosphate (PIP₂). *Biochim Biophys Acta* 979:105-112.
- Gao Z, Xiong Q, Sun H, Li M (2008) Desensitization of chemical activation by auxiliary subunits: convergence of molecular determinants critical for augmenting KCNQ1 potassium channels. *The Journal of biological chemistry* 283:22649-22658.
- Gillespie PG, Muller U (2009) Mechanotransduction by hair cells: models, molecules, and mechanisms. *Cell* 139:33-44.
- Goodyear RJ, Gale JE, Ranatunga KM, Kros CJ, Richardson GP (2008) Aminoglycoside-induced phosphatidylserine externalization in sensory hair cells is regionally restricted, rapid, and reversible. *J Neurosci* 28:9939-9952.
- Hadley JK, Noda M, Selyanko AA, Wood IC, Abogadie FC, Brown DA (2000) Differential tetraethylammonium sensitivity of KCNQ1-4 potassium channels. *British journal of pharmacology* 129:413-415.
- Halaszovich CR, Schreiber DN, Oliver D (2009) Ci-VSP is a depolarization-activated phosphatidylinositol-4,5-bisphosphate and phosphatidylinositol-3,4,5-trisphosphate 5'-phosphatase. *The Journal of biological chemistry* 284:2106-2113.
- Heidenreich M, Lechner SG, Vardanyan V, Wetzel C, Cremers CW, De Leenheer EM, Aranguiz G, Moreno-Pelayo MA, Jentsch TJ, Lewin GR KCNQ4 K(+) channels tune mechanoreceptors for normal touch sensation in mouse and man. *Nat Neurosci* 15:138-145.
- Hernandez CC, Zaika O, Shapiro MS (2008) A carboxy-terminal inter-helix linker as the site of phosphatidylinositol 4,5-bisphosphate action on Kv7 (M-type) K⁺ channels. *J Gen Physiol* 132:361-381.
- Hernandez CC, Falkenburger B, Shapiro MS (2009) Affinity for phosphatidylinositol 4,5-bisphosphate determines muscarinic agonist sensitivity of Kv7 K⁺ channels. *J Gen Physiol* 134:437-448.
- Hille B (2001) *Ion Channels of Excitable Membranes*, 3rd edition Edition. Sunderland, USA: Sinauer Associates, Inc.
- Holt JR, Stauffer EA, Abraham D, Geleoc GS (2007) Dominant-negative inhibition of M-like potassium conductances in hair cells of the mouse inner ear. *J Neurosci* 27:8940-8951.
- Housley GD, Ashmore JF (1992) Ionic currents of outer hair cells isolated from the guinea-pig cochlea. *The Journal of physiology* 448:73-98.
- Iwasaki H, Murata Y, Kim Y, Hossain MI, Worby CA, Dixon JE, McCormack T, Sasaki T, Okamura Y (2008) A voltage-sensing phosphatase, Ci-VSP, which shares sequence identity with PTEN, dephosphorylates phosphatidylinositol 4,5-bisphosphate. *Proc Natl Acad Sci U S A* 105:7970-7975.

R E F E R E N C E S

- Jentsch TJ (2000) Neuronal KCNQ potassium channels: physiology and role in disease. *Nat Rev Neurosci* 1:21-30.
- Jentsch TJ, Schroeder BC, Kubisch C, Friedrich T, Stein V (2000) Pathophysiology of KCNQ channels: neonatal epilepsy and progressive deafness. *Epilepsia* 41:1068-1069.
- Jiang H, Sha SH, Schacht J (2006a) Kanamycin alters cytoplasmic and nuclear phosphoinositide signaling in the organ of Corti in vivo. *J Neurochem* 99:269-276.
- Jiang H, Sha SH, Forge A, Schacht J (2006b) Caspase-independent pathways of hair cell death induced by kanamycin in vivo. *Cell Death Differ* 13:20-30.
- Johnson SL, Beurg M, Marcotti W, Fettiplace R (2011) Prestin-driven cochlear amplification is not limited by the outer hair cell membrane time constant. *Neuron* 70:1143-1154.
- Kennedy HJ, Crawford AC, Fettiplace R (2005) Force generation by mammalian hair bundles supports a role in cochlear amplification. *Nature* 433:880-883.
- Khan KM, Drescher MJ, Hatfield JS, Khan AM, Drescher DG (2002) Muscarinic receptor subtypes are differentially distributed in the rat cochlea. *Neuroscience* 111:291-302.
- Kharkovets T, Hardelin JP, Safieddine S, Schweizer M, El-Amraoui A, Petit C, Jentsch TJ (2000) KCNQ4, a K⁺ channel mutated in a form of dominant deafness, is expressed in the inner ear and the central auditory pathway. *Proc Natl Acad Sci U S A* 97:4333-4338.
- Kharkovets T, Dedek K, Maier H, Schweizer M, Khimich D, Nouvian R, Vardanyan V, Leuwer R, Moser T, Jentsch TJ (2006) Mice with altered KCNQ4 K⁺ channels implicate sensory outer hair cells in human progressive deafness. *EMBO J* 25:642-652.
- Kim HJ, Lv P, Sihm CR, Yamoah EN (2011) Cellular and Molecular Mechanisms of Autosomal Dominant Form of Progressive Hearing Loss, DFNA2. *The Journal of biological chemistry* 286:1517-1527.
- Kubisch C, Schroeder BC, Friedrich T, Lutjohann B, El-Amraoui A, Marlin S, Petit C, Jentsch TJ (1999) KCNQ4, a novel potassium channel expressed in sensory outer hair cells, is mutated in dominant deafness. *Cell* 96:437-446.
- Lacroix J, Halaszovich CR, Schreiber DN, Leitner MG, Bezanilla F, Oliver D, Villalba-Galea CA (2011) Controlling the activity of PTEN by membrane potential. *The Journal of biological chemistry*.
- Leitner MG, Halaszovich CR, Oliver D (2011) Aminoglycosides inhibit KCNQ4 channels in cochlear outer hair cells via depletion of phosphatidylinositol(4,5)bisphosphate. *Mol Pharmacol* 79:51-60.
- Leitner MG, Feuer A, Ebers O, Schreiber DN, Halaszovich CR, Oliver D (2012) Restoration of ion channel function in deafness-causing KCNQ4 mutants by synthetic channel openers. *British journal of pharmacology* 165:2244-2259.
- Li Y, Gamper N, Hilgemann DW, Shapiro MS (2005) Regulation of Kv7 (KCNQ) K⁺ channel open probability by phosphatidylinositol 4,5-bisphosphate. *J Neurosci* 25:9825-9835.
- Liberman MC, Gao J, He DZ, Wu X, Jia S, Zuo J (2002) Prestin is required for electromotility of the outer hair cell and for the cochlear amplifier. *Nature* 419:300-304.
- Lim DJ (1980) Cochlear anatomy related to cochlear micromechanics. A review. *J Acoust Soc Am* 67:1686-1695.
- Maehama T, Dixon JE (1998) The tumor suppressor, PTEN/MMAC1, dephosphorylates the lipid second messenger, phosphatidylinositol 3,4,5-trisphosphate. *The Journal of biological chemistry* 273:13375-13378.
- Mammano F, Ashmore JF (1996) Differential expression of outer hair cell potassium currents in the isolated cochlea of the guinea-pig. *The Journal of physiology* 496 (Pt 3):639-646.

R E F E R E N C E S

- Marcotti W, Kros CJ (1999) Developmental expression of the potassium current $I_{K,n}$ contributes to maturation of mouse outer hair cells. *The Journal of physiology* 520 Pt 3:653-660.
- Marcotti W, van Netten SM, Kros CJ (2005) The aminoglycoside antibiotic dihydrostreptomycin rapidly enters mouse outer hair cells through the mechano-electrical transducer channels. *The Journal of physiology* 567:505-521.
- Marcotti W, Johnson SL, Holley MC, Kros CJ (2003) Developmental changes in the expression of potassium currents of embryonic, neonatal and mature mouse inner hair cells. *The Journal of physiology* 548:383-400.
- Martin P, Hudspeth AJ (1999) Active hair-bundle movements can amplify a hair cell's response to oscillatory mechanical stimuli. *Proc Natl Acad Sci U S A* 96:14306-14311.
- McCrossan ZA, Abbott GW (2004) The Mink-related peptides. *Neuropharmacology* 47:787-821.
- Meyer AC, Moser T (2010) Structure and function of cochlear afferent innervation. *Curr Opin Otolaryngol Head Neck Surg* 18:441-446.
- Mistrik P, Ashmore J (2009) The role of potassium recirculation in cochlear amplification. *Curr Opin Otolaryngol Head Neck Surg* 17:394-399.
- Moser T, Brandt A, Lysakowski A (2006) Hair cell ribbon synapses. *Cell Tissue Res* 326:347-359.
- Murata Y, Iwasaki H, Sasaki M, Inaba K, Okamura Y (2005) Phosphoinositide phosphatase activity coupled to an intrinsic voltage sensor. *Nature* 435:1239-1243.
- Nenov AP, Norris C, Bobbin RP (1997) Outwardly rectifying currents in guinea pig outer hair cells. *Hear Res* 105:146-158.
- Nie L (2008) KCNQ4 mutations associated with nonsyndromic progressive sensorineural hearing loss. *Curr Opin Otolaryngol Head Neck Surg* 16:441-444.
- Nouvian R, Ruel J, Wang J, Guitton MJ, Pujol R, Puel JL (2003) Degeneration of sensory outer hair cells following pharmacological blockade of cochlear KCNQ channels in the adult guinea pig. *Eur J Neurosci* 17:2553-2562.
- Okamura Y, Dixon JE (2011) Voltage-sensing phosphatase: its molecular relationship with PTEN. *Physiology (Bethesda)* 26:6-13.
- Oliver D, Fakler B (1999) Expression density and functional characteristics of the outer hair cell motor protein are regulated during postnatal development in rat. *The Journal of physiology* 519 Pt 3:791-800.
- Oliver D, Knipper M, Derst C, Fakler B (2003) Resting potential and submembrane calcium concentration of inner hair cells in the isolated mouse cochlea are set by KCNQ-type potassium channels. *J Neurosci* 23:2141-2149.
- Oliver D, Lien CC, Soom M, Baukowitz T, Jonas P, Fakler B (2004) Functional conversion between A-type and delayed rectifier K⁺ channels by membrane lipids. *Science* 304:265-270.
- Pickles JO (1988) *An Introduction to the Physiology of Hearing*. London: Academic Press.
- Piechotta PL, Rapedius M, Stansfeld PJ, Bollepalli MK, Ehrlich G, Andres-Enguix I, Fritzenschaft H, Decher N, Sansom MS, Tucker SJ, Baukowitz T (2011) The pore structure and gating mechanism of K2P channels. *EMBO J* 30:3607-3619.
- Ricci AJ, Crawford AC, Fettiplace R (2000) Active hair bundle motion linked to fast transducer adaptation in auditory hair cells. *J Neurosci* 20:7131-7142.
- Rusch A, Eatock RA (1996) A delayed rectifier conductance in type I hair cells of the mouse utricle. *J Neurophysiol* 76:995-1004.

R E F E R E N C E S

- Russell IJ, Richardson GP (1987) The morphology and physiology of hair cells in organotypic cultures of the mouse cochlea. *Hear Res* 31:9-24.
- Russell IJ, Richardson GP, Cody AR (1986a) Mechanosensitivity of mammalian auditory hair cells in vitro. *Nature* 321:517-519.
- Russell IJ, Cody AR, Richardson GP (1986b) The responses of inner and outer hair cells in the basal turn of the guinea-pig cochlea and in the mouse cochlea grown in vitro. *Hear Res* 22:199-216.
- Russell IJ, Kossl M, Richardson GP (1992) Nonlinear mechanical responses of mouse cochlear hair bundles. *Proc Biol Sci* 250:217-227.
- Ryan A, Dallos P (1975) Effect of absence of cochlear outer hair cells on behavioural auditory threshold. *Nature* 253:44-46.
- Rybak LP, Ramkumar V (2007) Ototoxicity. *Kidney Int* 72:931-935.
- Santagata S, Boggon TJ, Baird CL, Gomez CA, Zhao J, Shan WS, Myszkowski DG, Shapiro L (2001) G-protein signaling through tubby proteins. *Science* 292:2041-2050.
- Schaechinger TJ, Gorbunov D, Halaszovich CR, Moser T, Kugler S, Fakler B, Oliver D (2011) A synthetic prestin reveals protein domains and molecular operation of outer hair cell piezoelectricity. *EMBO J* 30:2793-2804.
- Schroeder BC, Kubisch C, Stein V, Jentsch TJ (1998) Moderate loss of function of cyclic-AMP-modulated KCNQ2/KCNQ3 K⁺ channels causes epilepsy. *Nature* 396:687-690.
- Schulze D, Krauter T, Fritzenschaft H, Soom M, Baukowitz T (2003) Phosphatidylinositol 4,5-bisphosphate (PIP₂) modulation of ATP and pH sensitivity in Kir channels. A tale of an active and a silent PIP₂ site in the N terminus. *The Journal of biological chemistry* 278:10500-10505.
- Schwander M, Kachar B, Muller U (2010) Review series: The cell biology of hearing. *J Cell Biol* 190:9-20.
- Sellick PM, Patuzzi R, Johnstone BM (1982) Measurement of basilar membrane motion in the guinea pig using the Mossbauer technique. *J Acoust Soc Am* 72:131-141.
- Shapiro MS, Roche JP, Kaftan EJ, Cruzblanca H, Mackie K, Hille B (2000) Reconstitution of muscarinic modulation of the KCNQ2/KCNQ3 K⁽⁺⁾ channels that underlie the neuronal M current. *J Neurosci* 20:1710-1721.
- Smith RJH, Hildebrand M (2008) DFNA2 Nonsyndromic Hearing Loss. In: Gene Reviews [Internet] (Pagon RA, Bird TC, Dolan CR, Stephens K, eds). Seattle (WA): University of Washington.
- Smith RJH, Hildebrand MS, Van Camp G (2008) Deafness and Hereditary Hearing Loss Overview.
- Sogaard R, Ljungstrom T, Pedersen KA, Olesen SP, Jensen BS (2001) KCNQ4 channels expressed in mammalian cells: functional characteristics and pharmacology. *Am J Physiol Cell Physiol* 280:C859-866.
- Strutz-Seebohm N, Seebohm G, Fedorenko O, Baltaev R, Engel J, Knirsch M, Lang F (2006) Functional coassembly of KCNQ4 with KCNE-beta- subunits in *Xenopus* oocytes. *Cell Physiol Biochem* 18:57-66.
- Suh BC, Hille B (2002) Recovery from muscarinic modulation of M current channels requires phosphatidylinositol 4,5-bisphosphate synthesis. *Neuron* 35:507-520.
- Suh BC, Inoue T, Meyer T, Hille B (2006) Rapid chemically induced changes of PtdIns(4,5)P₂ gate KCNQ ion channels. *Science* 314:1454-1457.

REFERENCES

- Tatulian L, Delmas P, Abogadie FC, Brown DA (2001) Activation of expressed KCNQ potassium currents and native neuronal M-type potassium currents by the anti-convulsant drug retigabine. *J Neurosci* 21:5535-5545.
- Van Eyken E, Van Laer L, Franssen E, Topsakal V, Lemkens N, Laureys W, Nelissen N, Vandeveld A, Wienker T, Van De Heyning P, Van Camp G (2006) KCNQ4: a gene for age-related hearing impairment? *Hum Mutat* 27:1007-1016.
- Von Békésy G (1960) *Experiments in Hearing*. New York.
- Wang HS, Pan Z, Shi W, Brown BS, Wymore RS, Cohen IS, Dixon JE, McKinnon D (1998) KCNQ2 and KCNQ3 potassium channel subunits: molecular correlates of the M-channel. *Science* 282:1890-1893.
- Wang Q, Steyger PS (2009) Trafficking of systemic fluorescent gentamicin into the cochlea and hair cells. *J Assoc Res Otolaryngol* 10:205-219.
- Winter H, Braig C, Zimmermann U, Geisler HS, Franzer JT, Weber T, Ley M, Engel J, Knirsch M, Bauer K, Christ S, Walsh EJ, McGee J, Kopschall I, Rohbock K, Knipper M (2006) Thyroid hormone receptors TR α 1 and TR β differentially regulate gene expression of Kcnq4 and prestin during final differentiation of outer hair cells. *J Cell Sci* 119:2975-2984.
- Wulff H, Castle NA, Pardo LA (2009) Voltage-gated potassium channels as therapeutic targets. *Nat Rev Drug Discov* 8:982-1001.
- Xiong Q, Sun H, Li M (2007) Zinc pyrithione-mediated activation of voltage-gated KCNQ potassium channels rescues epileptogenic mutants. *Nat Chem Biol* 3:287-296.
- Xiong Q, Sun H, Zhang Y, Nan F, Li M (2008) Combinatorial augmentation of voltage-gated KCNQ potassium channels by chemical openers. *Proc Natl Acad Sci U S A* 105:3128-3133.
- Xu T, Nie L, Zhang Y, Mo J, Feng W, Wei D, Petrov E, Calisto LE, Kachar B, Beisel KW, Vazquez AE, Yamoah EN (2007) Roles of alternative splicing in the functional properties of inner ear-specific KCNQ4 channels. *The Journal of biological chemistry* 282:23899-23909.
- Yeung SY, Pucovsky V, Moffatt JD, Saldanha L, Schwake M, Ohya S, Greenwood IA (2007) Molecular expression and pharmacological identification of a role for K(v)7 channels in murine vascular reactivity. *British journal of pharmacology* 151:758-770.
- Zenner HP, Reuter G, Zimmermann U, Gitter AH, Fermin C, LePage EL (1994) Transitory endolymph leakage induced hearing loss and tinnitus: depolarization, biphasic shortening and loss of electromotility of outer hair cells. *Eur Arch Otorhinolaryngol* 251:143-153.
- Zhang D, Thimmapaya R, Zhang XF, Anderson DJ, Baranowski JL, Scanio M, Perez-Medrano A, Peddi S, Wang Z, Patel JR, DeGoey DA, Gopalakrishnan M, Honore P, Yao BB, Surowy CS (2011) KCNQ2/3 openers show differential selectivity and site of action across multiple KCNQ channels. *J Neurosci Methods* 200:54-62.
- Zheng J, Shen W, He DZ, Long KB, Madison LD, Dallos P (2000) Prestin is the motor protein of cochlear outer hair cells. *Nature* 405:149-155.

6 Publications

- A. Aminoglycosides inhibit KCNQ4 channels in cochlear outer hair cells via depletion of phosphatidylinositol(4,5)bisphosphate. *Molecular Pharmacology*. 2011 Jan;79(1):51-60
- B. Restitution of ion channel function in deafness-causing KCNQ4 mutants by synthetic channel openers. *British Journal of Pharmacology* (2012) 165 2244-2259
- C. Probing the regulation of TASK potassium channels by PI(4,5)P₂ with switchable phosphoinositide phosphatases. *Journal of Physiology*. 2011 Jul 1:589 (Pt 13):3149-62
- D. Controlling the activity of PTEN by membrane potential. *Journal of Biological Chemistry*. 2011 May 20:286(20):17945-53

Aminoglycosides Inhibit KCNQ4 Channels in Cochlear Outer Hair Cells via Depletion of Phosphatidylinositol(4,5)bisphosphate^S

Michael G. Leitner, Christian R. Halaszovich, and Dominik Oliver

Department of Neurophysiology, Institute for Physiology and Pathophysiology, Philipps University of Marburg, Marburg, Germany

Received August 12, 2010; accepted October 8, 2010

ABSTRACT

Aminoglycoside antibiotics (AGs) are severely ototoxic. AGs cause degeneration of outer hair cells (OHCs), leading to profound and irreversible hearing loss. The underlying mechanisms are not fully understood. OHC survival critically depends on a specific K^+ conductance ($I_{K,n}$) mediated by KCNQ4 (Kv7.4) channels. Dysfunction or genetic ablation of KCNQ4 results in OHC degeneration and deafness in mouse and humans. As a common hallmark of all KCNQ isoforms, channel activity requires phosphatidylinositol(4,5)bisphosphate [PI(4,5)P₂]. Because AGs are known to reduce PI(4,5)P₂ availability by sequestration, inhibition of KCNQ4 may be involved in the action of AGs on OHCs. Using whole-cell patch-clamp recordings from rat OHCs, we found that intracellularly applied AGs inhibit $I_{K,n}$. The inhibition results from PI(4,5)P₂ depletion indicated by fluorescence imaging of cellular

PI(4,5)P₂ and the dependence of inhibition on PI(4,5)P₂ availability and on PI(4,5)P₂ affinity of recombinant KCNQ channels. Likewise, extracellularly applied AGs inhibited $I_{K,n}$ and caused substantial depolarization of OHCs, after rapid accumulation in OHCs via a hair cell-specific apical entry pathway. The potency for PI(4,5)P₂ sequestration, strength of $I_{K,n}$ inhibition, and resulting depolarization correlated with the known ototoxic potential of the different AGs. Thus, the inhibition of $I_{K,n}$ via PI(4,5)P₂ depletion and the resulting depolarization may contribute to AG-induced OHC degeneration. The KCNQ channel opener retigabine and zinc pyrithione rescued KCNQ4/ $I_{K,n}$ activity from AG-induced inhibition. Pharmacological enhancement of KCNQ4 may thus offer a protective strategy against AG-induced ototoxicity and possibly other ototoxic insults.

Introduction

Aminoglycoside antibiotics (AGs) are highly efficient in the treatment of infections caused by Gram-negative bacteria, but clinical use is restricted by severe ototoxic side effects (Forge and Schacht, 2000; Rybak and Ramkumar, 2007). The hearing loss induced by clinical doses of AGs results from degeneration of OHCs and is therefore profound and irreversible. Inner hair cells (IHCs) show little vulnerability to AGs, and susceptibility of OHCs shows a marked cochlear base-to-apex gradient. Basal, high-frequency OHCs are most sensitive, which leads to initial high-frequency hearing loss that proceeds to lower frequencies with continued administration of AGs (Fausti et al., 1984). AG-induced ablation of

OHCs is also widely used to study hair cell regeneration in animal models. However, the underlying mechanisms are not fully understood, and the basis of the differential susceptibility of hair cells remains elusive.

Hair cell damage occurs after the uptake of AGs from the endolymph via endocytosis or mechano-electrical transduction (MET) channels (Hashino and Shero, 1995; Marcotti et al., 2005). After entry, AGs seem to initiate multiple pathways, leading to necrotic or apoptotic cell death. These pathways may involve caspase-dependent and -independent signals (Jiang et al., 2006a), formation of reactive oxygen species (Rybak and Ramkumar, 2007), mitochondrial dysfunction (Dehne et al., 2002), and disruption of phosphoinositide homeostasis (Jiang et al., 2006b; Goodyear et al., 2008). In addition, it is known that AGs interact with phosphoinositides via strong electrostatic interactions and can thereby functionally deplete these phospholipids (Gabev et al., 1989).

OHC function is directly linked to phosphoinositide metabolism, because the major K^+ current of OHCs, $I_{K,n}$, is mediated by KCNQ4 (Kv7.4) channels (Kubisch et al., 1999; Kharkovets et al., 2000, 2006). Activity of all KCNQ isoforms,

This work was supported by the Deutsche Forschungsgemeinschaft [Grants SFB 593, TP A12]; and by the University Medical Center Giessen and Marburg [Grant 42/2010 MR].

Article, publication date, and citation information can be found at <http://molpharm.aspetjournals.org>.

doi:10.1124/mol.110.068130.

^S The online version of this article (available at <http://molpharm.aspetjournals.org>) contains supplemental material.

ABBREVIATIONS: AG, aminoglycoside antibiotic; OHC, outer hair cell; IHC, inner hair cell; PI(4,5)P₂, phosphatidylinositol(4,5)bisphosphate; TR, Texas Red fluorescent dye; NTR, neomycin Texas Red conjugate; GTTR, gentamicin Texas Red conjugate; MET, mechano-electrical transduction; GFP, green fluorescent protein; TIRF, total internal reflection; CHO, Chinese hamster ovary; ZnP, zinc pyrithione; XE991, 10,10-bis(4-pyridinylmethyl)-9(10H)-anthracenone dihydrochloride.

including KCNQ4, essentially depends on PI(4,5)P₂ (Li et al., 2005; Suh et al., 2006). Strikingly, $I_{K,n}/KCNQ4$ activity is essential for OHC survival. Pharmacological block and genetic ablation of KCNQ4 result in OHC degeneration and hearing loss (Nouvian et al., 2003; Kharkovets et al., 2006). Remarkably, this degeneration totally resembles AG-induced outer hair cell loss, starting at the cochlear basis and proceeding to the apex. Mutations of KCNQ4 underlie the human hereditary deafness, DFNA2, further highlighting the importance of KCNQ4 for hair cell maintenance (Kubisch et al., 1999; Kharkovets et al., 2000).

Bringing together the knowledge on KCNQ channel regulation, interaction of AGs with phosphoinositides, and dependence of OHC survival on KCNQ4 leads to the idea that $I_{K,n}$ may be a primary molecular target of ototoxic AGs. Given the important implications for the etiology of AG-induced hair cell loss, we analyzed the effect of AGs on OHC currents and recombinant KCNQ4. We find that both are inhibited by intracellular AGs. Imaging of PI(4,5)P₂ concentrations, experimental manipulation of PI(4,5)P₂ levels, and differential responses of KCNQ isoforms with different PI(4,5)P₂ affinities indicate that this inhibition results from depletion of free PI(4,5)P₂. Moreover, entry of AGs into OHCs through stereociliary MET channels is sufficient to substantially block $I_{K,n}$ and to depolarize the hair cell. Thus, inhibition of $I_{K,n}$ may contribute to AG ototoxicity.

Materials and Methods

Acute Organ of Corti Preparation. Animals were kept according to German law and institutional guidelines at the Philipps University (Marburg, Germany). Apical cochlear turns of Wistar rats (12–20 days after birth) were isolated as described previously (Oliver et al., 2000). The preparation was placed in a recording chamber and continuously perfused with standard extracellular solution containing 144 mM NaCl, 5.8 mM KCl, 1.3 mM CaCl₂, 0.9 mM MgCl₂, 0.7 mM NaH₂PO₄, 10 mM HEPES, and 5.6 mM D-glucose, pH 7.4 (adjusted with NaOH), 305 to 310 mOsmol/kg. Experiments were performed within 3 h after the preparation.

Cell Culture and Transfection. Chinese hamster ovary (CHO) cells were plated on glass coverslips and transfected with jetPEI (Polyplus Transfection, Illkirch, France). The following expression vectors were used: pEGFP-C1-KCNQ4 (NM_004700.2); pBK-CMV-KCNQ3 (NM_004519.2) (plus pEGFP for identification of transfected cells); and pEGFP-C1-tubby-Cterm (NP_068685.1, amino acids 243–505) pRFP-C1-PI(4)P-5 kinase (NM_008846.1). Experiments were performed 24 to 48 h after transfection.

Electrophysiological Recordings from OHCs and CHO Cells. Whole-cell recordings were done with an Axopatch 200B amplifier (Molecular Devices, Sunnyvale, CA) in voltage-clamp or current-clamp mode. Data were sampled with an ITC-18 interface (HEKA, Lambrecht/Pfalz, Germany) controlled by PatchMaster software (HEKA). Currents were low pass-filtered at 2 kHz and sampled at 5 kHz. Patch pipettes were pulled from quartz glass to an open pipette resistance of 1.5 to 3 MΩ when filled with intracellular solution containing 135 mM KCl, 2.41 mM CaCl₂ (free Ca²⁺, 0.1 μM), 3.5 mM MgCl₂, 5 mM HEPES, 5 mM EGTA, and 2.5 mM Na₂ATP, pH 7.3 (adjusted with KOH), 290 to 295 mOsmol/kg. In some experiments, neomycin trisulfate, kanamycin disulfate, G418 (Geneticin) disulfate, or poly(D-lysine) hydrobromide (molecular weight, 1000–4000) (all from Sigma-Aldrich, Munich, Germany) was added to the intracellular solution at the concentrations indicated under *Results*. Series resistance (R_S) was less than 10 MΩ, and R_S compensation (80–90%) was applied. For perforated patch-clamp experiments, pipettes were pulled from borosilicate glass to an open pipette resis-

tance of 1.5 to 3 MΩ. Pipettes were tip-filled with standard intracellular solution and then back-filled with the same solution containing 120 μg/ml Nystatin (Sigma-Aldrich). R_S was less than 22 MΩ, and R_S compensation (75%–80%) was applied.

Experiments were performed on OHCs of the third row. Access to the basolateral membrane was achieved by gently removing adjacent supporting cells with a suction pipette. Only OHCs with visually intact stereocilia and a membrane potential more negative than –69 mV were used. Neomycin trisulfate, kanamycin disulfate, 10,10-bis(4-pyridinylmethyl)-9(10H)-anthracenone dihydrochloride (XE991), zinc-pyrithione (all purchased from Sigma-Aldrich), and retigabine (kindly provided by Neurosearch, Ballerup, Denmark) were added to the extracellular solution at the concentrations indicated under *Results* and applied locally via a glass capillary. All experiments were performed at room temperature. Membrane potentials shown are not corrected for liquid junction potential (–4 mV).

Total Internal Reflection Imaging. Total internal reflection (TIRF) microscopy was performed as described previously (Halaszovich et al., 2009). In brief, experiments were performed using a BX51WI upright microscope (Olympus, Hamburg, Germany) equipped with a TIRF condenser (numerical aperture of 1.45; Olympus) and a 488 nm laser (20 mW; Picarro, Sunnyvale, CA). Fluorescence was imaged by a LUMPlanFI/IR 40X/0.8 water immersion objective (Olympus). Fluorescence was acquired with an IMAGO-QE cooled charge-coupled device camera controlled by TILLvisION software (TILL Photonics, Gräfelfing, Germany). CHO cells transiently expressing Tubby-Cterm-GFP (Santagata et al., 2001; Halaszovich et al., 2009) were simultaneously imaged and voltage-clamped. Experiments were included for analysis when the access resistance was less than 5 MΩ to ensure consistent and rapid dialysis of AGs. F/F_0 traces were calculated from the background-corrected TIRF signal (F) and initial fluorescence intensity (F_0), averaged over the footprint of the patch-clamped cell excluding cell margins to avoid movement artifacts.

Aminoglycoside Labeling and Confocal Microscopy. Gentamicin and neomycin (both from Sigma-Aldrich) were conjugated with Texas Red (TR) according to published protocols (Sandoval et al., 1998). In brief, gentamicin sulfate or neomycin trisulfate (both 50 mg/ml in 100 mM K₂CO₃, pH 8.5) were agitated with Texas Red-X succinimidyl ester (TR; Invitrogen, Carlsbad, CA) at a molar ratio of 330:1 for 36 h at 4°C (final AG concentration, 50 mM; final TR, concentration 0.150 mM). As a control, TR was diluted in 100 mM K₂CO₃, pH 8.5, and processed accordingly. The obtained gentamicin-Texas Red (GTTR) and neomycin-Texas Red (NTR) conjugates were diluted (1:50) to final concentrations of 1 mM with standard extracellular solution. Control TR solution was diluted accordingly to obtain equal concentrations of the fluorescent dye in control experiments (1:50). For some experiments, NTR was diluted in extracellular solution containing 144 mM KCl, 5.8 mM NaCl, 1.3 mM CaCl₂, 0.9 mM MgCl₂, 0.7 mM NaH₂PO₄, 10 mM HEPES, and 5.6 mM D-glucose, pH 7.4 (adjusted with NaOH), 305 to 310 mOsmol/kg.

Confocal live-cell imaging was performed with an upright LSM 710 Axio Examiner.Z1 microscope equipped with a W Plan/Apochromat 20×/1.0 DIC M27 75-mm water immersion objective (Carl Zeiss GmbH, Jena, Germany). Texas Red was excited at 561 nm with a diode-pumped solid-state laser (Carl Zeiss), and fluorescence emission was sampled at 565 to 609 nm. All preparations were imaged with the same laser power and gain settings. Fluorescence was averaged from regions of interest at various levels of OHCs, background-corrected, and is presented normalized to the initial background fluorescence F_0 at the beginning of an experiment.

Data Analysis and Statistics. Electrophysiological data were analyzed using PatchMaster (HEKA) and Igor Pro (Wavemetrics, Lake Oswego, OR). Recombinant KCNQ current amplitudes were derived from monoexponential fits to current activation at 0 mV. $I_{K,n}$ was activated at a holding potential of –60 mV, and the current was

quantified as the XE991-sensitive tail current amplitude from this holding potential at -130 mV and corrected for leak current remaining after channel deactivation. Different voltage protocols were used for recombinant KCNQ4 and $I_{K,n}$ to account for the large difference in their activation voltage ranges (Kubisch et al., 1999; Marcotti and Kros, 1999).

Fluorescence time series were analyzed using TILLvisION (TILL Photonics), Zen 2009 (Carl Zeiss), ImageJ (<http://rsbweb.nih.gov/ij/>), and Igor Pro (Wavemetrics).

Statistical analysis was performed with (paired) t test, and significance was assigned at $P \leq 0.05$. Data are presented as mean \pm S.E.M., with n representing the number of independent experiments (individual cells).

Results

Inhibition of $I_{K,n}$ and KCNQ4 by Intracellular Aminoglycosides. Because hair cell degeneration occurs after the entrance and cytoplasmic accumulation of AGs (Hiel et al., 1993; Hashino and Shero, 1995), we first analyzed the effects of intracellular AGs on $I_{K,n}$ by introducing AGs through the patch pipette. $I_{K,n}$ current amplitude was measured as the deactivating tail current at -130 mV sensitive to the KCNQ channel blocker XE991 (Fig. 1A), showing that the used voltage protocol is qualified to monitor the KCNQ conductance in OHCs.

After the establishment of the whole-cell configuration, KCNQ4-mediated currents rapidly decreased by approximately 60% of initial amplitude, when the prototypical AG, neomycin (1 mM) was included in the pipette solution (Fig. 1, B and C). In contrast, only minor channel rundown was

observed in the absence of neomycin (Fig. 1D). These results indicate the inhibition of $I_{K,n}$ by neomycin entering the cell. As shown in Fig. 1F, patching OHCs with various neomycin concentrations yielded dose-dependent inhibition of $I_{K,n}$ with a half-blocking concentration of 0.59 mM. XE991-insensitive K^+ currents in OHCs that are not carried by KCNQ channels were not affected by neomycin (Supplemental Fig. S1).

Other AG antibiotics were also tested for their effect on $I_{K,n}$. Both G418 (an AG that is similar in structure to gentamicin) and kanamycin inhibited $I_{K,n}$, albeit with lower potency than neomycin (35 and 30% at 1 mM, respectively; Fig. 1, E and G). Poly(D-lysine) (200 μ g/ml), another polycationic molecule, which is structurally unrelated to AGs, strongly inhibited $I_{K,n}$ when applied via the pipette (Fig. 1G). In contrast, ampicillin, a structurally unrelated antibiotic that lacks net positive charge, had no effect on $I_{K,n}$. These findings suggest that the polycationic nature of AGs is essential for the inhibiting effect on $I_{K,n}$. The rapid time course of inhibition suggested an immediate action of AGs on the channels rather than involvement of intracellular signaling pathways that have been implicated in AG action.

We therefore examined the interaction of AGs with KCNQ4 in a simple recombinant system. Whole-cell voltage-clamp experiments were done on CHO cells heterologously expressing KCNQ4. The introduction of neomycin via the patch pipette robustly inhibited KCNQ4 currents (Fig. 2, B and E). Sensitivity toward neomycin was somewhat higher than observed in hair cells, yielding a half-inhibiting concentration of 0.13 mM (Fig. 2D). Similar to native $I_{K,n}$, G418,

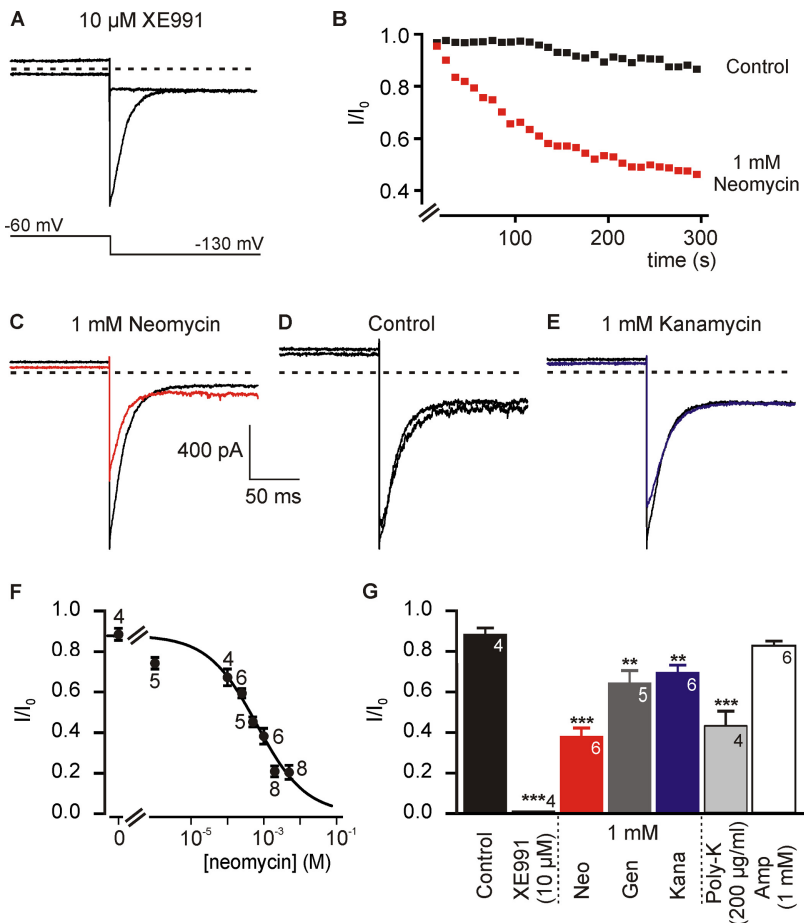


Fig. 1. Intracellular aminoglycoside antibiotics inhibit $I_{K,n}$. A, $I_{K,n}$, measured from rat OHCs as the deactivating inward tail current upon hyperpolarization (voltage command as indicated). Complete block by application of XE991 identifies this current as being carried by KCNQ channels. B, time course of current amplitude after establishment of whole-cell configuration in the absence (black) and presence (red) of neomycin in the pipette solution. Traces are representative recordings obtained from two different OHCs. Currents are presented normalized to the amplitude immediately after patch rupture (I_0). C, D, and E, representative currents immediately (black) and 10 min after (colored) patch rupture obtained with pipette solutions containing neomycin (C), no aminoglycosides (control; D) or kanamycin (E). Scale bars apply to A, C, D, and E. F, dose-dependent inhibition of $I_{K,n}$ by intracellular neomycin measured as in C. Continuous line shows a fit with the Hill equation, yielding an IC_{50} of 0.59 mM and a Hill coefficient of 1.3. G, steady-state inhibition of $I_{K,n}$ by various antibiotics and polycations. Neo, neomycin; Gen, G418; Kana, kanamycin; poly-K, poly(D-lysine); Amp, ampicillin. Numbers of experiments are indicated. **, $P \leq 0.01$; ***, $P \leq 0.001$.

kanamycin, and poly(D-lysine) also inhibited recombinant KCNQ4, whereas ampicillin was ineffective (Fig. 2E). The order of sensitivities toward these polycations was the same obtained from hair cells, suggesting the same mechanism of inhibition for $I_{K,n}$ and recombinant KCNQ4.

Aminoglycosides Interfere with the Availability of PI(4,5)P₂ to Channels. It is well established that neomycin

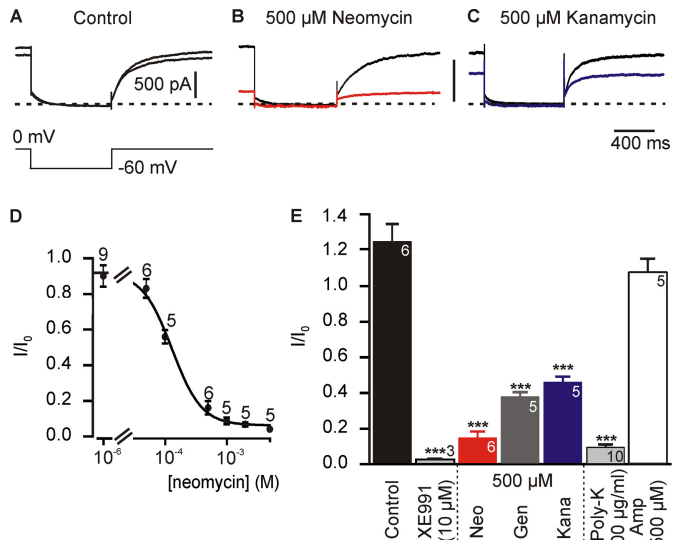


Fig. 2. Inhibition of recombinant KCNQ4 channels by intracellular aminoglycosides. A, representative whole-cell currents recorded from a CHO cell transiently expressing homomeric KCNQ4 channels, immediately (top trace) and 10 min after establishment of whole-cell configuration. Voltage protocol was performed as indicated in inset. B and C, recordings as in A with neomycin (B) or kanamycin (C) included in the patch pipette solution. Steady-state currents after dialysis of aminoglycosides into the cell are indicated in color. D, dose-dependent inhibition of KCNQ4 by intracellular neomycin measured as in B. Steady-state currents were normalized to current amplitude immediately after patch rupture (I_0) for each cell. Fit of the Hill equation to the data set (continuous line) yields IC_{50} of 0.13 mM and Hill coefficient of 1.8. E, summarized steady-state inhibition of KCNQ4 by the various antibiotics and polycations indicated. ***, $P \leq 0.001$.

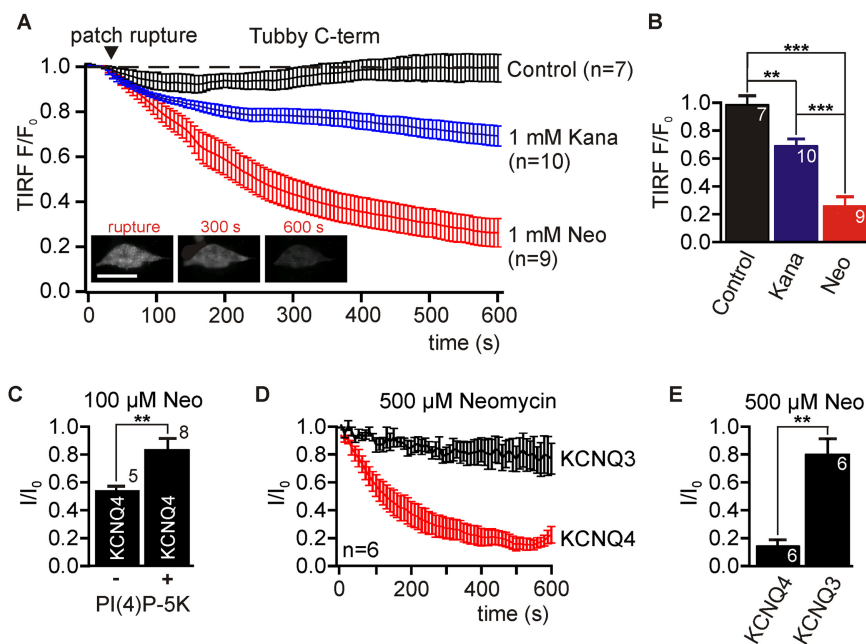


Fig. 3. Aminoglycosides decrease free PI(4,5)P₂ in the plasma membrane. A, combined TIRF imaging and patch-clamp experiments on CHO cells transfected with the PI(4,5)P₂ sensor domain Tubby-Cterm. Fluorescence intensity (TIRF F/F_0) signifies the degree of membrane association of the sensor, and is shown normalized to signal intensity (F_0) before establishing whole-cell configuration (patch rupture). Note that inclusion of neomycin and kanamycin in the patch pipette displaced the PI(4,5)P₂ sensor from the membrane. Representative TIRF images of Tubby-Cterm are shown at three time points with neomycin applied via the patch pipette (inset; scale bar, 20 μm). B, averaged relative changes in TIRF signals upon introduction of aminoglycosides into CHO cells. C, coexpression of a constitutively active PI(4)P-5 kinase significantly attenuated neomycin-induced KCNQ4 current inhibition in CHO cells. Voltage-clamp experiments were performed as in Fig. 2. D and E, differential inhibition of homomeric KCNQ4 and KCNQ3 channels by aminoglycosides. D, whole-cell currents during introduction of 500 μM neomycin through the patch pipette were measured and normalized as in Fig. 2. E, steady-state inhibition of KCNQ4, characterized by low PI(4,5)P₂ affinity, is significantly stronger than inhibition of KCNQ3, exhibiting high PI(4,5)P₂ affinity. **, $P \leq 0.01$; ***, $P \leq 0.001$.

and poly(D-lysine) bind PI(4,5)P₂ via electrostatic interaction with the anionic head groups (Gabev et al., 1989), thereby effectively chelating these lipids. Because activity of all KCNQ channels requires binding of PI(4,5)P₂, inhibition of $I_{K,n}$ may result from reduced availability of PI(4,5)P₂ to the channels. Indeed, sequestration by polycations has been used previously to define the role of phosphoinositides in the regulation of ion channels (Oliver et al., 2004; Suh and Hille, 2007).

To address the involvement of PI(4,5)P₂ in AG-induced inhibition of $I_{K,n}$ /KCNQ4, we first examined the ability of AGs to effectively deplete free PI(4,5)P₂ under our experimental conditions. To this end, we used a genetically encoded sensor for PI(4,5)P₂, the GFP-fused C terminus of the tubby protein (tubby-Cterm) (Santagata et al., 2001; Halaszovich et al., 2009). The degree of binding of this protein domain to the plasma membrane is a direct measure for the concentration of free PI(4,5)P₂. We measured membrane association of Tubby-Cterm using total internal reflection (TIRF) microscopy as described previously (Halaszovich et al., 2009). In brief, TIRF was used to selectively excite GFP bound to the plasma membrane, such that the obtained fluorescence signal directly reported the amount of membrane-associated PI(4,5)P₂ sensor and thus the concentration of free PI(4,5)P₂. As before, cells were dialyzed with either neomycin or kanamycin via a patch pipette (1 mM each). Upon the introduction of neomycin into the cell, the TIRF signal rapidly decreased to 26% of the initial signal amplitude, reporting full dislocation of Tubby from the membrane (Halaszovich et al., 2009) and thus depletion of free PI(4,5)P₂ (Fig. 3, A and B). In contrast, without neomycin in the pipette (control, Fig. 3, A and B) only an initial minor reduction of membrane fluorescence was observed, probably because of washout and bleaching of the fluorescent probe upon rupture of the membrane patch. Kanamycin also reduced free PI(4,5)P₂ concentration (to 70%), as indicated by a decrease of membrane fluorescence exceeding control recordings (Fig. 3, A and B).

However, the change of the TIRF signal and thus reduction of PI(4,5)P₂ concentration was significantly smaller than that observed with the same concentration of neomycin (Fig.

3B). Thus, the efficacy of both AGs for shielding PI(4,5)P₂ corresponds to the potency of KCNQ4 channel inhibition, consistent with the idea that inhibition results from depletion of PI(4,5)P₂.

If so, the degree of channel inhibition by AGs should depend on the PI(4,5)P₂ concentration in the plasma membrane. We therefore increased PI(4,5)P₂ levels in CHO cells by coexpression of a PI(4)P-5 kinase (e.g., Li et al., 2005; Suh and Hille, 2007). In these cells, the degree of KCNQ4 current inhibition by neomycin (100 μM) was significantly reduced compared with control cells (Fig. 3C).

The different KCNQ channel subtypes show marked differences in their apparent PI(4,5)P₂ binding affinities. Thus, homomeric KCNQ3 channels display a more than 50-fold higher apparent affinity compared with KCNQ4, rendering KCNQ4 more sensitive to PI(4,5)P₂ depletion than KCNQ3 (Li et al., 2005; Hernandez et al., 2009). We therefore compared the sensitivity of both channels to neomycin inhibition. As shown in Fig. 3, D and E, neomycin inhibition matched the channels' PI(4,5)P₂ affinity: KCNQ4 currents decreased to $14.9 \pm 4.0\%$ ($n = 6$) upon diffusion of 500 μM neomycin into the cells, whereas KCNQ3 currents were only slightly affected (reduction to $80.6 \pm 10.6\%$, $n = 6$). Taken together, these findings strongly indicate that AGs inhibit KCNQ4 channels via the sequestration of PI(4,5)P₂ in the plasma membrane.

Extracellular Aminoglycosides Inhibit $I_{K,n}$ in OHCs but Not KCNQ4 in CHO Cells. In the above experiments, we directly delivered AGs into the OHC's cytoplasm. However, in an ototoxic insult, AGs reach the hair cells from the endolymph (Hashino and Shero, 1995; Wang and Steyger, 2009). We thus tested whether entry of AGs from the extracellular space is sufficient to induce substantial inhibition of $I_{K,n}$.

Extracellular application of neomycin (1 mM) onto OHCs robustly inhibited $I_{K,n}$ to $65.8 \pm 1.6\%$ ($n = 12$) of preapplication current amplitude. Representative current traces, time course of current inhibition, and mean inhibition are shown in Fig. 4, A, B, and C, respectively.

In contrast, application of kanamycin (1 mM) only slightly diminished $I_{K,n}$ current amplitudes (to $87.0 \pm 2.0\%$, $n = 9$). However, this reduction was not significantly different from the slight current rundown observed in control experiments (to $93.4 \pm 1.1\%$, $n = 8$) (Fig. 4, B and C). The current inhibition induced by the application of neomycin was not fully reversible, consistent with the uptake into the OHC and intracellular retention after extracellular wash-off (Fig. 4A). Because intracellular accumulation of AGs may be limited under whole-cell conditions by diffusional loss into the patch pipette, we performed additional recordings in the perforated patch configuration, preventing any washout of neomycin. Under perforated-patch conditions, application of neomycin

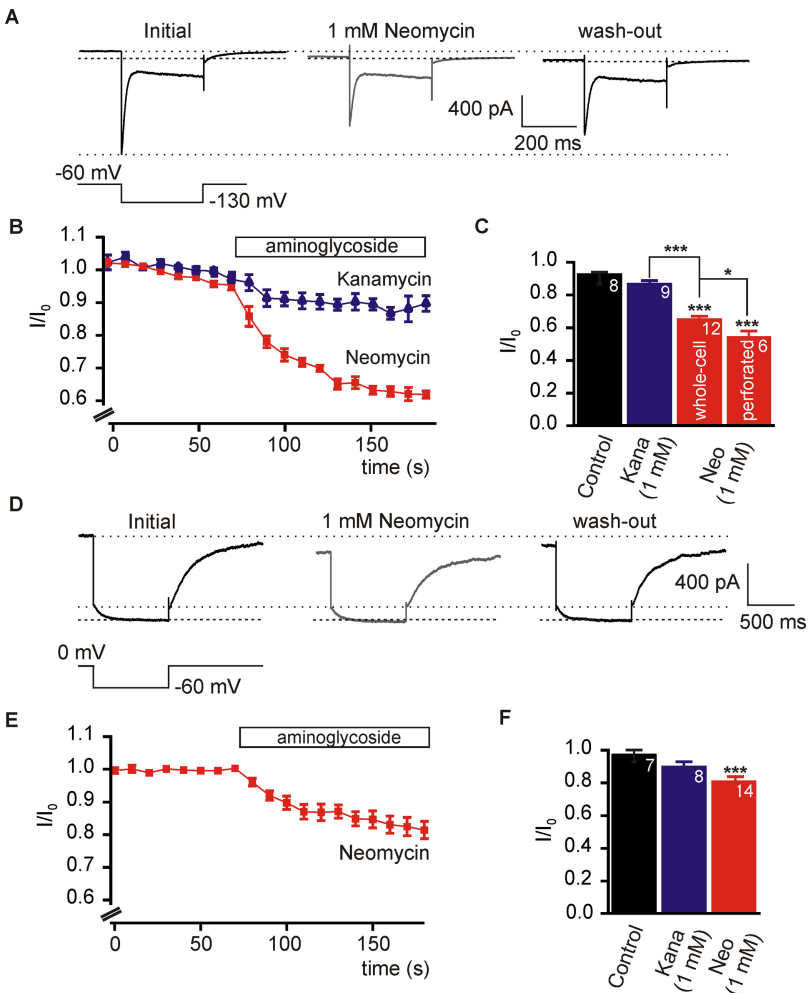


Fig. 4. Inhibition of $I_{K,n}$ in OHCs by extracellular aminoglycosides. A, representative current traces of $I_{K,n}$ before (left), during (middle), and after the extracellular application of neomycin (right). B, averaged time course of current amplitudes upon application of neomycin (1 mM, red) and kanamycin (1 mM, blue) onto OHCs, obtained as shown in A. C, summary of steady-state inhibition by extracellular aminoglycosides measured either in whole-cell or perforated-patch configuration. Note that inhibition by neomycin was significantly increased in the perforated-patch configuration compared with whole-cell. D, E, and F, effect of extracellular aminoglycosides on recombinant KCNQ4 channels expressed in CHO cells. D, representative whole-cell current traces before, during, and after application of neomycin. E, time course of currents upon application of neomycin. F, summary of relative steady state current amplitudes. Measurements were done in whole-cell configuration. *, $P \leq 0.05$; ***, $P \leq 0.001$.

induced a stronger inhibition of $I_{K,n}$ to $54.9 \pm 3.7\%$ ($n = 6$) compared with whole-cell recordings ($P = 0.02$), as shown in Fig. 4C. This finding is consistent with a higher degree of intracellular accumulation of the AG and thus supports an intracellular action of AGs on $I_{K,n}$.

To further scrutinize this conclusion, we also examined the effect of neomycin applied onto recombinant KCNQ4 channels in CHO cells, which lack the specific AG entry pathways of hair cells (Supplemental Fig. S2). Application of neomycin (1 mM) only slightly reduced KCNQ4 currents in a partially reversible manner (Fig. 4, D–F). Combined with the earlier finding of a substantially higher sensitivity of recombinant KCNQ4 to intracellular application of AGs, this result confirmed that AGs inhibit KCNQ4 only after uptake into the cell and do not considerably block channels from the extracellular side.

In summary, these results suggest that AGs inhibit KCNQ4-mediated $I_{K,n}$ after uptake and possibly accumulation via a hair cell-specific entry pathway.

Aminoglycoside Uptake into OHCs Is Fast. Although inhibition of $I_{K,n}$ by intracellular AGs is entirely consistent with the previously described entry of AGs into OHCs, the fast time course of current inhibition seemed surprising. Imaging studies are consistent with fast entry of AGs (Tiede et al., 2009); however, to our knowledge, the kinetics of AG entry have not been examined in detail at the relevant time scale.

Uptake of AGs into hair cells has been monitored previously using fluorescent Texas Red-derivatives of gentamicin (GTTR) (Dai et al., 2006). We used this approach to quantitatively record the entry of neomycin into OHCs in acutely isolated organs of Corti by confocal microscopy. Incubation with NTR or GTTR (1 mM each) for 5 min produced robust fluorescence inside OHCs and IHC but not in supporting cells and surrounding tissue (Fig. 5, A and B). Incubation with Texas Red alone did not increase hair cell fluorescence (Fig. 5C), confirming that the observed accumulation results from hair cell-specific entry of AGs but not from an unspecific permeation of the fluorescent group.

As shown in Fig. 5D, time-resolved imaging revealed the rapid accumulation of intracellular NTR in OHCs. Fluorescence increase was fastest and most pronounced in confocal sections through the hair bundles (time constant obtained from monoexponential fit to fluorescence increase, 69 s) and somewhat slower in optical sections through the medial and basal (subnuclear) regions of hair cells (281 and 241 s, respectively). These findings point to AG entry into OHCs at the level of the stereocilia and subsequent intracellular diffusion to the OHC's base, where $I_{K,n}$ /KCNQ4 is located (Kharkovets et al., 2000).

AGs may enter via the hair cell's MET channels located at the stereociliary tips (Marcotti et al., 2005). Consequently, apical membrane potential must contribute to the driving force for permeation, with hyperpolarization increasing the rate of entry of these cationic molecules. We addressed voltage-dependence of AG uptake by applying NTR while depolarizing or hyperpolarizing the cells with high or low extracellular K^+ concentrations, respectively (Fig. 5, E and F). When NTR was applied to OHCs depolarized by 144 mM extracellular K^+ , cellular fluorescence increased slowly (relative increase in the subnuclear region of OHCs, 0.02 s^{-1}). Subsequent hyperpolarization upon washout of extracellular

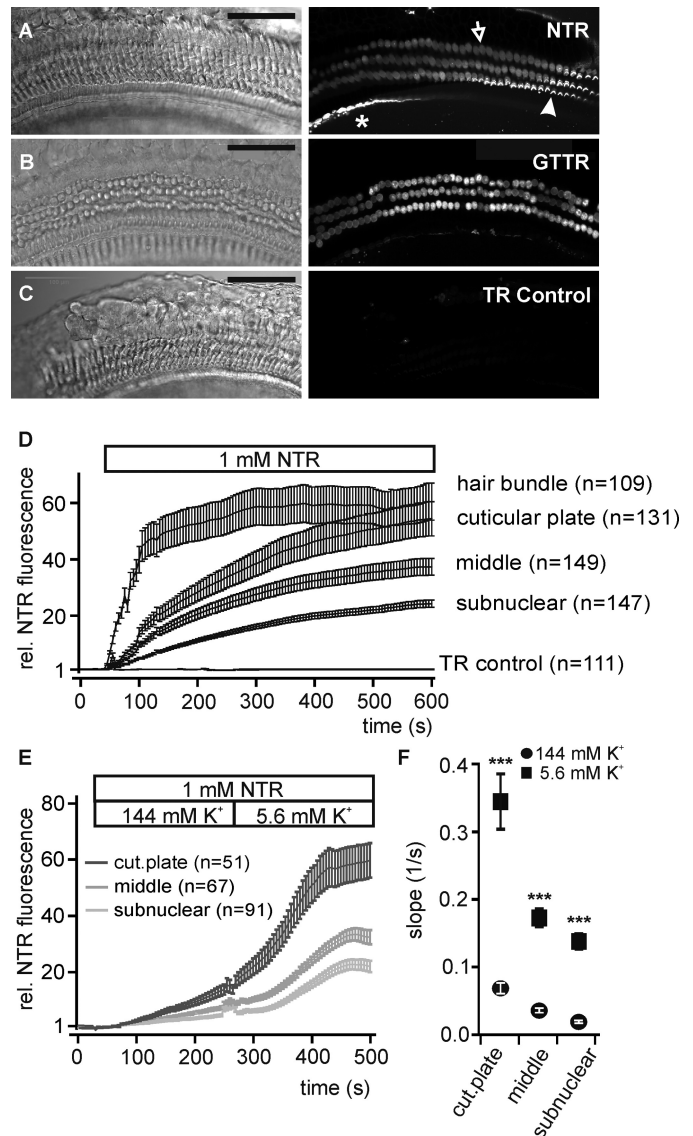


Fig. 5. Confocal imaging reveals rapid and voltage-dependent entry of aminoglycosides into OHCs. A, representative differential interference contrast (left) and confocal fluorescence (right) images of an isolated organ of Corti from rat, after incubation with fluorescently labeled neomycin (NTR; 1 mM) for 5 min (at room temperature). Note the selective uptake of NTR into OHCs and inner hair cells (*). The oblique orientation of the preparation allows visualization of labeled OHC hair bundles (filled arrow) and cell bodies (open arrow) (scale bars, 100 μm). B, images as in A after application of fluorescently labeled gentamicin (GTTR; 1 mM). C, no increase of cellular fluorescence was detected upon application of Texas Red not conjugated to aminoglycosides (TR; same TR concentration as in A and B). D, time course of entry of NTR (1 mM) into OHCs. Fluorescence intensities were sampled from confocal optical sections through hair bundles, apical region (level of the cuticular plate), middle, and subnuclear regions of OHCs. Application of TR did not produce any detectable increase in fluorescence (bottom trace). Numbers of individual OHCs analyzed are indicated (from five independent preparations). E, voltage dependence of NTR entry. Increase of OHC fluorescence during application of NTR (1 mM) was slow in depolarizing extracellular medium (144 mM K^+) and accelerated upon exchange by repolarizing medium (5.6 mM K^+). Note that the onset of increased entry is delayed because of the time needed for full solution exchange in the recording chamber. F, quantification of NTR uptake kinetics. Relative increase was derived from linear fits to the fluorescence traces from single OHCs ($n = 51$ –91, from four independent preparations). Asterisks indicate significantly faster fluorescence increase at 5.6 mM K^+ compared with 144 mM K^+ . ***, $P \leq 0.001$.

K^+ resulted in acceleration of fluorescence buildup (relative increase, 0.14 s^{-1}), indicating a strongly increased rate of aminoglycoside entry. Note that the onset of accelerated entry upon hyperpolarization is delayed because of the time needed for full exchange of the solutions inside the recording chamber (Fig. 5E).

In conclusion, AGs rapidly enter OHCs in a voltage-dependent manner, indicating permeation through MET channels. Moreover, the kinetics of AG entry into OHCs are consistent with the rapid inhibition of $I_{K,n}$ observed under similar experimental conditions.

AG-Induced Inhibition of $I_{K,n}$ Depolarizes OHCs. Loss of functional KCNQ4, and therefore $I_{K,n}$, results in OHC loss. The mechanisms that couple reduced $I_{K,n}$ to hair cell degeneration are not fully understood, but it seems likely that depolarization and subsequent Ca^{2+} overload play a major role (Oliver et al., 2003; Kharkovets et al., 2006), because $I_{K,n}$ is the principal determinant of membrane potential of OHCs (Marcotti and Kros, 1999; Kharkovets et al., 2006). Therefore, we next monitored membrane potential to investigate the immediate consequences of AG-mediated inhibition of $I_{K,n}$ (Fig. 6).

Under control conditions, membrane potentials of OHCs were constant during whole-cell recordings (V_M change, $+0.4 \pm 0.2 \text{ mV}$ at 10 min after establishing the whole-cell configuration; $n = 8$). In contrast, neomycin (1 mM) depolarized OHCs both when introduced via the patch pipette (by $+7.0 \pm 2.4 \text{ mV}$; $n = 6$) and when applied from the extracel-

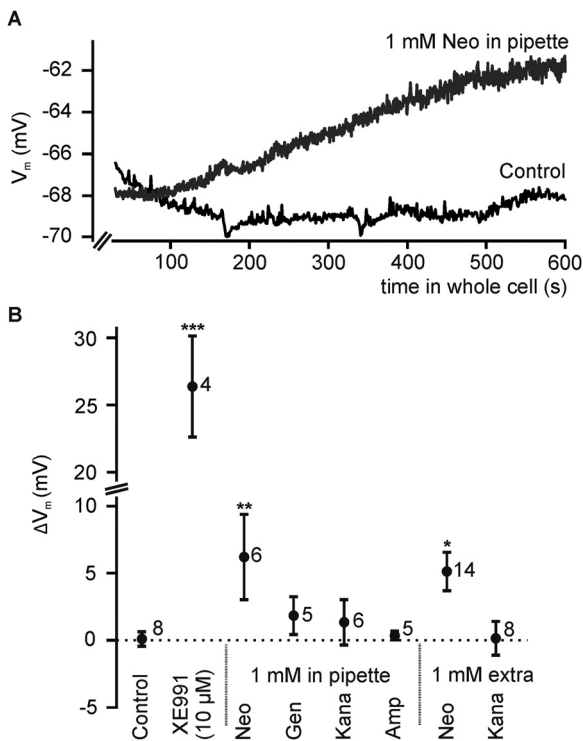


Fig. 6. Neomycin depolarizes OHCs. A, representative recordings of OHC membrane potential in current clamp mode. Patch pipettes contained either standard intracellular solution (control) or additional 1 mM neomycin. The establishment of whole-cell configuration at $t = 0$. B, summary of membrane potential changes, recorded as in A upon application of XE991, aminoglycosides or ampicillin, either via the patch pipette or by application through the extracellular solution as indicated. Note robust depolarization by intracellular and extracellular neomycin. *, $P \leq 0.05$; **, $P \leq 0.01$; ***, $P \leq 0.001$.

lular side ($+5.5 \pm 1.0 \text{ mV}$; $n = 14$). Fully blocking $I_{K,n}$ resulted in even stronger depolarization of OHCs by $+26.8 \pm 3.4 \text{ mV}$ ($n = 4$), as assessed by application of the KCNQ-specific antagonist XE991 ($10 \mu\text{M}$). Kanamycin and G418 had a small, albeit not significant, depolarizing effect when applied through the pipette, and ampicillin was entirely ineffective. Given the presumed relevance of depolarization in OHC degeneration upon dysfunction of KCNQ4, these findings point to $I_{K,n}$ inhibition as a mechanism contributing to AG ototoxicity.

Rescue of $I_{K,n}$ from Inhibition by Chemical KCNQ Channel Openers. If inhibition of $I_{K,n}$ contributes to hair cell loss, the reversal of current block by recently discovered activators of KCNQ channels (Wulff et al., 2009) might provide protection against AG ototoxicity. Therefore, we examined whether KCNQ channel openers could be used to rescue the $I_{K,n}$ conductance inhibited by AGs. We tested the channel openers retigabine (Rundfeldt and Netzer, 2000) and zinc pyrithione (ZnP) (Xiong et al., 2007). Both compounds slightly enhanced $I_{K,n}$ in the presence of intracellular neomycin ($500 \mu\text{M}$) at concentrations of up to $10 \mu\text{M}$ (Supplemental Fig. S3). However, combined application of retigabine and ZnP ($10 \mu\text{M}$ each) robustly enhanced $I_{K,n}$ amplitudes (Fig. 7A).

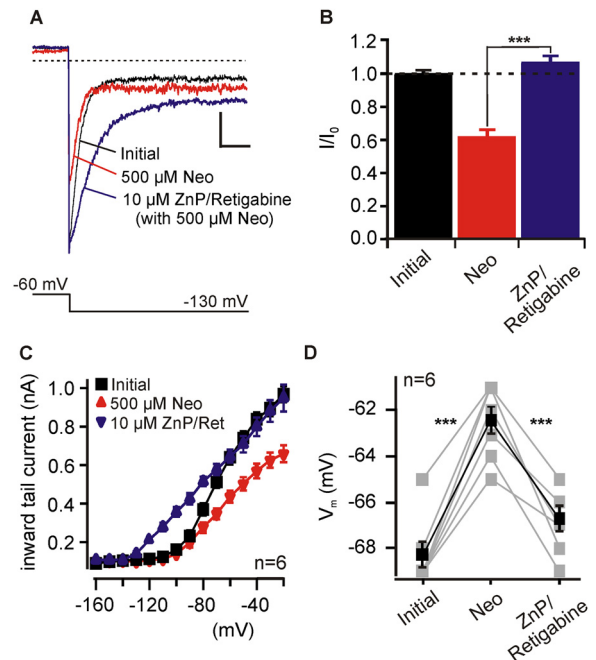


Fig. 7. Rescue of $I_{K,n}$ currents by chemical channel openers. A, representative $I_{K,n}$ tail currents recorded from an OHC immediately after patch rupture (black; control), after dialysis of neomycin from the patch pipette into the cell (red), and during additional extracellular application of zinc pyrithione (ZnP) and retigabine ($10 \mu\text{M}$ each; blue) (scale bars represent 200 pA and 50 ms). B, averaged current amplitudes, obtained as in A at a membrane potential of -70 mV . Note the full reversal of neomycin-induced $I_{K,n}$ inhibition by ZnP plus retigabine. C, mean I-V curves for $I_{K,n}$, obtained from tail currents at -130 mV and plotted as a function of prepulse voltage. Experimental conditions correspond to A and B ($n = 6$). D, OHC membrane potentials measured with a pipette containing 0.5 mM neomycin shortly after establishment of whole-cell conditions, after neomycin diffusion into the cell and during additional extracellular application of ZnP plus retigabine ($10 \mu\text{M}$ each). Gray symbols signify the recordings from individual OHCs and average potentials for each condition are shown in black. Note the reversal of aminoglycoside-induced depolarization by the channel openers. ***, $P \leq 0.001$.

At a physiological membrane potential of -70 mV, the channel activators fully recovered $I_{K,n}$ current to the control amplitude before dialysis of neomycin into the OHCs (Fig. 7, B and C). Accordingly, AG-induced depolarization was largely reversed by the application of the channel openers (Fig. 7D). The effects on current amplitude and membrane potential resulted exclusively from the openers' action on $I_{K,n}$, because increase of OHC currents was fully occluded in the presence of the specific KCNQ channel blocker XE991 (Supplemental Fig. S4). Current enhancement by the channel openers resulted from an increase in saturating $I_{K,n}$ conductance and from a pronounced leftward shift of the activation curve (Fig. 7D and Supplemental Fig. S5). Thus, application of retigabine plus ZnP induced an over-recovery of $I_{K,n}$ at potentials more negative than -70 mV (Fig. 7C). In conclusion, these results show that chemical KCNQ openers can reverse the inhibition of $I_{K,n}$ by AGs and stabilize the OHC membrane potential despite AG entry.

Discussion

Inhibition of KCNQ4-Mediated $I_{K,n}$ via PI(4,5)P₂ Sequestration. Here, we show for the first time that AGs have an immediate inhibiting effect on the major K⁺ conductance of OHCs, $I_{K,n}$. Moreover, we demonstrate that the mechanism underlying current deactivation is the decrease of free plasma membrane PI(4,5)P₂ as a result of sequestration by AGs. This conclusion is consistent with a recent report showing that intracellular polyocations, including neomycin, can inhibit heteromeric KCNQ2/3 channels by electrostatic interaction with PI(4,5)P₂ (Suh and Hille, 2007). Adding to the previous work, our data strongly support this mechanism of $I_{K,n}$ inhibition by directly demonstrating that AGs efficiently bind to membrane PI(4,5)P₂ using a fluorescent PI(4,5)P₂ sensor, Tubby (Santagata et al., 2001). The potency of different AGs to inhibit KCNQ4 correlates with the strength of PI(4,5)P₂ binding, derived from their efficacy in displacing Tubby. Moreover, the susceptibility to AG-induced block of different KCNQ channel isoforms is in agreement with their distinct PI(4,5)P₂ affinities as determined previously using independent methods (Li et al., 2005; Hernandez et al., 2009). $I_{K,n}$ seemed moderately less sensitive to the depletion of PI(4,5)P₂ induced by intracellularly applied AGs compared with recombinant KCNQ4. Different possible explanations may be considered. First, diffusional access of AGs to the PI(4,5)P₂ pool associated with the channels may be restricted (e.g., by subsurface cisternae, lamellar membrane sheets that are tightly stacked below the lateral plasma membrane). However, the localization of KCNQ4 has only little overlap with the membrane regions associated with cisternae (Kharkovets et al., 2000). Second, OHCs may possess higher basal PI(4,5)P₂ concentrations than mammalian culture cells such as CHO cells. Finally, the PI(4,5)P₂ affinity of native $I_{K,n}$ channels may differ from recombinant KCNQ4. Pronounced differences between $I_{K,n}$ and recombinant channels have been noted previously. In particular, native channels are characterized by a strikingly more negative activation range and faster kinetics (Kubisch et al., 1999; Marcotti and Kros, 1999). The present data extend these differences, suggesting a functional adjustment of KCNQ4 in OHCs (e.g., by post-translational modification or accessory channel subunits).

Mechanism of AG Entry into Hair Cells. Inhibition of $I_{K,n}$ by extracellular neomycin indicated rapid uptake into the OHC cytosol, supporting the existence of a hair cell-specific entry pathway for AGs. Uptake of AGs into hair cells has been determined as the first step leading to the ototoxic action of AGs (Forge and Schacht, 2000), and two different mechanisms for entry of AGs into hair cells have been suggested: endocytotic uptake at the apical surface (de Groot et al., 1990; Hashino and Shero, 1995), or permeation through the MET channels located in the stereocilia (Marcotti et al., 2005).

Our data strongly support entry through MET channels: the rapid inhibition of $I_{K,n}$ and the rapid uptake of fluorescent NTR are difficult to reconcile with endocytosis. Moreover, PI(4,5)P₂ sequestration requires cytosolic localization of free AGs immediately after uptake, whereas endocytosis would deliver AGs into the lumen of organelles. Accordingly, the increase of fluorescence was first detected in the hair bundle, followed by slower accumulation of NTR in the apical pole of the OHC. This indicates that the hair bundle, but not the apical surface, is the site of AG entry. Finally, the observed voltage dependence of entry is consistent with electrically driven permeation.

The mode of AG entry has important implications for the intracellular concentration that can be reached at a given extracellular concentration. We show here that some 100 μ M intracellular neomycin is required to substantially inhibit $I_{K,n}$. A comparable degree of inhibition resulted from the application of 1 mM extracellular neomycin. However, systemic administration of AGs yields lower endolymphatic concentrations in the micromolar range (de Groot et al., 1990; Marcotti et al., 2005). Can this result in relevant reduction of $I_{K,n}$?

In vivo, membrane potential and endocochlear potential provide a -150 -mV electrical driving force for cation entry into the hair cell, which allows for the generation of huge concentration gradients. Maximum intracellular concentration is reached at electrochemical equilibrium, which is quantitatively described by the Nernst equation. For a tetravalent cation such as neomycin (valence 4.5 at pH 7), the calculated potential intracellular concentration would exceed extracellular concentration by approximately 10^{10} at an electrical driving force of -150 mV. Using the dihydrostreptomycin entry rate estimated by Marcotti et al. (2005) of 0.05 fmol/h at an extracellular concentration of 1 μ M, intracellular concentrations of several hundred micromoles may be reached within hours. Thus, even micromolar endolymphatic concentrations can produce intracellular concentrations that result in massive inhibition of $I_{K,n}$. It is noteworthy that, because of the endocochlear potential, the electrical driving force is much larger in vivo than in the patch-clamp and imaging experiments presented here, allowing for higher cytoplasmic accumulation. Yet, cytoplasmic accumulation can be appreciated from NTR uptake, in which intracellular NTR fluorescence rapidly exceeds extracellular fluorescence.

Inhibition of $I_{K,n}$ and AG Ototoxicity. Strikingly, the interaction of AGs with phosphoinositides as a potential mechanism underlying AG-induced hair cell loss was recognized approximately three decades ago (Lodhi et al., 1980). Our data now identify KCNQ4, the channel that mediates $I_{K,n}$, as a molecular target affected by AG-phosphoinositide interaction. Other channels present in OHCs were not af-

ected by aminoglycosides (Supplemental Fig. S1), or their loss does not affect OHC survival (Vetter et al., 1999; Murthy et al., 2009). Because it is well documented that $I_{K,n}$ is essential for the survival of OHCs (Nouvian et al., 2003; Kharkovets et al., 2006), it seems likely that AG-induced inhibition of this current contributes to ototoxicity.

This idea is supported by a conspicuous correlation between the ototoxic potency of AG antibiotics and their efficacy in inhibiting $I_{K,n}$. Thus, neomycin exhibits higher cochleotoxicity than gentamicin and kanamycin *in vivo* and *in vitro* (Lodhi et al., 1980). Likewise, vulnerability to AGs of the different hair cell types correlates well with the expression of KCNQ4 and the requirement of KCNQ4 for cell survival. Most obviously, the highest susceptibility to damage by AGs is found in OHCs, in which KCNQ4/ $I_{K,n}$ provides essentially all of the resting K^+ conductance (Marcotti and Kros, 1999; Kharkovets et al., 2006). Moreover, the higher vulnerability of basal OHCs that results in the characteristic high-frequency hearing loss upon administration of AGs (Fausti et al., 1984), corresponds to a base-to-apex gradient of KCNQ4 expression (Kharkovets et al., 2000) and $I_{K,n}$ conductance (Mammano and Ashmore, 1996). We have shown previously that IHC express KCNQ4, in which it contributes to setting the membrane potential (Oliver et al., 2003). However, IHC function and survival do not obviously depend on this current (Nouvian et al., 2003; Kharkovets et al., 2006). In agreement with this difference to OHCs, IHCs are little, if at all, affected by AGs (Forge and Schacht, 2000).

A similar correlation is found for vestibular hair cells. Here, KCNQ4 is specifically expressed in type I but not in type II cells (Kharkovets et al., 2000). In analogy to cochlear hair cells, KCNQ4-expressing type I cells are more susceptible to AG-induced hair cell death (Forge and Schacht, 2000). It remains to be shown whether KCNQ-mediated currents in vestibular type I hair cells are inhibited by AGs and whether KCNQ4 is required for their survival.

Despite these considerations, it seems unlikely that inhibition of $I_{K,n}$ is the unique or predominant cause of AG-induced hair cell loss. Detailed analyses have demonstrated that multiple intracellular signaling pathways mediate OHC death by necrotic and/or apoptotic mechanisms (Jiang et al., 2006a). Considerable evidence, both from *in vitro* and *in vivo* experiments, points to the generation of reactive oxygen species as a major mechanism leading to AG-induced hair cell loss (Forge and Schacht, 2000). Additional mechanisms such as phospholipid scrambling triggered by interaction of AGs with phosphoinositides (Goodyear et al., 2008) may contribute as well. At present, it is not known how impairment of KCNQ4-mediated currents leads to OHC loss. However, cellular depolarization may be critical, possibly by initiating voltage-dependent Ca^{2+} influx (Oliver et al., 2003; Kharkovets et al., 2006). Excessive intracellular Ca^{2+} is involved in triggering several signals that promote cell death (Stefanis, 2005). It is noteworthy that such Ca^{2+} -sensitive signals have been implicated in AG-induced hair cell death, including the activation of calpain and subsequent release of cathepsins (Jiang et al., 2006a). Moreover, increased intracellular Ca^{2+} can contribute to mitochondrial dysfunction, which is implicated in hair cell degeneration (Dehne et al., 2002).

In conclusion, AG-induced depolarization may add to and act cooperatively with previously identified mechanisms of hair cell death. We propose that the dependence of outer hair

cells on KCNQ-mediated conductances may be an important determinant of their vulnerability to AGs.

Rescue of $I_{K,n}$ by KCNQ Channel Openers. Given that insufficient KCNQ4 activity leads to the degeneration of OHCs (Nouvian et al., 2003; Kharkovets et al., 2006), strategies for the prevention of current inhibition might have important therapeutic potential. Here, we demonstrate that the chemical KCNQ openers retigabine and zinc pyrithione enhance $I_{K,n}$ in OHCs and fully reverse inhibition by AGs.

Retigabine is being evaluated for use as an anticonvulsant drug in clinical trials (Wulff et al., 2009). In addition, potential clinical applications of retigabine and other recently identified KCNQ channel activators include treatment of pain and neuropsychiatric conditions (Wulff et al., 2009). Our data suggest that KCNQ activators may be evaluated for antagonism of AG ototoxicity. Despite the requirement of relatively high concentrations of channel activators (10 μ M) for $I_{K,n}$ rescue, the recent discovery and ongoing development of further KCNQ openers (Wulff et al., 2009) seems promising with respect to compounds with improved potency for $I_{K,n}$ enhancement. Moreover, the combinatorial action of different channel openers may increase their therapeutic potential in inner ear disease. Additive current enhancement by retigabine and zinc pyrithione was described previously for recombinant neuronal KCNQ2 channels (Xiong et al., 2008). The combinatorial effect seems to result from simultaneous binding to distinct binding sites, and distinct molecular determinants for the action of each channel opener have been identified (Xiong et al., 2008). Because the determinant amino acid residues are fully conserved between KCNQ2 and KCNQ4, we presume that binding sites and mechanism of action on $I_{K,n}$ are the same as identified previously for KCNQ2 channels.

We note that KCNQ4 openers might be useful in further conditions leading to hearing loss as a result of OHC degeneration. It will be interesting to see whether the openers can rescue the phenotype of human KCNQ4 mutations underlying DFNA2, similar to the rescue of epileptogenic mutations of KCNQ2 (Xiong et al., 2007). Moreover, correlations between KCNQ4 gene polymorphisms and both age-related and noise-induced hearing loss have been found (Van Eyken et al., 2006), suggesting that rather subtle changes in KCNQ4 expression or function may contribute to deafness. Thus, these frequent conditions might benefit from drugs modulating KCNQ4-mediated currents. In summary, the present data suggest that the spectrum of potential therapeutic use of KCNQ channel activators may include hearing loss.

Acknowledgments

cDNA constructs were kindly provided by Drs. Thomas Jentsch (Leibniz Institut für Molekulare Pharmakologie FMP and Max Delbrück Centrum für Molekulare Medizin MDC, Berlin, Germany; KCNQ4 and KCNQ3) and Lawrence Shapiro (Department of Biochemistry and Molecular Biophysics, Columbia University, New York, NY; tubby-Cterm). We gratefully acknowledge excellent technical assistance by O. Ebers and S. Petzold.

Authorship Contributions

Participated in research design: Leitner, Halaszovich, and Oliver.
Conducted experiments: Leitner.
Contributed new reagents or analytic tools: Halaszovich.
Performed data analysis: Leitner and Oliver.
Other: Oliver acquired funding for the research.

References

- Dai CF, Mangiardi D, Cotanche DA, and Steyger PS (2006) Uptake of fluorescent gentamicin by vertebrate sensory cells in vivo. *Hear Res* **213**:64–78.
- de Groot JC, Meeuwse F, Ruizendaal WE, and Veldman JE (1990) Ultrastructural localization of gentamicin in the cochlea. *Hear Res* **50**:35–42.
- Dehne N, Rauen U, de Groot H, and Lautermann J (2002) Involvement of the mitochondrial permeability transition in gentamicin ototoxicity. *Hear Res* **169**:47–55.
- Fausti SA, Rappaport BZ, Schechter MA, Frey RH, Ward TT, and Brummett RE (1984) Detection of aminoglycoside ototoxicity by high-frequency auditory evaluation: selected case studies. *Am J Otolaryngol* **5**:177–182.
- Forge A and Schacht J (2000) Aminoglycoside antibiotics. *Audiol Neurootol* **5**:3–22.
- Gabev E, Kasianowicz J, Abbott T, and McLaughlin S (1989) Binding of neomycin to phosphatidylinositol 4,5-bisphosphate (PIP₂). *Biochim Biophys Acta* **979**:105–112.
- Goodyear RJ, Gale JE, Ranatunga KM, Kros CJ, and Richardson GP (2008) Aminoglycoside-induced phosphatidylserine externalization in sensory hair cells is regionally restricted, rapid, and reversible. *J Neurosci* **28**:9939–9952.
- Halaszovich CR, Schreiber DN, and Oliver D (2009) Ci-VSP is a depolarization-activated phosphatidylinositol-4,5-bisphosphate and phosphatidylinositol-3,4,5-trisphosphate 5'-phosphatase. *J Biol Chem* **284**:2106–2113.
- Hashino E and Shero M (1995) Endocytosis of aminoglycoside antibiotics in sensory hair cells. *Brain Res* **704**:135–140.
- Hernandez CC, Falkenburger B, and Shapiro MS (2009) Affinity for phosphatidylinositol 4,5-bisphosphate determines muscarinic agonist sensitivity of Kv7 K⁺ channels. *J Gen Physiol* **134**:437–448.
- Hiel H, Erre JP, Arousseau C, Bouali R, Dulon D, and Aran JM (1993) Gentamicin uptake by cochlear hair cells precedes hearing impairment during chronic treatment. *Audiology* **32**:78–87.
- Jiang H, Sha SH, Forge A, and Schacht J (2006a) Caspase-independent pathways of hair cell death induced by kanamycin in vivo. *Cell Death Differ* **13**:20–30.
- Jiang H, Sha SH, and Schacht J (2006b) Kanamycin alters cytoplasmic and nuclear phosphoinositide signaling in the organ of Corti in vivo. *J Neurochem* **99**:269–276.
- Kharkovets T, Dedek K, Maier H, Schweizer M, Khimich D, Nouvian R, Vardanyan V, Leuwer R, Moser T, and Jentsch TJ (2006) Mice with altered KCNQ4 K⁺ channels implicate sensory outer hair cells in human progressive deafness. *EMBO J* **25**:642–652.
- Kharkovets T, Hardelin JP, Safieddine S, Schweizer M, El-Amraoui A, Petit C, and Jentsch TJ (2000) KCNQ4, a K⁺ channel mutated in a form of dominant deafness, is expressed in the inner ear and the central auditory pathway. *Proc Natl Acad Sci USA* **97**:4333–4338.
- Kubisch C, Schroeder BC, Friedrich T, Lütjohann B, El-Amraoui A, Marlin S, Petit C, and Jentsch TJ (1999) KCNQ4, a novel potassium channel expressed in sensory outer hair cells, is mutated in dominant deafness. *Cell* **96**:437–446.
- Li Y, Gamper N, Hilgemann DW, and Shapiro MS (2005) Regulation of Kv7 (KCNQ) K⁺ channel open probability by phosphatidylinositol 4,5-bisphosphate. *J Neurosci* **25**:9825–9835.
- Lodhi S, Weiner ND, Mechigian I, and Schacht J (1980) Ototoxicity of aminoglycosides correlated with their action on monomolecular films of polyphosphoinositides. *Biochem Pharmacol* **29**:597–601.
- Mammano F and Ashmore JF (1996) Differential expression of outer hair cell potassium currents in the isolated cochlea of the guinea-pig. *J Physiol* **496**:639–646.
- Marcotti W and Kros CJ (1999) Developmental expression of the potassium current IK_n contributes to maturation of mouse outer hair cells. *J Physiol* **520**:653–660.
- Marcotti W, van Netten SM, and Kros CJ (2005) The aminoglycoside antibiotic dihydrostreptomycin rapidly enters mouse outer hair cells through the mechano-electrical transducer channels. *J Physiol* **567**:505–521.
- Murthy V, Maison SF, Taranda J, Haque N, Bond CT, Elgoyhen AB, Adelman JP, Liberman MC, and Vetter DE (2009) SK2 channels are required for function and long-term survival of efferent synapses on mammalian outer hair cells. *Mol Cell Neurosci* **40**:39–49.
- Nouvian R, Ruel J, Wang J, Guitton MJ, Pujol R, and Puel JL (2003) Degeneration of sensory outer hair cells following pharmacological blockade of cochlear KCNQ channels in the adult guinea pig. *Eur J Neurosci* **17**:2553–2562.
- Oliver D, Klöcker N, Schuck J, Baukrowitz T, Ruppersberg JP, and Fakler B (2000) Gating of Ca²⁺-activated K⁺ channels controls fast inhibitory synaptic transmission at auditory outer hair cells. *Neuron* **26**:595–601.
- Oliver D, Knipper M, Derst C, and Fakler B (2003) Resting potential and submembrane calcium concentration of inner hair cells in the isolated mouse cochlea are set by KCNQ-type potassium channels. *J Neurosci* **23**:2141–2149.
- Oliver D, Lien CC, Soom M, Baukrowitz T, Jonas P, and Fakler B (2004) Functional conversion between A-type and delayed rectifier K⁺ channels by membrane lipids. *Science* **304**:265–270.
- Rundfeldt C and Netzer R (2000) The novel anticonvulsant retigabine activates M-currents in Chinese hamster ovary-cells transfected with human KCNQ2/3 subunits. *Neurosci Lett* **282**:73–76.
- Rybak LP and Ramkumar V (2007) Ototoxicity. *Kidney Int* **72**:931–935.
- Sandoval R, Leiser J, and Molitoris BA (1998) Aminoglycoside antibiotics traffic to the Golgi complex in LLC-PK1 cells. *J Am Soc Nephrol* **9**:167–174.
- Santagata S, Boggon TJ, Baird CL, Gomez CA, Zhao J, Shan WS, Myszkka DG, and Shapiro L (2001) G-protein signaling through tubby proteins. *Science* **292**:2041–2050.
- Stefanis L (2005) Caspase-dependent and -independent neuronal death: two distinct pathways to neuronal injury. *Neuroscientist* **11**:50–62.
- Suh BC and Hille B (2007) Electrostatic interaction of internal Mg²⁺ with membrane PIP₂ seen with KCNQ K⁺ channels. *J Gen Physiol* **130**:241–256.
- Suh BC, Inoue T, Meyer T, and Hille B (2006) Rapid chemically induced changes of PtdIns(4,5)P₂ gate KCNQ ion channels. *Science* **314**:1454–1457.
- Tiede L, Steyger PS, Nichols MG, and Hallworth R (2009) Metabolic imaging of the organ of Corti—a window on cochlea bioenergetics. *Brain Res* **1277**:37–41.
- Van Eyken E, Van Laer L, Franssen E, Topsakal V, Lemkens N, Laureys W, Nelissen N, Vandeveldel A, Wienker T, Van De Heyning P, et al. (2006) KCNQ4: a gene for age-related hearing impairment? *Hum Mutat* **27**:1007–1016.
- Vetter DE, Liberman MC, Mann J, Barhanin J, Boulter J, Brown MC, Saffioti-Kolman J, Heinemann SF, and Elgoyhen AB (1999) Role of alpha9 nicotinic ACh receptor subunits in the development and function of cochlear efferent innervation. *Neuron* **23**:93–103.
- Wang Q and Steyger PS (2009) Trafficking of systemic fluorescent gentamicin into the cochlea and hair cells. *J Assoc Res Otolaryngol* **10**:205–219.
- Wulff H, Castle NA, and Pardo LA (2009) Voltage-gated potassium channels as therapeutic targets. *Nat Rev Drug Discov* **8**:982–1001.
- Xiong Q, Sun H, and Li M (2007) Zinc pyrithione-mediated activation of voltage-gated KCNQ potassium channels rescues epileptogenic mutants. *Nat Chem Biol* **3**:287–296.
- Xiong Q, Sun H, Zhang Y, Nan F, and Li M (2008) Combinatorial augmentation of voltage-gated KCNQ potassium channels by chemical openers. *Proc Natl Acad Sci USA* **105**:3128–3133.

Address correspondence to: Dr. Dominik Oliver, Department of Neurophysiology, Institute for Physiology and Pathophysiology, Philipps-Universität Marburg, Deutschhausstr. 2, 35037 Marburg, Germany, E-mail: oliverd@staff.uni-marburg.de

RESEARCH PAPER

Restoration of ion channel function in deafness-causing KCNQ4 mutants by synthetic channel openers

Michael G Leitner, Anja Feuer, Olga Ebers, Daniela N Schreiber, Christian R Halaszovich and Dominik Oliver

Department of Neurophysiology, Institute of Physiology and Pathophysiology, Philipps-University Marburg, Marburg, Germany

Correspondence

Professor Dr Dominik Oliver,
Institute of Physiology and
Pathophysiology,
Philipps-University Marburg,
35037 Marburg, Germany.
E-Mail:
oliverd@staff.uni-marburg.de

Keywords

DFNA2; hereditary hearing loss;
organ of Corti; outer hair cell;
KCNQ4; neurodegeneration

Received

29 April 2011

Revised

4 September 2011

Accepted

13 September 2011

BACKGROUND AND PURPOSE

DFNA2 is a frequent hereditary hearing disorder caused by loss-of-function mutations in the voltage-gated potassium channel KCNQ4 (Kv7.4). KCNQ4 mediates the predominant K^+ conductance, $I_{K,n}$, of auditory outer hair cells (OHCs), and loss of KCNQ4 function leads to degeneration of OHCs resulting in progressive hearing loss. Here we explore the possible recovery of channel activity of mutant KCNQ4 induced by synthetic KCNQ channel openers.

EXPERIMENTAL APPROACH

Whole cell patch clamp recordings were performed on CHO cells transiently expressing KCNQ4 wild-type (wt) and DFNA2-relevant mutants, and from acutely isolated OHCs.

KEY RESULTS

Various known KCNQ channel openers robustly enhanced KCNQ4 currents. The strongest potentiation was observed with a combination of zinc pyrithione plus retigabine. A similar albeit less pronounced current enhancement was observed with native $I_{K,n}$ currents in rat OHCs. DFNA2 mutations located in the channel's pore region abolished channel function and these mutant channels were completely unresponsive to channel openers. However, the function of a DFNA2 mutation located in the proximal C-terminus was restored by the combined application of both openers. Co-expression of wt and KCNQ4 pore mutants suppressed currents to barely detectable levels. In this dominant-negative situation, channel openers essentially restored currents back to wt levels, most probably through strong activation of only the small fraction of homomeric wt channels.

CONCLUSIONS AND IMPLICATIONS

Our data suggest that by stabilizing the KCNQ4-mediated conductance in OHCs, chemical channel openers can protect against OHC degeneration and progression of hearing loss in DFNA2.

Abbreviations

BFNC, benign familial neonatal convulsion; DFNA2, deafness autosomal dominant locus 2; OHC, outer hair cell; wt, wild-type; ZnP, zinc pyrithione; ZnP/Ret, zinc pyrithione plus retigabine

Introduction

Loss-of-function mutations in the voltage-gated potassium channel KCNQ4 (Kv7.4) cause a non-syndromic, progressive form of hereditary deafness, deafness autosomal dominant locus 2 (DFNA2) (Kubisch *et al.*, 1999; Beisel *et al.*, 2000; Kharkovets *et al.*, 2000; 2006). DFNA2 is characterized by

symmetric hearing loss that is progressive at all frequencies (Jentsch, 2000; Nie, 2008). Hearing impairment is moderate at young ages, but most affected individuals develop severe-to-profound high-frequency hearing loss by the age of 70 (Smith and Hildebrand, 2008). KCNQ4 is strongly expressed in sensory outer hair cells (OHCs) in the organ of Corti, where it mediates the predominant K^+ conductance, $I_{K,n}$ (Mammano

and Ashmore, 1996; Kubisch *et al.*, 1999; Marcotti and Kros, 1999; Kharkovets *et al.*, 2006; Holt *et al.*, 2007). KCNQ4 has an essential role for OHC function, as pharmacological inhibition, genetic ablation and loss of function by dominant-negative mutations lead to progressive loss of OHCs and subsequent hearing loss in animal models, recapitulating the human DFNA2 phenotype (Kubisch *et al.*, 1999; Nouvian *et al.*, 2003; Kharkovets *et al.*, 2006). KCNQ4 is also expressed in inner hair cells (Oliver *et al.*, 2003) and in neurons in the central auditory system (Kharkovets *et al.*, 2000; Beisel *et al.*, 2005), but the physiological relevance in these cells is not known. To date, eight distinct KCNQ4 point mutations generating non-functional channel subunits, two mutations producing truncated protein (Coucke *et al.*, 1999; Kamada *et al.*, 2006) and a six-amino acid deletion in the linker between the fourth and fifth transmembrane segment (Baek *et al.*, 2011) have been identified in DFNA2-affected humans. Most point mutations were located within the channel's pore region, where mutations inhibit channel function presumably by disrupting ion permeation (Coucke *et al.*, 1999; Kubisch *et al.*, 1999; Talebizadeh *et al.*, 1999; Van Hauwe *et al.*, 2000; Akita *et al.*, 2001; Van Camp *et al.*, 2002; Topsakal *et al.*, 2005) or by reducing channel surface expression (Mencia *et al.*, 2008; Kim *et al.*, 2011). A mutation in a putative splicing site in the third transmembrane region was hypothesized to produce a non-functional KCNQ4 isoform specifically in OHCs (Su *et al.*, 2007; Kim *et al.*, 2011), and a mutation in the proximal C-terminus renders channels non-functional (Coucke *et al.*, 1999; Kim *et al.*, 2011), possibly by disrupting channel gating. Voltage-gated potassium channels are homo- or heteromeric assemblies of four pore-forming subunits. Therefore, mutations in one single subunit can disrupt channel function of the tetramer in a dominant-negative manner (Biervert *et al.*, 1998; Charlier *et al.*, 1998; Schroeder *et al.*, 1998; Singh *et al.*, 1998). Accordingly, DFNA2-causing mutations are thought to reduce native $I_{K,n}$ via dominant-negative suppression of channel function in individuals heterozygous for the mutation (Kubisch *et al.*, 1999; Holt *et al.*, 2007). A variety of potassium channel openers has been identified over the last years that strongly and specifically potentiate currents through KCNQ channels (Wulff *et al.*, 2009). Some of these KCNQ openers are already in use or in clinical trials for the treatment of various neurological disorders (Wulff *et al.*, 2009). Interestingly, the KCNQ openers, retigabine and zinc pyrithione (ZnP), were recently shown to restore the channel function of epileptogenic KCNQ2-mutants (Xiong *et al.*, 2007; 2008). These channel subunits mediate the neuronal M-currents (Wang *et al.*, 1998; Shapiro *et al.*, 2000) and loss-of-function mutations cause a specific form of neonatal epilepsy [benign familial neonatal convulsion (BFNC)] (Biervert *et al.*, 1998; Charlier *et al.*, 1998; Schroeder *et al.*, 1998; Singh *et al.*, 1998). In analogy, if KCNQ openers restored channel function in DFNA2-relevant KCNQ4 mutants, these agonists may have therapeutic potential to protect against OHC degeneration and hearing loss.

Here we investigated the effects of synthetic KCNQ openers on native $I_{K,n}$ and heterologously expressed KCNQ4 and found enhancement of both currents. Channel function of the DFNA2-causing mutation that is located close to the sixth transmembrane segment, G321S, was partially restored by a combination of zinc-pyrithione and retigabine

(ZnP/Ret). Moreover these KCNQ openers rescued KCNQ4 from dominant-negative inhibition by DFNA2-mutations. Channel activity was recovered substantially to wild-type (wt) levels by activation of residual homomeric wt channels. Taken together, our data suggest that channel activators have the potential to stabilize the essential KCNQ4-mediated conductance in OHCs in DFNA2.

Methods

Cell culture, transfection and mutagenesis

CHO cells were maintained in MEM Alpha Medium (Invitrogen GmbH, Darmstadt, Germany) supplemented with 10% fetal calf serum and 1% penicillin/streptomycin (both Invitrogen). For experiments cells were plated on glass cover slips (Carl Roth, Karlsruhe, Germany) and transfected with jetPEI transfection reagent (Polyplus Transfection, Illkirch, France). Experiments on transfected cells were performed 24 h to 48 h post-transfection. The expression vectors used were pEGFP-C1-KCNQ4 and pRFP-C1-KCNQ4 (NM_004700.2), and pBK-CMV-KCNQ3 (NM_004519.2). The expressed channels are referred to as KCNQ4 wt and KCNQ3 wt (Kv7.4 and Kv7.3, respectively) according to the Guide to Receptors and Channels (Alexander *et al.*, 2009). Based on pEGFP-C1-KCNQ4 six DFNA2-relevant point mutations were generated by site-directed mutagenesis using the QuickChangeII XL Site-Directed mutagenesis kit (Stratagene, Santa Clara, CA, USA), and mutagenesis was verified by sequencing (SEQLAB-Sequence Laboratories Göttingen GmbH, Göttingen, Germany). KCNQ4 wt and mutations were co-expressed to examine the action of channel openers in a setting corresponding to heterozygote DNFA2 carriers. In these experiments wt and mutant plasmids were transfected at various ratios as indicated while keeping the total amount of DNA constant. To verify co-expression of wt and mutated protein, wt KCNQ4-mRFP was co-expressed with the GFP-fused mutant. The expected fraction of homomeric wt channels was calculated for each proportion assuming random assembly of channel tetramers.

Tandem concatamers consisting of KCNQ4 wt subunits or of one wt and one mutant subunit (W276S, G285S or G321S) were generated by fusing the subunits N-terminus to C-terminus. Molecular cloning of the concatamers was based on KCNQ4 in the pBK-CMV-rev vector. An AgeI cutting site was introduced 3' of the KCNQ4 insert and the stop codon was removed by mutagenesis. The resulting construct was digested with AgeI and NheI, yielding a 2367 bp fragment encoding KCNQ4 that was subsequently subcloned into the KCNQ4-pEGFP-C1 plasmid to create the wt concatamer plasmid. For concatamers containing one of the mutations (W276S, G285S or G321S) we used the same cloning strategy with source vectors that carried one of the mutations. Mutagenesis and cloning were verified by sequencing.

Organ of Corti preparation

All experiments utilizing animal tissue were performed according to German law and to institutional guidelines at the Philipps-University Marburg. Organs of Corti of Wistar rats (12–20 days after birth) were acutely isolated as previ-

ously reported (Oliver *et al.*, 2000). Briefly, animals were anaesthetized using Isofluran (Baxter Deutschland GmbH, Unterschleißheim, Germany) and killed by decapitation. The cochlea was dissected, separated from modiolus, stria vascularis and tectorial membrane and then was continuously perfused with standard extracellular solution containing (mM) 144 NaCl, 5.8 KCl, 1.3 CaCl₂, 0.9 MgCl₂, 0.7 NaH₂PO₄, 10 HEPES and 5.6 D-glucose, pH 7.4 (with NaOH), 305–310 mOsm·kg⁻¹. Experiments were performed within 3 h after the preparation at room temperature (22–25°C).

Electrophysiological recordings

Patch clamp recordings were performed in the whole cell configuration with an Axopatch 200B amplifier (Molecular Devices, Union City, CA, USA). Data were sampled with an ITC-18 interface (HEKA Elektronik, Lambrecht, Germany) controlled by PatchMaster software (HEKA) via a Macintosh PowerPC (Apple Inc, Cupertino, CA, USA). Some experiments were performed using an EPC10-USB patch clamp amplifier (HEKA). Currents were low-pass filtered at 2 kHz and sampled at 5 kHz, and whole cell capacitance was compensated in whole-cell configuration. Patch pipettes were pulled from borosilicate glass (Sutter Instrument Company, Novato, CA, USA) to an open pipette resistance of 1.5–3 MΩ after back-filling with intracellular solution containing (mM) 135 KCl, 2.4 CaCl₂ (0.1 μM free Ca²⁺), 3.5 MgCl₂, 5 HEPES, 5 EGTA, 2.5 Na₂ATP, pH 7.3 (with KOH), 290–295 mOsm·kg⁻¹. Series resistance (R_s) typically was below 8 MΩ and R_s compensation (80–90%) was applied throughout the recordings. Experiments were performed on OHCs of the third row of apical cochlear turns, and recordings were only included in analysis if the membrane potential was more hyperpolarized than –69 mV. Access to the basolateral membrane of OHCs was achieved by gently removing surrounding tissue with a suction pipette. In CHO cells robust expression of wt and/or mutant KCNQ4 was verified by GFP and/or RFP fluorescence, and only one CHO cell was investigated per cover slip. All experiments were performed at room temperature (22–25°C). Membrane potentials shown are not corrected for liquid junction potentials (approximately 4 mV).

Chemicals

Retigabine {[N-(2-amino-4-(4-fluorobenzylamino)-phenyl) carbamic acid ethyl ester]}, flupirtine {N-[2-amino-6-(4-fluorophenyl)methyl]-3-pyridinyl}carbamic acid}, BMS-204352 {maxipost; [(S)-3-(5-chloro-2-methoxyphenyl)-3-fluoro-6-(trifluoromethyl)-1,3-dihydro-2H-indole-2-one]} (all kindly provided by Neurosearch, Ballerup, Denmark), ZnP (Sigma-Aldrich, Munich, Germany) and XE991 [10,10-bis(4-pyridinylmethyl)-9(10H)-anthracenone dihydrochloride] (Tocris Bioscience, Bristol, UK) were applied from the extracellular side via a glass capillary at the concentrations indicated in results.

Data analysis and statistics

Data were analysed with PatchMaster (HEKA) and IGOR Pro (Wavemetrics, Lake Oswego, OR, USA). Steady-state KCNQ4 currents were quantified as the outward current 1200 ms after a voltage pulse (as indicated) from the holding potential (–60 mV). Data are presented normalized to membrane

capacitance as the measure for membrane area, yielding current densities (pA/pF). Membrane capacitance was determined with the C_M compensation circuitry of the patch clamp amplifier. Drug-induced changes in current amplitudes were calculated by normalizing to the current amplitude at the beginning of each experiment prior to application of the respective channel opener (I/I_{control}). Concentration-response relations were derived from normalized KCNQ4 steady-state currents at 0 mV at various drug concentrations. Responses were fitted with a Hill equation with $I/I_b = I_b + (I_{max} - I_b)/(1 + (EC_{50}/[S])^{n_H})$, where I is the normalized current, I_b and I_{max} denote the minimal and maximal currents at low and high drug concentrations, EC₅₀ is the concentration at the half maximal effect, [S] is the drug concentration and n_H is the Hill coefficient. Voltage-dependence of channel activation was derived from tail current amplitudes using the voltage protocols given in the figures. Current-voltage curves were derived from tail currents and were fitted with a two-state Boltzmann function with $I = I_{min} + (I_{max} - I_{min}) / (1 + \exp[(V - V_h)/s])$, where I is current, V is the membrane voltage, V_h is the voltage at half maximal activation, and s describes the steepness of the curve. Results are shown as conductance-voltage curves, obtained by normalizing to (I_{max}–I_{min}), obtained from fits to the data of the individual experiments. To account for biophysical differences between heterologous KCNQ4 and native I_{K,n} (i.e. hyperpolarized voltages of activation for I_{K,n}), different voltage protocols were used for OHCs and CHO cells (Kubisch *et al.*, 1999; Marcotti and Kros, 1999; Oliver *et al.*, 2003). Thus, I_{K,n} current amplitudes were measured as the tail currents at –120 mV following pre-pulses to voltages between –160 and +40 mV (increments of 10 mV), and heterologous KCNQ4 tail currents were recorded at 0 mV from pre-pulses between –100 and +50 mV.

Statistical analysis was performed with (paired) *t*-test and Dunnett test for multi-comparison, and significance was assigned at $P \leq 0.05$ (* $P \leq 0.05$, ** $P \leq 0.01$, *** $P \leq 0.001$). Data are presented as mean ± SEM, with *n* representing the number of independent experiments (individual cells).

Results

Potentiation of heterologous KCNQ4 by channel openers

The effects of channel openers on heterologously expressed KCNQ channels have been investigated previously. However, the efficacy of current potentiation differs between channel openers and depends on the KCNQ isoform (Schroder *et al.*, 2001; Tatulian *et al.*, 2001; Xiong *et al.*, 2007). To identify the most potent activator of KCNQ4, we systematically compared the potencies of openers that have been described previously, namely flupirtine, retigabine, BMS-204352 and ZnP.

At concentrations of 10 μM, all openers except flupirtine strongly increased steady-state KCNQ4 currents (at 0 mV) 4- to 12-fold (Figure 1A,B; Supporting Information Figure S1). In these experiments the rank order of current potentiation was: flupirtine < retigabine < BMS-204352 < ZnP < ZnP/Ret. Despite different degrees of current augmentation, heterologous KCNQ4 showed comparable sensitivities for flupirtine

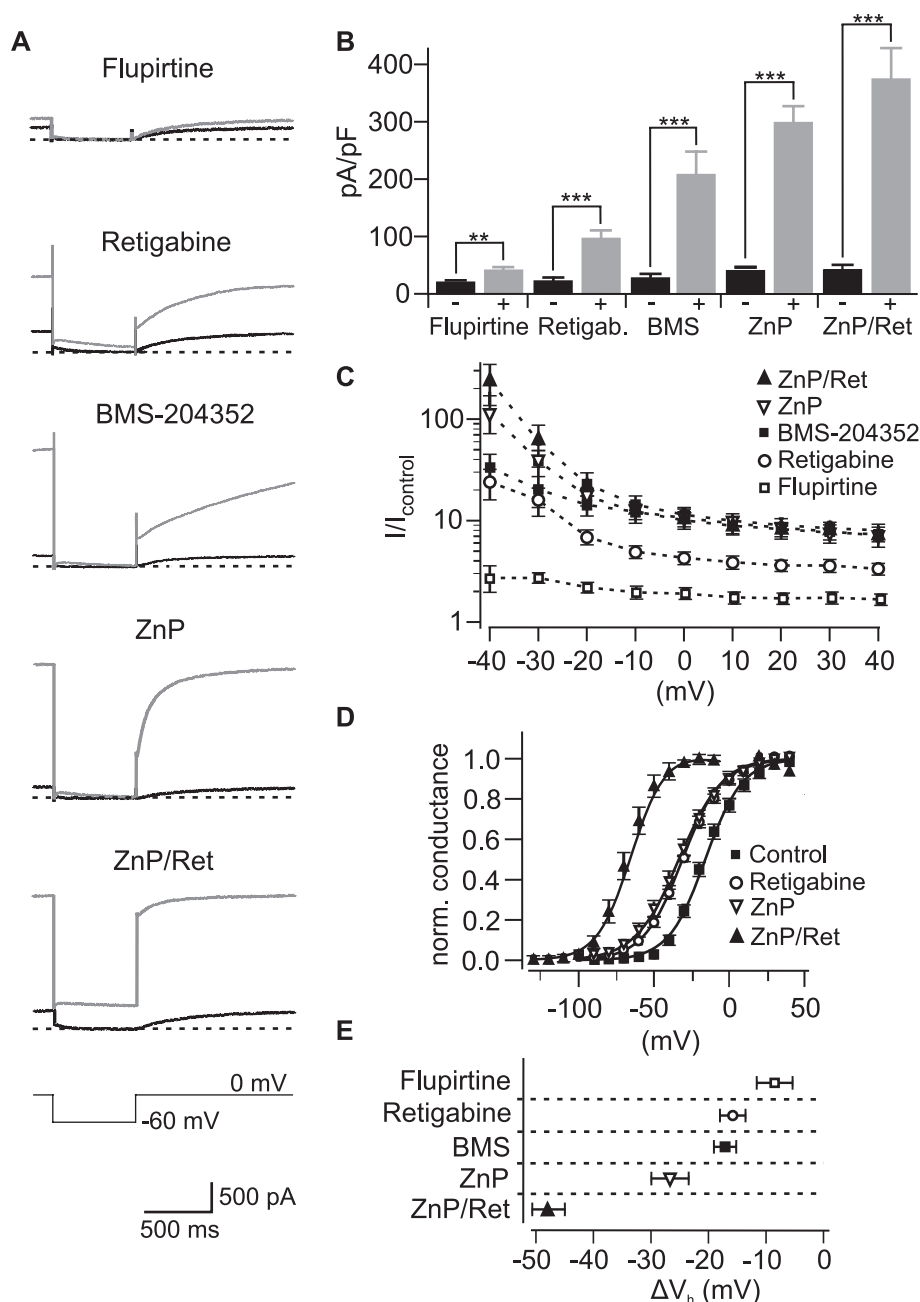


Figure 1

Potentiation of heterologous KCNQ4 currents by channel openers. (A) Representative recordings from CHO cells transiently transfected with wt KCNQ4 under control conditions and after application of flupirtine, retigabine, BMS-204352, zinc pyrithione (ZnP) or a combination of zinc pyrithione and retigabine (ZnP/Ret) (10 μ M each, voltage command as indicated). Dashed lines indicate zero currents, and scale bar applies to all recordings. (B) Summary of steady-state currents at 0 mV normalized to plasma membrane area (membrane capacitance), obtained from recordings as presented in (A). Concentration of all openers was 10 μ M. (C) KCNQ4 current potentiation by KCNQ openers was voltage-dependent. Steady-state currents at different holding potentials were normalized to currents obtained before the application of KCNQ channel openers. KCNQ4 current increase was more pronounced at hyperpolarized voltages, and saturated at approximately 10 mV for all openers. (D) Voltage-dependence of KCNQ4 currents with and without KCNQ channel openers. Conductance-voltage relations were derived from tail current recordings as shown in Supporting Information Figure S2 and normalized to maximum currents derived from Boltzmann fits to the data. Continuous lines indicate a Boltzmann fit to the averaged data. Fits to current-voltage relation of individual measurements yielded V_h -21.8 ± 2.0 mV for controls, -31.7 ± 2.7 mV with retigabine, -33.4 ± 2.9 mV with ZnP, and -64.0 ± 2.5 mV with ZnP/Ret (all openers at 10 μ M). Current-voltage relationships for BMS-204352 and flupirtine are shown in Supporting Information Figure S1. (E) Summary of the shifts of the half-maximal voltage of activation (ΔV_h) induced by application of KCNQ openers, calculated from recordings as in (D). Flupirtine, retigabine and BMS-204352 exhibited modest shifts (approximately -10 to -20 mV), ZnP (-26.7 ± 3.3 mV) and ZnP/Ret (-47.8 ± 2.9 mV) extremely shifted voltages of activation to hyperpolarized potentials. (Numbers of cells for all panels were 11 flupirtine, 11 retigabine, 12 BMS-204352, 11 ZnP and 8 ZnP/Ret)

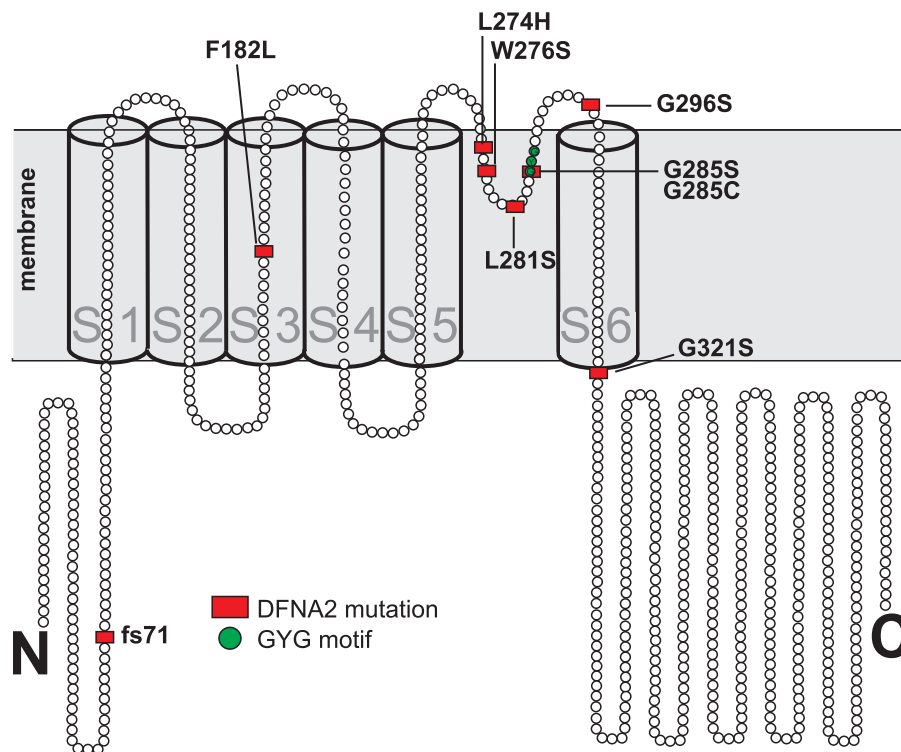


Figure 2

Topology of DFNA2-relevant mutations in the KCNQ4 channel protein. Point mutations described as causative for DFNA2 are presented in red and the K⁺ channel pore motif glycine–tyrosine–glycine (GYG) is depicted in green.

($EC_{50} = 2.9 \mu\text{M}$), retigabine ($EC_{50} = 3.7 \mu\text{M}$), BMS-204352 ($EC_{50} = 3.5 \mu\text{M}$), and for ZnP ($EC_{50} = 6.8 \mu\text{M}$) (Supporting Information Figure S1). Thus, $10 \mu\text{M}$ produced saturating or nearly saturating effects for all openers and this concentration was therefore used in the further studies. Figure 1C shows that current potentiation was stronger at hyperpolarized voltages, with highest current gain observed with ZnP/Ret. The voltage-dependence of current enhancement resulted from a shift of the voltage-dependence of activation to hyperpolarized potentials for all openers, as reported previously (Figure 1D) (Schroder *et al.*, 2001; Tatulian *et al.*, 2001; Xiong *et al.*, 2007). Taken together these results show that combined application of ZnP/Ret produced the strongest amplification of KCNQ4 currents. By enhancing steady-state conductance at 0 mV by a factor of approximately 11 (Figure 1B,C), and by shifting the voltage of half-maximal activation from -21.8 ± 2.0 mV to -64.0 ± 2.5 mV (Figure 1D,E), ZnP/Ret-mediated current potentiation amounted to more than 200-fold at -40 mV (Figure 1C). These results are consistent with a previous report, showing strong and additive enhancement of KCNQ currents by ZnP and retigabine via distinct molecular interaction sites in the channel protein (Xiong *et al.*, 2008). In fact, the shift in voltage sensitivity by ZnP/Ret produced currents that closely resembled the native $I_{K,n}$ currents from OHCs, which are characterized by their unique negative activation range (Supporting Information Figure S2) (Mammano and Ashmore, 1996; Marcotti and Kros, 1999; Oliver *et al.*, 2003).

KCNQ4 mutations in the pore region cannot be restored by ZnP/Ret

We next explored whether channel openers might be able to rescue channel function of the various KCNQ4 loss-of-function mutants that cause DFNA2 (Figure 2). To this end, we used the combination of ZnP and retigabine that exhibited the highest efficacy in potentiation of the wt channel.

Figure 3 summarizes the effects of ZnP/Ret ($10 \mu\text{M}$ both) on KCNQ4 channels carrying mutations within or close to the pore. None of the mutant channels produced detectable currents when expressed in CHO cells, consistent with previous reports (Kubisch *et al.*, 1999; Holt *et al.*, 2007; Baek *et al.*, 2011; Kim *et al.*, 2011). Application of the channel opener combination did not uncover detectable currents for W276S, L281S and G285S (Figure 3A–E, G). In cells transfected with the G296S mutant subunits ZnP/Ret produced small outward currents (approximately 1 pA/pF at 0 mV) that were clearly identified as KCNQ-mediated currents, since they were abolished by the KCNQ antagonist XE991 ($10 \mu\text{M}$; Figure 3D,G). However, equivalent currents were also found in non-transfected cells (Figure 3E, G) and thus most likely arise from a minuscule expression of endogenous channels that is uncovered by the KCNQ openers. Apparently, expression of the pore mutants (W276S, L281S and G285S) suppressed endogenous currents by the dominant-negative effect described previously (Kubisch *et al.*, 1999; Holt *et al.*, 2007). In contrast to these mutations, channel dysfunction of G296S

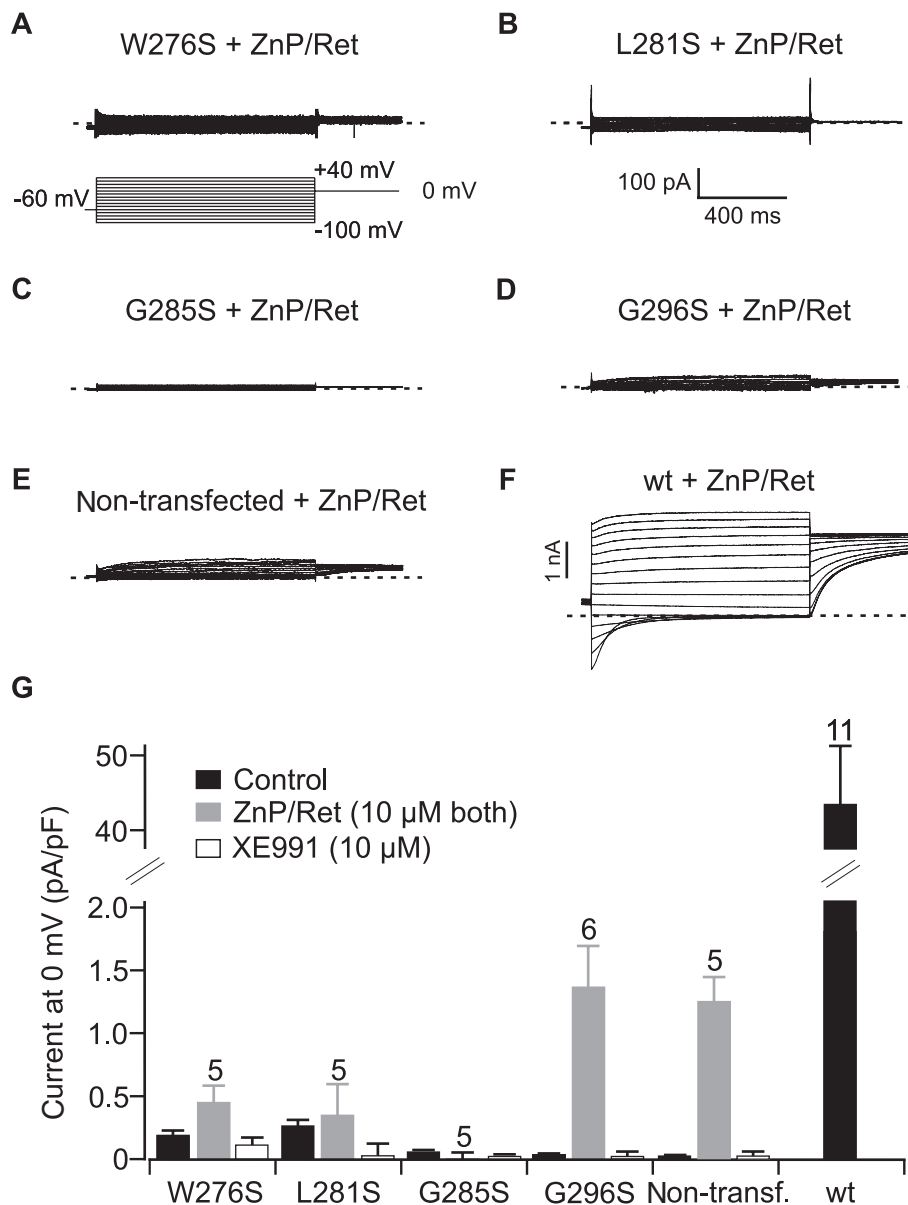


Figure 3

KCNQ4 mutations in the pore region cannot be rescued by ZnP/Ret. (A–E) Representative currents measured from cells expressing the DFNA2 mutations W276S (A), L281S (B), G285S (C) and G296S (D), and from non-transfected CHO cells (E) in the presence of ZnP/Ret (10 μM each). Scale bars apply to (A–E). Voltage protocol as indicated in (A). (F) wt KCNQ4 currents in the presence of ZnP/Ret. Voltage protocol as indicated in (A). Note the different current scaling. (G) Summarized steady-state current densities at 0 mV obtained from experiments as in (A–F), under control conditions, with ZnP/Ret and during subsequent application of the KCNQ antagonist XE991. None of the mutations produced substantial currents either in the absence or presence of ZnP/Ret. Application of the openers revealed small currents in non-transfected cells and in cells transfected with G296S that most likely arose from endogenous expression of KCNQ-like channels in CHO cells (see text). Note the compressed axis scaling for wt currents.

appeared not to interfere with the function of the endogenous channels, in line with a recent report of defective membrane targeting of this mutation (Mencia *et al.*, 2008). It should be noted that the currents recorded from non-transfected CHO cells or cells transfected with G296S were extremely small when compared with wt KCNQ4 currents (Figure 3D–G).

Taken together, these experiments show that homomeric KCNQ4 channels composed of subunits carrying a mutation

in or close to the pore region cannot be rescued by application of the most potent KCNQ openers tested in this study, ZnP/Ret.

Partial restoration of channel function of a mutation in the proximal C-terminus

Two DFNA2 mutations have been identified within or close to transmembrane regions distinct from the pore structure (F182L and G321S, respectively; see Figure 2) (Coucke *et al.*,

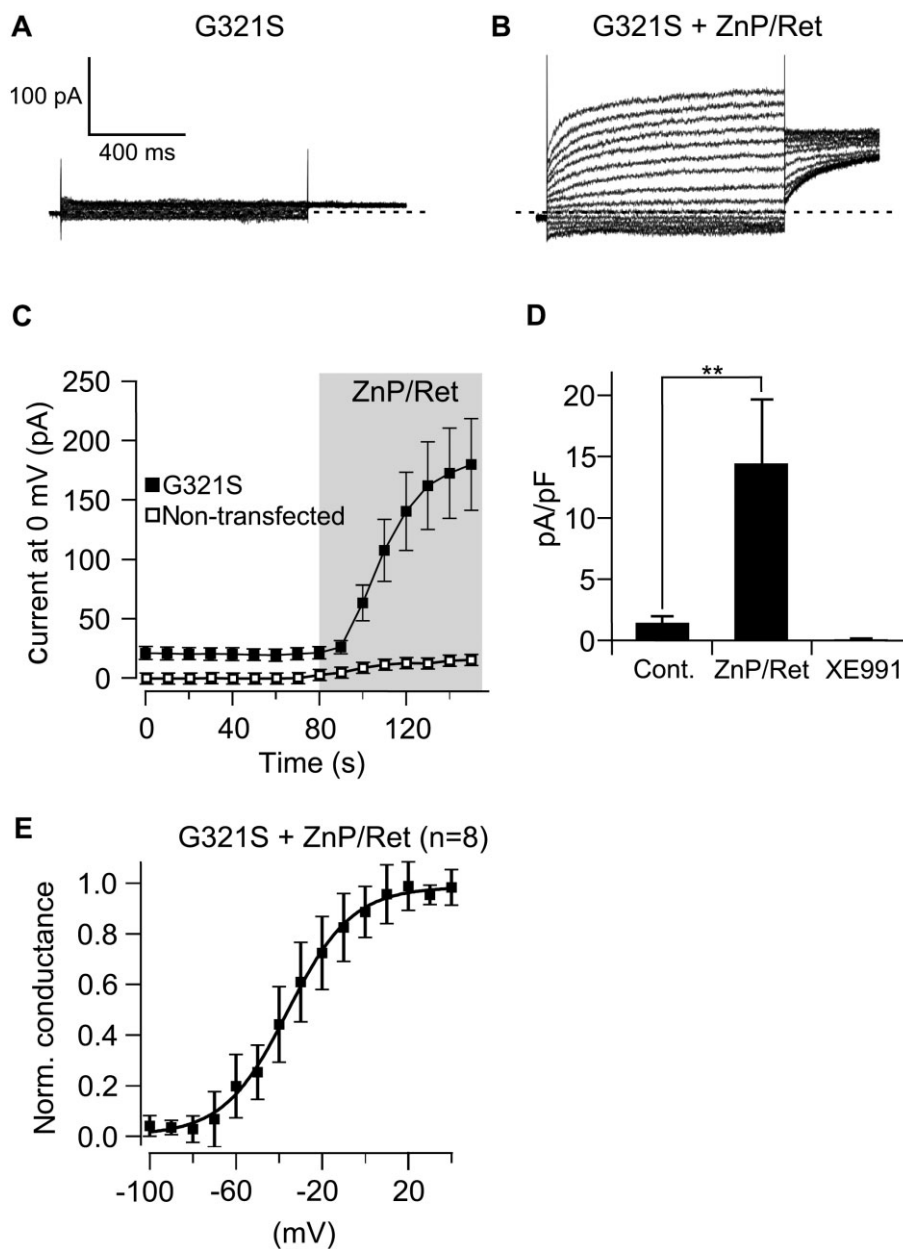


Figure 4

Partial rescue of a KCNQ4 mutation in the proximal C-terminus by ZnP/Ret. (A, B) Representative recordings from the same CHO cell transfected with KCNQ4-G321S under control conditions (A) and in the presence of ZnP/Ret (10 μ M both) (B). Voltage protocol as in Figure 3. (C) Time course of current potentiation by application of ZnP/Ret in cells transfected with KCNQ4-G321S ($n = 14$) and in non-transfected CHO cells ($n = 5$). Steady-state currents were measured at 0 mV. (D) Average current densities obtained from the experiments shown in (C). Potentiated currents were fully blocked by XE991 (10 μ M, $n = 14$). (E) Voltage-dependence of G321S-mediated currents in the presence of ZnP/Ret. Conductance-voltage relations were derived from tail current recordings as shown in (B) and derived from Boltzmann fits to the data (see Figure 1 and Supporting Information Figure S2). Continuous line indicates a Boltzmann fit to the averaged data. Fits to current-voltage relation of individual measurements yielded $V_n = -36.0 \pm 4.3$ mV and $k = -14.8 \pm 1.2$ mV ($n = 8$). Currents without channel openers were too small to determine voltage-dependence.

1999; Su *et al.*, 2007). We reasoned that these mutant channels may be more promising targets for functional restoration by channel openers.

The G321S mutation is located at the interface of S6 and the cytoplasmic C-terminus, which we refer to as the proximal C-terminus (see Figure 2) (Coucke *et al.*, 1999). Consis-

tent with a recent report (Kim *et al.*, 2011), homomeric KCNQ4-G321S did not produce clearly detectable voltage-dependent currents under control conditions (Figure 4A,C). However, a standing outward current at 0 mV was apparent that was significantly larger than in non-transfected cells (1.5 ± 0.6 pA/pF, $n = 14$; Figure 4A,C and D). Application of

ZnP/Ret (10 μ M both) elicited substantial voltage-activated outward currents of 14.4 ± 5.1 pA/pF (at 0 mV; $n = 14$; Figure 4B–E). These currents were significantly larger than the endogenous KCNQ-like currents induced by ZnP/Ret in non-transfected CHO cells (Figure 4C) and were blocked by XE991 (Figure 4D), unequivocally identifying them as carried by KCNQ4-G321S. These G321S-mediated currents activated at somewhat more hyperpolarized voltages than KCNQ4 wt currents under control conditions ($V_h = -36.0 \pm 4.3$ mV, slope = -14.8 ± 1.2 mV, $n = 8$, $P \leq 0.01$; Figure 4E). ZnP/Ret potentiated G321S-mediated currents 15- to 20-fold, yielding a conductance that was about 40% of wt currents in the absence of channel openers (also see Figure 3G). Yet, the ZnP/Ret-augmented G321S conductance was sufficient to hyperpolarize CHO cells from a membrane potential of -25.4 ± 0.7 mV to -50.3 ± 4.0 mV ($n = 8$; $P \leq 0.001$), which is indistinguishable from the membrane potential of cells expressing wt KCNQ4 (-48.5 ± 2.3 mV, $n = 12$; $P = 0.50$). Taken together, the current amplitudes, voltage-dependence, and subsequent hyperpolarization of CHO cells demonstrate the partial restoration of G321S channel function by ZnP/Ret.

We also examined F182L, a DFNA2 mutation located in the third transmembrane domain of KCNQ4 (Su *et al.*, 2007). In line with recent findings (Kim *et al.*, 2011), current amplitudes and voltage-dependence of this mutation were indistinguishable from wt KCNQ4. Similar to wt, application of ZnP/Ret (10 μ M) shifted the voltage range of activation to hyperpolarized voltages and potentiated F182L currents (Supporting Information Figure S3). Apparently, in the case of the F182L mutant impaired channel conductance is not the cause for deafness. We therefore did not investigate this mutation further.

ZnP/Ret rescues KCNQ4 from dominant-negative suppression by DFNA2 mutations

DFNA2 is a dominantly inherited disease, i.e. a single mutant KCNQ4 allele is sufficient to severely affect function of the channel. On the molecular level, the dominant nature of these loss-of-function mutations can be explained by the tetrameric structure of the channels. Thus, channel function may be disrupted by a single mutant subunit per tetrameric channel complex. If wt and mutant subunits are synthesized at the same level and assemble in a stochastic manner, this leaves only one functional (i.e. homomeric wt) channel out of 16 (6.25%), yielding a strong dominant-negative effect of the mutation. Indeed, stoichiometric co-expression of KCNQ4 with DFNA2 mutants resulted in strong suppression of channel activity (Kubisch *et al.*, 1999; Holt *et al.*, 2007), supporting this model. Moreover, in a mouse model heterozygous for the DFNA2 mutation (G285S) the native KCNQ4 equivalent in OHCs, I_{K_n} , was strongly diminished in a manner compatible with this dominant-negative action (Kharkovets *et al.*, 2006). We therefore tested for effects of channel openers on KCNQ4 currents suppressed by dominant-negative inhibition. To this end, wt KCNQ4 was co-expressed with subunits carrying mutations in the selectivity filter motif, GYG (G285S), near the channel pore (W276S), or in the proximal C-terminus (G321S) (Figure 2).

As reported previously (Kubisch *et al.*, 1999; Holt *et al.*, 2007; Baek *et al.*, 2011; Kim *et al.*, 2011), co-expression of mutant subunits with wt KCNQ4 strongly reduced current

amplitudes compared with wt currents alone (Figure 5A–C). Supporting Information Figure S4 confirms that this current reduction was not simply due to the lower amount of wt DNA used for transfection in these experiments, as wt current amplitudes were unaffected by decreasing the amount of DNA amount to the same level used in co-transfection experiments. Thus, the current reduction resulted from a dominant-negative interaction of the mutant channel subunits with the wt subunits. Co-expression of wt KCNQ4 with the pore mutants (1:1) reduced current densities at 0 mV to $2.4 \pm 0.3\%$ (wt/G285S; 1.0 ± 0.1 pA/pF, $n = 6$) and $5.7 \pm 1.7\%$ (wt/W276S; 2.3 ± 0.5 pA/pF, $n = 8$) of wt currents (obtained from the same batches of cells, Supporting Information Figure S4) (Figure 5A–C, lower panel). This is roughly compatible with the 6% (1/16) of functional homomeric wt channels expected to result from the assembly of co-synthesized wt and mutant subunits, assuming that co-assembly into tetrameric channels is stochastic and that a single mutated subunit is sufficient to abolish ion conductance of a channel (Kubisch *et al.*, 1999; Holt *et al.*, 2007). As shown in Figure 5A and B, application of ZnP/Ret (10 μ M each) strongly potentiated these residual currents to 18.9 ± 6.8 pA/pF (wt/G285S; $n = 6$) and 28.5 ± 4.7 pA/pF (wt/W276S; $n = 8$). These potentiated current amplitudes were statistically indistinguishable from wt control currents in the absence of channel openers (43.5 ± 7.8 pA/pF, $n = 5$, Supporting Information Figure S4 for the same batch of cells), indicating full compensation for dominant-negative suppression of channel function by ZnP/Ret. Similar to the pore mutants, co-expression of the G321S mutant suppressed wt KCNQ4 currents (to 5.3 ± 2.1 pA/pF at 0 mV, $12.2 \pm 2.7\%$ of wt; $n = 7$; Figure 5C, top and lower panel). Interestingly, the remaining current was larger than the 6.3% of wt currents expected from disrupted channel function by a single mutant subunit. ZnP/Ret robustly increased these currents to 75.2 ± 16.5 pA/pF ($n = 7$; Figure 5, C lower panel), which was even larger than wt control currents in the absence of channel openers. In addition to the strong enhancement of maximum current amplitude, restored currents from cells co-expressing mutant and wt channels exhibited negatively shifted activation ranges, similar to ZnP/Ret-potentiated wt currents (Figure 5D,E).

How do openers rescue current amplitudes from dominant-negative suppression?

The channel population under conditions of dominant-negative suppression by DFNA2 mutants consists of homomeric mutant channels, homomeric wt channels and heteromeric channels containing both wt and mutant subunits. As shown above, ZnP/Ret strongly activates the homomeric wt channels and potentiates homomeric G321S channels but has no effect on homomeric pore mutant channels (G285S and W276S; Figures 2 and 3). However, at this point it is not clear if the current potentiation, in the dominant-negative situation may also comprise the restoration of activity of otherwise dysfunctional heteromeric wt/mutant channels.

To address this issue we first consider the degree of current enhancement. ZnP/Ret increased currents from cells co-expressing wt and pore mutant channels by factors of 17.3 ± 4.5 ($n = 6$; wt/G285S) and 15.1 ± 2.8 ($n = 8$;

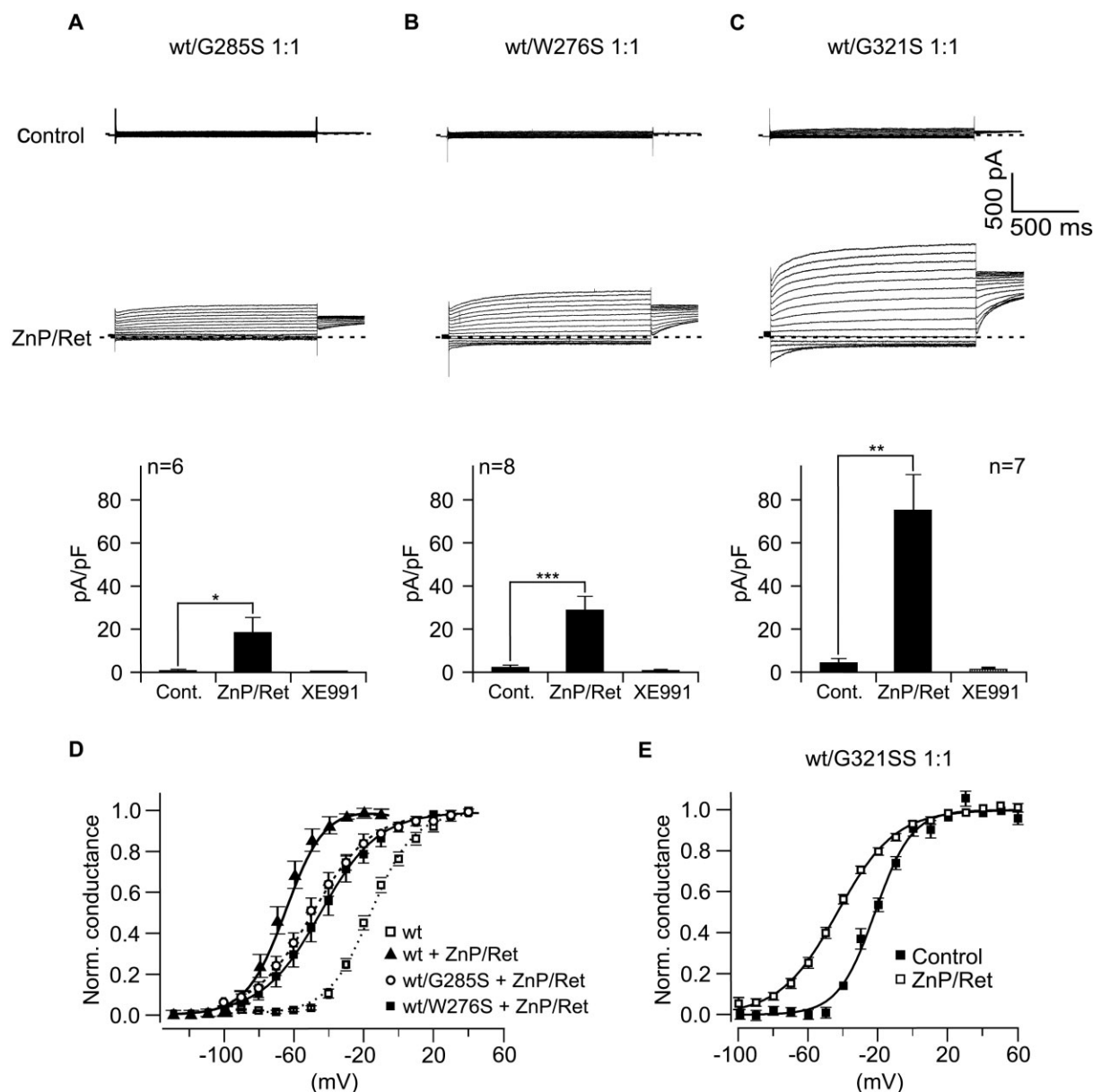
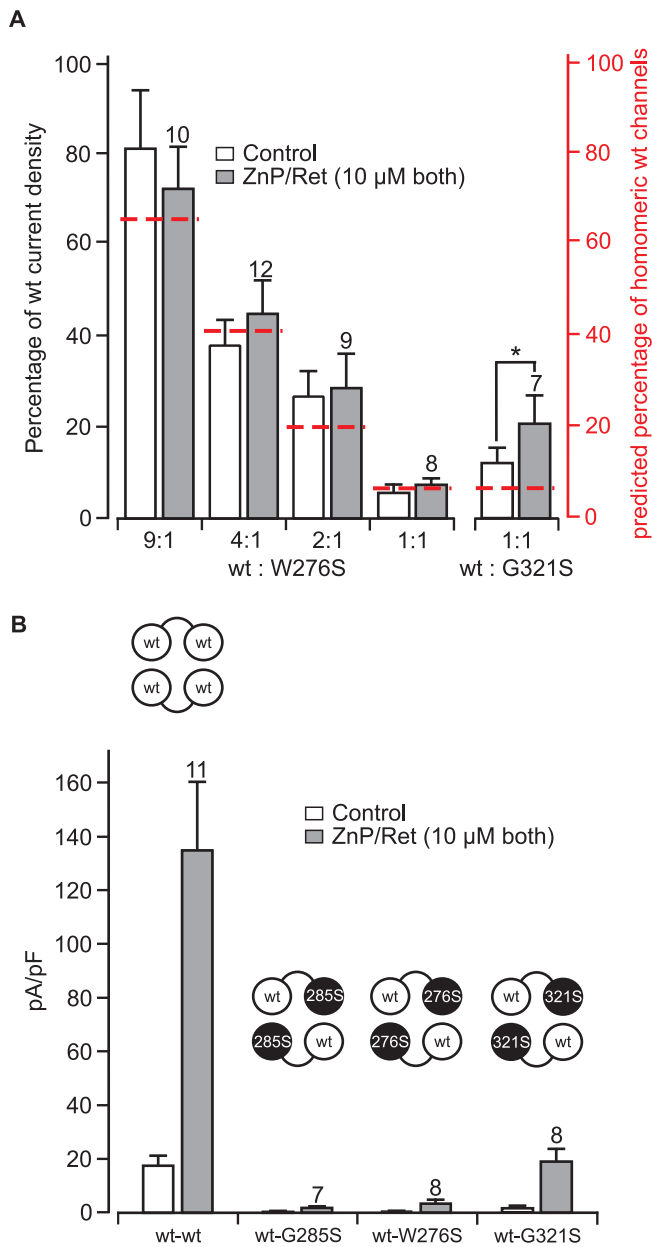


Figure 5

ZnP/Ret rescues KCNQ4 currents from dominant-negative inhibition. (A–C) Representative recordings from cells co-transfected with wt KCNQ4 and the DFNA2 mutants indicated. Current amplitudes were strongly suppressed by co-expression of the mutant channel subunits (upper panels). Application of ZnP/Ret (10 μ M both) strongly increased currents for all three mutants (middle panel; same cells). Voltage protocol as presented in Figure 3. Lower panels summarize current densities (at 0 mV) before and during application of ZnP/Ret and after application of XE991 (10 μ M). (D) Voltage-dependence of ZnP/Ret-induced currents in cells co-transfected with KCNQ4 wt and G285S or W276S, obtained from experiments as in (A and B): $V_h = -49.1 \pm 4.0$ mV, $n = 6$ (wt/G285S); $V_h = -46.8 \pm 3.4$ mV, $n = 8$ (wt/W276S). Under control conditions, currents were too small to reliably determine current-voltage relations. Conductance-voltage curves from wt KCNQ4 without and with ZnP/Ret ($V_h = -64.0 \pm 2.5$ mV) are shown for comparison. (E) Conductance-voltage relations were determined from cells co-expressing wt KCNQ4 and G321S as in (C) before ($V_h = -22.2 \pm 1.2$ mV) and during application of ZnP/Ret ($V_h = -43.5 \pm 1.2$, $n = 7$).

wt/W276S). This is similar to the 11-fold increase in current densities obtained with wt channels (11.4 ± 2.0 -fold; $n = 11$; see Figure 1). Therefore, the restored current may be explained solely by potentiation of the residual homomeric wt channels without the need to invoke a functional restoration of channels containing one or more mutant subunits.

However, since the above values of current enhancement may be spurious due to the minute residual current amplitudes in the absence of openers, we aimed at a more robust and quantitative examination of the degree of current enhancement. To this end, we titrated the relation between homomeric and heteromeric channel tetramers by



systematically varying the ratio of wt and W276S plasmids transfected into the cells.

As shown in Figure 6A, variation of the wt-to-mutant ratio from 9:1 to 1:1 resulted in an incremental suppression of whole-cell currents. For each plasmid ratio, the remaining current under control conditions (normalized to the current from cells expressing only wt homomers; Figure 6A, open columns) matched well with the predicted fraction of homomeric wt channels (Figure 6A, red axis), assuming random assembly of channel subunits and a linear relation between concentration of plasmid and synthesis of the respective subunit (9:1 $81.4 \pm 12.6\%$; 4:1 $38.1 \pm 5.4\%$; 2:1 $26.9 \pm 5.4\%$; 1:1 $5.7 \pm 1.7\%$). This finding strongly supports the previous notion that only homomeric wt channels are functional under these conditions, i.e. a single mutant subunit close to the pore region is sufficient to render the tetrameric channel non-functional (Kubisch *et al.*, 1999; Holt *et al.*, 2007). Simi-

Figure 6

For pore mutants, extrication from dominant-negative inhibition is mediated by activation of residual wt channels. (A) Co-expression of KCNQ4 wt with mutant subunits reduced whole cell currents by dominant-negative inhibition. Currents were recorded from CHO cells co-transfected at the indicated ratios of wt to mutant plasmid. Current densities recorded under control conditions are presented normalized to wt control current densities recorded from control cells transfected with wt plasmid only. Currents measured with ZnP/Ret are normalized to wt current densities in the presence of the same openers. For each subunit co-expression ratio of wt and the pore mutant W276S, the level of control and potentiated currents matched the predicted fraction of residual homomeric wt channels (red dashed lines), indicating that only homomeric wt channels contributed to the currents under all conditions. In contrast, for co-expression of wt subunits with G321S (1:1), current levels normalized to pure wt currents exceeded the predicted fraction of homomeric wt channels (calculated fractions: 9:1 65.6%; 4:1 41.0%; 2:1 19.9%; 1:1 6.3%). (B) Current densities of KCNQ4 channels assembled from tandem concatamers in the absence and presence of KCNQ4 channel openers. Insets indicate the subunit stoichiometry of channels assembled from the respective concatameric constructs.

larly, the ZnP/Ret-potentiated current also agreed closely with the predicted fraction of homomeric wt channels for each subunit ratio (Figure 6A, grey columns) (9:1 $72.1 \pm 9.3\%$; 4:1 $45.5 \pm 6.6\%$; 2:1 $29.2 \pm 7.0\%$; 1:1 $7.6 \pm 1.3\%$).

These results suggest that in the dominant-negative situation both control and opener-enhanced currents are mediated exclusively by the residual homomeric wt channels, since the fraction of currents did not increase upon application of the channel opener. Consequently, all channels containing at least one pore mutant subunit are non-conducting and cannot be rescued by the channel openers. The rescue of dominant-negative suppression by pore mutants therefore occurs through exclusive activation of the small fraction of homomeric wt channels.

Notably, the proximal C-terminal mutant, G321S, showed a different behaviour. In cells co-expressing wt and G321S (1:1), currents in the presence and absence of ZnP/Ret were larger than the predicted fraction of homomeric wt channels (Figure 6A). This suggests that in the case of G321S, channels containing mutant subunits may be functional under control conditions and furthermore can be activated by ZnP/Ret. These findings are fully consistent with the current recovered in homomeric G321S channels (Figure 4) (control 1:1 $12.2 \pm 2.7\%$; ZnP/Ret $21.0 \pm 3.2\%$).

Finally, we directly tested the sensitivity of heteromeric wt : mutant channels to the channel openers. Homogeneous populations of heteromeric channels were achieved by generation of concatamer of a wt and a mutant subunit, which were expected to assemble into tetramers containing two wt and two mutant subunits (Figure 6B). Channels assembled from wt : wt concatamer exhibited currents indistinguishable from monomeric wt channels, and were potentiated by ZnP/Ret to the same degree (10.3 ± 2.4 , $n = 11$; Figure 6B) as wt KCNQ4 assembled from monomeric subunits. Expression of wt:W276S or wt:G285S concatamer did not produce detectable currents. Moreover, application of ZnP/Ret did not produce currents beyond those seen in non-transfected cells, indicating that these channels containing pore mutant sub-

units cannot be activated by the channel agonists. In contrast, wt:G321S concatamer showed small currents under control conditions, and application of ZnP/Ret uncovered robust KCNQ currents. Thus heteromeric channels containing G321S subunits are not fully dysfunctional and can be restored, at least partially, by KCNQ channel openers (Figure 6B).

In conclusion, these data show that KCNQ channel openers can rescue the whole-cell KCNQ4 conductance from suppression by dominant-negative mutant subunits. For pore mutants, the recovery exclusively relies on the activation of residual homomeric wt channels. For the proximal C-terminal mutation, potentiation probably involves channels of all wt : mutant proportions and accordingly is stronger.

Chemical KCNQ openers potentiate native $I_{K,n}$ in OHCs

In DFNA2, OHC degeneration and deafness in heterozygotes results from the substantial suppression of the native KCNQ4-mediated current, $I_{K,n}$ by a dominant-negative action of the mutant subunits (Kubisch *et al.*, 1999; Kharkovets *et al.*, 2000; 2006; Holt *et al.*, 2007). Our findings suggest that KCNQ channel openers, by removing this suppression, are a promising strategy for the stabilization of $I_{K,n}$ in DFNA2. Since native $I_{K,n}$ and recombinant KCNQ4 show marked biophysical differences (Mammano and Ashmore, 1996; Kubisch *et al.*, 1999; Marcotti and Kros, 1999; Kharkovets *et al.*, 2006) (see Supporting Information Figure S2), we next examined the effects of KCNQ openers on $I_{K,n}$.

Figure 7 summarizes the potentiation of native $I_{K,n}$ by retigabine (10 and 100 μ M), BMS-204352, ZnP and ZnP/Ret (all applied at 10 μ M). We quantified tail currents at -120 mV from voltage-steps ranging from -160 to -20 mV before and during application of KCNQ openers to measure pure $I_{K,n}$ currents not contaminated by other OHC currents that activate at more positive potentials (Figure 7A-D) (Mammano and Ashmore, 1996; Kubisch *et al.*, 1999; Marcotti and Kros, 1999; Oliver *et al.*, 2003), as demonstrated recently (Leitner *et al.*, 2011). Under control conditions $I_{K,n}$ currents were activated at around -110 mV with V_h of -75.7 ± 1.3 mV ($n = 26$; Figure 7A,E). Application of chemical openers robustly augmented current amplitudes and shifted voltage-dependence to hyperpolarized potentials (Figure 7C). Figure 7D shows relative current increase upon application of chemical KCNQ openers. Retigabine and ZnP/Ret (all 10 μ M) robustly increased $I_{K,n}$ currents 1.4-fold (at -60 mV) to 2.2-fold (at -110 mV) with no relevant differences at physiological membrane potentials between the substances tested. Both substances quite specifically augmented $I_{K,n}$ without involvement of other OHC potassium currents, since XE991-insensitive currents were not affected by the openers, as we recently reported (Leitner *et al.*, 2011). Interestingly, BMS-204352 was barely effective, especially at membrane potentials around -70 mV, despite its high efficacy at potentiating KCNQ4-mediated currents in CHO cells. Since BMS-204352 failed to potentiate $I_{K,n}$ and thus is unlikely to be useful in the case of DFNA2, we did not further investigate the effects of this substance on native OHCs.

As for heterologous KCNQ4 channels, KCNQ openers shifted voltage-dependence of $I_{K,n}$ to hyperpolarized potentials (Figure 7E,F). These shifts were comparable for retigabine

at 10 and 100 μ M to V_h of -86.0 ± 3.3 mV ($n = 9$) and -92.1 ± 2.0 mV ($n = 8$), respectively, and for ZnP/Ret (both 10 μ M) to -92.5 ± 3.29 mV ($n = 11$). In contrast, ZnP and BMS-204352 produced rather modest shifts of V_h to -79.7 ± 4.4 mV ($n = 6$) and -82.0 ± 3.5 mV ($n = 8$), respectively. These data show that 10 μ M retigabine is a saturating concentration, yielding comparable sensitivities for this chemical opener for $I_{K,n}$ as for heterologous KCNQ4. Additionally, the recordings suggest equal sensitivity of $I_{K,n}$ for ZnP and retigabine, without additional current potentiation by the combination of the two substances (see also Figure 1) (Xiong *et al.*, 2008). This is also represented by the average shifts of V_h by the openers: Application of retigabine resulted in V_h shifts of -14.0 ± 1.7 mV ($n = 8$) and -15.4 ± 0.9 mV ($n = 8$) at 10 and 100 μ M, respectively. Similarly, ZnP/Ret shifted V_h by -17.2 ± 1.9 mV ($n = 11$) (Figure 7F), which was not higher than the effect of retigabine alone. This is in strong contrast to heterologous KCNQ4, and suggests retigabine has equivalent effects on OHCs to ZnP/Ret. Thus, retigabine may be used to stabilize the KCNQ conductance in OHCs, similar to ZnP/Ret for heterologous KCNQ4.

Discussion

Here we showed for the first time that synthetic channel openers can functionally rescue KCNQ4-mediated currents from deafness-causing mutations. While homomeric pore mutant channels remained non-functional even in the combined presence of ZnP/Ret, these openers were able to activate channels carrying the DFNA2-related mutation, G321S, located in the proximal C-terminus. Moreover, ZnP/Ret rescued KCNQ4 currents from dominant-negative suppression by co-expressed mutant channel subunits irrespective of the specific mutant, that is, both with pore mutants and the mutant located in the proximal C-terminus. For the pore mutants the restored function resulted exclusively from potentiation of the small population of channels assembled from wt channel subunits. Current enhancement in the case of G321S also involved activation of channels containing mutant subunits.

Implications of the rescue of DFNA2 mutants

In DFNA2, patients suffer from slowly progressing hearing loss that amounts to severe to profound deafness (Kharkovets *et al.*, 2006; Smith and Hildebrand, 2008). As KCNQ4 mediates the predominant K^+ conductance of OHCs, $I_{K,n}$, DFNA2 most likely results from OHC dysfunction. Indeed, a mouse model for KCNQ4 shows progressive OHC degeneration and hearing loss (Kharkovets *et al.*, 2006). KCNQ4 is also expressed in inner hair cells, where it mediates an $I_{K,n}$ -like conductance (Kharkovets *et al.*, 2000; Oliver *et al.*, 2003). Yet, this inner hair cell current seems to be less critical, since IHC function was not impaired in the KCNQ4 knock-out mouse model (Kharkovets *et al.*, 2006). Apart from sensory hair cells, KCNQ4 is also expressed in various neurons along the central auditory pathway (Kharkovets *et al.*, 2000; Beisel *et al.*, 2005); however, it is currently not known whether neuronal defects contribute to the pathology of DFNA2. Given the importance of KCNQ4 for the maintenance of hearing, the restoration of

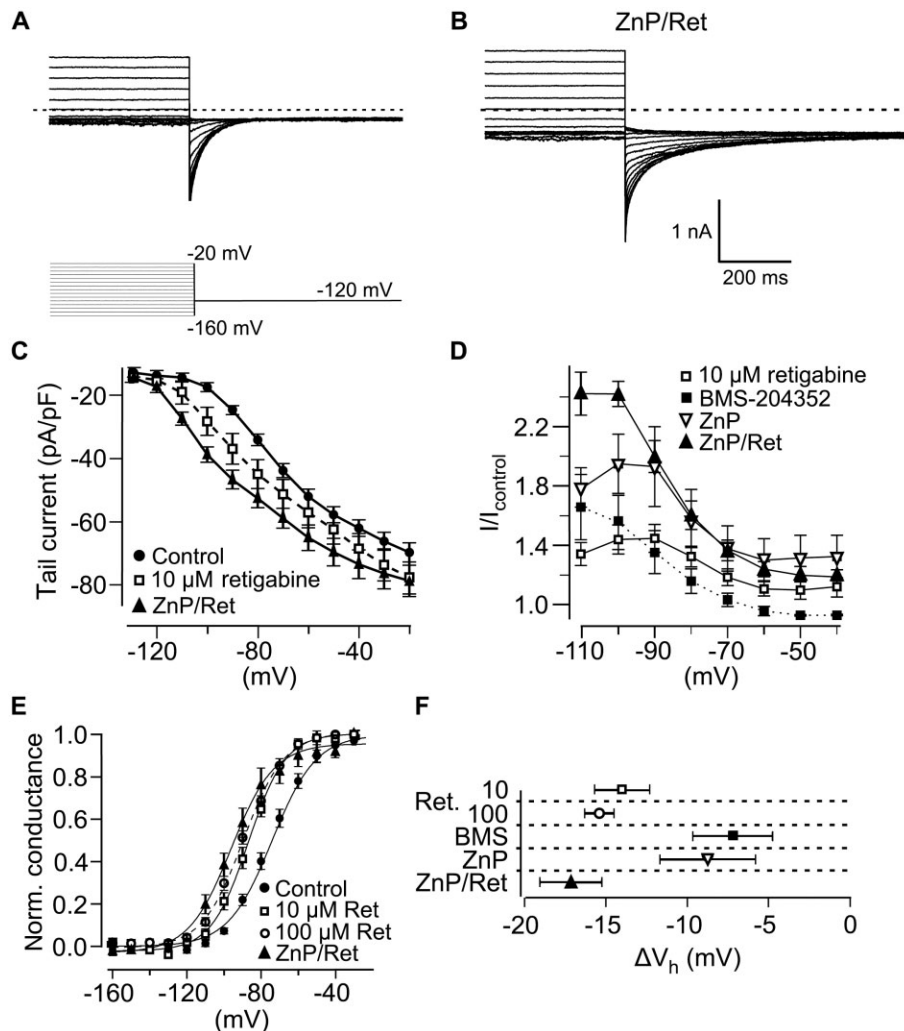


Figure 7

Native $I_{K,n}$ in OHCs is sensitive to chemical KCNQ openers. (A, B) Representative recordings of $I_{K,n}$ currents from an OHC before (A) and during application of ZnP/Ret (10 μ M each) (B). Scale bars and voltage protocol apply to (A) and (B). (C) Summary of tail current densities recorded as in (A, B) in presence of retigabine and ZnP/Ret (all 10 μ M). Retigabine and ZnP/Ret increased $I_{K,n}$ current amplitudes and shifted voltages of activation to hyperpolarized voltages. (D) Potentiation of $I_{K,n}$ by KCNQ openers (all 10 μ M). The relative current potentiation at different holding potentials is presented, calculated from tail currents as in (A–C). (E) Hyperpolarizing shifts in the voltage-dependence of $I_{K,n}$ currents induced by chemical openers. Voltage-dependence was derived from tail currents as in (C), normalized to the maximal current and fitted to a Boltzmann function. Under control conditions V_h was -75.7 ± 1.3 mV ($n = 26$), and was shifted to -82.0 ± 3.5 mV by BMS-204352 (10 μ M; $n = 8$), to -86.0 ± 3.3 mV by 10 μ M retigabine ($n = 9$), to -92.1 ± 2.0 mV by 100 μ M retigabine ($n = 8$), to -79.7 ± 4.4 mV by ZnP (10 μ M; $n = 6$), and to -92.5 ± 3.29 mV by ZnP/Ret (10 μ M; $n = 11$). (F) Averaged shifts of half-maximal voltages of activation (ΔV_h) upon application of the various KCNQ openers obtained from the data shown in (E).

channel function by chemical channel openers immediately suggests that these compounds may be of clinical use to stabilize the KCNQ conductance and prevent or retard OHC loss. It is worth noting that since DNFA2 is a dominant deafness, most patients present with a heterozygous genotype. Pathology therefore usually results from dominant-negative suppression of channel function by the mutant channel subunits transcribed from the mutated allele (Kubisch *et al.*, 1999; Holt *et al.*, 2007; Smith and Hildebrand, 2008). Here we demonstrated essentially full restoration of currents in this situation, at least in a heterologous expression system. Thus, enhancement of KCNQ4-mediated cur-

rents by channel openers might be a therapeutic option for most DFNA2 patients irrespective of the particular mutation in the KCNQ4 gene.

Native $I_{K,n}$ currents were potentiated by chemical openers similar to heterologously expressed KCNQ4, but current gain was substantially smaller. Since the action of the openers includes a substantial shift in the activation voltage range to more hyperpolarized potentials, the degree of current potentiation that can be reached *in vivo* must also depend on the membrane potential (V_M) of OHCs. The V_M of OHCs *in vivo* is not known precisely. While it has been reported as about -80 mV (Mammano and Ashmore, 1996; Marcotti and Kros,

1999), which is close to the half-activating voltage of $I_{K,n}$, V_M might be much more depolarized *in vivo* due to the large depolarizing transducer conductance that is lost with the usual recording conditions *in vitro* (He *et al.*, 2004; Johnson *et al.*, 2011). The lower efficacy of openers on the native channel may impose a limitation to any therapeutic use of channel openers, unless activators with higher potency are found. However, it should be noted that in human DFNA2, hearing loss is slowly progressive (Smith and Hildebrand, 2008) and its progressive nature was recapitulated in a mouse model. Hearing loss in mice heterozygous for the dominant-negative pore mutation G285S progressed significantly slower than after full deletion of KCNQ4 (Kharkovets *et al.*, 2006). Thus, even the minute current levels retained under dominant-negative suppression of KCNQ-mediated currents are obviously sufficient to substantially delay hair cell degeneration. Hence, even a moderate enhancement of native $I_{K,n}$, as observed with the channel openers, may provide significant protection against hair cell loss in DFNA2. We expect that chemical KCNQ openers enhance the current of residual wt channels in the dominant-negative mouse model (Kharkovets *et al.*, 2006) as also seen for native $I_{K,n}$ in OHCs. However, if this current increase is sufficient to delay the onset of hearing loss or even protect OHCs from degeneration, this should be further investigated directly *in vivo*.

Another issue that deserves attention is the finding that channel openers examined here do not only act on KCNQ4 channels within the inner ear but also strongly potentiate M-currents mediated by KCNQ2, -3 and -5 subunits in many central and peripheral neurons (Xiong *et al.*, 2007; Lv *et al.*, 2010). Of note, ZnP alone showed the highest potency for KCNQ4 as compared with other KCNQ isoforms (Xiong *et al.*, 2007). However, the various openers available to date have different potencies towards KCNQ4 and also differ in their potencies towards the different KCNQ isoforms (Schroder *et al.*, 2001; Tatulian *et al.*, 2001; Xiong *et al.*, 2007), suggesting that it may be possible to develop openers with higher specificity for KCNQ4.

Mechanism of current enhancement

It was shown previously that ZnP increases the open probability of KCNQ channels, rather than altering single channel conductance (Xiong *et al.*, 2007). This indicates that ZnP, and most likely other KCNQ openers, are primarily modifiers of channel gating, which is consistent with the shifted voltage-dependence observed here and in previous studies (Schroder *et al.*, 2001; Tatulian *et al.*, 2001; Xiong *et al.*, 2007). DFNA2 mutations may abolish channel function via different mechanisms: most obviously, mutations in the channel pore are expected to impair ion permeation, rendering channels constitutively non-functional independent of channel gating. This is consistent with our observation that KCNQ openers were completely ineffective in uncovering any channel activity in the pore mutants. For the mutation in the proximal C-terminus, G321S, there is no obvious reason to expect an impairment of ion permeation, as this region does not contribute to the pore structure. It seems more likely that this mutation disrupts channel gating, since in KCNQ channels, the C-terminus mediates channel gating by various physiological signals, including phosphatidylinositol(4,5) bisphosphate (Hernandez *et al.*, 2008; 2009), Ca^{2+} -calmodulin

(Gamper *et al.*, 2005) and phosphorylation (Li *et al.*, 2004). Consistent with this hypothesis, we found that the gating modifiers, ZnP/Ret, partially restored channel activity in G321S, but not in homomeric or heteromeric pore mutant channels.

Recently, disruption of targeting to the plasma membrane has been proposed as an alternative explanation for the dysfunction of DFNA2 mutants, including the pore mutations and G321S (Mencia *et al.*, 2008; Kim *et al.*, 2011). Such a mechanism would also be consistent with the lack of effect of channel openers on the pore mutants. However, the ZnP/Ret-induced currents through KCNQ4-G321S clearly show trafficking of this mutant channel to the plasma membrane, although we cannot exclude a reduction of surface expression.

Pharmacological properties and the molecular nature of $I_{K,n}$

There is strong evidence indicating that the OHC current $I_{K,n}$ is mediated by KCNQ4 channels (Marcotti and Kros, 1999; Kharkovets *et al.*, 2000; 2006; Holt *et al.*, 2007; Oliver *et al.*, 2003). Nevertheless, the functional properties of $I_{K,n}$ differ from those of heterologously expressed KCNQ4 channels in various aspects. Most strikingly, the activation voltage of $I_{K,n}$ is much more negative and the activation kinetics are faster (Mammano and Ashmore, 1996; Marcotti and Kros, 1999). Here we show that the differences extend to the pharmacological properties. Thus, current potentiation by retigabine, ZnP, and a combination of both openers was much less pronounced with $I_{K,n}$ than with heterologously expressed KCNQ4. Similarly, the drug-induced hyperpolarizing shift in the voltage of activation was smaller for the native channel. The differential sensitivity to channel openers is particularly pronounced for BMS-204352: this opener produced a 10-fold potentiation of recombinant KCNQ4 at saturating voltages, but was essentially ineffective on native $I_{K,n}$.

The molecular basis of these differences has remained elusive so far. An attractive hypothesis, however, is that $I_{K,n}$ characteristics result from the presence of as yet unknown accessory subunits within the native ion channel complex. KCNE β -subunits are obvious candidates for such accessory subunits, as they co-assemble with KCNQ α -subunits and are determinants of biophysical and pharmacological channel properties (McCrossan and Abbott, 2004). KCNE expression has been detected in the cochlea and all KCNE isoforms appear to co-assemble with KCNQ4 upon heterologous expression (Strutz-Seebohm *et al.*, 2006). However, none of the KCNE1-5 isoforms alters the biophysical properties of KCNQ4 currents in a manner consistent with the native current, $I_{K,n}$ (Strutz-Seebohm *et al.*, 2006). Another possibility is that native $I_{K,n}$ channels may be heteromeric KCNQ3/KCNQ4 channels (Kubisch *et al.*, 1999). Among the KCNQ channels, KCNQ3 is least sensitive to channel openers (Xiong *et al.*, 2007; 2008) and might decrease the sensitivity of KCNQ4 in the heteromers. In OHCs, the expression of KCNQ3 cannot be excluded unequivocally (Kubisch *et al.*, 1999; Jentsch, 2000; Kharkovets *et al.*, 2006). Thus, we tested the properties of heteromeric channels in CHO cells co-transfected with KCNQ3 and KCNQ4. Voltage-dependence and sensitivity towards channel openers of KCNQ3/4 heteromers were not different from homomeric KCNQ4

channels, indicating that co-assembly with KCNQ3 in OHCs cannot explain the unusual pharmacological and biophysical properties of $I_{K,n}$ (Supporting Information Figure S5). Thus, the molecular underpinnings of the native current remain unknown.

Mechanistically, one explanation for the relative insensitivity of $I_{K,n}$ might be that endogenous hair cell-specific modifiers of gating increase open probability via the same mechanism that is exploited by the synthetic channel openers, thereby occluding additive effects. In fact, recombinant KCNQ4 in the presence of ZnP/Ret closely resembles the native current in terms of voltage-dependence and kinetics (Supporting Information Figure S2). One prerequisite for the dramatic current enhancement by channel openers is the low open probability of KCNQ channels even at saturating voltages (Li *et al.*, 2005). For recombinant KCNQ4, ZnP was shown to increase the open probability at 0 mV from 0.01 to 0.33 (Xiong *et al.*, 2007). The similarity of $I_{K,n}$ with KCNQ4 currents potentiated by ZnP/Ret may indicate high basal open probabilities of the native channels. For pharmacological restoration of $I_{K,n}$ in DFNA2, a high endogenous open probability may pose a fundamental obstacle, as it limits the enhancement that can be reached. Therefore, it will be interesting to see, if basal open probabilities of native channels mediating $I_{K,n}$ are indeed higher than those of the corresponding channel in an expression system.

In conclusion, we have shown that the dominant-negative suppression of ion channel function underlying hearing loss in DFNA2 can be overcome using synthetic channel openers. Beyond hereditary deafness, KCNQ channel openers may prove useful in forms of deafness that involve hair cell loss, as we have recently shown that ZnP and retigabine can also antagonize the suppression of $I_{K,n}$ by ototoxic aminoglycoside antibiotics (Leitner *et al.*, 2011).

Acknowledgements

The authors gratefully acknowledge the kind gift of KCNQ4 cDNA constructs from Dr. T.J. Jentsch (Berlin, Germany) and thank S. Petzold for excellent technical assistance, and B. Wilke and A.K. Schlusche for generating KCNQ4 mutants and for performing preliminary experiments. This work was supported by a research grant of the Medical Center Giessen and Marburg, UKGM (42/2010 MR) to D.O.

Conflict of Interest

The authors have no conflict of interest to declare.

References

Akita J, Abe S, Shinkawa H, Kimberling WJ, Usami S (2001). Clinical and genetic features of nonsyndromic autosomal dominant sensorineural hearing loss: KCNQ4 is a gene responsible in Japanese. *J Hum Genet* 46: 355–361.

Alexander SP, Mathie A, Peters JA (2009). Guide to Receptors and Channels (GRAC). 4th edn. *Br J Pharmacol* 158 (Suppl. 1): S1–S254.

Baek JI, Park HJ, Park K, Choi SJ, Lee KY, Yi JH *et al.* (2011). Pathogenic effects of a novel mutation (c.664_681del) in KCNQ4 channels associated with auditory pathology. *Biochim Biophys Acta* 1812: 536–543.

Beisel KW, Nelson NC, Delimont DC, Fritzsche B (2000). Longitudinal gradients of KCNQ4 expression in spiral ganglion and cochlear hair cells correlate with progressive hearing loss in DFNA2. *Brain Res Mol Brain Res* 82: 137–149.

Beisel KW, Rocha-Sanchez SM, Morris KA, Nie L, Feng F, Kachar B *et al.* (2005). Differential expression of KCNQ4 in inner hair cells and sensory neurons is the basis of progressive high-frequency hearing loss. *J Neurosci* 25: 9285–9293.

Biervert C, Schroeder BC, Kubisch C, Berkovic SF, Propping P, Jentsch TJ *et al.* (1998). A potassium channel mutation in neonatal human epilepsy. *Science* 279: 403–406.

Charlier C, Singh NA, Ryan SG, Lewis TB, Reus BE, Leach RJ *et al.* (1998). A pore mutation in a novel KQT-like potassium channel gene in an idiopathic epilepsy family. *Nat Genet* 18: 53–55.

Coucke PJ, Van Hauwe P, Kelley PM, Kunst H, Schatteman I, Van Velzen D *et al.* (1999). Mutations in the KCNQ4 gene are responsible for autosomal dominant deafness in four DFNA2 families. *Hum Mol Genet* 8: 1321–1328.

Gamper N, Li Y, Shapiro MS (2005). Structural requirements for differential sensitivity of KCNQ K⁺ channels to modulation by Ca²⁺/calmodulin. *Mol Biol Cell* 16: 3538–3551.

He DZ, Jia S, Dallos P (2004). Mechano-electrical transduction of adult outer hair cells studied in a gerbil hemicochlea. *Nature* 429: 766–770.

Hernandez CC, Zaika O, Shapiro MS (2008). A carboxy-terminal inter-helix linker as the site of phosphatidylinositol 4,5-bisphosphate action on Kv7 (M-type) K⁺ channels. *J Gen Physiol* 132: 361–381.

Hernandez CC, Falkenburger B, Shapiro MS (2009). Affinity for phosphatidylinositol 4,5-bisphosphate determines muscarinic agonist sensitivity of Kv7 K⁺ channels. *J Gen Physiol* 134: 437–448.

Holt JR, Stauffer EA, Abraham D, Geleoc GS (2007). Dominant-negative inhibition of M-like potassium conductances in hair cells of the mouse inner ear. *J Neurosci* 27: 8940–8951.

Jentsch TJ (2000). Neuronal KCNQ potassium channels: physiology and role in disease. *Nat Rev Neurosci* 1: 21–30.

Johnson SL, Beurg M, Marcotti W, Fettiplace R (2011). Prestin-driven cochlear amplification is not limited by the outer hair cell membrane time constant. *Neuron* 70: 1143–1154.

Kamada F, Kure S, Kudo T, Suzuki Y, Oshima T, Ichinohe A *et al.* (2006). A novel KCNQ4 one-base deletion in a large pedigree with hearing loss: implication for the genotype-phenotype correlation. *J Hum Genet* 51: 455–460.

Kharkovets T, Hardelin JP, Safieddine S, Schweizer M, El-Amraoui A, Petit C *et al.* (2000). KCNQ4, a K⁺ channel mutated in a form of dominant deafness, is expressed in the inner ear and the central auditory pathway. *Proc Natl Acad Sci U S A* 97: 4333–4338.

Kharkovets T, Dedek K, Maier H, Schweizer M, Khimich D, Nouvian R *et al.* (2006). Mice with altered KCNQ4 K⁺ channels implicate sensory outer hair cells in human progressive deafness. *EMBO J* 25: 642–652.

- Kim HJ, Lv P, Sihm CR, Yamoah EN (2011). Cellular and molecular mechanisms of autosomal dominant form of progressive hearing loss, DFNA2. *J Biol Chem* 286: 1517–1527.
- Kubisch C, Schroeder BC, Friedrich T, Lutjohann B, El-Amraoui A, Marlin S *et al.* (1999). KCNQ4, a novel potassium channel expressed in sensory outer hair cells, is mutated in dominant deafness. *Cell* 96: 437–446.
- Leitner MG, Halaszovich CR, Oliver D (2011). Aminoglycosides inhibit KCNQ4 channels in cochlear outer hair cells via depletion of phosphatidylinositol(4,5)bisphosphate. *Mol Pharmacol* 79: 51–60.
- Li Y, Langlais P, Gamper N, Liu F, Shapiro MS (2004). Dual phosphorylations underlie modulation of unitary KCNQ K(+) channels by Src tyrosine kinase. *J Biol Chem* 279: 45399–45407.
- Li Y, Gamper N, Hilgemann DW, Shapiro MS (2005). Regulation of Kv7 (KCNQ) K⁺ channel open probability by phosphatidylinositol 4,5-bisphosphate. *J Neurosci* 25: 9825–9835.
- Lv P, Wei D, Yamoah EN (2010). Kv7-type channel currents in spiral ganglion neurons: involvement in sensorineural hearing loss. *J Biol Chem* 285: 34699–34707.
- Mammano F, Ashmore JF (1996). Differential expression of outer hair cell potassium currents in the isolated cochlea of the guinea-pig. *J Physiol* 496: 639–646.
- Marcotti W, Kros CJ (1999). Developmental expression of the potassium current IK,n contributes to maturation of mouse outer hair cells. *J Physiol* 520: 653–660.
- McCrossan ZA, Abbott GW (2004). The MinK-related peptides. *Neuropharmacology* 47: 787–821.
- Mencia A, Gonzalez-Nieto D, Modamio-Hoybjor S, Etxeberria A, Aranguiz G, Salvador N *et al.* (2008). A novel KCNQ4 pore-region mutation (p.G296S) causes deafness by impairing cell-surface channel expression. *Hum Genet* 123: 41–53.
- Nie L (2008). KCNQ4 mutations associated with nonsyndromic progressive sensorineural hearing loss. *Curr Opin Otolaryngol Head Neck Surg* 16: 441–444.
- Nouvian R, Ruel J, Wang J, Guitton MJ, Pujol R, Puel JL (2003). Degeneration of sensory outer hair cells following pharmacological blockade of cochlear KCNQ channels in the adult guinea pig. *Eur J Neurosci* 17: 2553–2562.
- Oliver D, Klocker N, Schuck J, Baukowitz T, Ruppertsberg JP, Fakler B (2000). Gating of Ca²⁺-activated K⁺ channels controls fast inhibitory synaptic transmission at auditory outer hair cells. *Neuron* 26: 595–601.
- Oliver D, Knipper M, Derst C, Fakler B (2003). Resting potential and submembrane calcium concentration of inner hair cells in the isolated mouse cochlea are set by KCNQ-type potassium channels. *J Neurosci* 23: 2141–2149.
- Schroder RL, Jespersen T, Christophersen P, Strobaek D, Jensen BS, Olesen SP (2001). KCNQ4 channel activation by BMS-204352 and retigabine. *Neuropharmacology* 40: 888–898.
- Schroeder BC, Kubisch C, Stein V, Jentsch TJ (1998). Moderate loss of function of cyclic-AMP-modulated KCNQ2/KCNQ3 K⁺ channels causes epilepsy. *Nature* 396: 687–690.
- Shapiro MS, Roche JP, Kaftan EJ, Cruzblanca H, Mackie K, Hille B (2000). Reconstitution of muscarinic modulation of the KCNQ2/KCNQ3 K(+) channels that underlie the neuronal M current. *J Neurosci* 20: 1710–1721.
- Singh NA, Charlier C, Stauffer D, DuPont BR, Leach RJ, Melis R *et al.* (1998). A novel potassium channel gene, KCNQ2, is mutated in an inherited epilepsy of newborns. *Nat Genet* 18: 25–29.
- Smith RJH, Hildebrand M (2008). DFNA2 nonsyndromic hearing loss. In: Pagon RA, Bird TC, Dolan CR, Stephens K (eds). *Gene Reviews* [Internet]. University of Washington: Seattle, WA. <http://www.ncbi.nlm.nih.gov/books/NBK1209/>.
- Strutz-Seeböhm N, Seeböhm G, Fedorenko O, Baltaev R, Engel J, Knirsch M *et al.* (2006). Functional coassembly of KCNQ4 with KCNE-beta- subunits in *Xenopus* oocytes. *Cell Physiol Biochem* 18: 57–66.
- Su CC, Yang JJ, Shieh JC, Su MC, Li SY (2007). Identification of novel mutations in the KCNQ4 gene of patients with nonsyndromic deafness from Taiwan. *Audiol Neurootol* 12: 20–26.
- Talebzadeh Z, Kelley PM, Askew JW, Beisel KW, Smith SD (1999). Novel mutation in the KCNQ4 gene in a large kindred with dominant progressive hearing loss. *Hum Mutat* 14: 493–501.
- Tatulian L, Delmas P, Abogadie FC, Brown DA (2001). Activation of expressed KCNQ potassium currents and native neuronal M-type potassium currents by the anti-convulsant drug retigabine. *J Neurosci* 21: 5535–5545.
- Topsakal V, Pennings RJ, te Brinke H, Hamel B, Huygen PL, Kremer H *et al.* (2005). Phenotype determination guides swift genotyping of a DFNA2/KCNQ4 family with a hot spot mutation (W276S). *Otol Neurotol* 26: 52–58.
- Van Camp G, Coucke PJ, Akita J, Franssen E, Abe S, De Leenheer EM *et al.* (2002). A mutational hot spot in the KCNQ4 gene responsible for autosomal dominant hearing impairment. *Hum Mutat* 20: 15–19.
- Van Hauwe P, Coucke PJ, Ensink RJ, Huygen P, Cremers CW, Van Camp G (2000). Mutations in the KCNQ4 K⁺ channel gene, responsible for autosomal dominant hearing loss, cluster in the channel pore region. *Am J Med Genet* 93: 184–187.
- Wang HS, Pan Z, Shi W, Brown BS, Wymore RS, Cohen IS *et al.* (1998). KCNQ2 and KCNQ3 potassium channel subunits: molecular correlates of the M-channel. *Science* 282: 1890–1893.
- Wulff H, Castle NA, Pardo LA (2009). Voltage-gated potassium channels as therapeutic targets. *Nat Rev Drug Discov* 8: 982–1001.
- Xiong Q, Sun H, Li M (2007). Zinc pyrithione-mediated activation of voltage-gated KCNQ potassium channels rescues epileptogenic mutants. *Nat Chem Biol* 3: 287–296.
- Xiong Q, Sun H, Zhang Y, Nan F, Li M (2008). Combinatorial augmentation of voltage-gated KCNQ potassium channels by chemical openers. *Proc Natl Acad Sci U S A* 105: 3128–3133.

Supporting information

Additional Supporting Information may be found in the online version of this article:

Figure S1 Chemical KCNQ openers augment heterologous KCNQ4. (A–D) Dose-response relationships of CHO cells expressing wt KCNQ4 for (A) retigabine (B) BMS-204352 (C) flupirtine and (D) zinc pyrithione. Current amplitudes at 0 mV were normalized to control currents prior the application of the KCNQ agonist, and were fitted to a Hill equation to calculate the concentration at half-maximal effect (EC_{50})

and the Hill coefficient (n). Note different potencies of current augmentation of the substances. (E, F) Voltage-dependence of heterologous KCNQ4 in presence of (E) 10 μ M BMS-204352 and (F) 10 μ M flupirtine. Conductance-voltage relations were derived from tail current recordings as shown in Supporting Information Figure S2, and currents were normalized to the maximum current and fitted by a two-state Boltzmann function. Continuous lines indicate the Boltzmann fit to the averaged data. Fits to the current-voltage relation of individual cells yielded (E) V_h under control conditions of -19.6 ± 1.9 mV, and in presence of 10 μ M BMS-204352 of -31.7 ± 1.2 mV. Note that application of BMS-204352 lowered k from -13.7 ± 3.7 to -6.0 ± 0.5 mV ($n = 7$). (F) In presence of flupirtine V_h was shifted from -17.2 ± 1.2 mV to -23.2 ± 1.2 mV ($n = 11$), without affecting the slope. (G) Summarized time course of KCNQ4 current potentiation at 0 mV by ZnP/Ret (10 μ M both, $n = 8$).

Figure S2 ZnP/Ret produces $I_{K,n}$ -like KCNQ4 currents in CHO cells. (A–C) Representative recordings of wt KCNQ4 in CHO cells (A), K^+ currents in OHCs (B) and wt KCNQ4 in presence of ZnP/Ret (10 μ M both) (C). A and C show recordings from the same cell. Voltage-protocols were as indicated. (D) Current-voltage relationship for native $I_{K,n}$ in OHCs and heterologous KCNQ4 in presence and absence of ZnP/Ret. ZnP/Ret shifted KCNQ4 currents by -40 mV to $V_h = -64.0 \pm 2.5$ mV ($n = 8$), producing an $I_{K,n}$ -like voltage range of activation ($V_h = -75.7 \pm 1.3$ mV, $n = 24$). Note that in presence of ZnP/Ret heterologous KCNQ4 currents showed marked inactivation at voltages more depolarised than +20 mV that was not further investigated in this study. Data are reproduced for comparisons from Figures 1 and 7 in the main text.

Figure S3 KCNQ4-F182L is fully functional and sensitive to ZnP/Ret. (A, B) Representative currents of the same CHO cell expressing KCNQ4-F182L. Voltage command as indicated, scale bar corresponds to A and B. Dashed lines indicate zero current. (C) Current-voltage relationship for F182L under control conditions (*black*) and with ZnP/Ret (*red*) derived from Boltzmann fits to the tail currents as recorded in (A, B). Control F182L currents showed the same voltage-dependence as wt KCNQ4 (F182L: $V_h = -18.0 \pm 1.8$ mV), and ZnP/Ret shifted voltage-dependence as for wt ($V_h = -62.9 \pm 4.7$ mV; $n = 8$). (D) KCNQ4-F182L current amplitudes at 0 mV in

presence and absence of the KCNQ channel opener. For F182L ZnP/Ret-mediated current potentiation and sensitivity to the KCNQ antagonist XE991 were similar as for wt KCNQ4.

Figure S4 KCNQ4 current amplitudes do not depend on the DNA amount used for transfection. (A, B) Co-expression experiments of wt and mutant KCNQ4 (1:1) required the halving of the DNA concentration for each plasmid used for transfection. Using equal DNA amounts in control experiments did not affect homomeric wt KCNQ4 current amplitudes. Thus reduction of current amplitudes by co-expressed mutants was caused by dominant-negative suppression of wt subunits (compare with Figure 5 in the main text). (A) Shows a representative recording of a CHO cell expressing wt KCNQ4 with half[DNA] used for transfection. (B) Current amplitudes using half[DNA] were indistinguishable from control cells using the normal amount of DNA (recordings from the same batch of cells).

Figure S5 KCNQ4 homomeric channels and KCNQ3/KCNQ4 heterotetramers show comparable sensitivity towards chemical openers. (A) Retigabine (*left panel*, 2.5 μ M) and ZnP (*right panel*, 2.5 μ M) robustly potentiated currents from CHO cells transfected either with KCNQ4 alone or co-transfected with KCNQ4 and KCNQ3. Values shown are current densities at 0 mV. Note that control currents from co-transfected cells are several folds larger than in KCNQ4-transfected cells, indicating coassembly of KCNQ3/KCNQ4 hetero-tetramers (cg. Kubisch *et al.*, 1999) (recordings from the same batch of cells). The drug concentrations were chosen close to their EC_{50} values (see Supporting Information Figure S1). (B) Current potentiation by retigabine (*left*) and ZnP (*right*) was comparable and statistically indistinguishable for KCNQ4 homomers and KCNQ3/4 heteromers. Values shown indicate relative current increase at 0 mV calculated from the same set of recordings shown in (A). (C) Current-voltage relationship for KCNQ4 homomers and KCNQ3/4 heteromers. KCNQ4 homomeric channels ($V_h = -21.7 \pm 0.8$ mV) show the same voltage-dependence as KCNQ3/4 ($V_h = -23.3 \pm 1.3$ mV; recordings from the same batch of cells).

Please note: Wiley-Blackwell are not responsible for the content or functionality of any supporting materials supplied by the authors. Any queries (other than missing material) should be directed to the corresponding author for the article.

Probing the regulation of TASK potassium channels by PI(4,5)P₂ with switchable phosphoinositide phosphatases

Moritz Lindner¹, Michael G. Leitner¹, Christian R. Halaszovich¹, Gerald R. V. Hammond² and Dominik Oliver¹

¹Institute of Physiology and Pathophysiology, Department of Neurophysiology, Philipps University, Deutschhausstrasse 1-2, 35037 Marburg, Germany

²Department of Pharmacology, University of Cambridge, Tennis Court Road, Cambridge CB2 1PD, UK

Non-technical summary The electrical activity of nerve cells is produced by the flux of ions through specialized membrane proteins called ion channels. Some ion channels can be regulated by the signalling lipid PIP₂, a component of the channels' membrane environment. Here we examine the relevance of PIP₂ for the regulation of one specific channel type, termed TASK. Many chemical transmitters in the brain change neural activity by shutting off TASK channels and it has been suggested that this results from reduction of PIP₂. By using novel techniques to alter the concentration of PIP₂ in living cells, we find that the activity of TASK is independent of PIP₂. Besides demonstrating that another signalling mechanism must control the activity of nerve cells via TASK inhibition, we delineate a general approach for clarifying the relevance of PIP₂ in many cell types and organs.

Abstract TASK channels are background K⁺ channels that contribute to the resting conductance in many neurons. A key feature of TASK channels is the reversible inhibition by Gq-coupled receptors, thereby mediating the dynamic regulation of neuronal activity by modulatory transmitters. The mechanism that mediates channel inhibition is not fully understood. While it is clear that activation of Gα_q is required, the immediate signal for channel closure remains controversial. Experimental evidence pointed to either phospholipase C (PLC)-mediated depletion of phosphatidylinositol-4,5-bisphosphate (PI(4,5)P₂) as the cause for channel closure or to a direct inhibitory interaction of active Gα_q with the channel. Here, we address the role of PI(4,5)P₂ for G-protein-coupled receptor (GPCR)-mediated TASK inhibition by using recently developed genetically encoded tools to alter phosphoinositide (PI) concentrations in the living cell. When expressed in CHO cells, TASK-1- and TASK-3-mediated currents were not affected by depletion of plasma membrane PI(4,5)P₂ either via the voltage-activated phosphatase Ci-VSP or via chemically triggered recruitment of a PI(4,5)P₂-5'-phosphatase. Depletion of both PI(4,5)P₂ and PI(4)P via membrane recruitment of a novel engineered dual-specificity phosphatase also did not inhibit TASK currents. In contrast, each of these methods produced robust inhibition of the *bona fide* PI(4,5)P₂-dependent channel KCNQ4. Efficient depletion of PI(4,5)P₂ and PI(4)P was further confirmed with a fluorescent phosphoinositide sensor. Moreover, TASK channels recovered normally from inhibition by co-expressed muscarinic M1 receptors when resynthesis of PI(4,5)P₂ was prevented by depletion of cellular ATP. These results demonstrate that TASK channel activity is independent of phosphoinositide concentrations within the physiological range. Consequently, Gq-mediated inhibition of TASK channels is not mediated by depletion of PI(4,5)P₂.

(Received 15 March 2011; accepted after revision 30 April 2011; first published online 3 May 2011)

Corresponding author D. Oliver: Institute of Physiology and Pathophysiology, Deutschhausstrasse 2, 35037 Marburg, Germany. Email: oliverd@staff.uni-marburg.de

Abbreviations CHO, Chinese hamster ovary; Ci-VSP, *Ciona intestinalis* voltage-sensitive phosphatase; GPCR, G-protein-coupled receptor; m1R, muscarinic m1 acetylcholine receptor; Oxo-M, oxotremorine-M; PH, pleckstrin homology; PI, phosphoinositide; PI(4)P, phosphatidylinositol-4-phosphate; PI(4,5)P₂, phosphatidylinositol-4,5-bisphosphate; PLC, phospholipase C; TIRF, total internal reflection fluorescence.

Introduction

TWIK-related acid sensitive potassium channels (TASK-1 and TASK-3) are members of the two-pore-domain potassium channel (K_{2P}) family (Duprat *et al.* 1997; Rajan *et al.* 2000). They are constitutively open K^+ -selective 'background' channels that dominate the resting or 'leak' K^+ conductance in many cells, thereby setting membrane potential and basal electrical properties (reviewed in Enyedi & Czirjak, 2010). TASK channels are broadly expressed in diverse neuronal populations throughout the central nervous system (Talley *et al.* 2001), but also in many peripheral tissues, e.g. adrenal cortex (Czirjak *et al.* 2000) and heart (Putzke *et al.* 2007).

Both TASK-1 and TASK-3 channels are potently inhibited by receptors that signal through the Gq/11 subgroup of G-proteins, including muscarinic acetylcholine receptors, metabotropic glutamate receptors and angiotensin receptors (Enyedi & Czirjak, 2010). This inhibition is rapid and reversible. It has been observed in various native cell types and is readily reconstituted in heterologous expression systems upon co-expression of recombinant TASK with Gq-coupled receptors (e.g. Czirjak *et al.* 2000; Millar *et al.* 2000; Chemin *et al.* 2003; Chen *et al.* 2006). As TASK channels are open at resting membrane potential, their inhibition generally results in depolarization and increased excitability. A well-studied example is the cerebellar granule neuron, where TASK channels determine membrane potential and enable fast action potential firing (Millar *et al.* 2000; Brickley *et al.* 2007). Activation of Gq-coupled muscarinic m3 acetylcholine receptors and group I metabotropic glutamate receptors inhibit the TASK-mediated conductance (Boyd *et al.* 2000; Chemin *et al.* 2003), consequently changing the firing behaviour of the granule cell (Watkins & Mathie, 1996). In adrenal zona glomerulosa cells, secretion of aldosterone is promoted by the depolarization that results from inhibition of TASK-3 channels by angiotensin II via Gq-coupled AT_1 receptors (Czirjak *et al.* 2000; Enyedi & Czirjak, 2010).

The molecular mechanism that leads to TASK channel closure remains elusive (reviewed in Mathie, 2007; Enyedi & Czirjak, 2010). While there is consensus that activation of $G\alpha_q/11$ is required (Chen *et al.* 2006), two alternative Gq-dependent mechanisms have been proposed to mediate channel inhibition.

First, channel closure may result from a direct interaction of activated $G\alpha_q$ with the channel protein. This mechanism is supported, among other observations, by inhibition of TASK by active $G\alpha_q$ even in a cell-free (excised patch) system and by co-immunoprecipitation of $G\alpha_q$ with the channel protein (Chen *et al.* 2006). However, this direct interaction awaits confirmation by independent

methods and the putative molecular interaction domains have not yet been identified.

Alternatively, TASK inhibition may result from depletion of $PI(4,5)P_2$ by PLC activated downstream of $G\alpha_q$. Evidence for this model includes an activating effect of $PI(4,5)P_2$ applied to excised patches containing TASK channels and channel inhibition by scavengers of polyanionic lipids (Chemin *et al.* 2003; Lopes *et al.* 2005). Regulation of TASK channels by $PI(4,5)P_2$ is an attractive model, as activity of many ion channels strictly depends on $PI(4,5)P_2$ as a cofactor. In fact, some channel types have been shown convincingly to be controlled by $PI(4,5)P_2$ dynamics (Suh & Hille, 2008). Specifically, Gq-mediated inhibition of KCNQ (Kv7) channels, which closely resembles inhibition of TASK by the same receptors, is directly mediated by depletion of $PI(4,5)P_2$ (Suh & Hille, 2002; Zhang *et al.* 2003; Suh *et al.* 2006).

One pivotal experimental strategy to distinguish between both mechanisms has been the use of the PLC inhibitor U73122, because PLC acts downstream of $G\alpha_q$ but upstream of $PI(4,5)P_2$ concentration changes (Horowitz *et al.* 2005). However, while occlusion of receptor-mediated TASK channel inhibition by U73122 was found in some studies (Czirjak *et al.* 2001; Chemin *et al.* 2003), U73122 was ineffective according to other reports (Boyd *et al.* 2000; Chen *et al.* 2006). Thus, the involvement of PLC is contentious.

In any case, if TASK inhibition results from PLC-induced depletion of $PI(4,5)P_2$, binding of this phospholipid must be essential for maintaining channel activity and, importantly, the channel's affinity for $PI(4,5)P_2$ must be low enough to warrant disruption of the interaction by reductions in the $PI(4,5)P_2$ concentration that occur under physiological conditions, i.e. receptor-induced activation of PLC. Following this reasoning, we here employ an arsenal of newly developed methods to alter the concentrations of endogenous $PI(4,5)P_2$ and related phosphoinositides in the living cell while monitoring TASK channel activity. These genetically encoded tools allowed for the acute depletion of $PI(4,5)P_2$ without activating any of the multiple other signals generated by the Gq-mediated pathway. Neither depletion of $PI(4,5)P_2$ and $PI(4)P$ by various methods nor blocking resynthesis of $PI(4,5)P_2$ after receptor-induced depletion by PLC interfered with TASK channel activity. In contrast, all of these manoeuvres reliably down-regulated the *bona fide* $PI(4,5)P_2$ -dependent channel, KCNQ4. Our results thus provide clear evidence that TASK channel activity does not require $PI(4,5)P_2$. Consequently, inhibition by GPCRs is not mediated by depletion of phosphoinositides but by another signal within the complex Gq signalling cascade.

Methods

Molecular biology and heterologous expression

The following expression vectors were used: TASK-1 (NM_002246) and TASK-3 (NM_016601) both in pcDNA3.1; KCNQ4 (NM_004700.2) in pEGFP-C1 (Clontech Laboratories, Mountain View, CA, USA); PH_{PLC δ 1}-GFP (P51178; pEGFP-N1) or PH_{PLC δ 1}-YFP (pcDNA3); Ci-VSP in pRFP-C1 (NP_001028998.1); human m1R (NM_000738.2) in pSGHV0; Lyn₁₁-FRB in pC₄R_HE; and CF-Inp in pCFP-N1 (Suh *et al.* 2006). Duplicate PH domains from Osh2p (NM_001180078, residues 256–424) were fused in tandem at XhoI/EcoRI and HindIII/KpnI sites in pEGFP-C1 (Clontech) with a short VNSKL linker, as previously described (Balla *et al.* 2008).

Construction of pseudojanin and its mutants were based around the mRFP-FKBP12 constructs previously reported (Varnai *et al.* 2006). The constructs were built using the pEGFP-C1 plasmid backbone (Clontech), with mRFP replacing the EGFP and FKBP12 fused to the 3' end of the mRFP with a flexible linker (SGLRSRSAAAGAGGAARAALG). Next, the cytosolic catalytic fragment of *S. cerevisiae* Sac1p (NM_001179777, residues 2–517) was fused with a flexible linker (SAGG SAGGSAGGSAGGSAGGPRAQASRLDA). Finally, after a third flexible linker (GGTARGAAAGAGGAGR) residues 214–644 of the human INPP5E 5-phosphatase (NM_019892) were inserted carrying a C641A mutation to remove the prenylation site. Inactivating mutations were then inserted into these phosphatase domains by site-directed mutagenesis, and the resulting mutant named for the activity they retain. Therefore, PJ-Sac carries an inactivating point mutation of the conserved DRVL motif of INPP5E (equivalent to D556A in the full length INPP5E), and thus only Sac is active. Conversely, PJ-5ptase carries an inactivating mutation in the conserved CX₅R(T/S) motif of the Sac domain (equivalent to C392S in full-length Sac1p), thus only INPP5E 5-phosphatase domain is active. PJ-Dead carries both of these mutations, and so has no phosphatase activity.

Chinese hamster ovary (CHO) cells were plated onto glass-bottom dishes (WillCo Wells B. V., Amsterdam, the Netherlands) for total internal reflection fluorescence (TIRF) imaging or onto glass coverslips for electrophysiology and confocal microscopy. Cells were transfected with jetPEI transfection reagent (Polyplus Transfection, Illkirch, France) according to the manufacturer's instructions. For co-expression of ion channels with Ci-VSP-RFP, cells were selected for clear membrane localization of RFP. For co-expression experiments involving the rapamycin system (3 plasmids), cells were selected for robust cyan fluorescent protein (CFP) or RFP fluorescence, tagging the translocatable enzymes Inp54p or PJ, respectively. Only those cells were included in

the analysis that showed translocation of CFP or RFP, respectively, to the plasma membrane upon application of rapamycin. This behaviour indicates successful expression of both the membrane anchor (Lyn11-FRB) and the translocatable fluorescence-tagged enzyme. The presence of PLC δ 1-PH-GFP and Osh2x2-PH-GFP for TIRF measurements was evidenced by the GFP fluorescence. Successful co-expression of channels was directly confirmed by the respective currents.

Electrophysiology

Whole-cell recordings were performed with an Axopatch 200B amplifier (Molecular Devices, Sunnyvale, CA, USA) in voltage-clamp mode. Data were sampled with an ITC-16 interface (Instrutech, HEKA, Lambrecht/Pfalz, Germany) controlled by PatchMaster software (HEKA). For experiments combining patch-clamp and fluorescence imaging, an EPC10 amplifier (HEKA) was used. Currents were low-pass filtered at 2 kHz and sampled at 5 kHz. Patch pipettes were pulled from borosilicate or quartz glass and had open pipette resistances of 1 to 3 M Ω when filled with pipette solution. Intracellular (pipette) solution contained (mM): 135 KCl, 2.41 CaCl₂, 3.5 MgCl₂, 5 Hepes, 5 EGTA, 2.5 Na₂ATP and 0.1 Na₂GTP, pH 7.3 (adjusted with KOH). Free [Ca²⁺] of this solution was 100 nM, as calculated with MaxChelator (maxchelator.stanford.edu). Series resistance was <10 M Ω and was not compensated. The extracellular solution was composed as follows (mM): 144 NaCl, 5.8 KCl, 0.7 NaH₂PO₄, 5.6 glucose, 1.3 CaCl₂, 0.9 MgCl₂ and 10 Hepes, pH 7.4 (adjusted with NaOH). Experiments were performed at room temperature (~22°C).

Fluorescence imaging

TIRF imaging was performed as described elsewhere (Halaszovich *et al.* 2009). In brief, a BX51WI upright microscope (Olympus, Hamburg, Germany) equipped with a TIRF condenser (numerical aperture of 1.45; Olympus) and a 488 nm laser (20 mW; Picarro, Sunnyvale, CA, USA) was used. Fluorescence was imaged through a LUMPlanFI/IR 40 \times /0.8 NA water immersion objective (Olympus). Images were acquired with an IMAGO-QE cooled CCD camera (TILL Photonics GmbH, Gräfelfing, Germany). Wide-field fluorescence illumination was achieved with a monochromator (Polychrome IV, TILL Photonics GmbH) coupled to the BX51WI microscope through fibre optics. Green fluorescent protein (GFP) fluorescence was excited at 488 nm. The laser shutter for TIRF illumination, the monochromatic light source and image acquisition were controlled by TILLvisION software (TILL Photonics GmbH).

Confocal imaging of membrane translocation of the CF-Inp and RF-PJ constructs was performed with

an upright LSM 710 Axio Examiner.Z1 microscope equipped with a W-Plan/Apochromat 20×/1.0 DIC M27 75 mm water immersion objective (Carl Zeiss GmbH, Jena, Germany). RFP was excited at 561 nm with a diode-pumped solid-state laser (Carl Zeiss), and fluorescence emission was sampled at 582–754 nm. CFP was excited at 458 nm with an argon laser (Carl Zeiss) and emission was sampled at 454–581 nm.

Chemicals

Rapamycin was purchased as a solution in Me₂SO (from Merck KGaA, Darmstadt, Germany) and further diluted in extracellular solution to a concentration of 5 μM before use. 10,10-*bis*(4-pyridinylmethyl)-9(10H)-anthracenone (XE991; Tocris, Ellisville, USA) and oxotremorine-M (Oxo-M; Tocris) were prepared as 10 mM stock solutions in H₂O, and diluted with extracellular solution to their final concentration of 10 μM. Chemicals were delivered locally to the cells with a gravity-fed, custom-built application system.

Data analysis

Electrophysiological data were analysed using IgorPro (Wavemetrics, Lake Oswego, OR, USA) and imaging data were analysed with TILLVISION and IgorPro. Regions of interest (ROI) were defined to include the majority of a single cell's footprint. To avoid movement artifacts the margins of the cell were excluded from analysis. Normalized F/F_0 traces were calculated from the TIRF signal intensity F , averaged from the ROI, and the initial fluorescence intensity F_0 obtained before application of agonists or depolarization of the cell. Where appropriate, traces were corrected for bleaching according to a monoexponential fit to the signal decay during the pre-application interval. Fluorescence intensities were background-corrected. Time constants were obtained from monoexponential fits. All data are given as mean ± standard error of the mean (SEM), with n indicating the number of individual cells analysed. Statistical analysis was performed by ANOVA test followed by a two-tailed Dunnett t test. Significance was assigned for $P < 0.05$.

Results

Inhibition of TASK channels by Gq-coupled muscarinic receptor

When TASK-1 or TASK-3 channels were co-expressed with the Gq-coupled muscarinic m1 acetylcholine receptor (m1R) in CHO cells, application of the muscarinic agonist Oxo-M resulted in rapid and nearly complete inhibition of

TASK-mediated currents (Fig. 1A and B). After washout of Oxo-M, the current recovered to about 70% ($69.1 \pm 7.0\%$ for TASK-1 and $70.3 \pm 3.0\%$ for TASK-3) within 4 min.

It is well established that Gq-triggered activation of PLCβ can result in a pronounced decrease of the PI(4,5)P₂ concentration in the plasma membrane (e.g. Horowitz *et al.* 2005). Receptor-mediated PI(4,5)P₂ dynamics have been implicated in the regulation of numerous ion channels (Suh & Hille, 2008). Thus, it appeared that channel deactivation due to loss of PI(4,5)P₂ might be an attractive and straightforward mechanism explaining the inhibition of TASK currents by the Gq-coupled receptors, as suggested previously (Chemin *et al.* 2003; Lopes *et al.* 2005).

We tested for the putative PI(4,5)P₂ depletion in CHO cells using two distinct PI(4,5)P₂ biosensors, the GFP-fused pleckstrin homology (PH) domain of PLCδ1 (PH_{PLCδ1}-GFP (Stauffer *et al.* 1998) as an optical probe for PI(4,5)P₂, and the voltage-gated potassium channel KCNQ4 (Kv7.4). PH_{PLCδ1}-GFP specifically binds to PI(4,5)P₂ and has been used widely as a genetically encoded 'translocation biosensor' for PI(4,5)P₂. The degree of its membrane association directly reports on the concentration of PI(4,5)P₂ (Varnai & Balla, 2006). Here, we used live-cell TIRF microscopy to monitor membrane association of PH_{PLCδ1}-GFP (Halaszovich *et al.* 2009). In cells co-expressing m1R and PH_{PLCδ1}-GFP, TIRF fluorescence strongly decreased during activation of m1R, indicating dissociation of the sensor from the membrane, and thus robust depletion of PI(4,5)P₂ (Fig. 1E). Upon washout of the receptor agonist, the TIRF signal recovered, demonstrating reversibility of PI(4,5)P₂ depletion due to resynthesis of PI(4,5)P₂. It has been shown unequivocally that inhibition of KCNQ (Kv7) potassium channels by many Gq-coupled receptors results from Gq/PLC-mediated depletion of PI(4,5)P₂ (Suh & Hille, 2002; Zhang *et al.* 2003; Suh *et al.* 2006; Hernandez *et al.* 2009). In our experimental setting, homomeric KCNQ4 channels were also strongly inhibited by activation of m1R (Fig. 1C and D), confirming depletion of PI(4,5)P₂. Characteristics of inhibition resembled the inhibition observed with TASK channels: KCNQ4-mediated currents decreased by $88.0 \pm 5.5\%$ within a few seconds and recovered with a time course that matched recovery of TASK-mediated currents (Fig. 1C). However, the onset of inhibition of TASK-1 and TASK-3 occurred consistently faster than inhibition of KCNQ4 and PH_{PLCδ1}-GFP dissociation (Fig. 1E).

TASK channel activity is resistant to depletion of PI(4,5)P₂

To scrutinize the suggested role of PI(4,5)P₂ concentration changes in receptor-mediated TASK channel inhibition,

we used different molecular tools for the selective depletion of phosphoinositides in the intact cell.

First, we used the voltage-sensitive phosphoinositide phosphatase Ci-VSP (Murata *et al.* 2005; Murata & Okamura, 2007), a membrane-resident PI(4,5)

P₂-5-phosphatase, that is rapidly and reversibly activated by strong depolarization of the membrane potential. Upon activation, Ci-VSP efficiently removes PI(4,5)P₂ from the plasma membrane by dephosphorylation to PI(4)P (Halaszovich *et al.* 2009; Falkenburger *et al.* 2010).

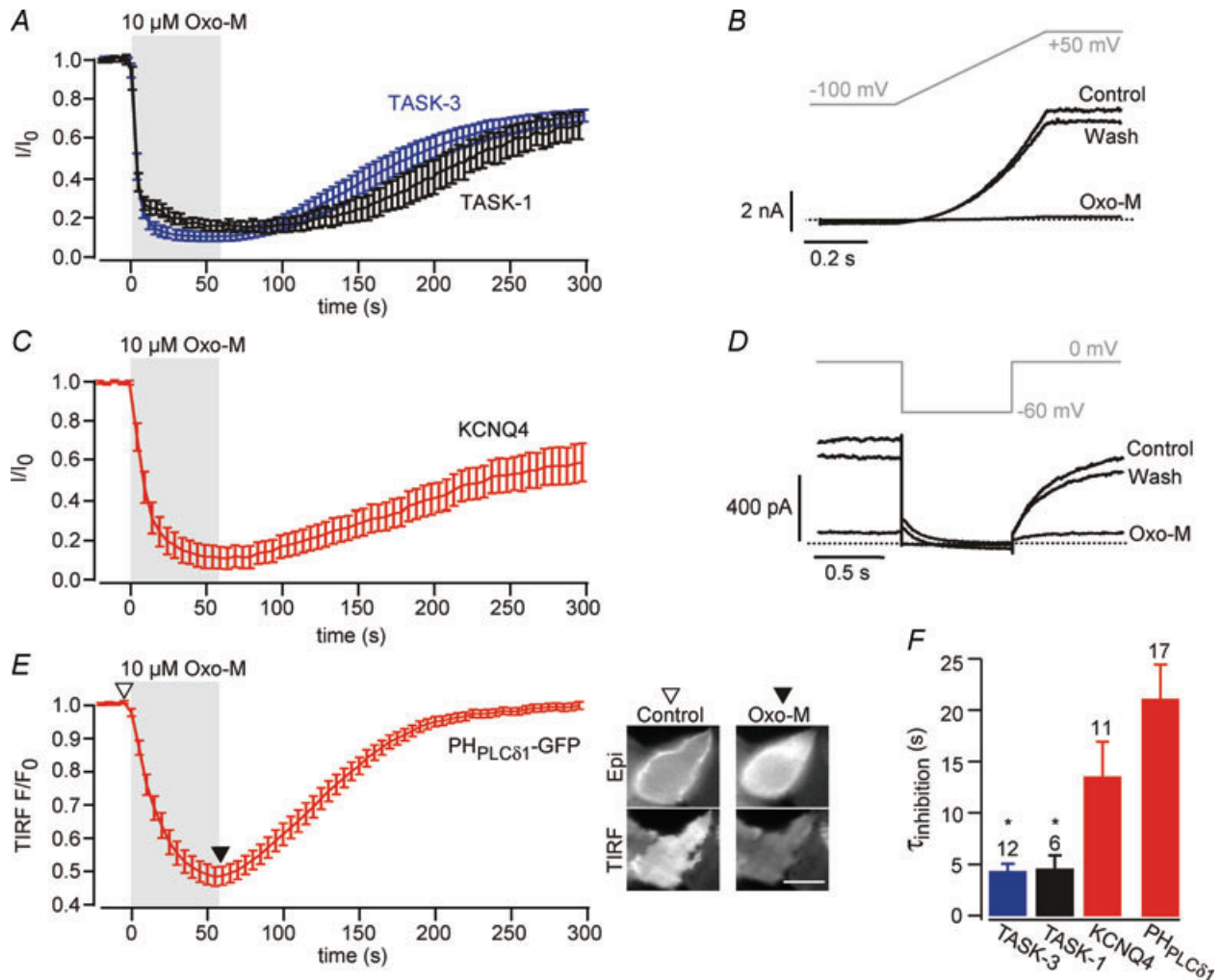


Figure 1. Receptor-mediated inhibition of TASK channels and concomitant depletion of PI(4,5)P₂

A, averaged time course of TASK currents upon activation of muscarinic m1 receptors. Data were obtained from CHO cells co-transfected with m1R and either TASK-1 ($n = 6$) or TASK-3 ($n = 12$). Application of the muscarinic agonist oxo-M ($10 \mu\text{M}$, 60 s) inhibited currents to $17.0 \pm 2.4\%$ for TASK-1 and $9.7 \pm 2.4\%$ for TASK-3. Cells were clamped at -60 mV and currents were measured in response to voltage ramps every 2 s. Traces show currents at $+50 \text{ mV}$, normalized to current amplitude prior to application for each cell before averaging. **B**, representative recordings for the experiments summarized in **A**. Current traces in response to the voltage ramp shown were obtained from a cell co-expressing m1R and TASK-3. Dashed line indicates zero current level. **C**, muscarinic inhibition of KCNQ4 channels measured from CHO cells co-transfected with m1R and KCNQ4 ($n = 11$). Currents obtained at 0 mV using the voltage step protocol shown in **D** at 5 s intervals (holding potential, 0 mV) were normalized to the current amplitude prior to application of Oxo-M for each cell before averaging. **D**, representative recordings and voltage protocol for the experiments summarized in **C**. **E**, TIRF recordings from CHO cells expressing m1R and PH_{PLC} δ 1-GFP ($n = 17$ cells from 3 independent experiments). Application of $10 \mu\text{M}$ Oxo-M triggered a strong and reversible decrease in TIRF, indicative of translocation of the GFP-fused sensor from the membrane to the cytosol. Insets show epifluorescence (upper) and TIRF image (lower panel) of a representative cell before and after application of Oxo-M. Scale bar, $10 \mu\text{m}$. **F**, average time constants of the onset of muscarinic current inhibition and of translocation of PH_{PLC} δ 1-GFP. Time constants were obtained from monoexponential fits to the data shown in (**A**–**E**). Asterisks indicate significantly faster time constants of TASK-1 and TASK-3 compared to KCNQ4 ($P \leq 0.05$).

As shown in Fig. 2A, TASK channels were completely insensitive to the activation of co-expressed Ci-VSP. After 50 s of depolarization to +80 mV, TASK-1 and TASK-3 current amplitudes were $102.0 \pm 3.2\%$ and $107.9 \pm 5.8\%$, respectively, of current amplitude before activation of Ci-VSP. In contrast, KCNQ4 currents were strongly inhibited by the same voltage protocol when co-expressed with Ci-VSP (residual current, $32.3 \pm 5.8\%$; Fig. 2A). This indicated efficient depletion of PI(4,5)P₂ by Ci-VSP, which was further confirmed by strong translocation of the fluorescent PI(4,5)P₂ probe PH_{PLC δ 1}-GFP upon depolarization (Fig. 2D).

We next applied an independent approach that was developed recently to acutely modify PI(4,5)P₂ concentrations (Suh *et al.* 2006; Varnai *et al.* 2006). Here, PI(4,5)P₂ is depleted by chemically triggered recruitment of a yeast polyphosphoinositide-5-phosphatase, Inp54p, that specifically dephosphorylates PI(4,5)P₂ at the 5' position. This method is based on the hetero-dimerization

of the FRB (FKBP/rapamycin binding) domain from mTOR and the FKBP (FK506 binding protein) in the presence of rapamycin. FRB is anchored to the plasma membrane by fusion to a membrane targeting motif from Lyn (Lyn₁₁-FRB) and Inp54p is fused to CFP-tagged FKBP (CF-Inp) (Suh *et al.* 2006). Consequently dimerization induced by the addition of rapamycin results in massive and rapid translocation of Inp54p to the membrane and thus consumption of PI(4,5)P₂. Recruitment can be monitored conveniently as the translocation of CFP fluorescence from the cytosol to the membrane (Fig. 3A, inset).

As shown in Fig. 3A, currents mediated by TASK-1 or TASK-3 were not affected by application of rapamycin to cells co-expressing either channel with Lyn₁₁-FRB and CF-Inp. For all recordings, efficient recruitment of Inp54p was verified by monitoring the translocation of CFP fluorescence to the membrane (insets). As before, we tested for depletion of PI(4,5)P₂ by rapamycin-triggered

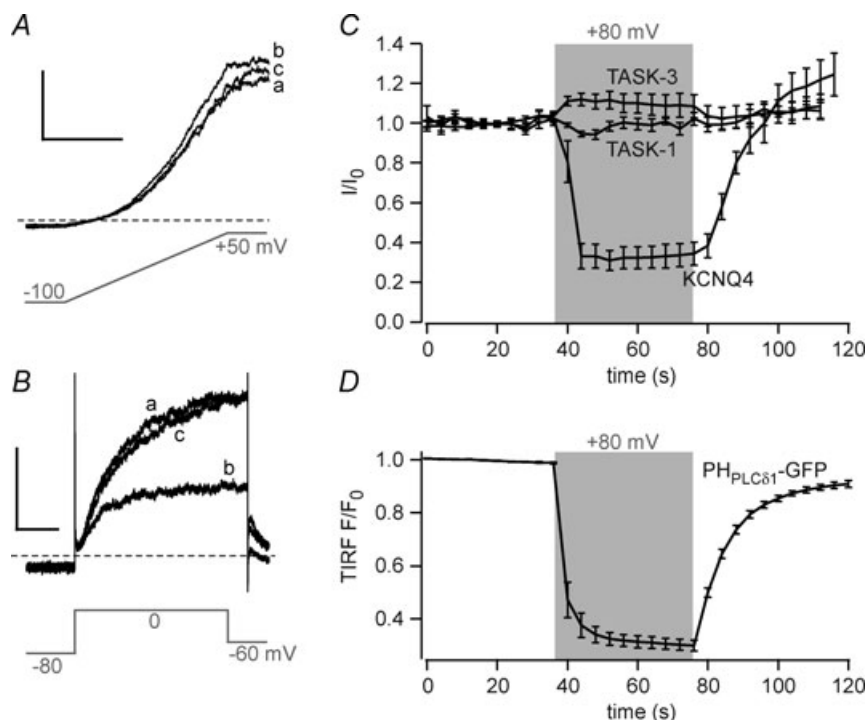


Figure 2. TASK currents are insensitive to depletion of PI(4,5)P₂ by Ci-VSP

A, representative whole-cell currents from CHO cells co-transfected with TASK-3 and Ci-VSP. Currents were recorded in response to brief voltage ramps from a holding potential of -80 mV (a). Holding potential was then depolarised to +80 mV for 40 s to activate Ci-VSP (b), followed by repolarisation to -80 mV (c). Scale bars, 0.5 nA and 100 ms. B, currents from cells co-transfected with KCNQ4 and Ci-VSP obtained with the same holding potential protocol as in A. Currents were evoked by brief intermittent voltage steps (-80 to 0 mV) as indicated. Scale bars, 0.1 nA and 200 ms. C, mean time course of currents obtained from experiments as in A and B from cells co-transfected with Ci-VSP and either TASK-1, TASK-3 or KCNQ4. The shaded area indicates depolarisation to +80 mV from an initial holding potential of -80 mV. Depolarisation induced rapid inhibition of KCNQ4 currents (to $34.1 \pm 5.8\%$ of initial current at the end of the depolarizing period; $n = 12$) but not of TASK-1 ($102.0 \pm 3.2\%$, $n = 6$) and TASK-3 ($107.9 \pm 5.8\%$, $n = 7$). Monoexponential fits to the recovery of KCNQ4 currents yielded time constants of 14.6 ± 2.2 s. D, mean TIRF intensities from voltage-clamped cells expressing Ci-VSP and PH_{PLC δ 1}-GFP obtained as in Fig. 1E ($n = 12$). Depolarization as in C induced fast and reversible translocation of the PI(4,5)P₂ probe. Monoexponential fits to the re-association of the PH domain yielded time constants of 10.2 ± 0.8 s.

translocation of Inp54p using the sensors KCNQ4 and PH_{PLC δ 1}-YFP. KCNQ4-mediated currents were robustly and rapidly suppressed by application of rapamycin to cells co-expressing KCNQ4, Lyn₁₁-FRB and CF-Inp (Fig. 3B). Rapamycin applied to cells transfected with the channel alone failed to affect current amplitude, confirming that channel inhibition resulted from recruitment of Inp54p to the membrane. Additionally, dissociation of PH_{PLC δ 1}-YFP from the membrane upon addition of rapamycin (Fig. 3C) demonstrated efficient depletion of PI(4,5)P₂ by recruitment of Inp54p.

Taken together, TASK channels remained fully active despite strong decrease in the concentration of membrane PI(4,5)P₂ in intact cells.

Combined depletion of PI(4,5)P₂ and PI(4)P does not affect TASK activity

Our experimental manipulation of PI(4,5)P₂ levels differed from receptor-mediated PI(4,5)P₂ depletion. The phosphatases used here stoichiometrically converted PI(4,5)P₂ to PI(4)P, probably keeping the overall phosphoinositide concentration in the membrane constant. In contrast, activation of PLC depletes both PI(4,5)P₂ and PI(4)P (Willars *et al.* 1998; Horowitz *et al.* 2005) without generating a structurally similar lipid. Since these two phosphoinositides constitute the majority of all phosphoinositides in the plasma membrane (Willars *et al.* 1998; Nasuhoglu *et al.* 2002), activation of Gq-coupled receptors triggers bulk depletion of phosphoinositides.

If TASK channels are activated by phosphoinositides with no or little specificity, the PI(4)P produced by Ci-VSP and Inp54p might be sufficient to sustain channel activity. We therefore sought to fully deplete both PI(4,5)P₂ and PI(4)P to closely recapitulate the changes in phosphoinositide concentrations during Gq/PLC activation, but without activating the various other cellular messengers involved in Gq signalling. We therefore used a modified heterodimerization approach, where an engineered dual-specificity phosphatase, pseudojanin (PJ), replaced Inp54p. As shown schematically in Fig. 4A, pseudojanin was engineered in analogy to the native dual-specificity phosphoinositide phosphatase synaptojanin (Mani *et al.* 2007) and consists of two functionally distinct phosphoinositide phosphatase domains separated by a linker region. The N-terminus of PJ consists of the yeast 4'-phosphatase Sac while the C-terminus harbours a human 5-phosphatase (INPP5E). To allow for rapamycin-driven membrane recruitment, PJ was fused to FKBP and mRFP (RF-PJ).

In cells co-transfected with RF-PJ and Lyn₁₁-FRB, application of rapamycin triggered efficient recruitment of PJ to the plasma membrane (Fig. 4A). The

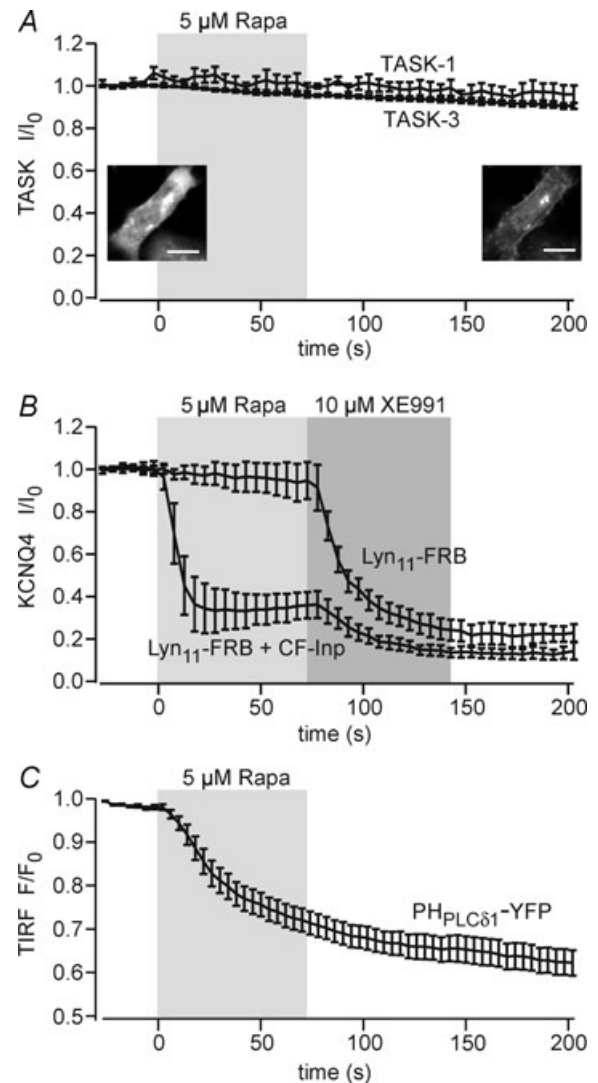


Figure 3. PI(4,5)P₂ depletion by chemically triggered recruitment of Inp54p fails to suppress TASK currents

A, normalized current amplitudes measured from cells co-expressing CF-Inp, Lyn₁₁-FRB and either TASK-1 or TASK-3. Currents were unaffected by application of rapamycin. Current amplitudes 2 min after application of rapamycin were $89.9 \pm 4.1\%$ ($n = 5$) and $89.6 \pm 2.5\%$ ($n = 6$) for TASK-1 and TASK-3, respectively. Translocation of CF-Inp to the membrane was verified for each experiment as shown in the representative confocal images before (left) and after (right) application of rapamycin. Scale bar, 10 μm . B, KCNQ4-mediated current in cells co-expressing CF-Inp and Lyn₁₁-FRB was robustly suppressed upon application of rapamycin ($n = 5$). When the translocatable phosphatase was omitted (Lyn₁₁-FRB only), currents were not affected by rapamycin, confirming current inhibition by depletion of PI(4,5)P₂. Residual currents were blocked by the KCNQ channel inhibitor, XE991. Voltage protocols used were as described in Fig. 1. C, TIRF recordings from cells co-transfected with PH_{PLC δ 1}-YFP, CF-Inp and Lyn₁₁-FRB. Application of rapamycin decreased TIRF intensity, indicating dissociation of PH_{PLC δ 1}-GFP from the membrane ($n = 15$ cells from 4 independent experiments).

resulting changes in phosphoinositide concentrations were examined by TIRF imaging of the $\text{PI}(4,5)\text{P}_2$ sensor, $\text{PH}_{\text{PLC}\delta 1}$ -GFP, and a probe for $\text{PI}(4)\text{P}$, $\text{PH}_{\text{OSH}2 \times 2}$ -GFP (Roy & Levine, 2004). The latter is a GFP-fused tandem

construct of two identical PH domains from yeast $\text{OSH}2\text{p}$ and has been shown to bind to the plasma membrane in a $\text{PI}(4)\text{P}$ -dependent manner (Balla *et al.* 2008). $\text{PH}_{\text{PLC}\delta 1}$ -GFP dissociated from the membrane upon

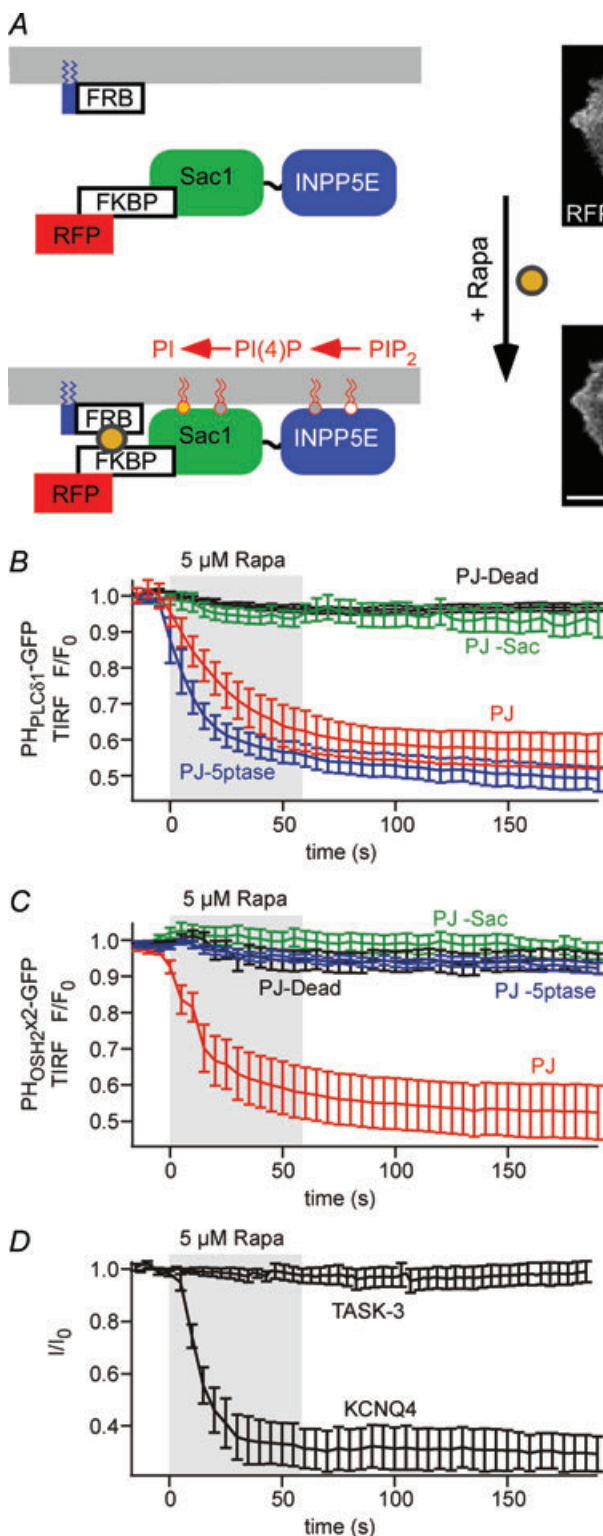


Figure 4. TASK-3 currents are insensitive to combined depletion of $\text{PI}(4,5)\text{P}_2$ and $\text{PI}(4)\text{P}$ by pseudojanin

A, schematic representation of the pseudojanin membrane targeting construct (RF-PJ) and its recruitment to the plasma membrane by rapamycin. Confocal images of RF-PJ before (top) and after addition of 5 μM rapamycin (bottom) show efficient translocation of PJ. Scale bar, 10 μm . **B**, TIRF recordings were performed on cells co-transfected with $\text{PH}_{\text{PLC}\delta 1}$ -GFP, Lyn_{11} -FRB, and either of the RF-PJ variants indicated. Dissociation of $\text{PH}_{\text{PLC}\delta 1}$ -GFP from the membrane upon application of rapamycin (shaded) was only observed with intact INPP5E 5-phosphatase domain. ($n = 9$ cells/5 independent experiments, 5/3, 10/4 and 21/8, for PJ, PJ-Sac, PJ-5ptase and PJ-Dead, respectively). **C**, TIRF recordings from cells co-transfected with $\text{PH}_{\text{OSH}2 \times 2}$ -GFP, Lyn_{11} -FRB and either of the RF-PJ variants indicated. Dissociation of $\text{PH}_{\text{OSH}2 \times 2}$ -GFP from the membrane required functional Sac1 and INPP5E phosphatase domains ($n = 14$ cells /8 independent experiments, 11/5, 15/5 and 14/21, for PJ, PJ-Sac, PJ-5ptase and PJ-Dead, respectively). **D**, whole-cell voltage-clamp recordings from cells co-transfected with Lyn_{11} -FRB, fully intact PJ and either TASK-3 or KCNQ4. While KCNQ currents were robustly inhibited by recruitment of PJ (residual currents, $30.6 \pm 7.8\%$, $n = 6$), TASK currents were not affected (residual currents, $97.4 \pm 3.9\%$, $n = 7$). Voltage protocols as shown in Fig. 1.

recruitment of PJ (Fig. 4B and C). Dissociation was also observed when the Sac1 domain was inactivated by a point mutation in its catalytic centre, but not when the INPP5E phosphatase or both phosphatase domains were inactivated by mutation. Thus, recruitment of PJ leads to depletion of PI(4,5)P₂ via its 5'-phosphatase domain. Similarly, recruitment of PJ resulted in dissociation of PH_{OSH2}×2-GFP (Fig. 4C) from the membrane. In contrast to PH_{PLCδ1}, mutational inactivation of either phosphatase domain abolished this dissociation. This indicates that PH_{OSH2}×2 can bind to PI(4,5)P₂ or PI(4)P and that the presence of only one of both phosphoinositides is sufficient for membrane localisation of this probe. However, this finding also provides clear evidence for depletion of PI(4)P by PJ recruitment. Taken together, TIRF imaging using both fluorescent probes demonstrates that rapamycin-triggered recruitment of PJ robustly and rapidly depletes both PI(4,5)P₂ and PI(4)P.

We went on to examine the effects of phosphoinositide depletion by PJ on TASK channels in cells co-expressing TASK-3 with RF-PJ and Lyn₁₁-FRB. As shown in Fig. 4D, application of rapamycin had no effect on TASK currents (remaining current, 97.4 ± 3.9%), despite successful membrane recruitment of PJ, as confirmed by association of RFP fluorescence with the plasma membrane for each recording. To independently confirm the proper activity of PJ under whole-cell patch-clamp, we also examined the effect of PJ recruitment on KCNQ4 channels. In contrast to TASK, KCNQ4-mediated currents were strongly suppressed to 30.6 ± 7.8% by PJ when subjected to the same experimental protocol (Fig. 4D). In conclusion, combined depletion of the most abundant phosphoinositides in the plasma membrane is insufficient to inhibit TASK channel activity.

Recovery from receptor-induced inhibition does not require resynthesis of PI(4,5)P₂

Finally, we probed for involvement of phosphoinositides in TASK channel regulation by interfering with the resynthesis of PI(4,5)P₂ after activation of Gq/PLC. If channel inhibition was due to PLC-mediated PI(4,5)P₂ depletion, current recovery must depend on replenishment of PI(4,5)P₂. Resynthesis occurs via sequential phosphorylation of phosphatidylinositol and PI(4)P and therefore involves ATP hydrolysis (Horowitz *et al.* 2005). The ATP requirement for recovery has previously been used as a criterion for defining involvement of PI(4,5)P₂ in the regulation of KCNQ channels (Suh & Hille, 2002).

We examined the recovery of TASK currents from inhibition by co-expressed m1R. ATP was omitted from the pipette solution and replaced by the non-hydrolysable analogue AMP-PCP, which fully prevents resynthesis of PI(4,5)P₂ as reported previously (Suh & Hille, 2002; Halaszovich *et al.* 2009). As shown in Fig. 5A, TASK3 currents recovered completely after withdrawal of the muscarinic agonist. The time course of recovery was not significantly different from control recordings obtained with 2.5 mM MgATP in the patch pipette (Fig. 5B). In contrast, recovery of KCNQ4 channels from m1R-mediated inhibition was completely abrogated by ATP removal as reported previously for KCNQ2/3 heteromeric channels (Suh & Hille, 2002). This finding confirmed that resynthesis was fully prevented and transient activation of PLC resulted in persistent depletion of PI(4,5)P₂.

In conclusion, our results demonstrate that TASK channels re-open despite maximal depletion of phosphoinositides by PLC. Consequently, channel activity

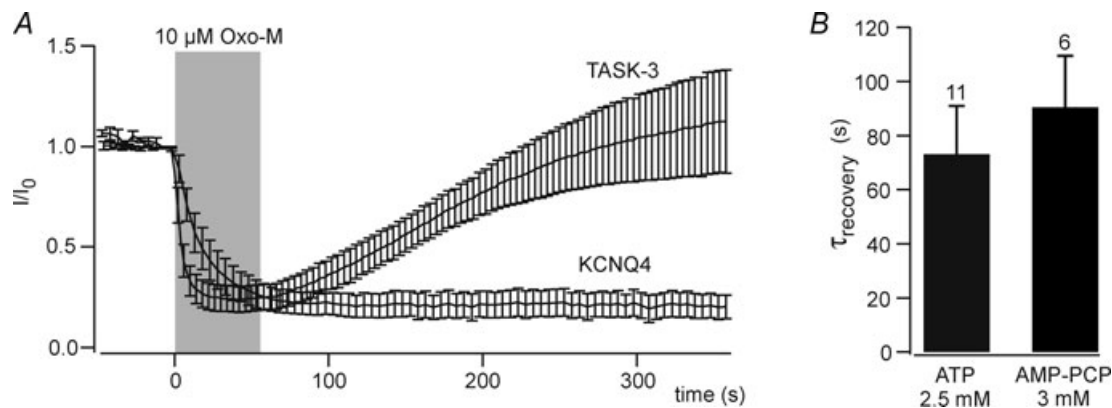


Figure 5. ATP is not required for recovery of TASK-3 currents

A, recovery of TASK-3 and KCNQ4 currents after removal of intracellular ATP. CHO cells co-expressing either TASK-3 or KCNQ4 with m1R were patch-clamped with a pipette solution containing no ATP and 3 mM AMP-PCP. Recordings were started after 4 min of dialysis with the pipette solution (TASK-3, $n = 5$; KCNQ4, $n = 6$). Voltage protocols as shown in Fig. 1. B, average time constants for recovery from muscarinic inhibition of TASK-3 were similar in the presence of 2.5 mM MgATP (data shown in Fig. 1C) or 3 mM AMP-PCP in the patch pipette. Time constants were derived from monoexponential fits to the current recovery for individual cells.

does not require PI(4,5)P₂ or other phosphoinositides, indicating that m1R-mediated current inhibition is not mediated by reduction of the concentrations of PI(4,5)P₂ or PI(4)P.

Discussion

PI(4,5)P₂ is dispensable for activity of TASK channels

We used various methods to deplete the endogenous PI(4,5)P₂ pool in living cells and consistently found no change in currents mediated by TASK-1 and TASK-3. These findings clearly demonstrate that TASK channel activity does not depend on the concentration of this phosphoinositide species in the plasma membrane.

Since this conclusion critically relies on the assumption that Ci-VSP and rapamycin-triggered recruitment of Inp54p efficiently degrade the PI(4,5)P₂ content of the membrane, it is worth considering the degree of PI(4,5)P₂ depletion achieved with these methods. We used two different sensors to follow the PI(4,5)P₂ concentration in our experimental setting: a fluorescent PI(4,5)P₂ probe that has been used extensively (PH_{PLCδ1}-GFP; (Varnai & Balla, 2006) and a PI(4,5)P₂-dependent ion channel, KCNQ4. Inhibition of KCNQ4 currents upon recruitment of Inp54p and PJ was faster than the dissociation of PLCδ1-PH-GFP (Figs 3 and 4) and current recovery was slower after activation of m1R or Ci-VSP (Figs 1 and 2). This difference may be explained by a lower apparent affinity of KCNQ4 for PI(4,5)P₂ when compared to the fluorescent sensor. In fact, less activation of Ci-VSP, and consequently a lower degree of PI(4,5)P₂ depletion, is needed to fully inhibit KCNQ4 channels than to displace PLCδ1-PH-GFP from the plasma membrane (A. Rjasanow, C. R. Halaszovich and D. Oliver, unpublished results). Notwithstanding, translocation of PH_{PLCδ1}-GFP from the membrane and inhibition of KCNQ4 channels during activation of Ci-VSP and membrane recruitment of the phosphatase quantitatively matched the responses following activation of m1R. Therefore, the degree of PI(4,5)P₂ depletion achieved with the genetically encoded tools was similar to the PLC-mediated depletion during receptor stimulation.

In agreement with our observations, recent work showed that channel inhibition by Ci-VSP and rapamycin-triggered phosphatase recruitment is remarkably consistent with the sensitivity to receptor-mediated PLC activation for other PI(4,5)P₂-regulated channels including voltage-gated calcium and potassium channels (Falkenburger *et al.* 2010; Suh *et al.* 2010). Moreover, even Kir2.1 inward rectifier K⁺ channels, which are characterized by particularly high affinity for PI(4,5)P₂ (Du *et al.* 2004), are strongly inhibited by Ci-VSP (Murata & Okamura, 2007; A. Rjasanow and D. Oliver, unpublished results). These

considerations clearly show that the genetically encoded tools used here are well suited to gauge the sensitivity of channels to PLC-mediated depletion of PI(4,5)P₂.

We further note that inhibition of TASK channels by m1R activation occurred consistently faster than inhibition of KCNQ4. The latter channel has a comparatively low affinity to PI(4,5)P₂, and is therefore highly sensitive to PLC activation (Hernandez *et al.* 2009). Thus, if depletion of PI(4,5)P₂ was causing loss of TASK channel activity due to a direct PI(4,5)P₂-channel interaction, the affinity of TASK channels for PI(4,5)P₂ would be predicted to be even lower compared to KCNQ4 and TASK would be highly sensitive to activation of the phosphatases used in our experiments. This was not the case. We therefore conclude that TASK channels are resistant to depletion of PI(4,5)P₂ within a physiological range of concentrations.

It was previously shown that application of PI(4,5)P₂ to excised membrane patches can enhance TASK-mediated currents (Chemin *et al.* 2003; Lopes *et al.* 2005). This is seemingly in contradiction to our results and has been taken to suggest a role of PI(4,5)P₂ in the regulation of these channels. However, it should be noted that our results do not necessarily exclude that a reduction of PI(4,5)P₂ to levels below those reached under physiological conditions (by PLC or phosphatases) may lead to channel closure. In other words, it remains possible that TASK channels bind PI(4,5)P₂ with a very high affinity, whereby PI(4,5)P₂ would be a permissive cofactor but not a physiological regulator of TASK (Gamper & Shapiro, 2007). Such a role of PI(4,5)P₂ may be consistent with the partial block of TASK-mediated currents by PI(4,5)P₂-scavenging polycations such as poly-lysine and neomycin observed previously (Chemin *et al.* 2003; Lopes *et al.* 2005). Alternatively, artificially high levels of PI(4,5)P₂, as may be reached by application to excised patches, may enhance TASK currents. In any case, our experiments exclude that inhibition of TASK channels by Gq-coupled receptors results from PLC-mediated depletion of PI(4,5)P₂.

A role for other phosphoinositides?

Although resistance to Ci-VSP and Inp54p unequivocally show that PI(4,5)P₂ depletion is not sufficient for channel down-regulation, it remained possible that other phosphoinositides might be involved in receptor-mediated inhibition of TASK. Specifically, PI(4)P might be relevant since it is present at similar concentrations as PI(4,5)P₂ in the resting plasma membrane and is also depleted during receptor-induced activation of PLC (Willars *et al.* 1998; Horowitz *et al.* 2005). If TASK channels had a non-selective dependence on phosphoinositides, similar to some inward rectifier K⁺ (Kir) channels (Rohacs *et al.*

1999; Tucker & Baukowitz, 2008), then activation of PI(4,5)P₂-5-phosphatases might not suffice for channel deactivation despite strong depletion of PI(4,5)P₂. In other words, the differential sensitivity of TASK to PLC *versus* phosphatases might result from the different changes in the overall concentration of phosphoinositides according to the different enzymatic activities.

To examine such a possible role of combined depletion of PI(4,5)P₂ and PI(4)P in receptor-induced TASK inhibition, we used PJ, a novel engineered dual-specificity phosphatase for dephosphorylation of PI(4,5)P₂ and PI(4)P. Recruitment of PJ to the membrane efficiently depleted both phosphoinositides as indicated by specific fluorescent sensors. However, the complete insensitivity of TASK to this manoeuvre indicated that neither PI(4,5)P₂ nor PI(4)P concentrations contribute to regulation of TASK channels by PLC. This conclusion is further strongly supported by the full reactivation of TASK channels from receptor-induced inhibition observed after substitution of ATP by the non-hydrolysable analogue AMP-PCP. Under this condition, resynthesis of PI(4)P and PI(4,5)P₂ is abrogated, resulting in persistent depletion of both phosphoinositides after activation of Gq-coupled receptors.

A TASK-associated pool of PI(4,5)P₂ inaccessible to exogenous phosphatases?

It has been suggested that the plasma membrane may harbour functionally distinct pools of PI(4,5)P₂ (Wang *et al.* 2004; Vasudevan *et al.* 2009). Such pools may correspond to PI(4,5)P₂ localized to spatially separated membrane domains, such as lipid rafts or caveolae *versus* non-raft membranes (Johnson *et al.* 2008; Cui *et al.* 2010), although such local domains are difficult to reconcile with the fast diffusion of phosphoinositides as determined in native plasma membranes (Hilgemann, 2007). Experimental findings suggested that localized PI(4,5)P₂ pools resulting from restricted diffusion may determine regulation of ion channels by PI(4,5)P₂ in cardiomyocytes (Cho *et al.* 2005). The efficient inhibition of KCNQ2/3 heteromeric channels by Gq-coupled muscarinic receptors in HEK cells required co-localization of channels and receptors to detergent-resistant membrane fractions (Oldfield *et al.* 2009). In principle, the observed differential action of receptor-activated PLC and recombinant phosphatases could be compatible with PI(4,5)P₂-mediated regulation of TASK channels, if the channels interacted with a distinct 'private' pool of PI(4,5)P₂ that is depleted by endogenous PLC but is inaccessible to the phosphatase constructs used in this study. However, any membrane pool of PI(4,5)P₂ must remain exhausted after depletion by PLC when replenishment of PI(4,5)P₂ is blocked. Therefore, such a

possibility is clearly ruled out by our finding of full current recovery in the absence of intracellular ATP.

In summary, our results obtained upon depletion of PI(4,5)P₂ and PI(4)P by exogenous phosphatases and inhibition of their resynthesis after depletion by endogenous PLC rule out a requirement of these phosphoinositides for TASK channel activity. Specifically, we conclude that the inhibition of TASK channels by Gq-coupled receptors is not mediated by depletion of phosphoinositides.

Possible mechanisms for Gq/PCR-mediated TASK channel inhibition

Since depletion of PI(4,5)P₂ can be ruled out as the signal that mediates channel closure downstream of Gq/PCR activation, which other mechanisms of channel inhibition remain? In principle, several other intermediates within the Gq-mediated signalling cascade may interact with TASK channels to induce channel closure.

The currently most complete evidence suggests that a direct interaction of activated Gαq protein (Gαq*) can deactivate TASK channels (Chen *et al.* 2006). This scenario is supported by elegant experiments including the demonstration of channel activation by purified Gαq* in excised patches and co-immunoprecipitation of Gαq* with TASK channels (Chen *et al.* 2006). However, it should be noted that previous studies demonstrated the suppression of GqPCR-mediated TASK channel inhibition by the PLC inhibitor U73122 (Czirjak *et al.* 2001; Chemin *et al.* 2003), suggesting at least a contribution of signals downstream of PLC activation. Among these signals, channel phosphorylation by PKC has been ruled out, since elimination of candidate phosphorylation sites did not impede Gq/PCR-dependent channel inhibition (Talley & Bayliss, 2002; Veale *et al.* 2007). This conclusion is supported by our current results showing that inhibition is unaffected by removal of the intracellular ATP required for phosphorylation.

Given the high physiological relevance of Gq/PCR-mediated inhibition of TASK-1 and TASK-3, further work is needed to unequivocally identify the mechanism of channel regulation.

Methods for probing the phosphoinositide regulation of ion channels

The combined methods used here provide a toolbox for probing the physiological relevance of phosphoinositides and their concentration dynamics for the regulation of ion channels. Many ion channels have been shown to be affected by PI(4,5)P₂ (Suh & Hille, 2008). However, in many cases the proposal of a functional role for PI(4,5)P₂ is solely based on the application of exogenous

phosphoinositides to excised membrane patches. In addition to TASK channels, examples for the alteration of channel behaviour by exogenous PI(4,5)P₂ include TREK channels as additional members within the K_{2P} channel family (Chemin *et al.* 2005), voltage-gated K⁺ (Kv) channels (Oliver *et al.* 2004), various TRP channels (Rohacs & Nilius, 2007) and HCN channels (Zolles *et al.* 2006), among others. As shown here, such sensitivity to applied phosphoinositides may not always provide strong evidence for a role in the regulation of channels under physiological conditions. Furthermore, pharmacological tools for alterations of phosphoinositide concentrations are poorly developed, and a control for the effectiveness of the intended changes is usually not performed. Thus, genetically encoded tools for the acute manipulation of endogenous phosphoinositide pools combined with fluorescence-based sensors for control of these manipulations should help substantially in obtaining a clearer picture of the genuine roles of PI(4,5)P₂ in ion channel regulation. Moreover, these methods are not limited to the analysis of ion channels but may be used to address the role of phosphoinositides in other cellular processes as well.

References

- Balla A, Kim YJ, Varnai P, Szentpetery Z, Knight Z, Shokat KM & Balla T (2008). Maintenance of hormone-sensitive phosphoinositide pools in the plasma membrane requires phosphatidylinositol 4-kinase III α . *Mol Biol Cell* **19**, 711–721.
- Boyd DF, Millar JA, Watkins CS & Mathie A (2000). The role of Ca²⁺ stores in the muscarinic inhibition of the K⁺ current I_{K(SO)} in neonatal rat cerebellar granule cells. *J Physiol* **529**, 321–331.
- Brickley SG, Aller MI, Sandu C, Veale EL, Alder FG, Sambhi H, Mathie A & Wisden W (2007). TASK-3 two-pore domain potassium channels enable sustained high-frequency firing in cerebellar granule neurons. *J Neurosci* **27**, 9329–9340.
- Chemin J, Girard C, Duprat F, Lesage F, Romey G & Lazdunski M (2003). Mechanisms underlying excitatory effects of group I metabotropic glutamate receptors via inhibition of 2P domain K⁺ channels. *EMBO J* **22**, 5403–5411.
- Chemin J, Patel AJ, Duprat F, Lauritzen I, Lazdunski M & Honore E (2005). A phospholipid sensor controls mechanogating of the K⁺ channel TREK-1. *EMBO J* **24**, 44–53.
- Chen X, Talley EM, Patel N, Gomis A, McIntire WE, Dong B, Viana F, Garrison JC & Bayliss DA (2006). Inhibition of a background potassium channel by Gq protein α -subunits. *Proc Natl Acad Sci U S A* **103**, 3422–3427.
- Cho H, Kim YA, Yoon J-Y, Lee D, Kim JH, Lee SH & Ho W-K (2005). Low mobility of phosphatidylinositol 4,5-bisphosphate underlies receptor specificity of Gq-mediated ion channel regulation in atrial myocytes. *Proc Natl Acad Sci U S A* **102**, 15241–15246.
- Cui S, Ho WK, Kim ST & Cho H (2010). Agonist-induced localization of Gq-coupled receptors and G protein-gated inwardly rectifying K⁺ (GIRK) channels to caveolae determines receptor specificity of phosphatidylinositol 4,5-bisphosphate signaling. *J Biol Chem* **285**, 41732–41739.
- Czirjak G, Fischer T, Spat A, Lesage F & Enyedi P (2000). TASK (TWIK-related acid-sensitive K⁺ channel) is expressed in glomerulosa cells of rat adrenal cortex and inhibited by angiotensin II. *Mol Endocrinol* **14**, 863–874.
- Czirjak G, Petheo GL, Spat A & Enyedi P (2001). Inhibition of TASK-1 potassium channel by phospholipase C. *Am J Physiol Cell Physiol* **281**, C700–C708.
- Du X, Zhang H, Lopes C, Mirshahi T, Rohacs T & Logothetis DE (2004). Characteristic interactions with phosphatidylinositol 4,5-bisphosphate determine regulation of Kir channels by diverse modulators. *J Biol Chem* **279**, 37271–37281.
- Duprat F, Lesage F, Fink M, Reyes R, Heurteaux C & Lazdunski M (1997). TASK, a human background K⁺ channel to sense external pH variations near physiological pH. *EMBO J* **16**, 5464–5471.
- Enyedi P & Czirjak G (2010). Molecular background of leak K⁺ currents: two-pore domain potassium channels. *Physiol Rev* **90**, 559–605.
- Falkenburger BH, Jensen JB & Hille B (2010). Kinetics of PIP₂ metabolism and KCNQ2/3 channel regulation studied with a voltage-sensitive phosphatase in living cells. *J Gen Physiol* **135**, 99–114.
- Gamper N & Shapiro MS (2007). Regulation of ion transport proteins by membrane phosphoinositides. *Nat Rev Neurosci* **8**, 921–934.
- Halaszovich CR, Schreiber DN & Oliver D (2009). Ci-VSP is a depolarization-activated phosphatidylinositol-4,5-bisphosphate and phosphatidylinositol-3,4,5-trisphosphate 5'-phosphatase. *J Biol Chem* **284**, 2106–2113.
- Hernandez CC, Falkenburger B & Shapiro MS (2009). Affinity for phosphatidylinositol 4,5-bisphosphate determines muscarinic agonist sensitivity of Kv7 K⁺ channels. *J Gen Physiol* **134**, 437–448.
- Hilgemann D (2007). Local PIP₂ signals: when, where, and how? *Pflugers Archiv* **455**, 55–67.
- Horowitz LF, Hirdes W, Suh B-C, Hilgemann DW, Mackie K & Hille B (2005). Phospholipase C in living cells: activation, inhibition, Ca²⁺ requirement, and regulation of M current. *J Gen Physiol* **126**, 243–262.
- Johnson CM, Chichili GR & Rodgers W (2008). Compartmentalization of phosphatidylinositol 4,5-bisphosphate signaling evidenced using targeted phosphatases. *J Biol Chem* **283**, 29920–29928.
- Lopes CMB, Rohacs T, Czirjak G, Balla T, Enyedi P & Logothetis DE (2005). PIP₂ hydrolysis underlies agonist-induced inhibition and regulates voltage gating of two-pore domain K⁺ channels. *J Physiol* **564**, 117–129.
- Mani M, Lee SY, Lucast L, Cremona O, Di Paolo G, De Camilli P & Ryan TA (2007). The dual phosphatase activity of synaptojanin 1 is required for both efficient synaptic vesicle endocytosis and reavailability at nerve terminals. *Neuron* **56**, 1004–1018.

- Mathie A (2007). Neuronal two-pore-domain potassium channels and their regulation by G protein-coupled receptors. *J Physiol* **578**, 377–385.
- Millar JA, Barratt L, Southan AP, Page KM, Fyffe RE, Robertson B & Mathie A (2000). A functional role for the two-pore domain potassium channel TASK-1 in cerebellar granule neurons. *Proc Natl Acad Sci USA* **97**, 3614–3618.
- Murata Y, Iwasaki H, Sasaki M, Inaba K & Okamura Y (2005). Phosphoinositide phosphatase activity coupled to an intrinsic voltage sensor. *Nature* **435**, 1239–1243.
- Murata Y & Okamura Y (2007). Depolarization activates the phosphoinositide phosphatase Ci-VSP, as detected in *Xenopus* oocytes coexpressing sensors of PIP₂. *J Physiol* **583**, 875–889.
- Nasuhoglu C, Feng S, Mao J, Yamamoto M, Yin HL, Earnest S, Barylko B, Albanesi JP & Hilgemann DW (2002). Nonradioactive analysis of phosphatidylinositides and other anionic phospholipids by anion-exchange high-performance liquid chromatography with suppressed conductivity detection. *Anal Biochem* **301**, 243–254.
- Oldfield S, Hancock J, Mason A, Hobson SA, Wynick D, Kelly E, Randall AD & Marrion NV (2009). Receptor-mediated suppression of potassium currents requires colocalization within lipid rafts. *Mol Pharmacol* **76**, 1279–1289.
- Oliver D, Lien CC, Soom M, Baukrowitz T, Jonas P & Fakler B (2004). Functional conversion between A-type and delayed rectifier K⁺ channels by membrane lipids. *Science* **304**, 265–270.
- Putzke C, Wemhoner K, Sachse FB, Rinne S, Schlichthorl G, Li XT, Jae L, Eckhardt I, Wischmeyer E, Wulf H, Preisig-Muller R, Daut J & Decher N (2007). The acid-sensitive potassium channel TASK-1 in rat cardiac muscle. *Cardiovasc Res* **75**, 59–68.
- Rajan S, Wischmeyer E, Xin Liu G, Preisig-Muller R, Daut J, Karschin A & Derst C (2000). TASK-3, a novel tandem pore domain acid-sensitive K⁺ channel. An extracellular histidine as pH sensor. *J Biol Chem* **275**, 16650–16657.
- Rohacs T, Chen J, Prestwich GD & Logothetis DE (1999). Distinct specificities of inwardly rectifying K⁺ channels for phosphoinositides. *J Biol Chem* **274**, 36065–36072.
- Rohacs T & Nilius B (2007). Regulation of transient receptor potential (TRP) channels by phosphoinositides. *Pflugers Archiv* **455**, 157–168.
- Roy A & Levine TP (2004). Multiple pools of phosphatidylinositol 4-phosphate detected using the pleckstrin homology domain of Osh2p. *J Biol Chem* **279**, 44683–44689.
- Stauffer TP, Ahn S & Meyer T (1998). Receptor-induced transient reduction in plasma membrane PtdIns(4,5)P₂ concentration monitored in living cells. *Curr Biol* **8**, 343–346.
- Suh BC & Hille B (2002). Recovery from muscarinic modulation of M current channels requires phosphatidylinositol 4,5-bisphosphate synthesis. *Neuron* **35**, 507–520.
- Suh BC & Hille B (2008). PIP₂ is a necessary cofactor for ion channel function: how and why? *Annu Rev Biophys* **37**, 175–195.
- Suh B-C, Inoue T, Meyer T & Hille B (2006). Rapid chemically induced changes of PtdIns(4,5)P₂ gate KCNQ ion channels. *Science* **314**, 1454–1457.
- Suh BC, Leal K & Hille B (2010). Modulation of high-voltage activated Ca²⁺ channels by membrane phosphatidylinositol 4,5-bisphosphate. *Neuron* **67**, 224–238.
- Talley EM & Bayliss DA (2002). Modulation of TASK-1 (Kcnk3) and TASK-3 (Kcnk9) potassium channels: volatile anesthetics and neurotransmitters share a molecular site of action. *J Biol Chem* **277**, 17733–17742.
- Talley EM, Solorzano G, Lei Q, Kim D & Bayliss DA (2001). CNS distribution of members of the two-pore-domain (KCNK) potassium channel family. *J Neurosci* **21**, 7491–7505.
- Tucker SJ & Baukrowitz T (2008). How highly charged anionic lipids bind and regulate ion channels. *J Gen Physiol* **131**, 431–438.
- Varnai P & Balla T (2006). Live cell imaging of phosphoinositide dynamics with fluorescent protein domains. *Biochim Biophys Acta* **1761**, 957–967.
- Varnai P, Thyagarajan B, Rohacs T & Balla T (2006). Rapidly inducible changes in phosphatidylinositol 4,5-bisphosphate levels influence multiple regulatory functions of the lipid in intact living cells. *J Cell Biol* **175**, 377–382.
- Vasudevan L, Jeromin A, Volpicelli-Daley L, De Camilli P, Holowka D & Baird B (2009). The β - and γ -isoforms of type I PIP5K regulate distinct stages of Ca²⁺ signaling in mast cells. *J Cell Sci* **122**, 2567–2574.
- Veale EL, Kennard LE, Sutton GL, MacKenzie G, Sandu C & Mathie A (2007). G α q-mediated regulation of TASK3 two-pore domain potassium channels: the role of protein kinase C. *Mol Pharmacol* **71**, 1666–1675.
- Wang YJ, Li WH, Wang J, Xu K, Dong P, Luo X & Yin HL (2004). Critical role of PIP5KI γ 87 in InsP₃-mediated Ca²⁺ signaling. *J Cell Biol* **167**, 1005–1010.
- Watkins CS & Mathie A (1996). A non-inactivating K⁺ current sensitive to muscarinic receptor activation in rat cultured cerebellar granule neurons. *J Physiol* **491**, 401–412.
- Willars GB, Nahorski SR & Challiss RA (1998). Differential regulation of muscarinic acetylcholine receptor-sensitive polyphosphoinositide pools and consequences for signaling in human neuroblastoma cells. *J Biol Chem* **273**, 5037–5046.
- Zhang H, Craciun LC, Mirshahi T, Rohacs T, Lopes CM, Jin T & Logothetis DE (2003). PIP₂ activates KCNQ channels, and its hydrolysis underlies receptor-mediated inhibition of M currents. *Neuron* **37**, 963–975.
- Zolles G, Klocker N, Wenzel D, Weisser-Thomas J, Fleischmann BK, Roeper J & Fakler B (2006). Pacemaking by HCN channels requires interaction with phosphoinositides. *Neuron* **52**, 1027–1036.

Author contributions

M.L. designed and performed most experiments, analysed data and wrote parts of the manuscript. M.G.L. and C.R.H. performed experiments and contributed to the design of the experiments. G.R.V.H. developed pseudojanin, advised on and designed experiments, and revised the manuscript. D.O. conceived the project, designed experiments, analysed data and wrote the manuscript. All authors approved the final version. Experiments were performed at the Philipps University Marburg.

Acknowledgements

We thank Drs Jürgen Daut and Thomas Baukowitz for insightful discussions. cDNA constructs used in this study were kindly provided by J. Daut (TASK-1/3), T. Jentsch (KCNQ4), T. Meyer (PH_{PLC δ 1}-GFP, rapamycin recruitment system) and Y. Okamura

(Ci-VSP). We are indebted to S. Petzold, O. Haeckel and G. Fischer for excellent technical assistance and to D. Schreiber for advice on molecular biological techniques. This work was supported by the Deutsche Forschungsgemeinschaft (SFB 593, TP A12; D.O.)

Controlling the Activity of a Phosphatase and Tensin Homolog (PTEN) by Membrane Potential*

Received for publication, November 8, 2010, and in revised form, February 21, 2011. Published, JBC Papers in Press, March 17, 2011, DOI 10.1074/jbc.M110.201749

Jérôme Lacroix^{†1}, Christian R. Halaszovich^{§1}, Daniela N. Schreiber[§], Michael G. Leitner[§], Francisco Bezanilla[‡], Dominik Oliver^{§2}, and Carlos A. Villalba-Galea^{¶3}

From the [†]Department of Biochemistry and Molecular Biology, The University of Chicago, Chicago, Illinois 60637, the [§]Institute of Physiology and Pathophysiology, Philipps University, 35037 Marburg, Germany, and the [¶]Department of Physiology and Biophysics, Virginia Commonwealth University, Richmond, Virginia 23298

The recently discovered voltage-sensitive phosphatases (VSPs) hydrolyze phosphoinositides upon depolarization of the membrane potential, thus representing a novel principle for the transduction of electrical activity into biochemical signals. Here, we demonstrate the possibility to confer voltage sensitivity to cytosolic enzymes. By fusing the tumor suppressor PTEN to the voltage sensor of the prototypic VSP from *Ciona intestinalis*, Ci-VSP, we generated chimeric proteins that are voltage-sensitive and display PTEN-like enzymatic activity in a strictly depolarization-dependent manner *in vivo*. Functional coupling of the exogenous enzymatic activity to the voltage sensor is mediated by a phospholipid-binding motif at the interface between voltage sensor and catalytic domains. Our findings reveal that the main domains of VSPs and related phosphoinositide phosphatases are intrinsically modular and define structural requirements for coupling of enzymatic activity to a voltage sensor domain. A key feature of this prototype of novel engineered voltage-sensitive enzymes, termed Ci-VSPPTEN, is the novel ability to switch enzymatic activity of PTEN rapidly and reversibly. We demonstrate that experimental control of Ci-VSPPTEN can be obtained either by electrophysiological techniques or more general techniques, using potassium-induced depolarization of intact cells. Thus, Ci-VSPPTEN provides a novel approach for studying the complex mechanism of activation, cellular control, and pharmacology of this important tumor suppressor. Moreover, by inducing temporally precise perturbation of phosphoinositide concentrations, Ci-VSPPTEN will be useful for probing the role and specificity of these messengers in many cellular processes and to analyze the timing of phosphoinositide signaling.

Many cellular processes, ranging from secretion of hormones and neurotransmitters to gene transcription, can be triggered by rapid changes in membrane potential. The canonical principle for transduction of membrane potential changes into intra-

cellular signals involves Ca^{2+} influx by activation of voltage-gated channels, resulting in an increase of the intracellular Ca^{2+} concentration, which in turn acts via downstream Ca^{2+} -sensitive proteins as effectors (1–3). The recent discovery of voltage-sensitive phosphatases (VSPs)⁴ (4, 5) has broadened this view fundamentally. In response to depolarization of the membrane potential, the prototypic VSP from *Ciona intestinalis*, Ci-VSP (5, 6), degrades both phosphatidylinositol 4,5-bisphosphate ($\text{PI}(4,5)\text{P}_2$) and phosphatidylinositol 3,4,5-trisphosphate ($\text{PI}(3,4,5)\text{P}_3$) by removing the phosphate group in position 5 of the inositol ring (5–8). These phosphoinositides are signaling molecules with pivotal roles in the regulation of various cellular processes such as cell proliferation and differentiation (9, 10), ion channel activity (11), synaptic exocytosis and endocytosis (12, 13), and neural development (9). Thus, VSPs constitute a novel mechanism of coupling of intracellular pathways to electrical activity at the plasma membrane, although their physiological role remains elusive.

VSPs are homologues of the tumor suppressor PTEN (phosphatase and tensin homolog deleted from chromosome 10) (14, 15), a key regulator of phosphoinositide signaling pathways. PTEN is a cytosolic 3'-phosphoinositide phosphatase, acting as an antagonist of the Akt/PI3K pathway. Loss-of-function mutations of PTEN are frequently found in human cancer, ranking this protein as one of the most important tumor suppressors known presently (16). Regulation of PTEN activity is highly complex, but in contrast to VSPs, it is independent of membrane potential because PTEN is a cytosolic protein. Because the membrane lipid $\text{PI}(3,4,5)\text{P}_3$ is the main substrate of PTEN, binding to the plasma membrane is a prerequisite for enzymatic activity. Targeting to the plasma membrane is mediated by two distinct domains located in the N and C termini (17–20). The C terminus harbors a C2 domain that binds phosphatidylserine; its binding affinity is regulated by phosphorylation (19, 21). The N terminus constitutes a phosphoinositide-binding motif (PBM) that recruits PTEN to the membrane by specifically binding to $\text{PI}(4,5)\text{P}_2$, the main catalytic product of PTEN (17, 22). Moreover, binding of the PBM to $\text{PI}(4,5)\text{P}_2$ allosterically activates PTEN (17, 22). Thus, the activity of PTEN relies not

* This work was supported, in whole or in part, by National Institutes of Health Grant GM030376 (to F.B.). This work was also supported by Deutsche Forschungsgemeinschaft Grant SFB593 TPA12 (to D.O.).

¹ Both authors contributed equally to this work.

² To whom correspondence may be addressed: Institut für Physiologie und Pathophysiologie, Deutschhausstr. 1-2, 35037 Marburg, Germany. Fax: 49-6421-2862306; E-mail: oliverd@staff.uni-marburg.de.

³ To whom correspondence may be addressed: Department of Physiology and Biophysics, 1101 E. Marshall St., Richmond, VA 23298. Fax: 1-804-828-7382; E-mail: cavillalbag@vcu.edu.

⁴ The abbreviations used are: VSP, voltage-sensitive phosphatase; CD, catalytic domain; OK, opossum kidney; PBM, phosphoinositide binding motif; PD, phosphatase domain; PH, pleckstrin homology domain; $\text{PI}(4,5)\text{P}_2$, phosphatidylinositol(4,5)bisphosphate; $\text{PI}(3,4)\text{P}_2$, phosphatidylinositol(3,4)bisphosphate; $\text{PI}(3,4,5)\text{P}_2$, phosphatidylinositol(3,4,5)trisphosphate; $\text{PI}(4)\text{P}$, phosphatidylinositol 4-phosphate.

Voltage-controlled PTEN Activity

only on the recognition of its substrate but also on binding to the membrane and on a membrane-delimited allosteric interaction with PI(4,5)P₂, which acts as an activating ligand. This complexity poses substantial challenges for further detailed examination of the mechanism of activation, enzymatic mechanism, and regulation of PTEN and of its multiple cellular functions (23). A robust method for experimental control of PTEN activity, analogous to the voltage control of the VSPs, might therefore greatly facilitate such examination.

In VSPs, voltage sensitivity is conferred by a voltage-sensing domain (VSD) located in the N terminus, which, in turn, controls the activity of the catalytic domain (CD) located within the C terminus (see Fig. 1A). Both domains are fully functional when expressed individually (5, 24). The modular nature of both domains suggested that the VSD initiates the catalytic activity by operating a molecular switch intrinsic to the CD. The N terminus of the CD of Ci-VSP also contains a PBM highly homologous to the PBM of PTEN (see Fig. 1B), which is critical for depolarization-triggered activity. In fact, it has been proposed that the mechanism of activation of the Ci-VSP involves binding of the PBM to the membrane (8, 24); accordingly, voltage sensitivity relies on the control of this binding step by the VSD. Thus, activation of VSPs resembles the PBM-mediated activation of PTEN. Moreover, the CD of Ci-VSP shares substantial sequence conservation with PTEN (8, 25). A structural homology model for the CD of Ci-VSP (see Fig. 1C) based upon the crystal structure of PTEN as a template (26) confirmed a high degree of structural similarity between Ci-VSP and PTEN, including an architecture consisting of a phosphatase domain (PD) and a C2 domain. These considerations suggested that it may be possible to impose voltage control upon PTEN if it was connected properly to a VSD. Following this idea, we here describe the successful generation and characterization of engineered voltage-activated enzymes (Venz), by conferring voltage sensitivity upon the cytoplasmic signaling enzyme PTEN.

EXPERIMENTAL PROCEDURES

Generation of Ci-VSPPTEN Chimera and Mutagenesis—Ci-VSPPTEN chimeras were built by swapping the DNA fragments encoding the codons 240–576 (Ci-VSPPTEN0), 255–576 (Ci-VSPPTEN16), and 260–576 (Ci-VSPPTEN21) of Ci-VSP by the DNA fragments encoding the codons 1–403 (Ci-VSPPTEN0), 16–403 (Ci-VSPPTEN16), and 21–403 (Ci-VSPPTEN21) of the mouse PTEN cDNA.⁵ For this, we employed a PCR-based primer extension strategy. Briefly, the PTEN DNA fragments were generated by PCR-amplification from a Sport6 plasmid containing the full-length PTEN cDNA. The 5' ends of the sense and antisense primers used for these PCR were complementary to the 5' and 3' regions immediately flanking the sequence to swap in the Ci-VSP cDNA. The obtained PCR products were purified and used as extended primers for a sec-

ond PCR reaction using a standard QuikChange mutagenesis protocol (Stratagene). The DNA template used for these second PCR was a pBSTA plasmid encoding the Ci-VSP cDNA under the T7 promoter. For expression in CHO and opossum kidney (OK) cells, Ci-VSPPTEN chimeras were subcloned from pBSTA into pRFP-C1. Ci-VSPPTEN mutants were generated by standard site-directed mutagenesis and verified by sequencing. Sensing current recordings and voltage clamp fluorometry, were performed with Ci-VSPPTEN containing the additional mutation C363S, equivalent to the catalytically inactive mutant C124S in PTEN.

Expression in *Xenopus* Oocytes—The DNA was linearized with NotI and transcribed using T7 RNA polymerase. 50 nl of 0.5–1 μg/μl RNA was injected per oocyte, followed by incubation at 18 °C in a solution containing 100 mM NaCl, 2 mM KCl, 1 mM MgCl₂, 1.8 mM CaCl₂, 2 mM sodium pyruvate, 50 μM EDTA, and 10 mM HEPES, pH 7.5 (27).

Sensing Currents and Voltage Clamp Fluorometry—Sensing currents were measured 2–4 days after injection with the cut-open oocyte voltage clamp technique (28) as described by Villalba-Galea *et al.* (27). Currents were measured in response to voltage steps (400 ms, 10-s interval) from a holding potential of –80 mV without leak subtraction during acquisition. Capacitance transient currents were compensated analogically using the amplifier compensation circuit. The external recording solutions contained 120 mM NMG-MeSO₃ (methanesulfonate), 10 mM HEPES, and 2 mM CaCl₂, pH 7.4, whereas internal solutions contained 120 mM NMG-MeSO₃, 10 mM HEPES, and 2 mM EGTA, pH 7.4. Labeling of oocytes with tetramethylrhodamine-5-maleimide and fluorometry were done as described previously (29). Briefly, tetramethylrhodamine-5-maleimide fluorescence was measured through a BX51WI microscope (Olympus) equipped with a LUMPlanFl 40× water immersion objective (numerical aperture, 0.80) and an appropriate filter set. Fluorescence intensity was monitored with a PhotoMax-201-PIN photodiode controlled by a PhotoMax 200 amplifier (Dagan). Electrophysiological and fluorescence data were filtered at 2–5 kHz and sampled at 5–20 kHz and recorded and analyzed with the acquisition system and programs described previously (27).

Expression in CHO and OK Cells—CHO and OK cells were grown as described (7, 30), plated onto glass-bottomed dishes (WillCo Wells B. V., Amsterdam, The Netherlands) or glass coverslips, respectively, and transfected using jetPEI (CHO cells; Polyplus Transfection, Illkirch, France) or Lipofectamine 2000 (OK cells; Invitrogen). Experiments were done 24–48 h post-transfection on cells selected for expression of mRFP-Ci-VSPPTEN and the presence of corresponding sensing currents. Vectors used for transfection were as follows: PLCδ1-PH-pEGFP-N1 (GenBank accession no. P51178); Akt1-PH-pEGFP-N1 (GenBank accession no. AAL55732.1); Btk-PH-pEGFP (GenBank accession no. AAC51347.1); OSBP-PH-pEGFP-N1 (GenBank accession no. NP_002547.1); TAPP1-PH-FUGW (GenBank accession no. NP_067635); bovine phosphatidylinositol 3-kinase p110α (constitutively active mutant K227E; GenBank accession no. NP_776999.1); and hTASK-3-pcDNA3.1 (GenBank accession no. NP_057685).

Combined Patch Clamp and TIRF Microscopy—CHO cells were whole-cell voltage clamped with an EPC-10 amplifier con-

⁵ PTEN from both human and mouse displays 96% identity in their nucleotide sequence, while only differing in a single amino acid in the distal region of the C terminus, particularly a Serine in position 398, instead of a Threonine, as in human. To our knowledge, there is no evidence showing any difference between the activities of these two enzymes.

trolled by PatchMaster software (HEKA, Lambrecht, Germany). Sensing currents were isolated using a P/-10 protocol. Patch pipettes were pulled from a quartz glass to an open pipette resistance of 1.5–4.0 M Ω when filled with intracellular solution: 135 mM KCl, 2.5 mM MgCl₂, 2.41 mM CaCl₂, 5 mM EGTA, 5 mM HEPES, and 3 mM Na₂ATP, pH 7.3 (with KOH). For perforated patch measurements Nystatin (100 μ g/ml) was added. The extracellular solution contained the following: 144 mM NaCl, 5.8 mM KCl, 0.7 mM NaH₂PO₄, 5.6 mM glucose, 1.3 mM CaCl₂, 0.9 mM MgCl₂, and 10 mM HEPES, pH 7.4 (with NaOH). For depolarization by K⁺, cells were initially kept in standard extracellular solution, and depolarization was induced by transient application of 150 mM K⁺ (150 mM KCl, 5.6 mM glucose, 1.3 mM CaCl₂, 0.9 mM MgCl₂, and 10 mM HEPES, pH 7.4). Total internal reflection fluorescence (TIRF) imaging was done as described previously (7). Briefly, a BX51WI upright microscope (Olympus) equipped with a TIRF condenser (numerical aperture, 1.45; Olympus) and a 488-nm laser (20 milliwatt; Picarro, Sunnyvale, CA) was used. Fluorescence was imaged through a LUMPlanFI/IR 40 \times /0.8 numerical aperture water-immersion objective. Images were acquired with a TILL-Imago QE cooled CCD camera (TILL Photonics, Gräfelfing, Germany) controlled by TILLvision software (TILL Photonics). Imaging data were analyzed using TILLvision and IgorPro (Wavemetrics, Lake Oswego, OR). Regions of interest encompassed the footprint of a single cell excluding cell margins to avoid movement artifacts. F/F_0 traces were calculated from the background-corrected TIRF signal intensity F , averaged over the region of interest and the initial fluorescence intensity F_0 during the baseline interval. F/F_0 traces were corrected for bleaching according to monoexponential fits to the baseline interval.

Confocal Imaging—OK cells were co-transfected with mRFP-Ci-VSPTEN16, Akt-PH-GFP, p110 α (K227E), and the TASK3 potassium channel. Cells were transiently depolarized by application of 150 mM K⁺. Confocal imaging was performed with a Zeiss Examiner upright microscope equipped with a LSM710 scan head (Carl Zeiss AG, Jena, Germany) and a W-Plan-Apochromat 20 \times /1.0 DIC M27 75 mm (Carl Zeiss AG). Laser lines used were 561 nm for mRFP and 488 nm for GFP, detection wavelength ranges were 582–754 and 493–582 nm, respectively. Time series recordings were taken in the GFP channel. Fluorescence (F) was averaged from regions of interest placed in cytosolic regions of individual cells and normalized to the baseline fluorescence (F_0), prior to stimulation.

All experiments were performed at room temperature. Data are given as means \pm S.E.

RESULTS

Designing Chimeras between Ci-VSP and PTEN—A chimera, hereafter named Ci-VSPTEN16, was built by replacing the CD of Ci-VSP with full-length PTEN (Fig. 1D). Because the PBM is critically involved in mediating activation both in Ci-VSP and PTEN, we particularly focused our attention on the motif linking PTEN to the VSD in the chimeras. Previous functional analysis showed that, in Ci-VSP, the VSD seems to control the binding of the PBM to the membrane, and this process is critically dependent on arginines 253 and 254. In fact, mutation of these

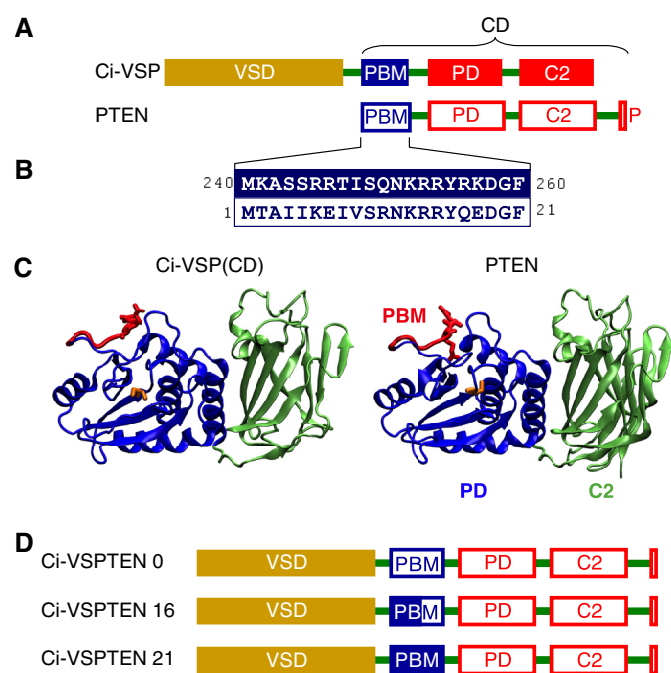


FIGURE 1. Design of chimeras between Ci-VSP and PTEN. *A*, comparison of the domain organization of Ci-VSP and PTEN. *P*, PDZ-binding motif. *B*, high sequence identity between the PBMs of Ci-VSP and PTEN. *Numbers* refer to the amino acid positions in Ci-VSP and PTEN, respectively. *C*, structural similarity between the catalytic domains of Ci-VSP and PTEN predicted by structural homology modeling of the CD of Ci-VSP (*left panel*) based on the crystal structure of PTEN (26), generated with ESyPred3D (48). PD and C2 domains are displayed in *blue* and *green*, respectively. Partially rendered PBMs are shown in *red*, with arginines 253 and 254 in Ci-VSP and arginines 14 and 15 in PTEN emphasized as *stick* models. Cysteines 363 (in Ci-VSP) and 124 (in PTEN) in the catalytic core are displayed as *yellow stick* models. *D*, design of Ci-VSPTEN chimeras. PTEN replaces the CD of Ci-VSP with different variants of the PBM (see text).

arginines eliminates coupling between electrical and catalytic activity (8, 24) even if the charges are conserved (8). In addition, arginines 245 and 246 are also critical for coupling since neutralization of these residues renders coupling inefficient (8). Despite overall similarity, the PBM of PTEN lacks the arginines equivalent to 245 and 246 of Ci-VSP, displaying no net charge at the corresponding position (Fig. 1B). To account for potential relevance of these residues for coupling of PTEN to the VSD, we replaced the DNA sequence coding from amino acid 17 of the PBM from Ci-VSP (including Arg^{245/246}), with the coding sequence of PTEN contributing the more distal part of the PBM (Ci-VSPTEN16; see Fig. 1, B and D).

In addition to positions Arg^{245/246}, there are further differences in the sequences of the PBMs from Ci-VSP and PTEN (see Fig. 1B), which may be relevant for coupling between VSD and PD. In fact, some of these amino acids are known to have a critical impact on the function of PTEN (18, 20, 31). To account for a potential impact of these residues on electrochemical coupling, we designed two additional chimeras containing either the full-length PBM (*i.e.* 21 residues) of Ci-VSP (termed Ci-VSPTEN21) or the full PBM of PTEN without contribution from the PBM of Ci-VSP (Ci-VSPTEN0) (see Fig. 1D).

Ci-VSPTEN16 Displays Voltage-activated Enzymatic Activity—Enzymatic activity of Ci-VSPTEN16 was assessed in living cells by imaging genetically encoded fluorescent phosphoinositide probes, following paradigms established previously for Ci-VSP

Voltage-controlled PTEN Activity

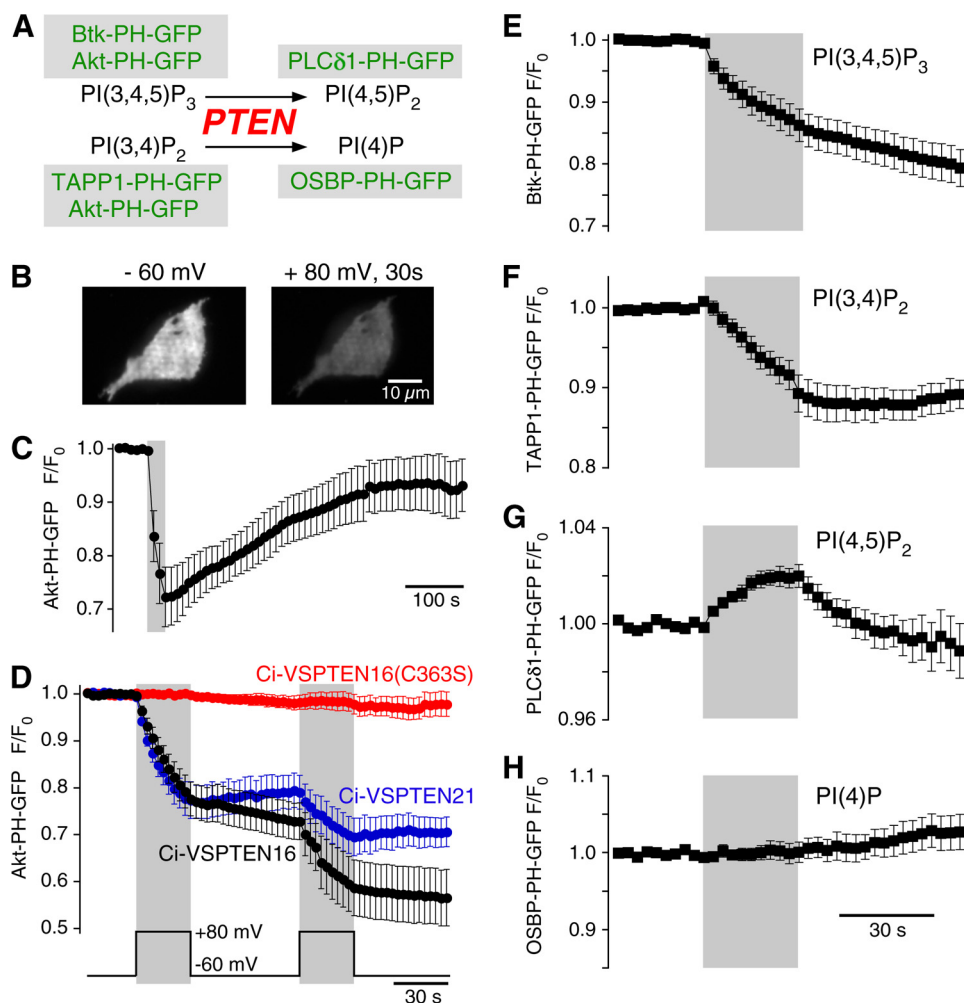


FIGURE 2. Ci-VSPTEN displays voltage-activated lipid phosphatase activity. *A*, schematic representation of the enzymatic activity of PTEN, a 3'-phosphatase that converts PI(3,4,5)P₃ into PI(4,5)P₂ and PI(3,4)P₂ into PI(4)P. GFP-fused sensor domains used in this study to detect concentration changes of the putative substrates and products of Ci-VSPTEN chimeras are indicated (green). *B*, TIRF images of a living CHO cell coexpressing the PI(3,4,5)P₂/PI(3,4)P₂ sensor Akt-PH-GFP and Ci-VSPTEN16 together with constitutively active PI3K p110αK227E (PI3K). Images were acquired before (left) and after 30 s of depolarization to +80 mV (right) in whole-cell configuration. Depolarization-induced loss of fluorescence results from reduced membrane association of Akt-PH and indicates depletion of 3'-phosphoinositides. *C*, depolarization-induced translocation of Akt-PH as in *B* is followed by slow recovery, indicating resynthesis of 3'-phosphoinositides by PI3K (recordings obtained with perforated patch configuration). The gray area indicates depolarization from -60 to +80 mV. *D*, normalized TIRF intensities in response to repetitive depolarization obtained as in *B*. Cells coexpressed Akt-PH-GFP, PI3K, and the Ci-VSPTEN chimeras indicated ($n = 10, 3$, and 7 cells, for Ci-VSPTEN16, Ci-VSPTEN21, and Ci-VSPTEN16-C363S, respectively). *E-H*, depolarization-triggered changes in membrane association of fluorescent probes that specifically bind various phosphoinositides, measured as in *D*. Cells expressed Ci-VSPTEN16 together with PI3K and either Btk-PH-GFP ($n = 16$), TAPP1-PH-GFP ($n = 5$), PLCδ1-PH-GFP ($n = 6$), or OSBP-PH-GFP ($n = 6$). Error bars indicate S.E.

(7). Briefly, membrane association of these probes reports the abundance of the specifically recognized lipid. Membrane association was determined by TIRF imaging of cells under whole-cell voltage clamp.

Upon depolarization (to +80 mV), cells co-expressing Ci-VSPTEN16 and the probe Akt-PH-GFP, specific for PI(3,4,5)P₃ and PI(3,4)P₂, displayed an unambiguous decrease in membrane-associated fluorescence intensity (Fig. 2, *B* and *C*). This observation showed that the concentration of PI(3,4,5)P₃ and/or PI(3,4)P₂ decreased during depolarization, indicating that Ci-VSPTEN16 has depolarization-triggered enzymatic activity. Following repolarization, the membrane-associated fluorescence recovered, indicating resynthesis of PI(3,4,5)P₃ and/or PI(3,4)P₂ (Fig. 2*C*). Activation of Ci-VSPTEN16 was rapidly reversible, as fluorescence decrease was observed only during depolarization and ceased upon repolarization to -60 mV, as demonstrated using double-pulse protocols (Fig. 2*D*).

Similar results were obtained with Ci-VSPTEN21 but not with the catalytically inactive mutant Ci-VSPTEN16-C363S (this mutation is equivalent to C124S in PTEN) (Fig. 2*C*), confirming that the fluorescence decrease was caused by enzymatic activity of the PTEN domain of the chimeras.

The decrease in Akt-PH-GFP fluorescence obtained with Ci-VSPTEN16 after 60 s of depolarization (+80 mV) was to $46.8 \pm 7.2\%$ of the initial signal ($n = 5$). Because a signal decrease to ~40% reports the full translocation of an initially fully membrane-resident probe (7), this finding indicates that Ci-VSPTEN16 can completely deplete the pool of PI(3,4,5)P₃ and PI(3,4)P₂ in the plasma membrane.

Ci-VSPTEN16 Preserves PTEN Substrate Selectivity—Having found that Ci-VSPTEN16 is both active and voltage-dependent, we next examined the catalytic specificity of this chimera using other phosphoinositide-specific probes (Fig. 2*A*). When co-expressed with Btk-PH-GFP or TAPP1-PH-GFP (32), which

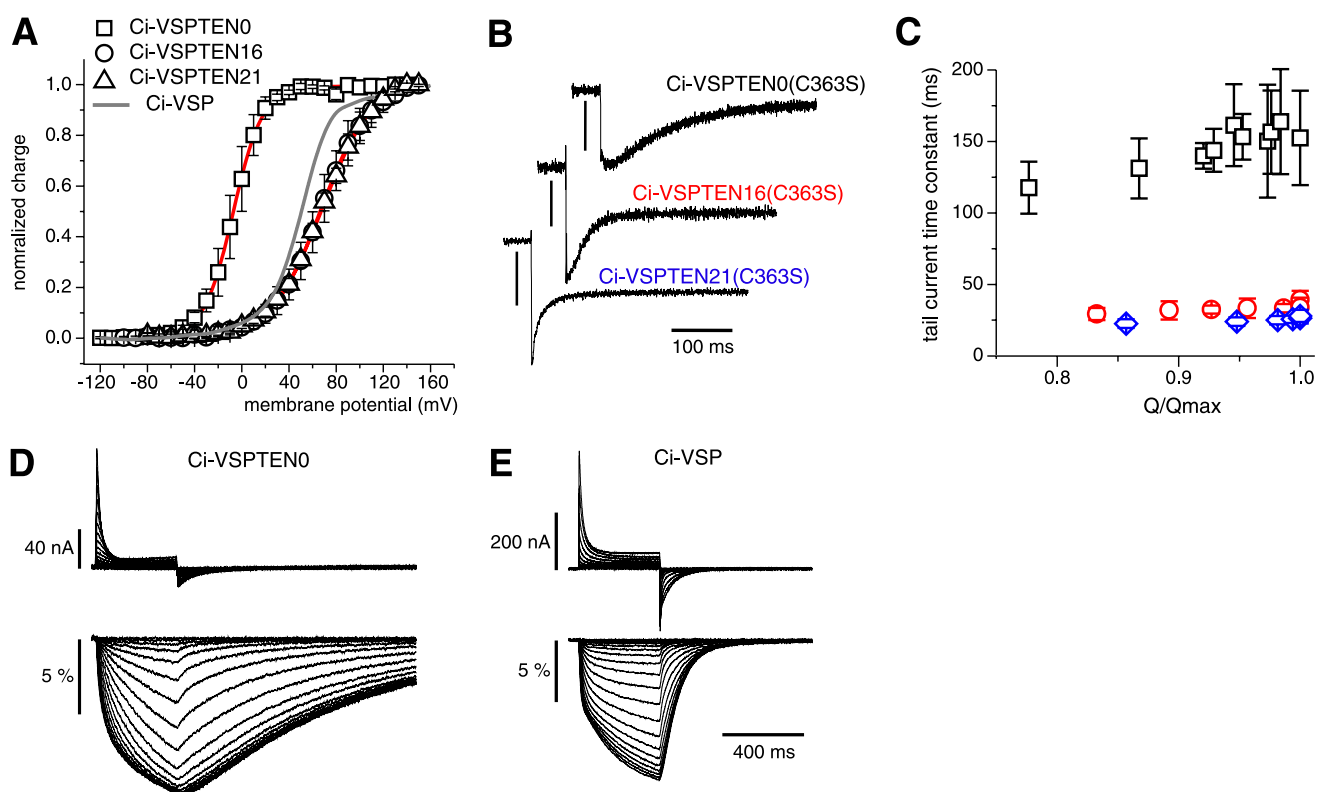


FIGURE 3. Effect of the PBM on the voltage sensor dynamics. *A*, voltage dependence of the sensing currents of the three Ci-VSPTEN chimeras were measured from *Xenopus* oocytes (27), using the catalytically inactive mutant C363S (equivalent to C124S in PTEN). Normalized Q - V curves were derived from the OFF sensing currents at -90 mV following a 400-ms step to the potentials indicated. The gray curve shows the voltage dependence of Ci-VSP-C363S recorded under the same conditions (27). Fits of a two-state Boltzmann distribution to the data (continuous red lines) yielded potentials at half-maximal charge transfer of -7 ± 0.2 mV ($n = 4$), $+67 \pm 0.4$ mV ($n = 3$), and $+69 \pm 0.3$ mV ($n = 4$), with charges of $2.0 \pm 0.03 e_0$, $1.2 \pm 0.02 e_0$ and $1.1 \pm 0.01 e_0$, for Ci-VSPTEN0, Ci-VSPTEN16, and Ci-VSPTEN21, respectively. *B*, OFF sensing currents of Ci-VSPTEN chimeras measured at -90 mV following a 400-ms test pulse to 0 mV for Ci-VSPTEN0 and $+100$ mV for Ci-VSPTEN16 and Ci-VSPTEN21. Current scale bars, 50 nA, 250 nA, and 100 nA, respectively. *C*, Weighted mean time constants of tail-sensing currents recorded as in *A* are shown for the nearly saturating region of the Q - V curves ($Q/Q_{\max} > 0.75$; $n = 5$) for Ci-VSPTEN (black), Ci-VSPTEN16 (red), and Ci-VSPTEN21 (blue). *D* and *E*, sensing currents and changes in fluorescence intensity ($\Delta F/F_0$) from tetramethylrhodamine-5-maleimide-labeled Ci-VSPTEN0-G214C-C363S (*D*) and Ci-VSP-G214C-C363S (*E*) in response to depolarizing voltage steps (-120 to 140 mV).

specifically bind $PI(3,4,5)P_3$ and $PI(3,4)P_2$, respectively, Ci-VSPTEN16 evoked a decrease in membrane fluorescence upon depolarization (Fig. 2, *E* and *F*). Thus Ci-VSPTEN16 dephosphorylates both $PI(3,4,5)P_3$ and $PI(3,4)P_2$, consistent with the enzymatic activity of PTEN (Fig. 2*A*). Conversely, membrane fluorescence from the $PI(4,5)P_2$ -specific probe, PLC δ 1-PH-GFP (33), increased during depolarization (Fig. 2*G*). This result indicated production of $PI(4,5)P_2$ from $PI(3,4,5)P_3$ and confirmed that Ci-VSPTEN16 behaves as a 3'-phosphatase. Membrane association of PLC δ 1-PH-GFP recovered rapidly following deactivation of Ci-VSPTEN, which most likely reflects rapid turnover of $PI(4,5)P_2$ (7, 34) and indicates that the $PI(4,5)P_2$ concentration is regulated independent of the $PI(3,4,5)P_3$ pool depleted by Ci-VSPTEN. Despite dephosphorylation of $PI(3,4)P_2$, membrane fluorescence of the $PI(4)P$ specific probe OSBP-PH-GFP (35) seemed unaffected by depolarization (Fig. 2*H*), indicating the lack of substantial changes of the $PI(4)P$ concentration by Ci-VSPTEN16 activation. However, this is expected, because the basal $PI(3,4)P_2$ content of the membrane is typically 1000-fold lower than its $PI(4)P$ content (36). Based on these observations, we conclude that Ci-VSPTEN16 retains the enzymatic specificity of PTEN.

Role of PBM in Coupling Exogenous Enzymatic Activity to Voltage Sensor—To understand the coupling of catalytic activity to membrane potential, we next characterized the behavior of the VSD. Thus, we measured sensing currents from the chimeras carrying the mutation C363S expressed in *Xenopus* oocytes. Sensing currents are mainly produced by the movement of charged residues within the putative fourth trans-membrane segment (S4) of the VSD (5). The net sensing charge movement versus potential relationship (Q - V curve) revealed that both Ci-VSPTEN16 and -21 display voltage dependences similar to Ci-VSP (Fig. 3*A*). However, a shift to negative potentials was observed for Ci-VSPTEN0. In addition, Ci-VSPTEN0 displayed much slower OFF-sensing currents than Ci-VSPTEN16 and Ci-VSPTEN21 (Fig. 3, *B* and *C*). We further examined the movement of the S4 segment using voltage clamp fluorometry. Tetramethylrhodamine-5-maleimide was attached covalently to a cysteine replacing glycine 214 in the extracellular end of this segment, such that S4 movements result in fluorescence intensity changes (27, 37). Ci-VSP (Fig. 3*E*) and Ci-VSPTEN0 (Fig. 3*D*) displayed voltage-dependent fluorescence changes with strikingly different kinetics during repolarization: consistent

Voltage-controlled PTEN Activity

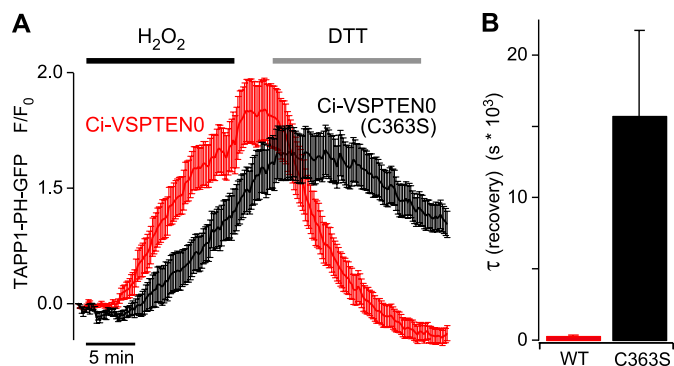


FIGURE 4. Basal PI-3'-phosphatase activity of Ci-VSPTE0 at resting membrane potential. *A*, membrane association of the PI(3,4)P₂ probe TAPP1-PH-YFP in cells either coexpressing Ci-VSPTE0 ($n = 47$ cells from nine independent experiments) or Ci-VSPTE0 with the inactivating mutation C363S ($n = 35$ cells from 10 experiments) was imaged by TIRF microscopy. H₂O₂ (1 mM) was applied for 15 min, followed by application of DTT (5 mM) for 15 min as indicated. *B*, average time constants obtained from monoexponential fits to the signal recovery upon application of DTT from the same experiments shown in *A*. Error bars indicate S.E.

with sensing currents (*upper panels*), fluorescence signals (*lower panels*) were much slower for Ci-VSPTE0.

Ci-VSPTE0 Displays High Basal Activity—Despite an intact catalytic domain, Ci-VSPTE0 produced no changes in membrane-associated fluorescence of Akt-PH-GFP during depolarization (data not shown). This might be a consequence of a strong negative shift in the voltage dependence of enzymatic activity in parallel with the voltage sensor behavior (Fig. 3*A*). Such a shift may render Ci-VSPTE0 active at resting potential and thereby preclude additional depletion of PI(3,4,5)P₃ and PI(3,4)P₂ upon depolarization. However, we did not succeed in detecting depolarization-induced enzymatic activity even after prolonged hyperpolarization to abolish any activity present at resting membrane potential. We therefore tested for basal activity of Ci-VSPTE0 under conditions of experimentally increased substrate concentration. To this end, cells were treated with H₂O₂, which is known to strongly increase the plasma membrane concentration of PI(3,4)P₂ (32, 38). The H₂O₂-triggered pathway leading to the PI(3,4)P₂ increase is not well understood but appears to involve the dysregulation of endogenous enzymes that otherwise control PI(3,4)P₂ levels, likely including inactivation of PTEN (32). It should be noted that H₂O₂ also inactivates PTEN, and consequently Ci-VSPTE0, by formation of a disulfide bond between Cys⁷¹ and catalytic Cys¹²⁴, corresponding to Cys³¹⁰ and Cys³⁶³ in the chimera (39). However, this inactivation is readily reversed in the presence of DTT (39). When H₂O₂ was applied to cells expressing Ci-VSPTE0 and the PI(3,4)P₂ sensor TAPP1-PH, accumulation of PI(3,4)P₂ was readily detected as an increase in membrane association of TAPP-PH-GFP (Fig. 4*A*). Subsequent application of DTT to reverse oxidative inactivation induced a rapid decrease of membrane fluorescence in cells expressing Ci-VSPTE0, indicating consumption of PI(3,4)P₂. In contrast, in cells expressing the inactive mutant Ci-VSPTE0-C363S, recovery of PI(3,4)P₂ after H₂O₂ treatment was delayed and occurred much more slowly (Fig. 4*A*). Time constants obtained from monoexponential fits to the fluorescence decay upon application of DTT quantitatively con-

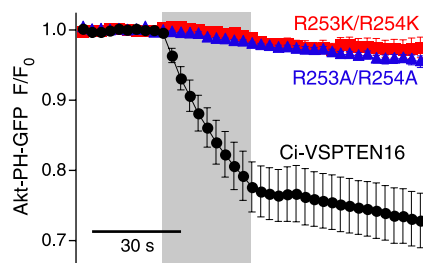


FIGURE 5. Binding of the PBM is essential for phosphatase activation by the VSD. Mutations that interfere with membrane binding of the PBM (R253A/R254A and R253K/R254K) abolish the depolarization-induced activation of enzymatic activity of Ci-VSPTE16 as monitored by measuring membrane association of Akt-PH-GFP ($n = 7$ cells for each mutant). Experiments were done as described in the legend to Fig. 2, and data for Ci-VSPTE16 are from Fig. 2*D* for comparison. The gray area indicates depolarization from -60 to $+80$ mV.

firmed the faster depletion of PI(3,4)P₂ with wild-type Ci-VSPTE0 (Fig. 4*B*).

In conclusion, the fast removal of PI(3,4)P₂ upon treatment with DTT provides direct evidence for enzymatic activity of Ci-VSPTE0 under basal conditions, *i.e.* at resting membrane potential. Additionally, the increase of PI(3,4)P₂ during H₂O₂ application was slightly stronger and faster in cells expressing Ci-VSPTE0. This finding might be explained by a lower initial concentration of PI(3,4)P₂, which is again consistent with basal activity of Ci-VSPTE0.

Mutations in PBM Abolished Ci-VSPTE16 Activity—Both the effect of the PBM on the VSD movement (Fig. 3) and the differential enzymatic activity of Ci-VSPTE16 *versus* Ci-VSPTE0 are consistent with a pivotal role of the PBM in electrochemically coupling the exogenous enzymatic activity to the VSD movement. We directly tested this suggestion by introducing mutations that have been shown previously to affect the activity of PTEN, namely of Arg^{14/15} of the PBM (15, 17). The corresponding amino acids (Arg^{253/254}) were also shown to be critical for electrochemical coupling of Ci-VSP (8, 24). Conversion of arginines Arg^{14/15} of the PBM to alanines or lysines completely abolished voltage-activated enzymatic activity of Ci-VSPTE16 (Fig. 5), despite functionality of the VSD as confirmed by sensing currents (data not shown). This demonstrates functional uncoupling of the CD from the VSD, confirming the essential role of the PBM for activation of exogenous catalytic domains by a VSD.

Activation of Ci-VSPTE16 in Intact Cells without Electrophysiological Instrumentation—So far, we have shown that Ci-VSPTE0 allows the activation of PTEN enzymatic activity and the depletion of both PI(3,4,5)P₃ and PI(3,4)P₂ when used with electrophysiological single-cell techniques. Obviously, methods for controlling enzymatic activity with more general methods that can also be used on cell populations would substantially increase the range of potential applications.

We therefore explored K⁺-induced depolarization as a means to activate Ci-VSPTE16. Thus, we transiently depolarized the membrane potential by application of high extracellular K⁺ concentration to otherwise undisturbed cells coexpressing Ci-VSPTE16 and Akt-PH-GFP. K⁺-induced depolarization triggered rapid depletion of both PI(3,4,5)P₃ and PI(3,4)P₂ as reported by translocation of Akt-PH-GFP from the

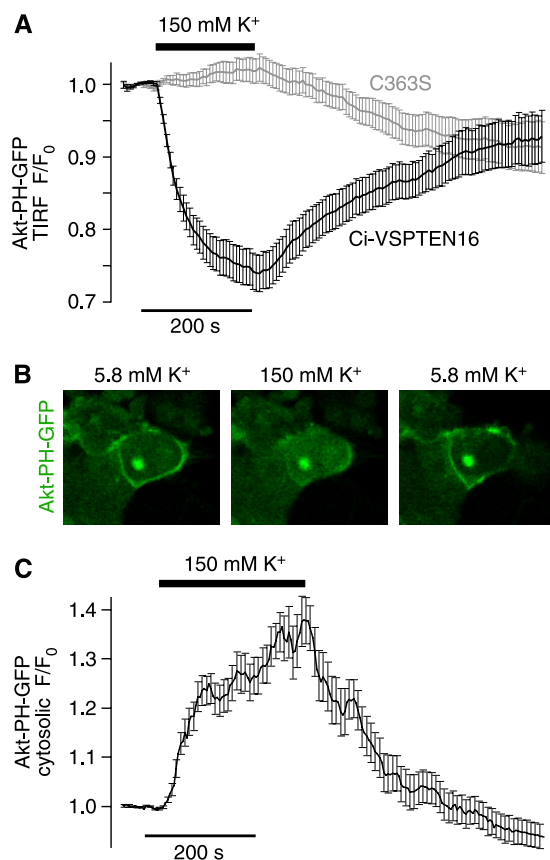


FIGURE 6. Experimental control of Ci-VSPTEN activity in intact cells without use of electrophysiological instrumentation. *A*, reversible dissociation of Akt-PH from the plasma membrane upon K^+ -induced depolarization observed with Ci-VSPTEN16 ($n = 30$ cells from five independent experiments) but not with the catalytically inactive Ci-VSPTEN16-C363S ($n = 29$ cells, from five independent experiments), measured by TIRF microscopy. CHO cells were cotransfected with Ci-VSPTEN16, Akt-PH-GFP, PI3K, and the potassium channel TASK3. *B*, confocal images of OK cells show reversible translocation of Akt-PH from the plasma membrane to the cytosol upon K^+ -induced depolarization. OK cells were cotransfected as described in *A*. *C*, averaged time course of K^+ -induced translocation of Akt-PH-GFP obtained from experiments as described in *B* ($n = 19$ cells from two independent experiments).

membrane into the cytosol measured either by TIRF (Fig. 6*A*) or confocal microscopy (Fig. 6, *B* and *C*). Upon lowering the extracellular concentration of K^+ back to the initial condition, Akt-PH-GFP reassociated to the membrane, indicating resynthesis of $PI(3,4,5)P_3$ and $PI(3,4)P_2$. These results show that Ci-VSPTEN can be activated precisely and in a readily reversible manner by simply altering the extracellular concentration of K^+ .

DISCUSSION

The recently discovered VSPs constitute a novel principle for the transduction of cellular electrical activity into intracellular biochemical signals, which differs fundamentally from the canonical principle for such transduction, *i.e.* influx of Ca^{2+} mediated by voltage-gated channels. Here, we explore molecular details of this novel principle and show that at least one exogenous enzyme can be operated by a voltage sensor domain. Specifically, fusing the VSD of Ci-VSP to PTEN, a key cytosolic modulator of intracellular signaling, yielded chimeric proteins that renders strictly voltage-dependent PTEN-like activity. To our knowledge, both Ci-VSPTEN16 and -21 represent the first

example of conferring voltage control to a cytoplasmic enzyme, and they constitute the first generation of engineered Venz.

Potential Applications for Engineered Venz—We note that dramatically improving experimental control over PTEN activity provides a novel paradigm for the study of this important signaling enzyme. Stringent control of activity will enable addressing details of the enzymatic mechanism, cellular regulation, disease-causing mutations, and pharmacology of PTEN.

Beyond analysis of PTEN operation, voltage-controlled enzymes such as Ci-VSPTEN provide novel tools for analyzing cellular signaling. By inducing rapid phosphoinositide concentrations changes, Ci-VSPTEN can be used to probe the role and specificity of these messengers in many cellular processes and to analyze the timing of phosphoinositide signaling. Various methods have been used previously to address the roles of phosphoinositides in the control of cellular function. For example, overexpression and knockdown of enzymes involved in phosphoinositide synthesis or homeostasis have been used widely (40–42). Many fundamental cellular processes occurring at a variety of time scales are affected by phosphoinositides, including protein targeting, cell differentiation, and transcription. Therefore, with the above-mentioned methods, it may often be difficult to unequivocally define the direct role of these lipid messengers for the process under observation. Moreover, compensatory mechanisms may complicate the actual changes of phosphoinositide concentrations resulting from long term manipulation of synthesis or degradation (43). To overcome these problems, methods for triggered recruitment of enzymes and signaling molecules to the plasma membrane by rapamycin-induced dimerization have been developed (43, 44). Such recruitment has been used to induce rapid, albeit irreversible, alterations of phosphoinositide concentrations during experimental observation (43, 44).

Voltage-controlled activation of enzymes, as introduced here, takes this approach one step further by rapidly switching enzymatic activity “on” and “off.” Thus, the precisely timed and reversible control of enzyme activation on a time scale of milliseconds provides a powerful tool for addressing temporal characteristics of signaling processes. Unlike the rapamycin-based approach, reversibility of activation allows the graded titration of phosphoinositide concentrations in the living cell (Fig. 2*D*) (7). Moreover, the recovery of phosphoinositide concentrations following a step-like perturbation (Fig. 2*C*) can yield unique insights into synthesis, homeostasis, and regulation of these messengers (7, 34). In analogy to Ci-VSPTEN, we envisage that fusion of different enzymatic domains to a VSD could provide novel tools for the temporally precise interference with diverse signaling pathways in the living cell, allowing for the experimental manipulation of cellular signaling networks beyond the level possible with the current cell biological or biochemical techniques.

Which enzymes or enzymatic domains may be amenable to functional coupling to VSDs? Here, we show that membrane binding of the PBM is critical for the activation of the exogenous enzymatic domain. The strong impact of the PBM on voltage sensor movement indicates that the VSD activates the exogenous enzyme by controlling the membrane binding of the PBM (see below), resembling electrochemical coupling in

Voltage-controlled PTEN Activity

native VSPs (8, 24). Although it has been shown that binding of the PBM to PI(4,5)P₂ increases the α -helicity of PTEN (22), it remains unknown whether activation occurs by the reorientation of the PD toward its membrane-resident substrate or by direct interaction of the PBM with the catalytic site. Although further work is needed to distinguish between these mechanisms, the latter model would suggest that generation of V_{enz} may be limited to CDs whose intrinsic activation mechanism involves a PBM-like motif. Such candidates may include, without being limited to, additional PTEN-related proteins, namely TPTE (45), TPIP (46), and PLIP (47). *In vitro*, these molecules may possess phosphoinositide phosphatase activities with distinct substrate specificities (46, 47). Generation of V_{enz} chimeras with these proteins may substantially help to address their function in intact cells, which has been largely unexplored.

Mechanism of Coupling in Engineered V_{enz}—The loss of electrically triggered enzymatic activity observed with PBM mutants (Fig. 5) clearly demonstrates that electrochemical coupling in Ci-VSPTEN16 involves the PBM. How might the PBM mediate the interaction of VSD and PD? For PTEN, it has been shown that the PBM mediates both membrane binding and activation of catalytic activity (17, 19, 20). Likewise, work on Ci-VSP suggested that binding of the PBM to the plasma membrane is involved in coupling and that VSD movement modulates the PBM binding to control enzymatic activity (8, 24). Thus, sensor movement following depolarization is thought to promote membrane binding of the PBM and thereby activate the PBM. According to this model, the membrane binding of the PBM will reciprocally affect voltage sensor movement. Specifically, binding of the PBM upon depolarization will restrict subsequent voltage sensor movement upon repolarization, thus slowing down OFF sensing currents (8, 24).

Our present results with Ci-VSPTEN chimeras are consistent with this idea. Thus, mutations in the PBM most probably abrogate electrochemical coupling by interfering with membrane binding, similar to previous results obtained with Ci-VSP (8). We further observed that the full PBM from PTEN drastically slowed down voltage sensor return to the resting state upon repolarization, when compared with both of the other chimeras. According to the model outlined above, this observation suggests distinct membrane binding affinities of the different chimeric PBMs, with the full PBM of PTEN (*i.e.* Ci-VSPTEN0) exhibiting the strongest binding.

Following this idea, the proposed distinct membrane binding affinities may point to a specific interaction between the different PDs and their associated PBM. Thus, we note that the chimeric PBMs of Ci-VSPTEN16 and 21 yielded the fastest OFF-sensing currents, which may indicate that their bound conformation is less stable compared with native PBMs of Ci-VSP or Ci-VSPTEN0 associated with their original PDs (Fig. 3 and Ref. 8). These combined observations suggest that for optimal membrane binding, the PBM must match the catalytic domain with which they couple. In this view, the PBM in Ci-VSP serves as an adapter for the binding between the membrane and the CD. Combinatorial exchange of PBMs in VSP chimeras designed to operate as Ci-VSPTEN should help in directly addressing such specific interaction of PBM and PD.

One caveat to this model comes from its failure to fully explain the apparent lack of control of the VSD over the CD in Ci-VSPTEN0. The basal activity at negative potentials may either indicate that PTEN is constitutively active at all potentials (*i.e.* uncoupled from the VSD) or that the activation range is also shifted to negative potentials, as found for the sensing current. Both scenarios are not mutually exclusive and may be consistent with a higher membrane binding affinity of the PBM of PTEN. For the first case, it is plausible that the control of the VSD can be overridden by a strong interaction between the membrane and the PBM. For the second case, the shift in voltage dependence may prevent the sensor from adopting a conformation in which the PBM cannot bind (as in the case of Ci-VSPTEN16, -21 and other VSPs at negative potentials), resulting in high basal activity.

Furthermore, it should be noted that the observed shift in the voltage dependence of Ci-VSPTEN0 might be explained by an alternative scenario, in which the PBM influences the profile of the focused electrical field across the voltage sensor. In this case, the PBM could increase the sensitivity of the VSD to depolarization and therefore self-promote the activation of the catalytic activity, rendering a high basal activity. To distinguish between these different possibilities, further work is required, which is beyond the scope of the current study.

In Ci-VSP, cationic residues Arg²⁴⁵, Arg²⁴⁶, Arg²⁵³, and Arg²⁵⁴ within the PBM are involved in electrochemical coupling, presumably by contributing to binding to negatively charged phospholipids in the membrane (8, 24). It is therefore remarkable that the PBM from PTEN, although lacking the positive charge at residue pair 245–246 (R245K-R246E; see Fig. 1B), produced slowed OFF-sensing currents and enhanced enzymatic activity at resting potentials, both consistent with enhanced membrane binding according to the coupling mechanism proposed above. This finding supports the idea that the PBM binds to membrane lipids in a stereo-specific manner rather than simply by electrostatic interaction with the membrane (8). This conclusion also is consistent with the elimination of electrochemical coupling by isocoulombic substitution of Arg²⁵³ and Arg²⁵⁴ to Lys (Fig. 5). Further detailed analysis of the role of individual residues within the PBM for membrane binding is required to fully resolve this issue.

In conclusion, we have been able to engineer a series of chimeric proteins conferring voltage sensitivity to the tumor suppressor PTEN *in vivo*. This work supports the idea that the PBM is a key element in the activation of VSP. In a broader view, this study constitutes a proof-of-concept to a novel approach for controlling enzymatic activity using VSDs.

Acknowledgments—We thank Drs. I. S. Ramsey, D. E. Logothetis, and L. J. DeFelice for helpful comments on the manuscript and S. Krieger and V. Petrou for excellent technical assistance. Constructs used in this work were kindly provided by Y. Okamura (Ci-VSP), T. Balla (PLC δ 1-PH, Akt-PH, Btk-PH, OSBP-PH), D. Alessi (TAPP1-PH), J. Downward (PI3K), and J. Daut (TASK3).

REFERENCES

1. Finkbeiner, S., and Greenberg, M. E. (1998) *J. Neurobiol.* 37, 171–189
2. Kingsbury, T. J., Bambrick, L. L., Roby, C. D., and Krueger, B. K. (2007)

- J. Neurochem.* **103**, 761–770
3. Wheeler, D. G., Barrett, C. F., Groth, R. D., Safa, P., and Tsien, R. W. (2008) *J. Cell Biol.* **183**, 849–863
 4. Hossain, M. I., Iwasaki, H., Okochi, Y., Chahine, M., Higashijima, S., Nagayama, K., and Okamura, Y. (2008) *J. Biol. Chem.* **283**, 18248–18259
 5. Murata, Y., Iwasaki, H., Sasaki, M., Inaba, K., and Okamura, Y. (2005) *Nature* **435**, 1239–1243
 6. Murata, Y., and Okamura, Y. (2007) *J. Physiol.* **583**, 875–889
 7. Halaszovich, C. R., Schreiber, D. N., and Oliver, D. (2009) *J. Biol. Chem.* **284**, 2106–2113
 8. Villalba-Galea, C. A., Miceli, F., Tagliatela, M., and Bezanilla, F. (2009) *J. Gen. Physiol.* **134**, 5–14
 9. Leslie, N. R., Batty, I. H., Maccario, H., Davidson, L., and Downes, C. P. (2008) *Oncogene* **27**, 5464–5476
 10. Ooms, L. M., Horan, K. A., Rahman, P., Seaton, G., Gurung, R., Kethesparan, D. S., and Mitchell, C. A. (2009) *Biochem. J.* **419**, 29–49
 11. Suh, B. C., and Hille, B. (2008) *Annu. Rev. Biophys.* **37**, 175–195
 12. Cremona, O., Di Paolo, G., Wenk, M. R., Lüthi, A., Kim, W. T., Takei, K., Daniell, L., Nemoto, Y., Shears, S. B., Flavell, R. A., McCormick, D. A., and De Camilli, P. (1999) *Cell* **99**, 179–188
 13. Haucke, V. (2005) *Biochem. Soc. Trans.* **33**, 1285–1289
 14. Maehama, T., and Dixon, J. E. (1998) *J. Biol. Chem.* **273**, 13375–13378
 15. Steck, P. A., Pershouse, M. A., Jasser, S. A., Yung, W. K., Lin, H., Ligon, A. H., Langford, L. A., Baumgard, M. L., Hattier, T., Davis, T., Frye, C., Hu, R., Swedlund, B., Teng, D. H., and Tavtigian, S. V. (1997) *Nat. Genet.* **15**, 356–362
 16. Wymann, M. P., and Schneider, R. (2008) *Nat. Rev. Mol. Cell Biol.* **9**, 162–176
 17. Campbell, R. B., Liu, F., and Ross, A. H. (2003) *J. Biol. Chem.* **278**, 33617–33620
 18. Das, S., Dixon, J. E., and Cho, W. (2003) *Proc. Natl. Acad. Sci. U.S.A.* **100**, 7491–7496
 19. Vazquez, F., Matsuoka, S., Sellers, W. R., Yanagida, T., Ueda, M., and Devreotes, P. N. (2006) *Proc. Natl. Acad. Sci. U.S.A.* **103**, 3633–3638
 20. Walker, S. M., Leslie, N. R., Perera, N. M., Batty, I. H., and Downes, C. P. (2004) *Biochem. J.* **379**, 301–307
 21. Rahdar, M., Inoue, T., Meyer, T., Zhang, J., Vazquez, F., and Devreotes, P. N. (2009) *Proc. Natl. Acad. Sci. U.S.A.* **106**, 480–485
 22. Redfern, R. E., Redfern, D., Furgason, M. L., Munson, M., Ross, A. H., and Gericke, A. (2008) *Biochemistry* **47**, 2162–2171
 23. Liu, Y., and Bankaitis, V. A. (2010) *Prog. Lipid Res.* **49**, 201–217
 24. Kohout, S. C., Bell, S. C., Liu, L., Xu, Q., Minor, D. L., Jr., and Isacoff, E. Y. (2010) *Nat. Chem. Biol.* **6**, 369–375
 25. Iwasaki, H., Murata, Y., Kim, Y., Hossain, M. I., Worby, C. A., Dixon, J. E., McCormack, T., Sasaki, T., and Okamura, Y. (2008) *Proc. Natl. Acad. Sci. U.S.A.* **105**, 7970–7975
 26. Lee, J. O., Yang, H., Georgescu, M. M., Di Cristofano, A., Maehama, T., Shi, Y., Dixon, J. E., Pandolfi, P., and Pavletich, N. P. (1999) *Cell* **99**, 323–334
 27. Villalba-Galea, C. A., Sandtner, W., Starace, D. M., and Bezanilla, F. (2008) *Proc. Natl. Acad. Sci. U.S.A.* **105**, 17600–17607
 28. Stefani, E., and Bezanilla, F. (1998) *Methods Enzymol.* **293**, 300–318
 29. Cha, A., Zerangue, N., Kavanaugh, M., and Bezanilla, F. (1998) *Methods Enzymol.* **296**, 566–578
 30. Schaechinger, T. J., and Oliver, D. (2007) *Proc. Natl. Acad. Sci. U.S.A.* **104**, 7693–7698
 31. Denning, G., Jean-Joseph, B., Prince, C., Durden, D. L., and Vogt, P. K. (2007) *Oncogene* **26**, 3930–3940
 32. Kimber, W. A., Trinkle-Mulcahy, L., Cheung, P. C., Deak, M., Marsden, L. J., Kieloch, A., Watt, S., Javier, R. T., Gray, A., Downes, C. P., Lucocq, J. M., and Alessi, D. R. (2002) *Biochem. J.* **361**, 525–536
 33. Várnai, P., and Balla, T. (1998) *J. Cell Biol.* **143**, 501–510
 34. Falkenburger, B. H., Jensen, J. B., and Hille, B. (2010) *J. Gen. Physiol.* **135**, 99–114
 35. Balla, A., Tuymetova, G., Tsiomenko, A., Várnai, P., and Balla, T. (2005) *Mol. Biol. Cell* **16**, 1282–1295
 36. Leslie, N. R., and Downes, C. P. (2002) *Cell Signal* **14**, 285–295
 37. Kohout, S. C., Ulbrich, M. H., Bell, S. C., and Isacoff, E. Y. (2008) *Nat. Struct. Mol. Biol.* **15**, 106–108
 38. Van der Kaay, J., Beck, M., Gray, A., and Downes, C. P. (1999) *J. Biol. Chem.* **274**, 35963–35968
 39. Lee, S. R., Yang, K. S., Kwon, J., Lee, C., Jeong, W., and Rhee, S. G. (2002) *J. Biol. Chem.* **277**, 20336–20342
 40. Chen, X., Talley, E. M., Patel, N., Gomis, A., McIntire, W. E., Dong, B., Viana, F., Garrison, J. C., and Bayliss, D. A. (2006) *Proc. Natl. Acad. Sci. U.S.A.* **103**, 3422–3427
 41. Milosevic, I., Sørensen, J. B., Lang, T., Krauss, M., Nagy, G., Haucke, V., Jahn, R., and Neher, E. (2005) *J. Neurosci.* **25**, 2557–2565
 42. Wang, Y. J., Li, W. H., Wang, J., Xu, K., Dong, P., Luo, X., and Yin, H. L. (2004) *J. Cell Biol.* **167**, 1005–1010
 43. Várnai, P., Thyagarajan, B., Rohacs, T., and Balla, T. (2006) *J. Cell Biol.* **175**, 377–382
 44. Suh, B. C., Inoue, T., Meyer, T., and Hille, B. (2006) *Science* **314**, 1454–1457
 45. Tapparel, C., Reymond, A., Girardet, C., Guillou, L., Lyle, R., Lamou, C., Hutter, P., and Antonarakis, S. E. (2003) *Gene* **323**, 189–199
 46. Walker, S. M., Downes, C. P., and Leslie, N. R. (2001) *Biochem. J.* **360**, 277–283
 47. Pagliarini, D. J., Worby, C. A., and Dixon, J. E. (2004) *J. Biol. Chem.* **279**, 38590–38596
 48. Lambert, C., Léonard, N., De Bolle, X., and Depiereux, E. (2002) *Bioinformatics* **18**, 1250–1256

7 Appendix

7.1 Table of Figures

Figure 1: The organ of Corti in the inner ear mediates the transduction of sound.....-2-

7.2 Curriculum Vitae

Personal Details

Name	Michael Georg Leitner
Address	Herrmannstraße 69 35037 Marburg (Germany)
Date of Birth	09.05.1980 in St. Johann in Tirol (Austria)

Scholastics

2001 - 2005	Leopold-Franzens-Universität Innsbruck (Austria) - Bachelors Programme Biology (11.4.2005 Bakk.rer.nat.)
-------------	--

2005 -2007	Leopold-Franzens-Universität Innsbruck (Austria) – Masters Programme Zoology (02.05.2007 Mag. Biol.)
------------	--

Diploma Thesis – Interaction of Nicotine and Menthol in Sensory Neurons (Department of Physiology and Medical Physics, Medical University Innsbruck)

2008 - 2012	Philipps-Universität Marburg (Germany) – Doctoral thesis in the group of Prof. Dr. Dominik Oliver (Neurophysiology) "Molecular Properties and Pathophysiological Relevance of the Predominant K ⁺ Conductance in Cochlear Outer Hair Cells"
-------------	---

Awards

2004 - 2006	Achievement oriented scholarship of the Leopold- Franzens Universität Innsbruck
-------------	--

2007	Incentive Scholarship of the Medical University Innsbruck
------	--

2009	Poster award at the 88 th annual meeting of the "Deutsche Physiologische Gesellschaft"
------	--

2010	2 nd position Dissertationspreis Philips-University Marburg
------	---

7.3 Verzeichnis der akademischen Lehrer

Meine Akademischen Lehrer waren die Damen und Herren...

...in Innsbruck (Österreich)

Dallinger, Doppler, Fürst, Haas, Haselwandter, Hobmeyer, Jennings, Kaufmann, Kress, Krumschnabl, Loidl, Maier, Maly, Meyer, Moser, Pelster, Pfaller, Psenner, Ravasio, Rieger, Sattler, Schinner, Schwerte, Sommaruga, Sturmbauer, Tappeiner, Thaler, Tuluc

...in Marburg (Deutschland)

Braun, Oberwinkler, Del Rey, Oliver

7.4 Acknowledgements

Hiermit möchte ich alle erwähnen, ohne die diese Arbeit wohl niemals in dieser Form möglich gewesen wäre:

An erster Stelle möchte ich mich bei Dominik (nicht weil ich muss, sondern will) für die Unterstützung während der Arbeit danken. Besonders auch dafür, dass ich auch messen durfte, was vielleicht (auf den ersten Blick) keinen Sinn gemacht hat....es hat ja doch ab und zu funktioniert. Und dafür, dass er die Arbeit dann doch noch gelesen hat ;)

Ich bedanke mich besonders bei allen Mitgliedern der Arbeitsgruppe für den sehr amüsanten Alltag und die immense Unterstützung bei der Arbeit. Vor allem natürlich Sigrid und Olga für die besten CHO Zellen des Universums, Christian (Herr Dr.) für die Hilfe und dafür, dass ich seine Arbeit machen durfte, und Herrn Nies, Moritz, Bettina, Anja und Angeliki für die kurzweiligen Pausen.

Ohne Ludwig und Simon (sowie natürlich alle anderen Feinmechaniker) wäre das Setup nicht so funktional, nicht so hübsch und schon gar nicht so abgerundet, wie es jetzt ist.

Ich bedanke mich bei Gisela, Eva und Daniela, die sich rührend um meine Plasmide gekümmert haben, obwohl ich wohl des Öfteren gar lästig war.

Meiner Familie danke ich dafür, dass sie mir das Studium überhaupt erst ermöglicht haben.

Abseits des Labors wäre es wohl nicht so lustig und nahrhaft gewesen, hätte es nicht Die Petzoldts, Bettina und Institutskino gegeben.

Abschließend möchte noch besonders Bettina für das Verständnis und die Freundschaft danken; wer weiß, wo das alles noch hinführt.....

DANKE EUCH ALLEN

7.5 Ehrenwörtliche Erklärung

Ich erkläre ehrenwörtlich, dass ich die dem Fachbereich Medizin Marburg zur Promotionsprüfung eingereichte Arbeit mit dem Titel

"Molecular Properties and Pathophysiological Relevance of the Predominant K⁺ Conductance in Cochlear Outer Hair Cells"

im Institut für Normale und Pathologische Physiologie unter der Leitung von Prof. Dr. Dr. Daut mit Unterstützung von Prof. Dr. Oliver ohne sonstige Hilfe selbst durchgeführt und bei der Abfassung der Arbeit keine anderen als die in der Dissertation aufgeführten Hilfsmittel benutzt habe. Ich habe bisher an keinem in- oder ausländischen Medizinischen Fachbereich ein Gesuch um Zulassung zur Promotion eingereicht, noch die vorliegende oder eine andere Arbeit als Dissertation vorgelegt.

Marburg, am 16.3.2012



Michael Leitner